

# DISSERTATION

## Development And Evaluation Of Silica-Based Mixed-Mode Weak Ion Exchangers Including Their Applications In Bioanalytics

Verfasser

Dipl.-Ing. Romain Dabre

angestrebter akademischer Grad

Doktor rerum naturalium

(Dr. rer. nat.)

Darmstadt, 16. März 2011

Studienkennzahl lt. Studienblatt:  
Dissertationsgebiet lt. Studienblatt:  
Betreuer:

A >091 419<  
Dr.-Studium der Naturwissenschaften Chemie UniStG  
O. Uni. Prof. Dr. Wolfgang Lindner



*The saddest aspect of life right now is that science gathers knowledge faster than society gathers wisdom.*  
Isaac Asimov, 1988

*La démarche scientifique n'utilise pas le verbe croire; la science se contente de proposer des modèles explicatifs provisoires de la réalité; et elle est prête à les modifier dès qu'une information nouvelle apporte une contradiction<sup>1</sup>.*  
Albert Jacquard, *Petite philosophie à l'usage des non-philosophes*, 1997

<sup>1</sup>*The scientific approach does not use the term “believe”; science is only proposing some temporary explicative models; and it is ready to amend them as soon as new information lead to contradiction.*





# Contents

<b>Preface</b>	<b>ix</b>
<b>Acknowledgments</b>	<b>xi</b>
<b>Nomenclature</b>	<b>xiii</b>
<b>Abstract</b>	<b>1</b>
<b>I. Introduction</b>	<b>3</b>
<b>1. Basis of chromatography</b>	<b>5</b>
1.1. Principle of chromatography . . . . .	5
1.2. Theory of chromatography . . . . .	6
1.2.1. Chromatogram . . . . .	6
1.2.2. Retention time . . . . .	6
1.2.3. Selectivity . . . . .	7
1.2.4. Efficiency . . . . .	7
1.2.5. Resolution . . . . .	8
1.2.6. Asymmetry . . . . .	8
<b>2. Chromatographic resins</b>	<b>9</b>
2.1. HPLC packings . . . . .	9
2.2. Reactive groups on the silica surface . . . . .	9
2.3. Characterization of the silica particles . . . . .	10
2.3.1. Particle size . . . . .	10
2.3.2. Surface area and porosity . . . . .	11
2.4. Carbon content and bonding density . . . . .	12
<b>3. Improving the selectivity</b>	<b>15</b>
3.1. Classical mono-type chromatography . . . . .	15
3.1.1. Normal phase and hydrophilic interaction . . . . .	15
3.1.2. Reversed phase and hydrophobic interaction . . . . .	16
3.1.3. Ion exchange chromatography . . . . .	17
3.2. Mixed-mode chromatography . . . . .	18
<b>II. Synthesis of mixed-mode stationary phases</b>	<b>21</b>
<b>1. Statistical optimization of the silylation reaction</b>	<b>23</b>
1.1. Introduction . . . . .	23
1.2. Experimental . . . . .	24
1.2.1. Chemicals . . . . .	24

1.2.2.	Silica pretreatment . . . . .	24
1.2.3.	Instrumentation . . . . .	24
1.2.4.	Determination of reactive surface thiols . . . . .	24
1.2.5.	Reaction procedure . . . . .	26
1.2.6.	Statistical method . . . . .	26
1.2.7.	NMR spectroscopy . . . . .	26
1.2.8.	Conditions for the chromatographic test . . . . .	26
1.2.9.	Stress treatment . . . . .	26
1.2.10.	LC-MS bleeding test . . . . .	27
1.3.	Results and discussion . . . . .	27
1.3.1.	Optimization of the silylation reaction . . . . .	27
1.3.2.	Characterization of thiol-modified particles by $^{29}\text{Si}$ CP-MAS NMR . . . . .	29
1.3.3.	Chromatographic characterization of the mercaptopropyl-modified silica particles . . . . .	31
1.3.4.	Stability of the phases . . . . .	34
1.4.	Concluding remarks . . . . .	36
<b>2.</b>	<b>Improvement of the stability of mixed-mode phases: endcapping and hydrolysis</b>	<b>39</b>
2.1.	Introduction . . . . .	39
2.2.	Experimental . . . . .	39
2.2.1.	Chemicals . . . . .	39
2.2.2.	Instrumentation . . . . .	41
2.2.3.	Reaction procedure . . . . .	41
2.3.	Results and discussion . . . . .	41
2.3.1.	Improvement of the endcapping reaction . . . . .	41
2.3.2.	Improvement of the hydrolysis process prior to the endcapping step . . . . .	42
2.4.	Concluding remarks . . . . .	43
<b>3.</b>	<b>Synthesis of RP-WAX selector and grafting</b>	<b>45</b>
3.1.	Introduction . . . . .	45
3.2.	Experimental . . . . .	46
3.2.1.	Chemicals . . . . .	46
3.2.2.	Instrumentation . . . . .	46
3.2.3.	Synthesis of N-(10-undecenoyl)-3-aminoquinuclidine . . . . .	46
3.2.4.	Grafting of RP-WAX selector to thiol-modified endcapped silica . . . . .	47
3.3.	Results and discussion . . . . .	48
3.3.1.	Synthesis of mixed-mode RP-WAX selector . . . . .	48
3.3.2.	Selector grafting on mercaptopropyl modified silica surface . . . . .	49
3.4.	Concluding remarks . . . . .	50
<b>4.</b>	<b>Improvement of the stability of mixed-mode phases: hypercrosslinking</b>	<b>51</b>
4.1.	Introduction . . . . .	51
4.2.	Experimental . . . . .	52
4.2.1.	Chemicals . . . . .	52
4.2.2.	Instrumentation . . . . .	52
4.2.3.	Reaction procedures . . . . .	52
4.3.	Results and discussion . . . . .	53
4.3.1.	Hypercrosslinking on tridentate silane . . . . .	53
4.3.2.	Hypercrosslinking on monodentate silane . . . . .	54
4.3.3.	Hypercrosslinking on cyclosiloxane . . . . .	54

4.4. Concluding remarks . . . . .	61
<b>5. Synthesis of other types of mixed-mode selectors</b>	<b>63</b>
5.1. Introduction . . . . .	63
5.2. Experimental . . . . .	64
5.2.1. Chemicals . . . . .	64
5.2.2. Selector synthesis . . . . .	64
5.2.3. Surface modification . . . . .	66
5.3. Results and discussion . . . . .	67
5.3.1. Mixed-mode Reversed Phase - Strong Anion eXchanger . . . . .	67
5.3.2. Mixed-mode Reversed Phase - Weak Cation eXchanger . . . . .	68
5.3.3. Mixed-mode Reversed Phase - Strong Cation eXchanger . . . . .	68
5.4. Concluding remarks . . . . .	69
 <b>III. HPLC method development on mixed-mode stationary phases</b>	 <b>71</b>
<b>1. Performance test and stability evaluation</b>	<b>73</b>
1.1. Introduction . . . . .	73
1.2. Experimental . . . . .	75
1.2.1. Chemicals . . . . .	75
1.2.2. Instrumentation . . . . .	75
1.2.3. Column classification system . . . . .	76
1.2.4. Sample preparation and chromatographic conditions for the specific RP-WAX test . . . . .	76
1.2.5. Stress test . . . . .	76
1.3. Results and discussion . . . . .	77
1.3.1. Column classification system . . . . .	77
1.3.2. Specific mixed-mode HPLC test . . . . .	78
1.3.3. Stability evaluation and benchmark comparison . . . . .	80
1.4. Concluding remarks . . . . .	86
 <b>2. Simultaneous determination of fat- and water-soluble vitamins</b>	 <b>89</b>
2.1. Introduction . . . . .	89
2.2. Material and methods . . . . .	91
2.2.1. Chemicals . . . . .	91
2.2.2. Instrumentation . . . . .	91
2.2.3. Sample preparation . . . . .	91
2.2.4. Chromatographic conditions . . . . .	92
2.2.5. Method validation . . . . .	92
2.3. Results and discussion . . . . .	95
2.3.1. Method development . . . . .	95
2.3.2. Elution order and mechanism . . . . .	98
2.3.3. Method validation . . . . .	100
2.3.4. Identification and determination of vitamins in multivitamin tablets	108
2.4. Conclusion . . . . .	108
 <b>3. Simultaneous separation of seven <math>\beta</math>-blockers</b>	 <b>111</b>
3.1. Introduction . . . . .	111
3.2. Material and methods . . . . .	113

3.2.1. Chemicals . . . . .	113
3.2.2. Instrumentation . . . . .	113
3.2.3. Determination of retention factors . . . . .	113
3.2.4. Method optimization . . . . .	113
3.3. Results and discussion . . . . .	118
3.3.1. Separation of 7 $\beta$ -blockers on conventional HPLC materials . . . . .	118
3.3.2. Effect of several parameters on the retention of 7 $\beta$ -blockers in iso- cratic mode . . . . .	120
3.3.3. Simultaneous separation of 7 $\beta$ -blockers on RP-WAX material . . . . .	121
3.4. Conclusion . . . . .	122
<b>4. Further applications of RP-WAX mixed-mode material</b>	<b>125</b>
4.1. Introduction . . . . .	125
4.2. Experimental . . . . .	125
4.2.1. Chemical . . . . .	125
4.2.2. Instrumentation . . . . .	125
4.3. Synthetic and biosimilar neutral, amphoteric, acidic, and basic active com- pounds . . . . .	126
4.3.1. Amphoteric compounds: fluoroquinolone antibiotics . . . . .	126
4.3.2. Isoprenoides . . . . .	131
4.3.3. Acidic compounds: anti-inflammatory drugs . . . . .	134
4.3.4. Human insulin . . . . .	137
4.3.5. Tri-Luma . . . . .	140
4.4. Conclusion . . . . .	143
<b>IV. Conclusion</b>	<b>145</b>
<b>Bibliography</b>	<b>149</b>
<b>List of Figures</b>	<b>157</b>
<b>List of Tables</b>	<b>161</b>
<b>Index</b>	<b>163</b>
<b>Addenda</b>	<b>165</b>
<b>Papers</b>	<b>167</b>
<b>Lectures</b>	<b>187</b>
<b>Posters</b>	<b>189</b>
<b>Zusammenfassung</b>	<b>195</b>
<b>Curriculum Vitae</b>	<b>197</b>

# Preface

The following work was funded by the company Merck KGaA (Darmstadt, Germany). The whole experimental work was achieved in the laboratory of Dr. Achim Schwämmle, from the group of Dr. Sven Andrecht, within the department *Performance & Life Science Chemicals - R&D Chromatography & Bioseparation* led by Dr. Robertus Hendriks.

Several parts of the presented work were published either in peer-reviewed journals, or as lectures or posters in different conferences.

The Chapter 1 in Part II was published in the Journal of Chromatography A [1]. Preliminary results from this paper were released in a poster at the HPLC 2008 in Baltimore, USA.

The Chapter 2 in Part III was published in the Journal of Separation Science in 2011 [2].

Several application examples presented in Part III were presented as lectures at the ISPPP 2008 in Baden-Baden, Germany, and at the ISPPP 2009 in Delray Beach, USA. Several posters were released based on the same part of the study at the Recovery 2008 in Quebec City, Canada, at the HPLC 2009 in Dresden, Germany, during the Euroanalysis 2009 in Innsbruck, Austria. The method validation from the Chapter 2 in Part III was described on a poster at the HPLC 2010 in Boston, USA. A poster presented at the HIC/RPC 2011 in Estoril, Portugal, summarized the applications presented in Part III.

Those different publications can be found in the addenda of this thesis.



# Acknowledgments

First of all, I would like to express Prof. Wolfgang Lindner my gratitude for giving me the opportunity to work on such an interesting project. I would also like to thank him for the latitude I had to manage my research work, for his support, and for his expertise. Even if it was not always easy, this combination gave me the perfect working conditions to get better.

My second thoughts are going to Dr. Michael Lämmerhofer. I learned a lot about scientific writing thanks to his meticulous review of my work, but I still have a very long way to go!

Many thanks also to all the students of the analytical group of Prof. Lindner at the University of Vienna. I was not so often there, but I always learned a lot working with them.

A very special thanks goes to Dr. Achim Schwämmle from Merck KGaA. We worked more than five years together on different projects, and I really enjoyed the confidence and the work climate. He had a very positive impact on my (professional) life, and he became more a friend than a supervisor.

I don't forget Dr. Sven Andrecht, Dr. Robertus Hendriks and Dr. Karl-Heinz Derwenskus for giving me the opportunity to work in perfect conditions.

Furthermore, I could not have achieved this work without the support of my colleagues at Merck Darmstadt, Arnd, Gabi, Helena, Nicole, Christian, Emese, Adeline, Céline, Flavie, Nazanin, Camille, and all those I forgot. My thoughts are also going to Dr. Johann Bauer for our late meetings, with german beers and constructive discussions.

A special thanks is going to my colleagues at Tosoh Bioscience. They gave me the opportunity to get already onto new challenges, but they also remembered me of the importance of this thesis.

I also would like to acknowledge my parents and my family for their never-ending support over the years.

At last, I cannot thank Jeanne enough for supporting my changing moods during this long-lasting work, especially within the last writing months. Now that this highly selfish project came to its end, let's start some new ones together!





# Nomenclature

## Abbreviations

AEC	Anion Exchange Chromatography
AFC	Affinity Chromatography
APCI	Atmospheric Pressure Chemical Ionization
CEC	Cation Exchange Chromatography
CP-MAS	Cross Polarization - Magic Angle Spinning
CRS	Chemical Reference Substance
CSP	Chiral Stationary Phase
CV	Column Volume
DAD	Diode Array Detection
DMAP	Dimethylaminopyridine
DoE	Design of Experiment
DPDS method	See DPDS in Chemical
ESI/MS	ElectroSpray Ionization / Mass Spectrometry
FDA	Food and Drug Administration
HETP	Height Equivalent to a Theoretical Plate
HIC	Hydrophobic Interaction Chromatography
HIC	Hydrophobic Interaction Chromatography
HILIC	Hydrophilic Chromatography
HMDS	Hexamethyldisilazane
HPLC	High Performance Liquid Chromatography
ICH	International Conference on Harmonization of Technical Requirements for Registration of Pharmaceuticals for Human Use
IEC	Ion Exchange Chromatography
IR	Infrared
LC-MS	Liquid Chromatography - Mass Spectrometry
LLOQ	Lower Limit of Quantitation

## *Nomenclature*

LOD	Limit of Detection
LOQ	Limit of Quantitation
NMR	Nuclear Magnetic Resonance
NPC	Normal Phase Chromatography
NPR	Non porous resin
POPLC	Phase OPTimized Liquid Chromatography
PSD	Particle Size Distribution
PTFE	Polytetrafluoroethylene
RP	Reversed Phase
RP-SAX	Reversed Phase - Strong Anion eXchange
RP-SCX	Reversed Phase - Strong Cation eXchange
RP-WAX	Reversed Phase - Weak Anion eXchange
RP-WCX	Reversed Phase - Weak Cation eXchange
RP18	Reversed Phase with 18 carbon units in alkyl chain
RT	Room Temperature
SC	Surface Coverage
SEC	Size Exclusion Chromatography
UHPLC	Ultra High Performance Liquid Chromatography
ULOL	Upper Limit of Linearity
ULOQ	Upper Limit of Quantitation
UV-Vis	Ultraviolet - Visible
WAX	Weak Anion Exchange
ZIC-HILIC	Zwitterionic Hydrophilic Interaction Chromatography

**Chemicals**

ACN	Acetonitrile
AIBN	Azobisisobutyronitrile
ATMS	(Diethylamino)trimethylsilane
BuLi	n-Butyllithium
DMAP	Dimethylaminopyridine
DMF	Dimethylformamide
DMSO	Dimethyl sulfoxide
DPDS	2,2'-Dipyridyl disulfide
FA	Formic acid
FPP	Farnesyl pyrophosphate
GGPP	Geranylgeranyl pyrophosphate
GPP	Geranyl pyrophosphate
HMDS	Hexamethyldisilazane
MPDMMS	3-Mercaptopropyltrimethoxymethylsilane
MPTMS	3-Mercaptopropyltrimethoxysilane
PMDMS	n-Propylmethyldimethoxysilane
PTMA	Pentaerythritoltetrakis(mercaptoacetate)
PTSA	p-Toluenesulfonic acid
TeMTeVTaS	Tetramethyltetravinyltetra-cyclosiloxane
TFA	Trifluoroacetic acid
THF	Tetrahydrofuran
TMCS	Trimethylchlorosilane
TMTVS	Trimethyltrivinyltrisiloxane
TRIS	Tris(hydroxymethyl)aminomethane
TVCH	1,2,4-Trivinylcyclohexane
TVCS	Trivinylchlorosilane
V65	2,2'-Azobis-(2,4-dimethyl)valeronitrile
VTMS	Vinyltrimethoxysilane

## Symbols

$\alpha$	Surface density ( $\mu\text{mol}/\text{m}^2$ )
$\alpha_{j/i}$	Selectivity between compound i and j
$\Delta t_R$	Distance between two peaks
$\sigma^2$	Variance of the statistical distribution
$a$	Fronting
$A_S$	Asymmetry
$b$	Tailing
$F$	Flow rate
$H$	see HETP in Abbreviations
$k'_i$	Reduced retention time of compound i
$L$	Length of the column
$M$	Molecular weight
$N$	Plate count
$n$	Number of atoms
$N_a$	Atomic weight
$p$	Percentage of carbon
$R_S$	Resolution
$S_0$	Specific surface area ( $\text{m}^2/\text{g}$ )
$t_{R_i}$	Retention time of compound i
$t_{\text{sys}}$	Dead time of the equipment
$t_{\text{total}}$	Dead time of the system
$t_0$	Dead time of the column
$v_0$	Dead volume
$w_i$	Width of peak corresponding to compound i

# Abstract

Silica resins have been used since the beginning of liquid chromatography for the separation of analytes depending on their steric characteristics due to the porosity of the silica. Afterwards, silica was used to separate polar compounds in normal mode. In this mode, the silanol groups on the surface of the bare silica act as interaction point between silica surface and analytes. However, the stability of those kind of gels and the range of application was limited due to the fixed composition of the surface.

Therefore, later on, reversed-phase materials were developed by adding some hydrophobic compounds to those silanol groups through silylation reactions. These more modern materials were less sensitive to aggressive conditions, and it allowed the analysis and purification of molecules with very different degree of hydrophobicity through changes in the content of organic solvent in the mobile phase. Other types of chromatographic resins were developed subsequently to address further separation issues. Hydrophobic interaction phases (HIC) were synthesized for the separation of hydrophobic compounds using a buffer-driven elution to analyze or purify molecules which are unstable in the presence of organic solvents (proteins, typically). Anion and cation exchange chromatography (AEC and CEC, respectively) were developed for the separation of charged molecules. Hydrophilic interaction phases (HILIC) were developed for the separation of polar compounds without the stability issue of bare silica. Chiral stationary phases (CSP) addressed the problematic of the separation of chiral molecules.

However, in the last decade, mixed-mode chromatography emerged to enable the separation of mixtures containing molecules with many different chemical characteristics within a single run on a single resin. In this study, we developed a ligand bearing a hydrophobic chain as well as a weak anion exchange head group. Grafting of the ligand to the surface of silica particles lead to the synthesis of a mixed-mode material combining both reversed phase (RP) and weak anion exchange (WAX) characteristics.

The first part of the study consisted in improving the synthesis of the patented ligand. Different chemicals and technical approaches were tested to simplify the synthesis and to increase the robustness of the method. The binding of the spacer onto the surface, the endcapping of the non-reacted silanol groups, the grafting of the ligand to the spacer were also investigated. After having optimized every step of the manufacturing process, the method was scaled up to 500 g, which corresponds to a pre-production scale.

In a second part, many different applications were developed to assess the operational range of such material. The RP-WAX material developed in our laboratories offers a wide range of applicability for the separation of neutral, acidic, basic, or amphoteric compounds. Chromatographic runs can be performed in many different interaction modes such as hydrophilic and hydrophobic interaction, ion exclusion or repulsion, ion exchange, or a combination of several of those modes. In order to demonstrate the versatility of our material, we studied the chromatographic behavior of hydrophobic and hydrophilic compounds, as well as molecules bearing acidic or basic moieties. We used therefore fat- and water-soluble vitamins, fluoroquinolone antibiotics, betablockers, non-steroidal anti-inflammatory, anti-hypercholesterolemia drugs, among others. We compared the sep-

## *Abstract*

aration on standard RP or HILIC material with the separation achieved using RP-WAX material. Separation of most of the considered complex mixtures could be improved by using the mixed-mode resin.

The RP-WAX material developed during this study should be commercially available at Merck KGaA in 2011.

**Part I.**

# **Introduction**





# 1. Basis of chromatography

## 1.1. Principle of chromatography

First chromatography techniques emerged in the middle of the 19<sup>th</sup> century. The chromatography grew up slowly to become one of the major analytical method nowadays. High-performance liquid chromatography (HPLC) really started in the 1970s with the miniaturization of silica particles, which lead to higher pressure and higher performances<sup>1</sup>. The first decade was dedicated to the understanding of the fundamentals, with groundbreaking studies performed by Guiochon, Halász, Horváth, Kirkland, among other scientists, with 5 to 10  $\mu\text{m}$  particles. In the 1990s, the particle size remained constant, and most of the improvements were made on standard material, with better batch-to-batch reproducibility for the synthesis of the basis material and improved derivatization, and packing techniques, with the input from Unger for example. Major change in the last decade was the decrease of particle size<sup>2</sup>, which lead to ultra high-performance chromatography (UHPLC). Even if the techniques and packings have evolved, the principle remains the same.

In chromatography, analytes are separated from each other through a partitioning between different phases. Most of the time, one phase is solid, whereas the other one is liquid or gaseous. Those different phases are moving relative to each other, due to driving forces. For electrokinetic chromatography, driving force is an electric field, and for counter-current chromatography, both phases are moving in opposite directions. In this study, we concentrate on HPLC, in which the stationary phase is a solid phase packed in a column whereas the liquid mobile phase is pumped through it. The stationary phase is also known as adsorbent, and the overall separation principle is based on the adsorption of analytes onto the surface (see Figure 1.1.1).

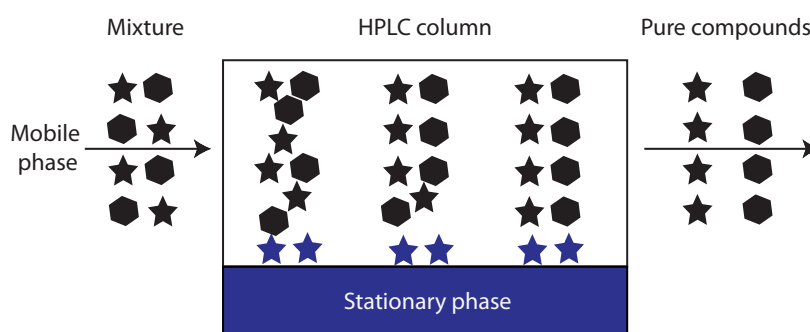


Figure 1.1.1.: Principle of chromatography.

In isocratic chromatography, all the settings remain constant over the entire analysis.

<sup>1</sup>Because of the higher pressure, the smaller particles are not the only factor to consider. The rapid development of HPLC in the last 30 years would not have been possible without improvements of the hardware, with pumps able to handle higher pressure, dedicated detectors, and informatics tools.

<sup>2</sup>Down to 1.7  $\mu\text{m}$ , known as sub-2 $\mu\text{m}$  particles.

## 1. Basis of chromatography

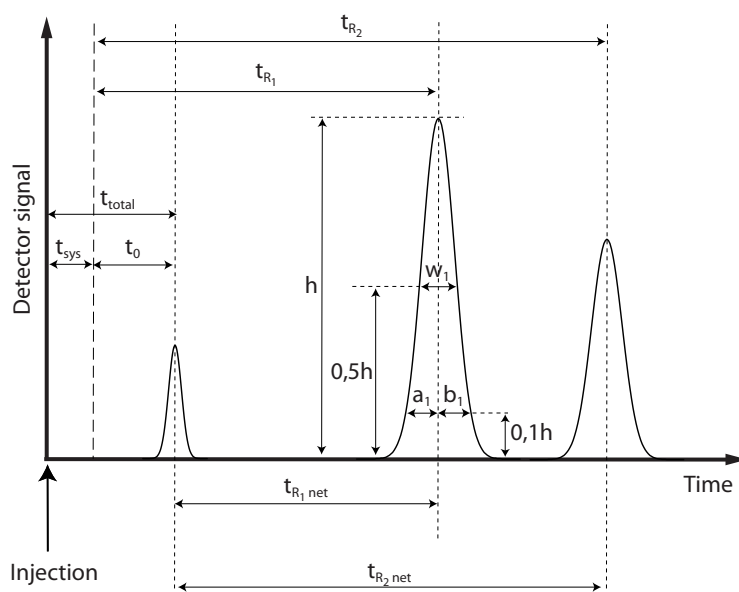


Figure 1.1.2.: Chromatogram of three components and corresponding parameters for the calculation of different chromatographic data [3].

For more complex separations, changing some parameters during a run can improve the quality of the separation. We speak then of gradient chromatography, and the most typical case consists in changing the mobile phase composition from high binding to low binding eluents. Other parameters can also be adapted such as temperature or flow rate.

## 1.2. Theory of chromatography

### 1.2.1. Chromatogram

Basic information obtained by injecting different molecules in a chromatographic column can be obtained from corresponding chromatogram plotted in Figure 1.1.2. It must be noted that, for explanation purposes, chromatogram is theoretical. First compound to elute is not retained by the column. Different abbreviations in following paragraphs are referring to this figure.

### 1.2.2. Retention time

Retention time  $t_{Ri}$  corresponds to the time spent by component  $i$  in the column. It is directly proportional to the affinity of the analyte with the substrate. A non-retained compound elutes at  $t_0$ , also known as dead time of the column<sup>3</sup>. For standard chromatographic methods, where no secondary interaction take place, specific non-interacting molecules (typically uracil in reversed phase mode) can be injected along the analytes

<sup>3</sup>For standard HPLC, the dead time of the equipment without the column  $t_{sys}$  should be negligible in comparison with the dead time of the column  $t_0$ . Therefore, most of the time, total dead time  $t_{total}$  is equated to  $t_0$ . The difference affects the calculation only if the system dead volume is very large, for an older preparative system for instance, or if the run time is very short, for example for UHPLC runs. In these cases, determining  $t_{sys}$  is primordial. In this study, we do not mention whether  $t_{sys}$  was determined or not. Generally,  $t_{sys}$  was taken in account only for fine gradient tuning using automated method development system.

to determine  $t_0$ . However, as mixed-mode phases principally exhibit different parallel interactions, it is very difficult to find a molecule which has no affinity to the substrate. Therefore, in the following, most of the dead volume value were determined through injection of methanol, which leads to the obtention of a solvent peak at  $t_0$ <sup>4</sup>.

In order to be able to compare results independently to the column geometry, we introduce reduced retention time  $k'_i$ . The reduced retention time is also known as retention factor<sup>5</sup>:

$$k'_i = \frac{t_{R_i} - t_0}{t_0} \quad (1.2.1)$$

### 1.2.3. Selectivity

The selectivity  $\alpha_{j/i}$ , also known as relative retention or separation factor, is defined as following:

$$\alpha_{j/i} = \frac{k'_j}{k'_i} \quad (1.2.2)$$

By convention, the suffix  $j$  relates to the longer-retained compound, and the suffix  $i$  to the less-retained one. Therefore, selectivity is always  $> 1$ .

### 1.2.4. Efficiency

Column efficiency is equivalent to plate count  $N$ , and it is also a measurement of the quality of the separation. It characterizes the peak dispersion:

$$N = \frac{L}{H} \quad (1.2.3)$$

where  $L$  is the length of the column and  $H$  the height equivalent to a theoretical plate (HETP).  $N$  can be seen as a reduced parameter of the HETP, which allows to characterize a sorbent independently of the column hardware. This is very useful for concurrence comparison and for marketing publication. However, HETP is more interesting to understand the principle of chromatography.

In the theory, we assume that each injected compound can be divided into narrow bands at the top of the column. During the migration along the column, each band becomes broader. In the mean time, two bands corresponding to two different compounds are moving at two different speeds. The band broadening is proportional to the square root of the column length, whereas the separation is proportional to the length of the column. The compound migration is then much faster than the band broadening, which leads to separation<sup>6</sup>. Those chromatographic bands represent a statistical distribution of molecules. This distribution can be characterized by its variance  $\sigma^2$  and, mathematically, the height equivalent to a theoretical plate is formulated as a differential equation:

$$H = \frac{d\sigma^2}{dL} \quad (1.2.4)$$

Integrated along the column, and neglecting the bed non-uniformity, equation 1.2.4 can be simplified and written as a function of chromatogram parameters:

<sup>4</sup>Dead volume  $v_0$  and dead time  $t_0$  of the column are linked through the trivial equation  $t_0 = F \cdot v_0$  where  $F$  is the flow rate.

<sup>5</sup>All the figures can be expressed as function of column dimensions. This would be closer to the chromatographic reality but in practical, chromatogram-derived value are mostly used.

<sup>6</sup>This explains why the column length decreased regularly since the invention of chromatography. Because of the improvement of the quality of resins, the band broadening decreased, and subsequently the efficiency increased and there were no more need of so long columns.

## 1. Basis of chromatography

$$H = \frac{\sigma^2}{L} = f \frac{w_i^2}{t_{R_i}^2} \quad (1.2.5)$$

where the factor  $f$  is dependent of the height at which the peak width was measured. Different  $f$ -value can be found in the work of Uwe D. Neue [4].

### 1.2.5. Resolution

The resolution  $R_S$  characterizes the quality of the separation between two peaks:

$$R_S = \frac{\Delta t_R}{1/2 \cdot (w_i + w_j)} \quad (1.2.6)$$

where  $\Delta t_R$  is the distance between the two considered peaks  $t_{R_j} - t_{R_i}$ .

The quality of the separation between two molecules can also be defined as a function of the efficiency, of the selectivity, and of the retention time:

$$R_S = \frac{\sqrt{N}}{4} \cdot \frac{\alpha - 1}{\alpha} \cdot \frac{k_2}{k_2 + 1} \quad (1.2.7)$$

where  $k_2$  is the retention factor of the second peak in the peak pair considered for the calculation of  $\alpha$ . This is known as Purnell equation.

### 1.2.6. Asymmetry

Quality of the column can be measured by peak asymmetry  $A_S$ :

$$A_S = \frac{b_i}{a_i} \quad (1.2.8)$$

$a$  and  $b$  can be determined at 5 or 10 % of peak height. Value were determined at 10 % in Figure 1.1.2<sup>7</sup>.  $a$  is called fronting and  $b$  tailing. When both are equal, peaks are close to Gaussian shapes. Improving column packing can help to improve asymmetry (i.e.  $A_S \approx 1$ ). However, several further parameters can influence peak shape, such as geometry of hardware or secondary interactions.

---

<sup>7</sup>This calculation method was used in the following work. However, several other measures can be found in the literature [5].

## 2. Chromatographic resins

### 2.1. HPLC packings

The most common chromatography materials for analytical purposes are based on silica. We will discuss in the following paragraphs about its characteristics and about the structure of its surface. Silica is a physically stable resin. This property is fundamental for HPLC because it can support very high pressure without collapsing. Reduction of the particle size to increase performance is only feasible because of this stability. Other advantages of silica are the porosity for maximizing the surface area<sup>1</sup> and the presence of reactive groups on the surface which allows adjusting the selectivity through ligand addition. Regarding all these properties, silica would be the perfect packing material, if the chemical stability was not an issue: silica is not stable at pH over 8 to 9 (depending on the porosity and surface derivatization).

Some applications need to run at higher pH, specially for regeneration and virus inactivation in bioprocessing. Therefore, polymeric packings based on poly(styrene-divinylbenzene), on polymethacrylates, or on polyvinyl-alcohol have been developed<sup>2</sup>. Advantage of chemical stability is countervailed by different drawbacks. Polymeric packings are rather soft, which leads to lower backpressure stability, they exhibit lower efficiency, and they swell and shrink depending on the mobile phase. The packing material has therefore to be chosen specifically depending on the application. Whereas preparative chromatography in down stream processing are preferably performed on polymeric materials, most of the standard analyzes run on silica-based resins. To paraphrase Neue, *a packing with all the advantages of silica, but with an expanded pH range is still the holy grail of HPLC* [6].

### 2.2. Reactive groups on the silica surface

The silica surface can be defined as a hydroxylated surface, on which the silicon atoms are not in an exactly regular geometrical arrangement. Hence, the hydroxyl groups attached to these silicon atoms (which interest us because they are directly related to the reactivity of the silica particles) will not be exactly equidistant from each other, as shown in Figure 1.2.1 [7]. This induces changes in the properties and reactivity of different silica materials. There are only three different types of reactive silanol groups, isolated, vicinal, and geminal silanols, as shown in Figure 1.2.2. The silanol number, that is, the number of hydroxyl groups per unit surface area, is considered to be about the same on different types of silica. For example on samples of silica dried at 170°C, containing total water equal to 8 OH-groups/nm<sup>2</sup>, about 2,3 seem to be adsorbed water, using Karl-Fischer and TAG methods [8]. Further study show that after thermal treatments at 200°C under vacuum, the amount of physisorbed water will be negligibly small and the surface concentration of hydroxyl groups will be around 8,0  $\mu\text{mol}/\text{m}^2$  or 4,8 hydroxyl-groups/nm<sup>2</sup> [9]. Further data

---

<sup>1</sup>Some newer media are only partly porous, such as Poroshell from Agilent which are based on core-shell technology, or completely non porous, like TSKgel NPR from Tosoh Bioscience.

<sup>2</sup>Poly(styrene-divinylbenzene) packings have been used since the 1960s for size-exclusion chromatography.

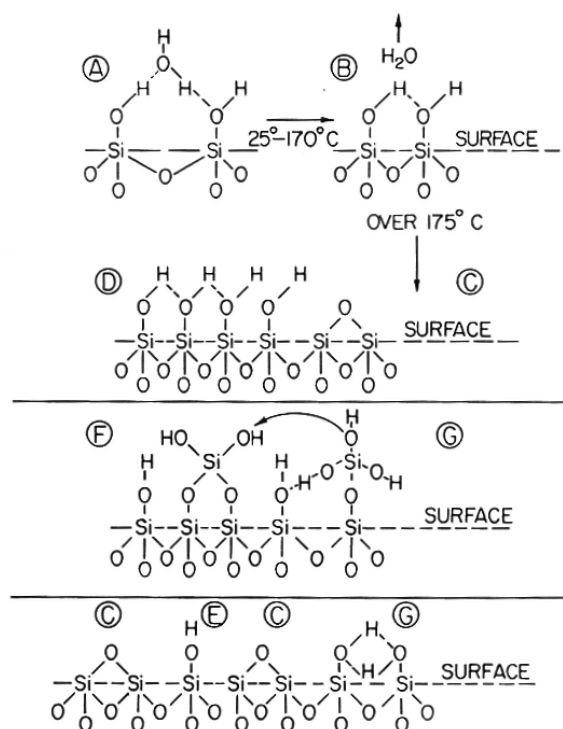


Figure 1.2.1.: Postulated types of hydroxyl groups on the surface of amorphous silica.

A, vicinal hydrated; B, vicinal anhydrous; C, siloxane-dehydrated; D, hydroxylated surface; E, isolated; F, geminal; G, vicinal, hydrogen bonded. Note: F and G probably do not actually exist on a dried surface

about the number of silanol groups on silica surface can be found in the Part II, Chapter 1.

## 2.3. Characterization of the silica particles

### 2.3.1. Particle size

The size of the silica particles is important because it influences the permeability of the column as well as the column efficiency. However, it is difficult to speak about defining the particle size of a packing, because the particles have different sizes (see Figure 1.2.3). We then tend to speak about a particle size distribution (PSD), and the value stated for a given packing is an average of the particle sizes. The PSD has not only an impact on the quality of the separation but also on the column backpressure. Modern materials exhibit narrower PSD, with higher reproducibility. PSD can be determined by different methods such as microscopy, laser diffraction, sedimentation, or electrozone sensing. The trend is going to smaller particles in order to increase resolution and to decrease analysis time. However, backpressure is increasing and new equipments are needed to handle such pressures (see also footnote 4 on page 11). Those newer materials lead to a newer technique known as Ultra High Performance Liquid Chromatography (UHPLC, or UPLC).

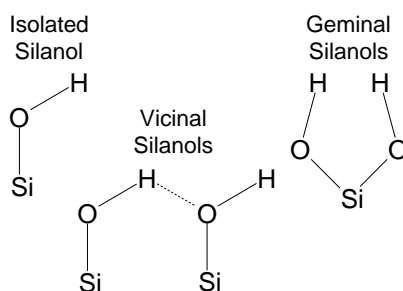


Figure 1.2.2.: Reactive silanols on silica surfaces.

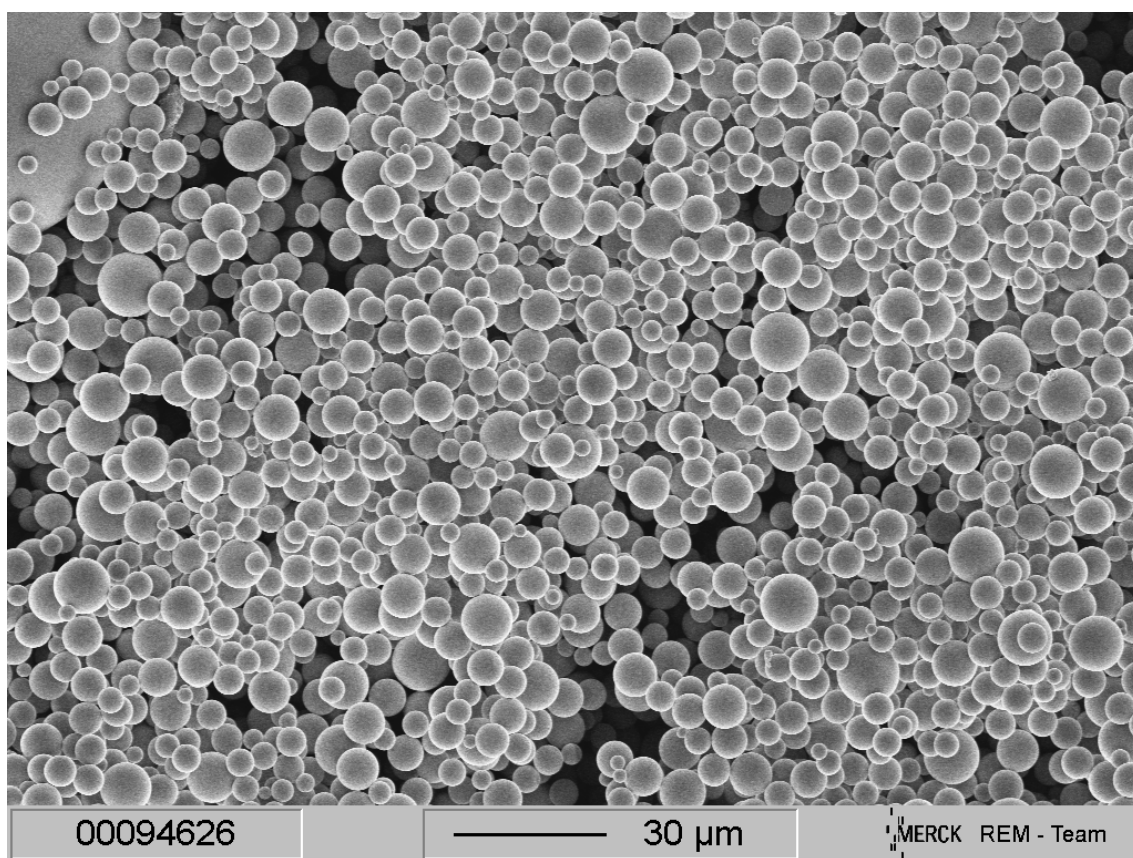


Figure 1.2.3.: Scanning electron microscopy of Merck in-house produced silica-based research sample.

### 2.3.2. Surface area and porosity

Most particles used for HPLC exhibit porous particles. Main advantage of using such porous material is the higher specific surface of the particles, which is needed for retention<sup>3</sup>. Principle of HPLC relies on this porosity to achieve high resolution and capacity<sup>4</sup>. A 5 μm

<sup>3</sup>For size exclusion chromatography, analytes do not interact with the surface and the whole separation principle relies on the porosity of the material.

<sup>4</sup>Backpressure in HPLC is mainly due to the porosity of the particles. Materials with smaller particles were developed to increase resolution and decrease analysis time. This leads to higher pressure, and to the need of dedicated equipments. In order to overcome these issues, two other kind of particles have

silica particle, for example, exhibit an external surface of only 0.02 m<sup>2</sup>/mL whereas its total surface reaches around 150 m<sup>2</sup>/mL. This value is however not directly usable for further concentration calculation (including inner-pore surface), because the density of the packing is not always known. Therefore, in the following, surface area will be expressed in m<sup>2</sup>/g.

Several methods can be employed to determine surface area. In practice, mostly used technique is the adsorption/desorption of a non-interacting gas such as nitrogen. Desorption curve of nitrogen adsorbed onto silica particles under high pressure is given in Figure 1.2.4.

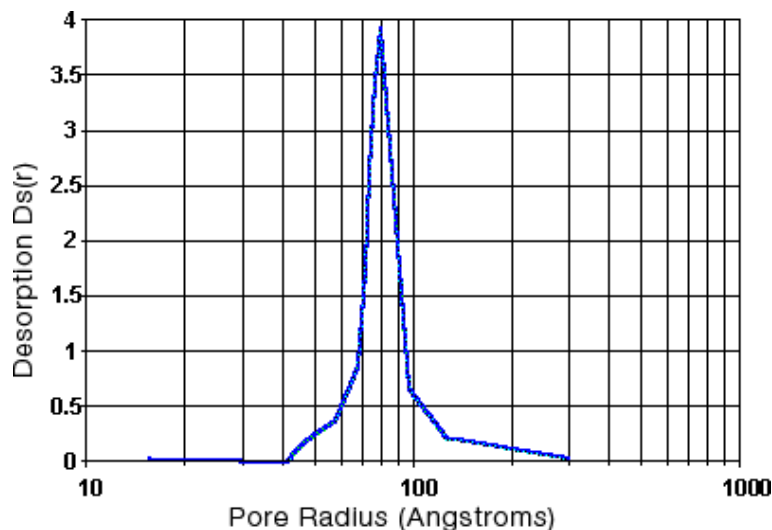


Figure 1.2.4.: Pore size distribution of silica material measured by nitrogen desorption [13].

## 2.4. Carbon content and bonding density

Using elemental analysis, it is possible to determine the percentage of several atoms within a material. Berendsen and de Galan developed in 1978 equations to determine surface density of ligands on the surface of silica depending of percentages of several atoms (C, S, N, O...) [14]. The number of micromoles per m<sup>2</sup> of native silica  $\alpha$  is given by:

$$\alpha = \frac{10^6 \cdot p}{S_0 \cdot (100 \cdot N_a \cdot n - p \cdot M)} \quad (2.4.1)$$

where  $p$  is the percentage of the considered atom,  $S_0$  the specific surface area of the native silica in m<sup>2</sup>/g,  $N_a$  the atomic weight of the considered atom,  $n$  the number of considered atoms per ligand, and  $M$  the molecular weight of ligand without reactive group. This equation can only be applied for first reaction on the silica surface. Sandoval developed

---

been commercialized:

- When resolution and capacity are less important than analysis time, some non-porous materials were developed to achieve very fast analysis [10].
- Some data tend to show that only the upper part of porous particles (or *shell*) are penetrated by analytes, and therefore the inner part (or *core*) has no impact on the quality of the separation. Newer materials consist therefore of a non-porous core enclosed by a porous shell. Such materials exhibit good efficiency in comparison with UPLC packing, and backpressure remains low [11].

A third technique was developed to limit the pressure and to keep high resolution. It consists of building a bi-modal pore network. Those monolithic columns exhibit macropores to keep low pressures and mesopores to get high resolution [12]. Drawback is the fixed hardware dimension.



in the late 1990s equations to determine the surface coverage of endcapping ligands, or more generally, the ligand density of a second reactive step [15]. In this case, we have to consider in the same equation both addition steps. Figures referring to first and second step will be indexed with 1 and 2, respectively. The number of micromoles per m<sup>2</sup> for endcapping reaction  $\alpha_2$  is given by:

$$\alpha_2 = \frac{10^8 \cdot N_a \cdot n_1 \cdot (p_2 - p_1)}{S_0(100 \cdot N_a \cdot n_1 - p_1 \cdot M_1)(100 \cdot N_a \cdot n_2 - p_2 \cdot M_2)} \quad (2.4.2)$$

For further surface modifications, one could expect that further straight-forward derivation of the same mathematical basis could lead to calculate surface density of further reactive steps. A theoretical approach confirmed the possibility to define a specific equation for every step. However, the use of several multi-functional ligands for each step is related to high calculation uncertainty. Calculations performed for the third or more modification step lead to incoherent results. Practically, we therefore had to limit the use of this method to the first two addition steps.



## 3. Improving the selectivity

As we have seen before, several parameters are describing the quality of a chromatogram, and subsequently of a separation. The chromatographic behavior is not only affected by the ligand on the surface of the particles, but also by the size and shape of the particles, by the porosity of the silica particles, and by the quality of the packing. The trend is going towards smaller particles with well-defined particle and pore sizes to reduce analysis time and to improve resolution. Those new types of materials known as UPLC resins have been performance-designed. However, this way of working leads mostly only to better separation of mixtures which are already separable on classic material. Compounds which are coeluting on 5  $\mu\text{m}$  particles may not be separated on smaller beads. Therefore, the current evolution of the chromatography materials is only addressing one need for the future of analysis<sup>1</sup>.

Separation of complex mixtures can only be improved by changing the selectivity of the separation. This can only be addressed by changing either the structure of chromatography beads or the ligand structure on the surface of such beads.

Two chromatography techniques will not be described in the following because the separation mechanism is not based on standard adsorption/desorption isotherms.

The first one, known as size exclusion chromatography (SEC), is also called gel-permeation chromatography or gel-filtration chromatography. This technique consists in separating molecules not through interactions with the surface (chemical separation) but through their steric sizes (physical separation). Bigger analytes will elute first, and smaller ones, which can enter the pores, will elute last.

The second one is called affinity chromatography (AFC). This technique is mostly used for separation of proteins. Some specific ligands are grafted to the surface, and a reversible interaction takes place between a special part of the protein and the ligand. The most used affinity material is modified either with protein A, or with parts of it. Specific purification or analysis of antibodies can be achieved with it.

The different types of chromatography based on chemical interactions between analytes and surface will be described in the next paragraphs.

### 3.1. Classical mono-type chromatography

#### 3.1.1. Normal phase and hydrophilic interaction

Normal phase chromatography (NPC) was the first chromatography mode to be developed, because the bare silica is suitable for such application. Normal phase gradient chromatography consists in adsorbing some polar compounds on the resin surface with a non-polar mobile phase, typically hexane or heptane, before eluting them through the addition of a more polar solvent to the mobile phase, like chloroform, methanol, ethanol... Bare silica

---

<sup>1</sup>As seen before in Paragraph 1.2.5, the resolution is not only a factor of the plate number but also related to the selectivity, which is influenced by the difference in affinity of both molecules to the substrate.

### 3. Improving the selectivity

is not the only normal phase modification. Some diol-, amino- or cyano-groups are also suitable for such separation. Those modified media are much more suitable because of their higher stability in more different mobile phases (organic solvents, high pH...). However, the use of such material in typical normal phase has a large drawback concerning the polarity of the analytes. Because of the use of low-polar mobile phases, this mode is only applicable to moderately polar compounds. If the molecules become too polar, the solubility in the mobile phase is too low, and separation is either impossible, or the retention times are so long, that the analysis is not practicable any more.

The hydrophilic interaction chromatography (or HILIC) is based on the same interaction between the analyte and the surface. Some of the derivatization developed for normal phase chromatography like the amino- or diol-groups have been used for this purpose. Further ligands bearing charged and non-charged groups like zwitterionic or amide-containing ligands have been developed in the last decades. Even if the HILIC behavior have been demonstrated and used before, Alpert gave its name to this technique in 1990 [16]. The main visible difference between HILIC and NPC is the mobile phase composition. Mobile phase for HILIC is composed of an organic solvent (typically acetonitrile in 95 to 60 % proportion), a protic solvent (typically water), and some buffering salts if necessary. The elution is driven by the protic solvent content. The use of water as co-solvent leads to a broader application range than NPC, because even very polar compounds can be separated on HILIC phases.

The principle of HILIC is based on polarity gradient of the mobile phase on the surface. Close to the surface, a water layer is formed, and going in the direction of the mobile phase, the acetonitrile amount is growing [17]. To simplify, a partitioning mechanism is occurring for the compounds between the water-rich layer directly on the surface and the less polar layers farther away (See Figure 1.3.1). This simplified model is not sufficient to fully understand HILIC mechanism. Deeper explanations can be found in the work of Irgum, who worked on both theoretical and practical aspect of HILIC and who is one of the “fathers” of ZIC-HILIC technology [18, 19].

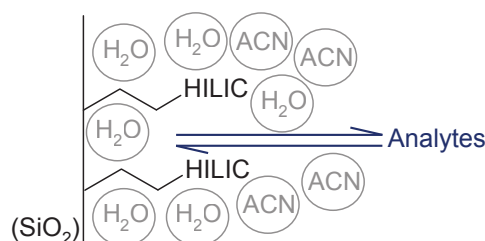


Figure 1.3.1.: Schematic illustration of the partitioning mechanism on the surface of HILIC modified silica.

#### 3.1.2. Reversed phase and hydrophobic interaction

The reversed phase mechanism can be described as an opposite to the normal and HILIC ones. A non-polar surface is built through the addition of hydrophobic ligands (typically hydrocarbon chains)<sup>2</sup> and the mobile phase consists of water (or buffer) with an organic

<sup>2</sup>This is the case for silica-based or polymeric chromatography material. Some other materials which are intrinsically hydrophobic and do not need any further modifications are seldom used. One of the main alternative to modified packing is porous graphitized carbon. Our study deals only with silica-based

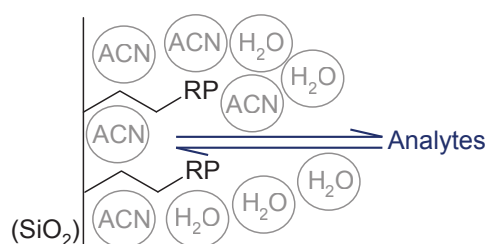


Figure 1.3.2.: Schematic illustration of the partitioning mechanism on the surface of RP modified silica.

polar modifier such as methanol or acetonitrile (See Figure 1.3.2).

The partitioning mechanism is very good understood - even better than for NPC and HILIC - and the method development is quite easy for the separation of hydrophobic compounds. Therefore more than 80 % of all HPLC applications are developed nowadays on RP materials [21]. We can however note that the proportion has declined within the last 15 years. Indeed, in the late 90s, more than 90 % of the methods were based on RP-HPLC [22].

Another technique based on the hydrophobicity of the surface was also developed to avoid using organic modifier in the mobile phase. The mechanism of hydrophobic interaction chromatography (HIC) is less understood, but it seems that hydrophobic compounds and ligands can undergo the formation of solvation layer at higher salt concentration. This leads to the adsorption of the hydrophobic compounds to the surface. Reducing the ionic strength of the mobile phase leads to elution of the desired molecules. The hydrophobicity of the ligands has to be lower for HIC, the carbon chain and the ligand density are rather smaller than for RPC, and this technique is only applicable for macromolecules with multiple interaction points. HIC is therefore very often used for the analysis and purification of proteins [23]. The absence of organic modifier is a great advantage for such separations, because most of proteins are denaturing in the presence of organic solvents.

### 3.1.3. Ion exchange chromatography

Ionic or ionizable compounds can be separated on ion exchange materials. The mechanism is based on the interaction between a charged surface and charged analytes. The term “exchange” refers to the counter ion, which is exchanged between the analyte and the fixed ion on the surface. The adsorption and elution are governed by the pH and the ionic strength of the mobile phase. In gradient chromatography, because of the difficulty of applying a linear pH gradient, the analytes are loaded onto the surface with a low-salt buffer and elution occurs through an increase of the salt concentration in the mobile phase. This technique is widely used for organic ions, amino-acids, peptides, proteins, and nucleic acids<sup>3</sup>. Inorganic ions can also be separated using the same technique, which is named “ion chromatography” for this special case.

Typical ligands for cation exchange chromatography are molecules containing sulfo- or carboxylic-groups (respectively strong and weak exchangers). For anion exchange chro-

materials, and further information can be found in the literature [20].

<sup>3</sup>Charged compounds can also be separated on reversed phase packings. Adding hydrophobic ions to the mobile phase leads to an increase of the retention of the analyte proportional to the surface concentration of the pairing reagent. This technique is known as ion pairing chromatography [24].

### 3. Improving the selectivity

matography, amino-ligands and diethylaminoethyl are widely used as strong and weak exchangers respectively. The term weak and strong does not refer to a binding capacity or whatsoever. The strong exchangers are charged at any pH, whereas the weak ones exhibit a pKa in the range 0 to 14, and their binding force is pH dependent. The weak exchangers offer more flexibility in the selectivity, but the robustness of the method is more critical if working at pH close to the pKa.

A specific use of those materials is the ion repulsion or ion exclusion chromatography. Instead of adsorbing the compounds to the surface through a positive-negative interaction, analytes and surface are equally charged, and the pores cannot be entered. This technique is normally not used as itself, but in combination with ion-exchange techniques, the selectivity between positively- and negatively-charged molecules can be dramatically enhanced.

## 3.2. Mixed-mode chromatography

The different modes that we investigated before can be used for the separation of different kind of molecules (polar, non polar, charged...). However, separation of mixtures containing a lot of different analytes with many different behaviors cannot be achieved within a single run on a mono-modal column.

One method to obtain better separation is to analyze the same mixture on different columns by multi-step chromatography. The easiest way to implement such method is to work off-line. After the first chromatographic run, several fractions are collected. Each fraction is then injected on a column with orthogonal properties<sup>4</sup>. Such multi-step processes are very often used to achieve very high purities. However, this method is barely applicable for routine analysis because of the too long run time. Therefore, some on-line techniques were developed with multi-columns systems connected with each other. Even if this system allows faster analysis and resolution of complex mixtures, both equipment and method development are quite complicated, because several pumps and switching valves are necessary to inject the right fraction to the right column with the right mobile phase at a very precise time.

Another technique consists in connecting different HPLC columns directly to each other. This can be done with any column, but the method development would be almost impossible, because of the number of parameters influencing the selectivity. The company Bischoff developed therefore an automated method development system with different resins packed in cartridges, with a specific connection hardware and a dedicated method development software [25]. This technique, called POPLC, can be very effective for the separation of complex mixtures, but once again, the method development remains a long procedure, with injections on single cartridges before finding the best column set-up. Another issue is the fixed hardware. No flexibility is possible in term of column dimensions.

In order to avoid the complexity of the previous methods, the idea was to develop a simple hardware packed with combined materials. Several publications describe the use of such mixed-bed columns, for example for the separation of proteins on mixed ion-exchangers [26] or for the separation of test solutes with mixed RP and IEC resins [27]. Even if the results in research laboratory was promising, no commercial product could

---

<sup>4</sup>For example, RP and HILIC methods are highly orthogonal to each other.

be successfully launched because of the packing issues. Because of the polar and charge differences between the beads, packing was not homogeneous neither reproducible.

True mixed mode phases implicate the presence of either mixed ligands on the surface of the particles, the synthesis of a mixed-mode ligand directly on the particles, or the addition of a single ligand on the silica surface (see Figure 1.3.3).

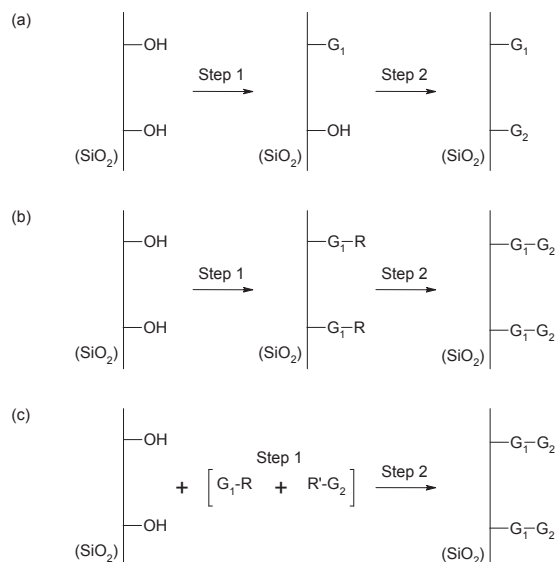


Figure 1.3.3.: Synthesis of different types of mixed-mode materials: mixed ligands (a), on-site ligand synthesis (b), and mixed-mode ligand addition (c).

Group G<sub>1</sub> is responsible for first mode, and G<sub>2</sub> for second mode.

Synthesis (b) and (c): A third step can be necessary before any other addition or reaction in order to add a linker to the surface.

Reproducibility of the synthesis of mixed-mode material using mixed ligands technology is quite unachievable if ligands have to be evenly distributed on whole particles (see Figure 1.3.3, a). One solution consists in using the remaining OH groups as G<sub>2</sub> groups. Hancock and Sparrow introduced therefore the term “mixed-mode chromatography” for the first time in 1981 [28]. They separated proteins and peptides on a C<sub>18</sub> material with low ligand density and without endcapping. The secondary interactions, which have to be minimized for standard materials, is there used to obtain different selectivities<sup>5</sup>. A second option consists in adding each group on different parts of the particles. Typically, one ligand is added inside the pores, and the other one is grafted onto the outer surface. This is known as restricted access material: the specific selectivity is depending on the size of the molecules [29, 30].

Further development consisted in adding a polar functionality at the surface, and grafting an hydrophobic ligand onto it in order to build up a more stable layer to enhance pH working range and to increase life time of columns (see Figure 1.3.3, b and c). Other advantages of such phases are reduced peak-tailing, and enhanced selectivity [31]. These materials are known as polar-embedded phases. However, even if synthesis principle is

<sup>5</sup>However, this use of the intrinsic silica drawbacks does not lead to reproducible methods. As a contrary, during the preparation of modern mixed-mode materials, uncontrolled secondary interactions have to be minimized, for example through endcapping, in order to enable the development of robust chromatographic methods and processes.

### 3. Improving the selectivity

similar to mixed-mode ones, main objective remains reverse-phase chromatography. We cannot therefore speak of mixed-mode materials due to their usage.

Dedicated mixed-mode phases can be synthesized through b and c techniques (see Figure 1.3.3). Both SIELC Technologies and Dionex launched mixed-mode columns in the past years (respectively Primesep and Acclaim Mixed-Mode series) [32, 33]. Further details on it can also be found in the introduction of Chapters 3 and 5 in Part II <sup>6</sup>. Several applications were developed in the last years using labor-made materials [35, 36, 37] or commercially available columns [38, 39, 40] <sup>7</sup>. Further development at Dionex lead to a three-mode material known as Acclaim Trinity [41]. Two applications were already published using this material, but method development feasibility remains questionable [42, 43].

The mixed-mode material developed in this study was described and patented in 2008 [44]. This initial work was the basis for further development that we performed. In a first part, we improved the synthesis in order to allow easier and cheaper preparation in larger scale. In a second time, we packed this material and used it for developing several analytical methods.

---

<sup>6</sup>Aim of this work is the development of analytical resins. However, in the last years, a few mixed-mode products were launched on the market of preparative purification, like Capto adhere and Capto MMC from GE Healthcare [34]. Main expected advantage would be the possibility to reduce the number of purification steps in down-stream processing.

<sup>7</sup>Those are only a few examples of applications. A large number of publications was already published using this technique. However, only two suppliers of analytical columns for mixed-mode chromatography can be found. Those are the two cited above, SIELC Technology and Dionex.



## **Part II.**

# **Synthesis of mixed-mode stationary phases**



# 1. Statistical optimization of the silylation reaction of a mercaptosilane with silanol groups on the surface of silica gel

## 1.1. Introduction

Thiol-modified silica is often used as an intermediate product for further synthesis of modified stationary phases for chromatography, amongst others chiral phases [45, 46], or mixed-mode reversed phase - weak anion exchange phases [47]. Many other uses of thiol-modified silica itself can be found in the literature, for example to analyze the very low amount of germanium in natural waters [48] or to recover homogeneous catalysts from the reaction mixture by interaction between the thiol-group and the metal center of the catalyst [49].

The study of mercaptopropylsilanes as silylating agent has started in the late seventies and the first synthesis route involved 3-mercaptopropyltrimethoxysilane (MPTMS) heated with silica gel at reflux for 1h in the presence of hexane and water [50]. Less common is the synthesis by heating the silica gel with MPTMS in DMF with imidazole as a catalyst at 100°C for 20h [51]. The surface coverage obtained by the latter was between 1.30  $\mu\text{mol}/\text{m}^2$  and 1.64  $\mu\text{mol}/\text{m}^2$ . In most of the publications, the general synthetic method consisted in slurrying the silica gel in toluene before adding MPTMS. Heating this suspension for 24 h leads to surface coverage between 1.8  $\mu\text{mol}/\text{m}^2$  and 2.6  $\mu\text{mol}/\text{m}^2$  [52]. Further study showed that adding a tertiary amine such as pyridine or its derivatives enhances the surface coverage. Heated at 80°C for 28 h, the mercaptopropylsilica reaches a surface coverage of 2.0  $\mu\text{mol}/\text{m}^2$  [53]. Lewis et al. obtained a surface coverage of 4.37  $\mu\text{mol}/\text{m}^2$  by heating the suspension at 115°C for 24 h [54]. Different studies with other small silanes such as trimethylchlorosilane which had been performed over the years show that surface coverage up to the average limit of 4.5 - 4.75  $\mu\text{mol}/\text{m}^2$  is principally possible [55, 56]. Scully et al. have performed an optimization of the silylation reaction with mercaptopropylsilane in supercritical carbon dioxide leading to surface coverage up to 6.0  $\mu\text{mol}/\text{m}^2$  [57]. Different conditions were used to synthesize thiol-modified stationary phases, but were seldom optimized by a systematic approach in which temperature and reaction time were both investigated over a wide range.

In our study, a design of experiment (DoE) has therefore been performed in order to optimize the reaction time and temperature. Commonly, silylations with tri-functional silanes induce much more silanol activity than di-functional silanes without improving the surface coverage. Tri-functional silanes yield an average linkage number of 1.6 which means that the third reactive leaving group of the silane (usually a methoxy substituent) remains always unreacted and enhances the silanol activity of the resulting silica gel [58, 59]. In preliminary experiments for this study, we compared the surface coverage after reaction of silica gel with MPTMS and with 3-mercaptopropyldimethoxymethylsilane (MPDMS) in toluene with addition of dimethylaminopyridine at different temperatures and reaction time. It turned out that the surface coverage is exactly the same for both reagents at given temperature, time and concentrations. The following study has there-

## 1. Statistical optimization of the silylation reaction

fore been performed with MPDMMS (see Fig. 2.1.1), because it was deemed beneficial in terms of its chromatographic performance and stability. Selected thiol-modified particles were characterized by solid-state NMR.

## 1.2. Experimental

### 1.2.1. Chemicals

Pharmprep Si 100 10  $\mu\text{m}$  was obtained from Merck, Darmstadt, Germany. The material exhibits a surface area of 300  $\text{m}^2/\text{g}$  and a specific pore volume of 0.81  $\text{ml/g}$ . Dimethylaminopyridine (DMAP) was obtained from AcrosOrganics (Geel, Belgium), MPDMMS, hexamethyldisilazane (HMDS) and n-propylmethyldimethoxysilane (PMDMS) from ABCR (Karlsruhe, Germany), azobisisobutyronitrile (AIBN), 1-tetradecene, toluene and 25% sulfuric acid from Merck, 2,2'-dipyridyl disulfide (DPDS) and 2-mercaptoethanol from Sigma-Aldrich (Steinheim, Germany). The chemicals were used without any further purification.

Mobile phases for chromatography were prepared from HPLC grade solvents (i.e. water, acetonitrile and methanol LiChrosolv from Merck) and analytical grade formic acid (FA) and trifluoroacetic acid (TFA) (Merck).

### 1.2.2. Silica pretreatment

The raw silica has been rehydroxylated in 25% sulfuric acid over 20 h at room temperature before being washed with deionized water and dried at 90°C under vacuum for at least 24 h until weight constancy.

### 1.2.3. Instrumentation

The elemental analyzes were carried out on an elemental (Hanau, Germany) vario EL III analyzer. The Berendsen- de Galan's equation was used to calculate the surface coverages (see Part I, Paragraph 2.4, and [15]) and the results are given in Table 2.1.1.

The chromatographic experiments were carried out on a VWR (Darmstadt, Germany) Hitachi LaChrom Elite HPLC system (three channels pump L-2130 with degasser, autosampler L-2200, oven L-2300, diode array detection (DAD) system L-2455). The data were processed using the Agilent (Waldbronn, Germany) EZChrom Elite version 3.21 software.

For the liquid chromatography - mass spectrometry (LC-MS) analysis, the chromatographic system was an Agilent 1100 Series equipment comprising a pump, a degasser, a column oven and an autosampler. MS-detection has been performed on a Bruker Daltonics (Bremen, Germany) Esquire 3000 plus device and the data were processed using the Esquire Control version 5.0 software from the same company.

### 1.2.4. Determination of reactive surface thiols

This method is based on a thiol-disulfide exchange reaction in acetonitrile with DPDS as reagent and HPLC-UV analysis of pyridyl-2-thione which is liberated in equimolar amounts to reactive sulfhydryls as validated and described in detail in ref. [60]. 2-Mercaptoethanol solutions in acetonitrile served as standards for calibration and the detailed procedure can be found elsewhere [60]. The experimental results along with the corresponding elemental analysis data are given in Table 2.1.1.

Material number	Temperature (°C)	Reaction time (h)	%C	%S	Surface coverage S (μmol/m <sup>2</sup> )		Reactive sulfhydryls by DPDS (μmol/m <sup>2</sup> )
					Low <sup>a</sup>	High <sup>b</sup>	
1	45	3.0	1.8	1.0	1.08	1.09	1.09
2		8.0	2.8	1.5	1.66	1.68	1.70
3		25.0	4.0	2.5	2.87	2.95	2.88
4	60	3.0	4.0	2.2	2.50	2.56	2.54
5		5.5	4.4	2.4	2.75	2.82	2.81
6		8.0	4.6	2.6	3.00	3.09	3.10
7		15.0	5.0	3.0	3.52	3.64	3.56
8		25.0	5.8	3.4	4.06	4.21	4.15
9	75	3.0	4.7	2.6	3.00	3.09	3.09
10		5.5	5.0	2.9	3.39	3.50	3.35
11		8.0	5.2	3.0	3.52	3.64	3.64
12		15.0	5.6	3.4	4.06	4.21	4.20
13		25.0	5.7	3.5	4.20	4.36	4.35
14	90	3.0	4.0	2.4	2.75	2.82	2.77
15		5.5	4.2	2.6	3.00	3.09	3.01
16		8.0	4.5	2.8	3.26	3.36	3.25
17		15.0	4.8	3.1	3.66	3.78	3.76
18		25.0	5.3	3.5	4.20	4.36	4.31
19	105	3.0	3.8	2.3	2.62	2.69	2.71
20		8.0	4.5	2.7	3.13	3.22	3.21
21		25.0	5.4	3.5	4.20	4.36	4.30

Table 2.1.1.: Characteristics of synthesized thiol-modified particles.

<sup>a</sup>As calculated for di-functionally bonded silane from %S of elemental analysis data.<sup>b</sup>As calculated for mono-functionally bonded silane from %S of elemental analysis data.

## 1. Statistical optimization of the silylation reaction

### 1.2.5. Reaction procedure

The apparatus was flushed with nitrogen flux during the whole reaction process. The silica was slurried in toluene and heated at reflux for 1.5 h using a Dean-Stark trap in order to remove the water adsorbed on the silica surface. After cooling down to room temperature, the reagents were added and the suspension was heated up to the temperature given by the DoE. After the predetermined time of reaction, the silica was directly washed with toluene and subsequently agitated three times in methanol at reflux for 20 min.

For preparation of mercaptopropyl-modified silica, the reagent was MPDMMS and for preparation of propyl-modified silica, PMDMS was used as reagent. For endcapping, the reagent was HMDS.

For C14-S-C3-e-silica, mercaptosilica ( $2.16 \mu\text{mol}/\text{m}^2$ ) endcapped with HMDS ( $0.32 \mu\text{mol}/\text{m}^2$ ) was heated at  $60^\circ\text{C}$  in presence of AIBN and 1-tetradecene in methanol before being washed as before.

### 1.2.6. Statistical method

The different surface modification experiments were planned using the statistical software Cornerstone (Applied Materials, Santa Clara, U.S.A.). This DoE software was used to calculate the 3-dimensional model whereas the Origin software (OriginLab, Northampton, U.S.A.) has been used to plot the 3D arch-shape plane of the surface coverage and to perform the 2-dimensional modeling on the whole range.

### 1.2.7. NMR spectroscopy

The NMR experiments were performed on Bruker AV 400 MHz spectrometer.

All spectra were acquired at 300 K. XWINNMR software version 3.5 (Bruker) was used for data acquisition and processing. 4 mm zirconia spinners were used.

The solid-state CP-MAS NMR experiments were performed at 400.13 MHz using TPPM-25 and a spinning rate of 5000 Hz. A total of 1188 data points were recorded and 4k scans were performed. The relaxation delay was set at 5 s and the contact time was set at 7 ms.

### 1.2.8. Conditions for the chromatographic test

The chromatographic conditions were optimized to achieve base-line separation for the test mixture (see below) in less than 10 minutes. The mobile phase was composed of a mixture of 0.1% TFA in water (A) and 0.1% TFA in methanol (B). A linear gradient was run from 20 to 80% B in 6 min followed by elution with 80% B for another 4 min. The temperature was maintained at  $25^\circ\text{C}$  and the flow rate was 1 ml/min. 10  $\mu\text{l}$  of the analyte mixture (benzylamine: 0.76  $\mu\text{l}/\text{ml}$ , caffeine: 0.26  $\mu\text{l}/\text{ml}$  and acetophenone: 0.98  $\mu\text{l}/\text{ml}$  dissolved in methanol-water-TFA 50:50:0.1% v/v/v) were injected. Peaks were detected at 212 nm. The methanol in the sample solution appeared as a solution peak and was used as  $t_0$  marker.

### 1.2.9. Stress treatment

Before each chromatographic test run using the method described above the column was rinsed with an acidic eluent (methanol-water 80:20 v/v, pH 2.0 by addition of TFA) at a flow rate of 1 ml/min for 2 h at  $45^\circ\text{C}$ .

### 1.2.10. LC-MS bleeding test

The bleeding of the material was tested with a linear gradient of acetonitrile, 0.1% FA (A) and water, 0.1% FA (B) from 10 to 90% A in 5 min, 90% A for 3 min and 10% A for 10 min. The column was kept at RT and the flow rate was 1 ml/min. The ionization was carried out in electrospray ionization in the positive ion mode (ESI(+) mode) and the extracted ion chromatogram was monitored. The column was flushed between each measurement run with 2-propanol, 0.1% FA for 60 min at a flow rate of 0.5 ml/min.

## 1.3. Results and discussion

### 1.3.1. Optimization of the silylation reaction

A systematic approach employing a DoE strategy was utilized to optimize the surface coverage of the thiol-modified particles. The parameter range for optimization was fixed from 3 h to 25 h for the reaction time and for 45°C to 105°C for the reaction temperature. After a first screening, we found that the response was quadratic between 45°C and 90°C. To reduce the number of experiments without losing information, a full factorial DoE was automatically generated between 60°C and 90°C. The individual experiments and the results in terms of carbon and sulfur contents, surface coverages and active sulfhydryl concentrations are given in Table 2.1.1.

The statistical software was then used to derive the coefficients for the subsequent model which describes the surface coverage (SC) as analyzed by elemental analysis and the DPDS test for active sulfhydryls, respectively, in dependence of temperature (T) and reaction time (t):

$$SC = A + B \times t + C \times T + D \times t^2 + E \times T^2 + F \times t \times T \quad (1.3.1)$$

where A, B, C, D, E and F are the coefficients of the model. A second order polynomial model has been chosen in order to study the impact of time and temperature. Interrelation of both effects (last term in the equation) has been excluded from the model after statistical fitting because of lack of statistical significance.

While the model fitted well to the experimental data in the T range between 45 and 90°C, larger deviations between experimental and calculated surface coverages were observed between 90°C and 105°C. Therefore, only the temperature range up to 90°C was considered in the three-dimensional (3D) model (Fig. 2.1.1). The estimated coefficients and their standard errors are given in Table 2.1.2 whereas adjusted R<sup>2</sup>, root mean square error (RMS-error) and residual degrees of freedom (n) are given in the caption of Fig. 2.1.1.

As can be seen from Fig. 2.1.1, the surface coverage is increasing slowly as a function of reaction time at any temperature before reaching a pseudo-plateau above 20 h. We can also conclude that the surface coverage cannot exceed the value of SC = 4.4 µmol/m<sup>2</sup> with the given reaction mixture, which corresponds to the maximum surface coverage. This value for the maximal surface coverage is in agreement with literature data [55, 61].

Concerning temperature dependency, a few aspects are noteworthy to be briefly outlined here. Below 45°C, barely any reaction could be observed. Between 45°C and 75°C, surface coverage increases whereas above 75°C, the surface coverage slowly decreases.

Further surface coverage data have been monitored at higher temperatures not covered by the depicted temperature range of Fig. 2.1.1 (i.e. 90°C-105°C). Combining these data with the former allows to derive information on the entire available reaction temperature range (i.e. 45°C-105°C). It is seen that above 90°C, surface coverage slowly reaches a plateau, which means that within high temperature range (i.e. 90°C-105°C), the amount

1. Statistical optimization of the silylation reaction

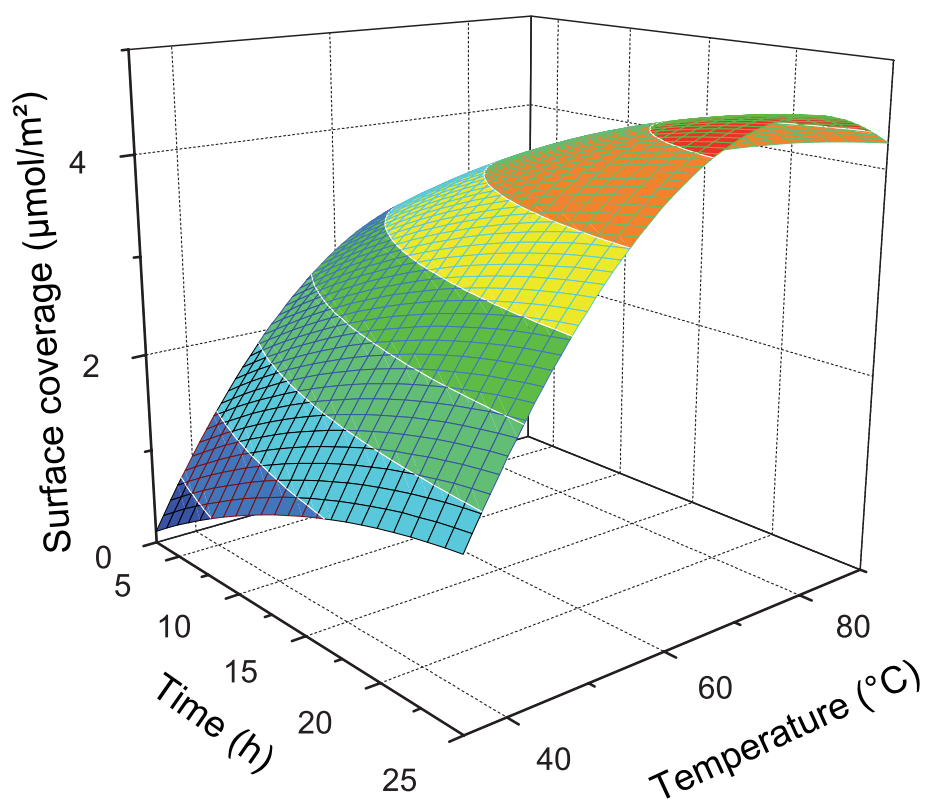


Figure 2.1.1.: Response surface illustrating the dependency of surface coverage (SC) on reaction time and temperature  $SC = A + B \times t + C \times T + D \times t^2 + E \times T^2 + F \times t \times T$  with adj.  $R^2=0.987976$ , RMS-error=0.09498 and  $n=13$ . For coefficient values and standard errors, see Table 2.1.2.



Coefficient	Coefficient value	Std. Error	P-value <sup>a</sup>
A	-810.355	0.468337	2.34E-10
B	0.281336	0.0141719	4.17E-11
C	0.127002	0.0142075	6.50E-07
D	-0.0018327	0.000102393	1.53E-10
E	-0.00204266	0.000487857	1.06E-03
F	-	-	0.07

Table 2.1.2.: Estimated coefficient values, standard errors and significance after model fitting from surface coverage determined for active sulfhydryls.

<sup>a</sup> P-value of <0.05 was set as statistical significance criterion for a term to be kept in model.

of silane bonded to the surface remains constant. A maximum in the surface coverage at 75°C could be read out, which corresponds to the overall temperature optimum at any reaction time.

Overall, performing a design of experiment to optimize the reaction conditions is a very efficient tool to obtain optimum surface coverage on silica material. Moreover, it is easier to find the most reasonable compromise in terms of high surface coverage, low energy input and short reaction time. For example, a surface coverage of more than 3  $\mu\text{mol}/\text{m}^2$  can be reached after only 3 h of reaction at 75°C, whereas the same degree of coverage at 105°C is obtained only after 6 h.

### 1.3.2. Characterization of thiol-modified particles by <sup>29</sup>Si CP-MAS NMR

Solid-state NMR was shown to be a powerful tool to investigate the bonding chemistry of modified silica surfaces [62, 63, 64, 65]. Herein, we utilized <sup>29</sup>Si crosspolarization-magic angle spinning NMR (<sup>29</sup>Si CP-MAS NMR) to derive information on the type of linkages that do exist on the surface of the modified particles. Representative <sup>29</sup>Si CP-MAS NMR spectra of two distinct materials, prepared by silylation at 60°C for 3h (top) and 90°C for 3 h (bottom) are shown in Fig. 2.1.2. Corresponding spectra of materials prepared with different reaction temperature and reaction time do feature similar signal patterns with slightly distinct signal intensities which are given for four different modified particles in Table 2.1.2.

As can be seen from Fig. 2.1.2 two different groups of signals are found in the spectra. The signals denoted with Q<sup>2</sup>, Q<sup>3</sup>, Q<sup>4</sup> come from the silica matrix and correspond to geminal silanol (- 92 ppm, Q<sup>2</sup>), isolated silanol (- 100 ppm, Q<sup>3</sup>) and siloxane (- 109 ppm, Q<sup>4</sup>), respectively. Further, there are signals that can be assigned to the surface-bonded silanes. The signal at - 8 ppm (D<sup>1</sup>) corresponds to the mono-functionally bonded silane. The signal denoted with D<sup>2</sup> is the difunctionally bonded silane species. Although the individual signals are partly overlapping, Gaussian decomposition allows to derive their individual signal intensities (Table 2.1.3). While the <sup>29</sup>Si CP-MAS NMR spectra suggest a similar surface structure of the materials prepared by different temperatures and reaction times, a closer inspection of the individual signal intensities may provide some minor peculiarities of the distinct materials. While the D<sup>1</sup>/D<sup>2</sup> ratio remained largely constant with higher temperatures and longer reaction time, some minor though characteristic alterations in relative signal intensities of the Q-species were noticed. Q<sup>2</sup> intensity diminishes and the Q<sup>4</sup> signal intensity grows relative to the Q<sup>3</sup> signal when the reaction temperature is raised from 60 over 75 to 90°C, as indicated by the Q<sup>3</sup>/Q<sup>4</sup> ratio. Both geminal and isolated

## 1. Statistical optimization of the silylation reaction

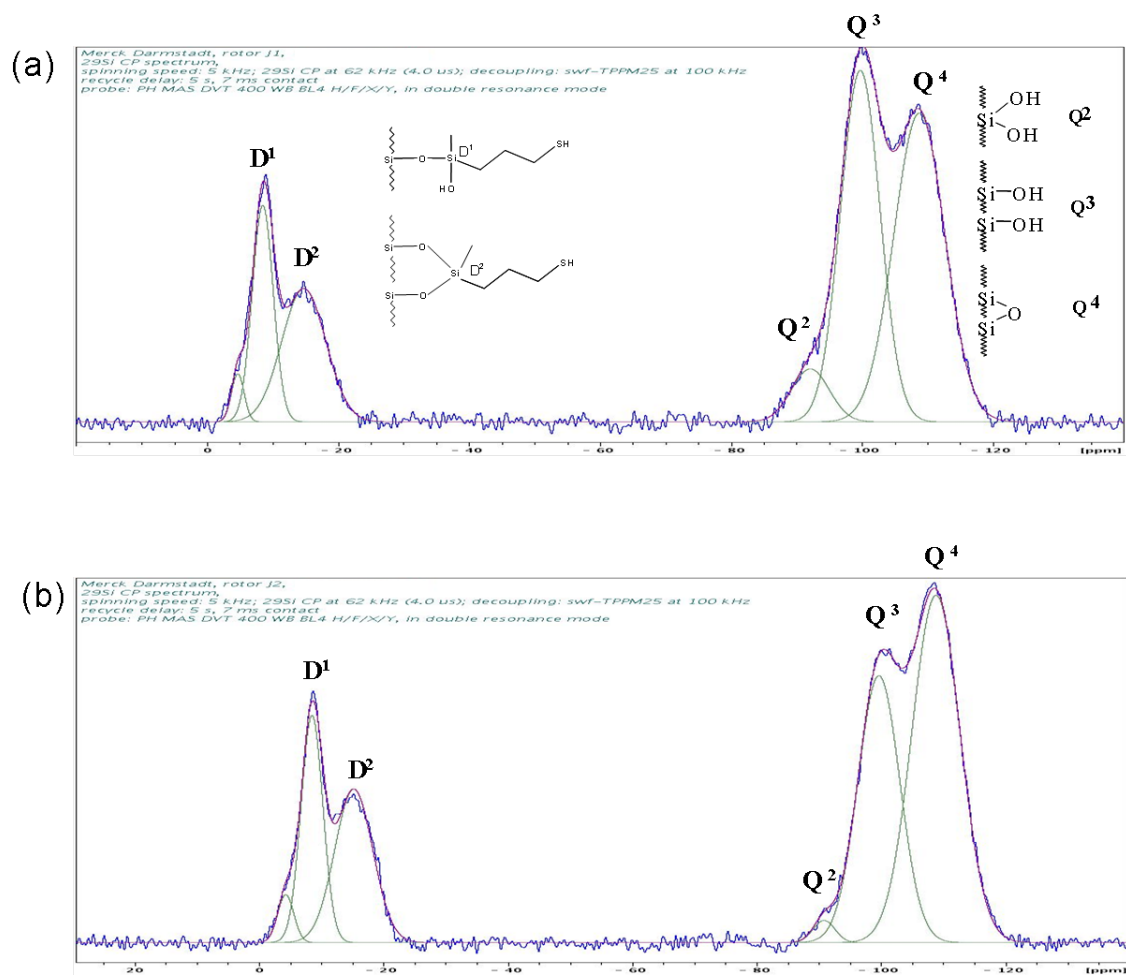


Figure 2.1.2.:  $^{29}\text{Si}$  CP-MAS NMR spectra of thiopropyl-modified silica particles prepared from 3-mercaptopropyldimethoxymethylsilane at 60°C (a) and 90°C (b) for 3 h.

Conditions	SC ( $\mu\text{mol}/\text{m}^2$ )	$D^1 + D^2$ -4 and -8 ppm	$D^3 + D^4$ -15 ppm	$Q^2$ -92 ppm	$Q^3$ , -100 ppm	$Q^4$ , -109 ppm	$\frac{D^1+D^2}{Q^3+Q^4}$	$\frac{Q^3}{Q^4}$
60°C for 3 h	2.54	12	14	4	33	37	0.86	0.89
75°C for 3 h	3.09	14	14	1	31	40	0.97	0.78
90°C for 3 h	2.77	14	15	1	28	42	0.99	0.67
90°C for 5.5 h	3.01	16	16	1	31	36	0.98	0.86

Table 2.1.3.: Relative signal intensities (%) as obtained by deconvolution of the  $^{29}\text{Si}$  CP-MAS NMR spectra.

silanol concentrations are reduced in favor of siloxane species. This would indicate a slightly lower silanol activity of the latter materials. However, when the reaction time is increased (90°C, for 5.5h), the  $Q^3/Q^4$  ratio drops back to the initial value which is hard to explain.

It is worth noting, however, that the present materials which are prepared from the difunctional silane appear to have less silanol groups stemming from the bonded silane as compared to previously described thiol-modified silica particles obtained from trifunctional silanes which showed  $T^1$ ,  $T^2$ ,  $T^3$  signals corresponding to monofunctionally bonded species ( $T^1$ ) leading to two free silanols, difunctionally bonded silane with single silanol ( $T^2$ ) and surface crosslinked siloxane ( $T^3$ ) [57, 66].  $T^1$  and  $T^2$  signals together are strongly dominating with regards to intensities as compared to  $T^3$  which may be regarded as tantamount to a higher silanol number. Hence, the present developed silica particles may also be expected to be more stable than corresponding former particles prepared from trifunctional silanes, because the number of silanol groups ( $D^1 + D^2$ ) remaining on the surface of our material (prepared from dialkoxy silane) is lower than that of material prepared from trialkoxy silane ( $T^1 + T^2$ ).

### 1.3.3. Chromatographic characterization of the mercaptopropyl-modified silica particles

In order to characterize the effect of the modification on the silica surface, we developed a specific chromatographic test. The purpose of this test was to describe chromatographically the SH activity and the silanol activity. Five different chromatographic materials have been synthesized with well-defined thiol modifications (see Table 2.1.4).

After having tested about twenty different compounds, we were able to pick out three analytes, which may be adequate to probe the two parameters, i.e. SH activity and silanol activity (see Fig. 2.1.3).

When the SH activity of considered material is increasing (material 1, 2 and 3 for example), the  $\alpha_{\text{caffeine/benzylamine}}$  value is decreasing. Decrease of silanol activity (material 2, 4 and 3) leads to an increase of the  $\alpha_{\text{acetophenone/caffeine}}$  value. These two parameters are regarded as sufficient to describe the material in a first approach: SH activity to verify the extent of surface modification and silanol activity to assess chromatographically the existence of residual silanols and their accessibility. This test is employed hereafter for testing the stability of the prepared bonded particles.

# 1. Statistical optimization of the silylation reaction

# Material	Modification	%C	%S	SH (DPDS) <sup>a</sup> ( $\mu\text{mol}/\text{m}^2$ )	Added ligand	Surface coverage of added ligand ( $\mu\text{mol}/\text{m}^2$ )	
						%C	DPDS <sup>a</sup>
1	Propyl (C3)	3.1	<0.3	-	Propyl	1.87/2.33 <sup>b</sup>	-
2	Mercaptopropyl LC <sup>c</sup> (S-C3)	3.2	1.9	2.16	Mercaptopropyl	1.93/2.41 <sup>b</sup>	2.16
3	Mercaptopropyl HC <sup>d</sup> (S-C3)	6.0	3.5	4.39	Mercaptopropyl	3.92/4.89 <sup>b</sup>	4.39
4	Mercaptopropyl LC + endcapping (S-C3-e)	3.5	1.9	2.15	TMS-endcapper	0.32 <sup>f</sup>	-
5	Mercaptopropyl LC + endcapping + C14 (C14-S-C3-e)	11.9	2.0	1.14	C14-residue	n.d. <sup>h</sup>	1.11 <sup>i</sup>

Table 2.1.4.: Modified silica materials with different surface modifications and corresponding surface coverages employed for the development of a specific chromatographic test.

<sup>a</sup>Reactive sulfhydryls by DPDS.

<sup>b</sup>Calculated for mono-functionally (low) and di-functionally (high) bonded silane from %C of elemental analysis data.

<sup>c</sup>LC: low coverage.

<sup>d</sup>HC: high coverage.

<sup>e</sup>Synthesized from material # 2.

<sup>f</sup> Surface coverage from %C of elemental analysis calculated by extended Berendsen-de Galan's equation [16].

<sup>g</sup> Synthesized from material # 4.

<sup>h</sup> n.d., not determined.

<sup>i</sup> Calculated from the difference of reactive sulfhydryls before and after adding C14 chain.

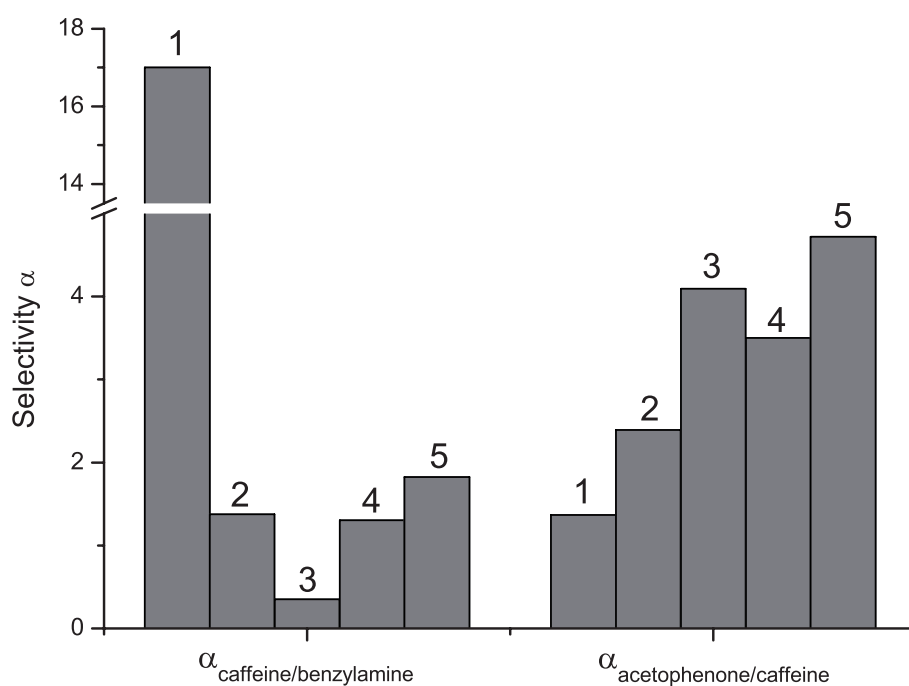


Figure 2.1.3.: SH activity ( $\alpha_{\text{caffeine/benzylamine}}$ ) and silanol activity ( $\alpha_{\text{acetophenone/caffeine}}$ ) of five different modified silica particles: 1, propyl; 2, mercaptopropyl LC; 3, mercaptopropyl HC; 4, mercaptopropyl LC + endcapping; 5, C14-S-C3 LC (see Table 2.1.3). In order to facilitate the readability of the figure the y-axis has been discontinued between 5 and 13.5.

Note that decreasing  $\alpha_{\text{caffeine/benzylamine}}$  values indicates increasing SH activities, while increasing  $\alpha_{\text{acetophenone/caffeine}}$  values are indicative for decreasing silanol activities.

### 1. Statistical optimization of the silylation reaction

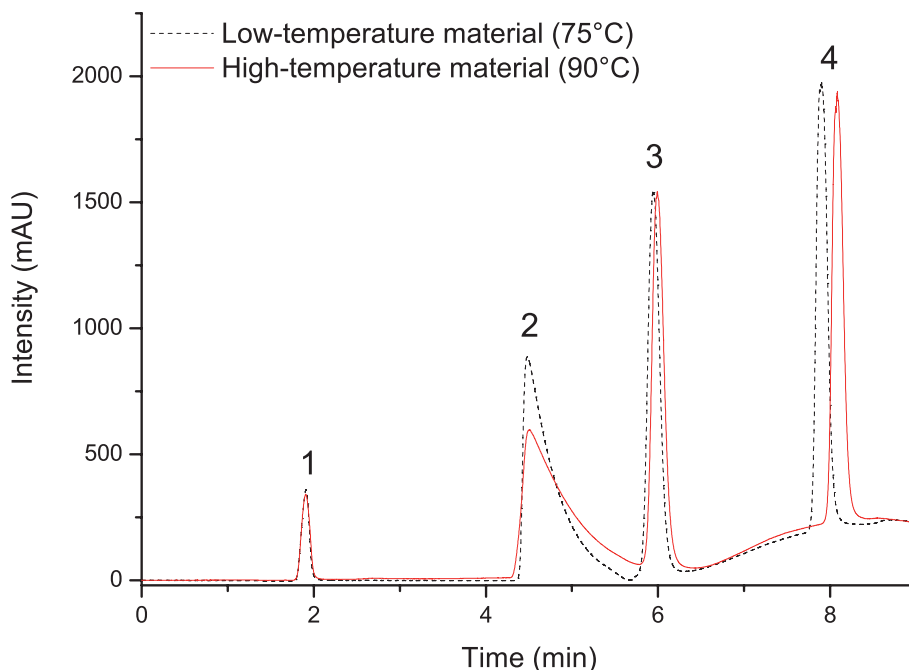


Figure 2.1.4.: Chromatograms of the developed HPLC test for columns packed with mercaptopropyl modified silica material synthesized at two different temperatures (75°C/4 h and 90°C/8 h) (see Section 1.2.5).

*Conditions:* water, 0.1 % TFA (A) and methanol, 0.1 % TFA (B), 20 % to 80 % B in 6 min, 80 % B for 4 min, temperature = 25°C, flow rate = 1 ml/min, injection volume = 10  $\mu$ l, detection at 212 nm.

*Analytes:* 1, methanol; 2, benzylamine; 3, caffeine; 4, acetophenone.

#### 1.3.4. Stability of the phases

The surface coverage of a silica material is only one of the important parameters to look at during an optimization. The corresponding stability of the material has also to be considered and must be investigated. The chromatographic test described in the experimental part (see section 1.2.8) was therefore established and the stability was studied by submitting the material to the specific stress treatment described in the section 1.2.9. Two different materials were selected for the test: the first one was a material synthesized at 4 h/75°C and the second one at 8 h/90°C. The surface coverage of both materials was 3.2  $\mu$ mol/m<sup>2</sup>. By selecting materials with the same surface coverage yet obtained at distinct reaction conditions for the chromatographic characterization and stress test, respectively, it was hoped that some information on possibly existing differences of the surface structure of the bonding can be derived. The chromatograms that were furnished for the two materials are illustrated in Fig. 2.1.4. The retention times for each analyte were essentially identical except for acetophenone for which a minor retention time shift was observed.

Next, the stabilities of these two mercaptopropyl bonded silica particles were examined (see Fig. 2.1.5). Both materials were submitted to the stress treatment described in the section 1.2.9. The reproducibility of the test has been investigated by replicating each measurement two times.

At the beginning the material synthesized by a 75°C reaction shows a faster increase in  $\alpha_{\text{caffeine/benzylamine}}$  being indicative for a stronger loss of thiol-ligand and thus of SH activity when compared to the material synthesized by a 90°C reaction. After a few cycles

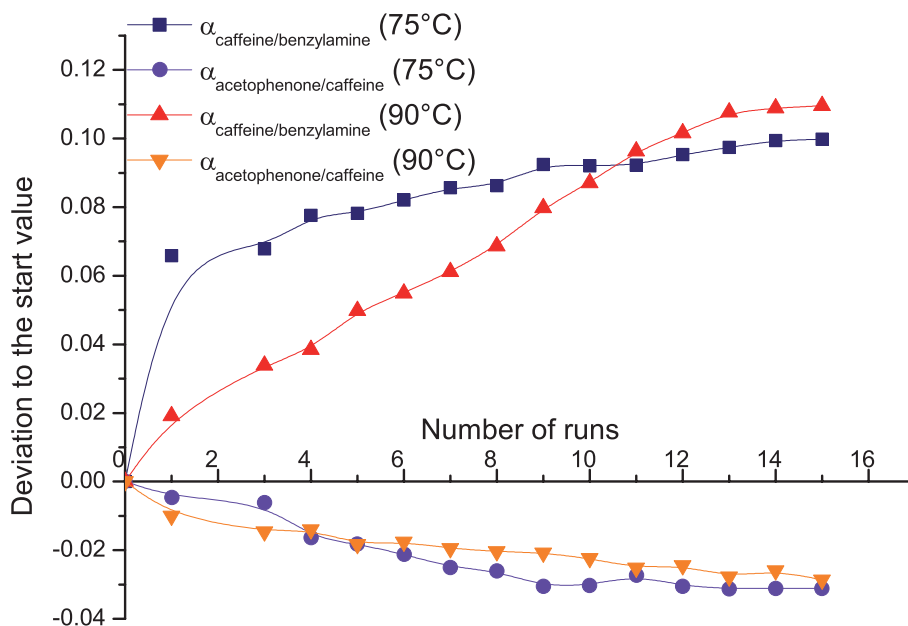


Figure 2.1.5.: Change of SH and silanol activity for two materials synthesized at two different temperatures in the course of the stability testing. SH activity:  $\alpha_{\text{caffeine/benzylamine}}$  and silanol activity:  $\alpha_{\text{acetophenone/caffeine}}$ . The deviation  $\Delta\alpha$  has been calculated as follows:  $\Delta\alpha = (\alpha - \alpha_0)/\alpha_0$  where  $\alpha$  is the selectivity at the respective run and  $\alpha_0$  the selectivity at the first measurement after packing the column. Note, that both  $\alpha$ -values are inversely proportional to the real activity.

of stress treatment, however, the SH loss leveled off and became largely comparable to the that of the 90°C material. On the other hand, the increase in silanol activity as indicated by a drop of  $\alpha_{\text{acetophenone/caffeine}}$  became less significant with increasing number of stress cycles and was largely comparable for the two tested materials.

It is striking that the optimum-temperature material exhibits a strong loss of SH activity during the first stress run whereas its silanol activity is not increasing proportionally. That is due to the fact that the first loss of SH activity involves probably the cleavage of mono-functionally bonded silane groups, the unreacted methoxy-groups of which were already hydrolyzed, so that one silane-silanol is replaced by one surface silanol. As a comparison, the evolution of the SH and silanol activity for the high-temperature material is much more equivalent.

To ensure these results, both materials were tested for bleeding by LC-MS as described in section 1.2.10. Submitted to acidic conditions, the silanes moieties are partially cleaved off the surface. The dihydroxy-silane originating from the cleavage of a di-functionally bonded silane is not ionizable in the positive mode whereas the hydroxy-methoxy-silane resulting from the cleavage of a mono-functionally bonded silane is ionizable and therefore easily detectable by ESI/MS detection ( $m/z=166.32$  Da). As can be seen from the plot of the amount of this fragment against the number of stress runs, an almost three times higher amount of mono-bonded silane is released from the optimum-temperature material compared to the high-temperature material (see Fig. 2.1.6).

As a conclusion for the stability study we can assume that material prepared at lower temperature does not necessarily exhibit lower stability because after excessive initial washing the change in thiol- and silanol activity is largely equivalent for the two materials.

## 1. Statistical optimization of the silylation reaction

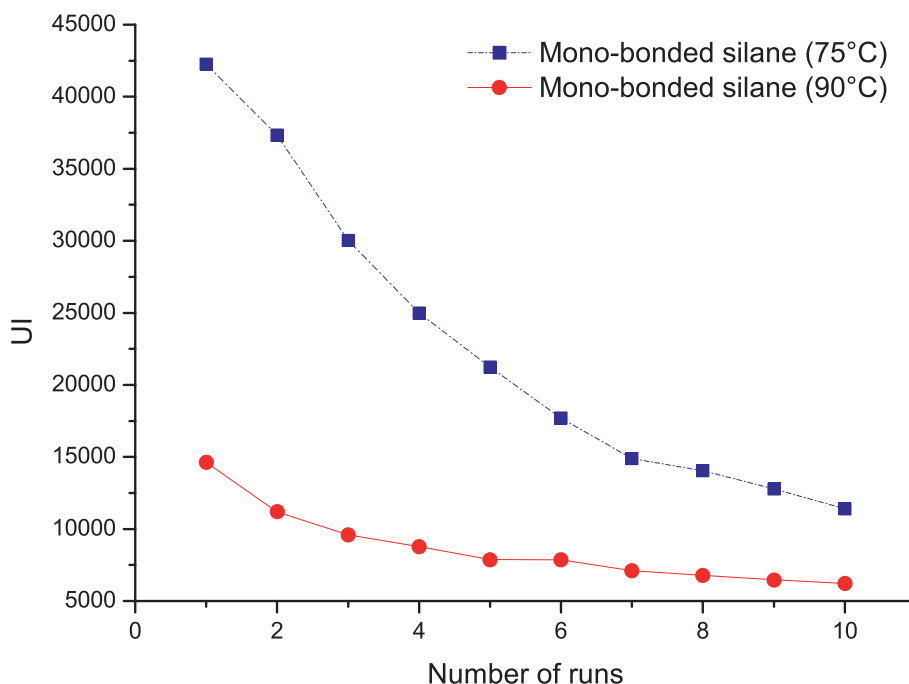


Figure 2.1.6.: Evolution of the  $m/z = 166.32$  Da response during ESI/MS runs (acetonitrile, 0.1% FA (A) and water, 0.1% FA (B) from 10 to 90% A in 5 min, 90% A for 3min and 10% A for 10 min, column kept at RT and flow rate 1 ml/min) monitored between washing runs (2-isopropanol, 0.1% FA for 60 min, 0.5 ml/min). The  $m/z$  value corresponds to the cleavage of mono-bonded silane (3-mercaptopropylmethoxymethylsilanol) from the silica surface.

Initially, however, the low-temperature (75°C) material shows a stronger bleeding of mono-functionally bonded silane and in general, the silanol activity of the low-temperature material seems to be slightly higher.

### 1.4. Concluding remarks

A new approach to thiol-modified silica particles is presented in which the formerly common trifunctional 3-mercaptopropyltrimethoxysilane was replaced by the difunctional 3-mercaptopropyldimethoxy-methylsilane. Such difunctional silane should lead to more stable bonding as compared to the trifunctional one. A systematic optimization of the silylation reaction by a design of experiment with reaction temperature and time was employed which revealed that optimal surface coverage can be accomplished at 75°C. Materials with same surface coverage but prepared at 75°C and 90°C, respectively, revealed differences in initial bleeding behavior. The low temperature material showed a stronger loss of ligand especially at the beginning of the stress test and a stronger monofunctional silane bleeding than the high temperature material. After a while the change in both thiol and silanol activity became insignificant for both of the materials suggesting that they show similar stability after excessive initial washings. The slightly higher silanol activity of material obtained at a lower reaction temperature could be seen as a disadvantage of the method, but a proper endcapping of the material should prevent the resulting material from a problematic silanol activity. The  $^{29}\text{Si}$  CP-MAS NMR spectra acquired for low and high temperature materials were qualitatively the same and showed only minute differences



regarding relative signal intensities of the individual Si species. While the ratio of D<sup>1</sup> to D<sup>2</sup> (monofunctional to difunctional silane bonding) was relatively constant for different temperature materials, the <sup>29</sup>Si CP-MAS NMR spectra suggested that the surface silanol activity should be lower for the high-temperature material as indicated by a decrease of the Q<sup>2</sup>-to-Q<sup>3</sup> ratio (ratio of isolated silanols versus siloxanes).

The fact that the optimum in terms of surface coverage is observed at 75°C has some other benefits. It should facilitate the on-column modification, because working at 75°C is much easier than running an in-line modification equipment at the reflux of toluene. This point is perhaps not so important for particulate material but in the case of monolithic columns, the implementation of an in-line modification becomes a relevant challenge.

Finally, this study has shown the usefulness of performing a statistical design of experiment for the optimization of chemical reactions, even if the reaction is already well described in the literature.



## 2. Improvement of the stability of mixed-mode phases: endcapping and hydrolysis

### 2.1. Introduction

As mentioned in Chapter 1, only about three third of the reactive silanol groups on the silica surface react with the mercaptopropylsilane. The residual silanol groups on RP material lead to secondary interactions such as peak broadening and lower performances for basic analytes [67]. The lowering of these effects can be obtained by endcapping, which consists in adding a small, very reactive silane to cap the residual silanol groups on the silica surface. The smallest silanes bear only methyl groups plus a reactive one. Trimethylsilylation of silica sorbent is mostly achieved with trimethylchlorosilane (TMCS) or hexamethyldisilazane (HMDS). Some studies indicated better surface coverage through reaction with a mixture of those two reagents [68]. Modification of silica surface with (dimethylamino)trimethylsilane was already investigated, but not for endcapping purposes [69].

The last step of the synthesis of RP-WAX material will consist in adding an hydrocarbon chain bearing an aminoquinuclidine group (see Chapter 3). It is already well established that aminoalkyl groups can hydrogen bond with silanol groups from the silica surface. Due to this property, aminosilane can graft horizontally as well as vertically, which reduces the surface coverage and interaction of amino groups with surface silanol weakens the bonding [70]. Thus, stability of the chromatographic amino material is rather low and efficiency of the endcapping is even more important.

Furthermore, the addition of dimethoxysilane described in Chapter 1 lead to a mix on the surface of mono-functionally bonded and di-functionally bonded silane. In the case of mono-functionally bonded silane, if no hydrolysis takes place during the manufacturing process, some methoxy groups are added to the surface along with the mercaptopropyl ones. A slow-going hydrolysis of those methoxy groups into silanol groups is then potentially taking place during chromatographic runs in aqueous conditions, leading to less stable material. Investigation of the LC-MS bleeding of the columns prepared without hydrolysis during the manufacturing process confirmed such phenomenon (see Figure 2.2.1) and implicates to implement an hydrolysis process prior to the endcapping step.

### 2.2. Experimental

#### 2.2.1. Chemicals

Purospher STAR Si 5  $\mu\text{m}$  was obtained from Merck (Darmstadt, Germany). The material exhibits a surface area of 300  $\text{m}^2/\text{g}$ .

Hexamethyldisilazane (HMDS), trimethylchlorosilane (TMCS), 3-mercaptopropyl-dimethoxymethylsilane (MPDMMS) were obtained from ABCR (Karlsruhe, Germany),

## 2. Improvement of the stability of mixed-mode phases: endcapping and hydrolysis

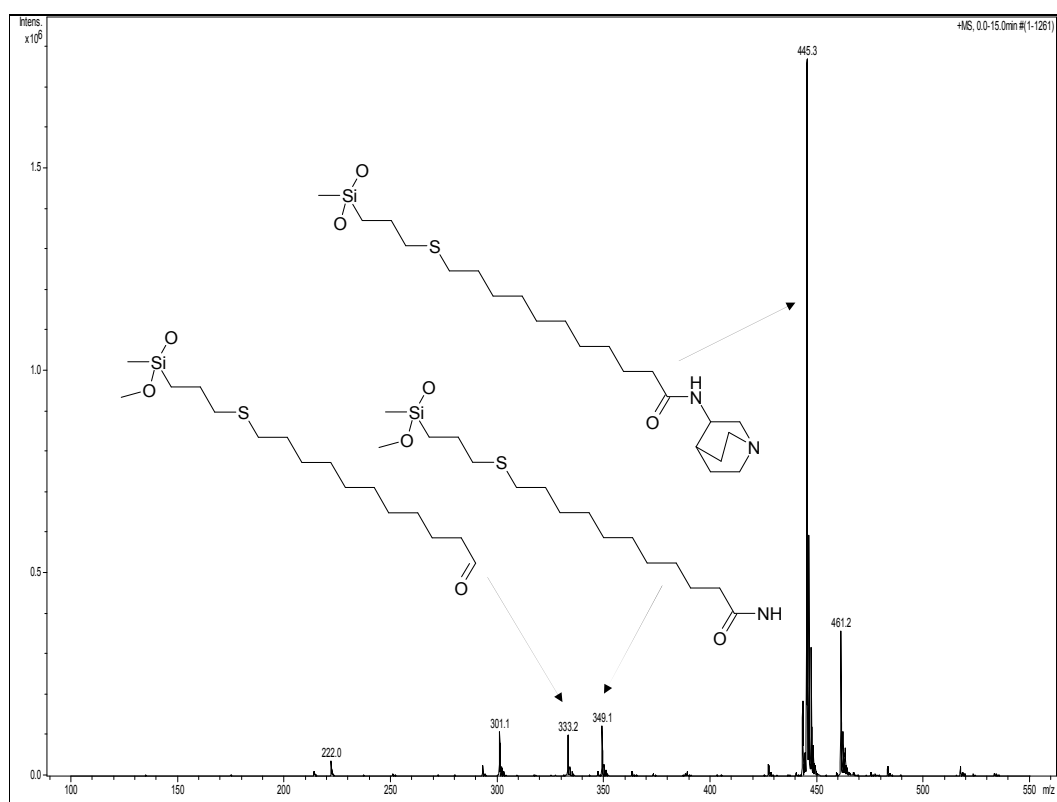


Figure 2.2.1.: Investigation of the bleeding of the RP-WAX material through LC-MS.

Conditions: water, 0.1% formic acid (A) and acetonitrile, 0.1 % formic acid (B), 10 % to 90 % B in 5 min, 90 % B for 3 min, 10 % B for 7 min (reconditioning), temperature = RT, flow rate = 0.5ml/min, detection MS in ESI(+) mode with target mass = 445 m/z.

(diethylamino)trimethylsilane (ATMS) from Bucher (Germany), dimethylaminopyridine (DMAP) from AcrosOrganics (Geel, Belgium), and toluene and methanol from Merck.

The chemicals were used without any further purification.

### 2.2.2. Instrumentation

The elemental analyzes were carried out on an elementar (Hanau, Germany) vario EL III analyzer. The Berendsen- de Galan's and Sandoval's equations were respectively used to calculate the surface coverages of the silane addition and of the endcapping step (see Part I, Chapter 2.4).

Reproducibility studies were performed on a Radleys (Saffron Walden, United Kingdom) Tornado IS6 + Carousel 6, a 6-post reaction station equipped with heating plate, nitrogen inlet, water cooling and mechanical agitator. Positions in Table 2.2.3 are given by the position of the reactor flask on the station.

### 2.2.3. Reaction procedure

Optimized procedure described in chapter 1 was used to prepare mercaptopropyl modified silica.

The apparatus was flushed with nitrogen flux during the whole reaction process. The silica was slurried in toluene and heated at reflux for 1.5 h using a Dean-Stark trap in order to remove the water adsorbed on the silica surface. After cooling down to room temperature, MPDMMS and DMAP were added and the suspension was heated up to 75°C. After 20 h, the silica was directly washed with toluene and subsequently agitated three times in methanol at reflux for 20 min. For the last part of the study, we also tried two further methods: the first one consisted in slurrying the modified silica in methanol - water (1:1, v/v) over night before the methanol washing step. For the second one, we used the same procedure as before but we exchanged the solvent from toluene to water - sodium acetate for the reaction.

Same basis technical procedure was followed for endcapping. Reagents given in Table 2.2.1 were added to the suspension and reaction temperature and time were set up to the value given in caption of Tables 2.2.2, 2.2.3 and 2.2.4. Modified silica was washed as above.

## 2.3. Results and discussion

### 2.3.1. Improvement of the endcapping reaction

First step to set up the endcapping reaction consisted in testing different small silanes in conditions described in section 2.2.3 in order to determine which silane could be reactive enough and appropriate for production. The data from elemental analyzes as well as the surface coverages calculated from the Sandoval equation are given in Table 2.2.1. The best endcapping coverage for HMDS/TMCS mixtures was achieved in 2:1 proportion, which confirms the results obtained by Sweeley et al. [68].

Endcapping performed with ATMS in same conditions exhibits however higher surface coverage. Kanan et al. showed that amine groups can catalyze the reaction between silanol groups from the surface and the silane molecules to form siloxane bonds [71]. Same phenomenon could occur in our case and lead to better endcapping through intra-molecular and inter-molecular catalysis. Furthermore, ATMS is affordable and can be bought from

## 2. Improvement of the stability of mixed-mode phases: endcapping and hydrolysis

Material number	Mercaptopropyl addition		Endcapping modification		
	%C	Carbon surface coverage <sup>a</sup> ( $\mu\text{mol}/\text{m}^2$ )	Endcapper	%C	Carbon surface coverage ( $\mu\text{mol}/\text{m}^2$ )
1			HMDS	5.8	0.12
2			TMCS	5.9	0.24
3	5.7	3.57 - 4.46	HMDS / TMCS 1:1	6.0	0.36
4			HMDS / TMCS 2:1	6.2	0.60
5			ATMS	6.5	0.96

Table 2.2.1.: Characteristics of endcapped thiol-modified particles from 4 different end-capper compositions at 120°C for 20 h.

<sup>a</sup>To understand the carbon surface coverage range, see Table 2.1.4, note *b*.

Endcapping temperature (°C)	%C	Carbon surface coverage ( $\mu\text{mol}/\text{m}^2$ )
120	6.5	0.96
75	6.5	0.96

Table 2.2.2.: Comparison of endcapping surface coverage with ATMS at 120°C and 75°C for 20 h.

several suppliers, which is essential for implementation on larger scale. ATMS was then selected as endcapper for the rest of the development and for synthesizing the final product.

Before testing the reproducibility of the endcapping reaction with ATMS, we adapted the temperature to that used for mercaptopropyl modification (see section 2.2.3). Results of tests are shown in Table 2.2.2. As the reaction at 75°C leads to similar surface coverage than the reaction at 120°C, this lower temperature was chosen as standard for the further reproducibility tests.

To ensure applicability of the ATMS reaction for production purposes, last step of the work on endcapping consisted in comparing endcapping value at two different reaction time and in testing the reproducibility. Results are shown in Table 2.2.3. As surface coverages after 6 h of reaction were similar to those after 20 h of reaction, the shorter reaction time was chosen as standard for further production steps.

Position	Reaction time (h)	%C	Carbon surface coverage ( $\mu\text{mol}/\text{m}^2$ )
1	6	6.4	0.84
2	6	6.5	0.96
3	6	6.5	0.96
4	20	6.5	0.96
5	20	6.6	1.09
6	20	6.6	1.09

Table 2.2.3.: Verification of reproducibility of the endcapping reaction after 6 h and 20 h of reaction at 75°C.

### 2.3.2. Improvement of the hydrolysis process prior to the endcapping step

As mentioned beforehand, the endcapping step can be as efficient as possible, it will not improve the stability of the packing if the methoxy groups added along the first step slowly hydrolyze to silanol groups during the chromatographic runs. We investigated therefore

# material	Reaction type	Mercaptopropyl addition		Endcapping modification	
		%C	Carbon surface coverage <sup>a</sup> ( $\mu\text{mol}/\text{m}^2$ )	%C	Carbon surface coverage ( $\mu\text{mol}/\text{m}^2$ )
1	Standard procedure	5.7	3.57 - 4.46	6.8	0.96
2	Hydrolysis	4.1	2.45 - 3.07	5.6	1.69
3	Reaction in water	5.9	3.71 - 4.64	7.0	1.35

Table 2.2.4.: Impact of hydrolysis on both mercaptopropyl and endcapping carbon surface coverage.

<sup>a</sup>To understand the carbon surface coverage range, see Table 2.1.4, note *b*.

the effect of an hydrolysis step between the mercaptopropyl addition and the endcapping (see Table 2.2.4).

Direct hydrolysis of the methoxy groups leads to lower carbon surface coverage for the dimethoxymercaptopropylsilane addition. Similar phenomenon potentially occurs on column during chromatographic runs in the presence of water and / or in acidic conditions. This technique is not suitable because it leads to low concentration of reactive thiol and therefore to low amount of WAX group on the surface. However, the very high carbon surface coverage cannot be linked to the hydrolyzed methoxy groups. Endcapping of the free surface silanols can very well be the reason for such high carbon load.

The second technique consisted in performing the addition of the dimethoxymercaptopropylsilane in water - sodium acetate, in order to directly hydrolyze the methoxy groups during the reaction process. On the one hand, results from the first step indicates slightly higher reactivity in comparison to the standard procedure in toluene, but the surface coverage remains in a similar range. On the other hand, the carbon surface coverage after the endcapping reaction is 40 % higher if the mercaptopropyl addition was performed in aqueous conditions. These results corroborate the need to hydrolyze the methoxy groups in order to improve the endcapping of our material.

## 2.4. Concluding remarks

The predominant use of HMDS and TMCS as endcapping reagent for chromatographic material has been contested. We showed that ATMS constitutes a very suitable alternative molecule to end-cap the remaining free silanol groups on the silica surface after a silane modification because of intra-molecular and inter-molecular catalysis phenomenon. Investigation of reaction time and temperature showed no manifest impact on the efficiency of the endcapping. However, we just verified some time and temperature value in a suitable working range without systematic optimization. The aim of the study was to determine some suitable working conditions for production purposes.

The stability issue, which is well-known for chromatographic sorbents bearing amino-groups, was addressed through a comprehensive approach of the phenomenon occurring on the surface during a chromatographic run. Those observations lead to investigate the effect of hydrolysis on the unreacted methoxy groups. Even if an hydrolysis of the material was not suitable, performing the reaction in aqueous conditions lead to an in-situ hydrolysis of the methoxy groups and therefore to an improvement of the endcapping procedure. The overall stability of the phases was ameliorated by these new procedures (see Part III Chapter 1). The MS results showed however no disappearing of the bleeding phenomenon, only an attenuation of it. Further actions were envisaged for the optimization of the MS stability of the RP-WAX material (see Chapter 4).

## *2. Improvement of the stability of mixed-mode phases: endcapping and hydrolysis*

Both ameliorations of the operating procedure (i.e. dimethoxymercaptopropylsilane addition performed in water and endcapping using (diethylamino)trimethylsilane) were retained for production purposes.



## 3. Synthesis of RP-WAX selector and grafting

### 3.1. Introduction

Mixed-mode chromatography material can be obtained by blending two different types of materials such as RP and ion-exchange material [26]. Preparation of such mixed beds can be delicate, especially the packing process. Other manufacturers are mixing two different ligands on the same particles, for example to obtain restricted access material [29, 30]. In that case, the control of the surface density for each species is rather difficult. Handier technique consists in bringing both RP and ion-exchange parts on a same ligand. Two approaches can be used. The ion-exchanger can be close to the surface and the hydrophobic chain is grafted on the hydrophilic layer. Such columns are commercially available from SIELC [72]. The opposite can also be achieved with the RP chain linked to the surface and the ion-exchanger located on the hydrophobic layer. This brush-type sorbents are commercially available from Dionex [73].

The RP-WAX material we developed corresponds to the latter method. The weak anion exchanger is based on a bicyclic aminoquinuclidine which bears the cationic group. The mixed-mode ligand is synthesized by creating an amide bond with 10-undecenoyl chloride. Its RP chain can then be linked to the thiol of the mercaptopropyl silica through the radical addition of the double bond (see Figure 2.3.1).

The addition of aminoquinuclidine dihydrochloride on an acid chloride was performed recently through a one step reaction in dichloromethane with a strong base like lithium hydroxide [74]. We adapted this method to a more suitable one using tetrahydrofurane as solvent and butyllithium as deprotonating agent (See Paragraph 3.2.3.1). However, after first successful experiments, we observed yield varying from 0 to 0.5 by stable operating conditions and we had therefore to abandon this one pot technique because we were not able to achieve reproducible process.

Another approach for the preparation of aminoquinuclidine derivatives consists in performing the reaction with the free base of the 3-aminoquinuclidine as base material [75]. We encountered the issue that 3-aminoquinuclidine is no longer commercially available as free base but only in its dihydrochloride form. Direct synthesis of the free base cannot be envisaged because of the complexity of the process [76].

The only remaining alternative was to perform a two-step synthesis where the desalting of the 3-aminoquinuclidine dihydrochloride is followed by reaction with the 10-undecenoyl chloride.

The grafting of the RP-WAX ligand on the thiol-modified silica surface is performed through a radical addition initiated by azobisisobutyronitrile [77]. Even if this reaction is well established, another radical initiator was tested because of regulatory and safety issues before evaluating the reproducibility of the process at different parameters.

## 3.2. Experimental

### 3.2.1. Chemicals

Purospher STAR Si 5  $\mu\text{m}$  was obtained from Merck (Darmstadt, Germany). The material exhibits a surface area of 300  $\text{m}^2/\text{g}$ .

2,2'-Azobis-(2,4-dimethyl)valeronitrile (V65) was obtained from Wako (Neuss, Germany), n-butyllithium, 1.6 M in hexane (BuLi) from AcrosOrganics (Geel, Belgium), 10-undecenoyl chloride, 3-aminoquinuclidine dihydrochloride, azobisisobutyronitrile (AIBN), potassium hydroxide (pellets and 2M in methanol), sodium sulfate, dichloromethane, toluene, tetrahydrofuran (THF), propyl acetate, 1 M sodium hydroxide, acetic acid, and methanol from Merck.

The chemicals were used without any further purification.

### 3.2.2. Instrumentation

The elemental analyzes were carried out on an elemental (Hanau, Germany) vario EL III analyzer. The Berendsen- de Galan's and Sandoval's equations were used to calculate the surface coverages (see Part I, Chapter 2.4).

Reproducibility studies were performed on a Radleys (Saffron Walden, United Kingdom) Tornado IS6 + Carousel 6, a 6-post reaction station equipped with heating plate, nitrogen inlet, water cooling and mechanical agitator. Positions in Table 2.3.3 are given by the position of the reactor flask on the station.

### 3.2.3. Synthesis of N-(10-undecenoyl)-3-aminoquinuclidine

#### 3.2.3.1. One-pot preparation of the RP-WAX selector

Closed reactor was dried under vacuum and nitrogen flow was maintained during whole procedure. Dried aminoquinuclidine dihydrochloride was solved in THF before cooling down the mixture to 0°C. BuLi was added drop-wise under absolute water-free conditions. 10-Undecenoyl chloride solved in THF was then added drop-wise, ice bath was removed and agitation was continued during 30 minutes. After evaporation of the solvent, the product is solved in propyl acetate and sodium hydroxide is added for liquid-liquid extraction. Organic phase was then evaporated and a yellowish oil was obtained.

#### 3.2.3.2. Two-step preparation of the RP-WAX selector

##### Free base preparation

Two different procedures were used for free base preparation (see Table 2.3.1):

1. Aminoquinuclidine dihydrochloride was solved in methanol and potassium hydroxide 2M in methanol was added drop-wise to the mixture. Agitation is continued during 3 h before filtration. Filtrate was evaporated and a whitely substance was obtained. Product was directly solved in toluene for storage for Version a. Version b consisted in evaporating the toluene to absolute dryness before solving the obtained product in same solvent again and filtrating the solution before storage.
2. Aminoquinuclidine dihydrochloride was solved in water and potassium hydroxide pellets solved in water was added drop-wise to the mixture. Agitation is continued during 2 h before filtration. Residue was solved in dichloromethane and filtrate was extracted with dichloromethane. Both organic phases were combined before drying

or not on sodium sulfate (see Table 2.3.1). Filtration and evaporation lead to a whitely substance. Product was directly solved in toluene for storage.

### Reaction of free base with undecenoyl chloride

Two different procedures were used for the reaction of the free base with undecenoyl chloride (see Table 2.3.1):

1. The free base solved in toluene from previous step is cooled down to 0°C. Undecenoyl chloride is solved in toluene before being added so slowly that the temperature in the mixture remains under 10°C, which leads to precipitation of a whitely powder. Agitation is continued during 3 h before letting the mixture heating up slowly to room temperature. Product is finally centrifuged and a yellowish gel is obtained.
2. Undecenoyl chloride is solved in toluene before being cooled down to 0°C. The free base solved in toluene from previous step is added so slowly that the temperature in the mixture remains under 10°C, which leads to precipitation of a whitely powder. Agitation is continued during 3 h before letting the mixture heating up slowly to room temperature. Product is finally centrifuged and a yellowish gel is obtained.

#### 3.2.3.3. <sup>1</sup>H-NMR of the RP-WAX selector

<sup>1</sup>H NMR-spectra were monitored at 400 MHz in DMSO. Proton numbering is given in figure 2.3.1.

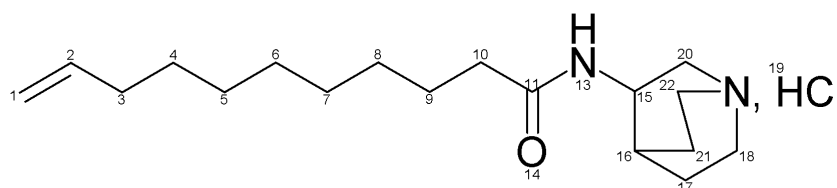


Figure 2.3.1.: Structure of the RP-WAX selector and proton numbering.

$\delta_H$ (ppm) 1.20 - 1.58 (m, 12 H, 6  $\text{CH}_2$ , 4 to 9), 1.71 - 1.82 (m, 5H, 1  $\text{CH}$  and 2  $\text{CH}_2$ , 17, 16 and 21), 2.02 (q, 2 H,  $=\text{CH}-\text{CH}_2$ , 3), 2.11 (t, 2 H,  $\text{CH}_2-\text{CO}$ , 10), 2.87 - 2.99 (m, 4 H, 2  $\text{CH}_2$ , 18 and 22), 3.16 (dd, 2 H,  $\text{CH}_2-\text{N}, \text{HCl}$ , 20), 3.58 (ddd, 1 H,  $\text{NH}-\text{CH}$ , 15), 4.92 (q, 2 H,  $\text{CH}_2=\text{CH}$ , 1), 5.72 (qt, 1 H,  $\text{CH}_2=\text{CH}$ , 2), 8.38 (d, 1 H,  $\text{CO}-\text{NH}$ , 13)

A molecular modelisation of the selector linked to the spacer was also performed using a Schrödinger software (Jaguar application) in order to have a spatial representation of the selector (see Figure 2.3.2).

#### 3.2.4. Grafting of RP-WAX selector to thiol-modified endcapped silica

Mercaptopropyl modified and endcapped silica is prepared as presented in Chapters 1 and 2. It is slurried in methanol in the presence of 2 mmol acetic acid per gram of silica. The N-(10-undecenoyl)-3-aminoquinuclidine is added to the mixture under nitrogen flow before adding the radical initiator AIBN or V65 (see Table 2.3.1). After heating at 65°C for desired time, the product is filtrated, washed three times with hot methanol, and dried at RT under vacuum until weight consistency.

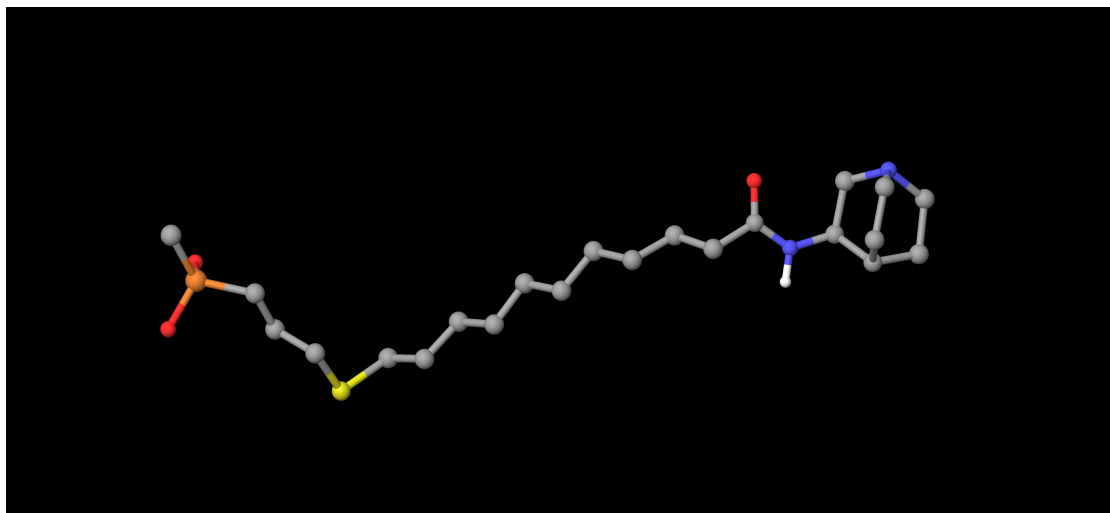


Figure 2.3.2.: Spatial representation of the RP-WAX selector.

To determine the surface coverage of the selector on the silica surface, elemental analysis was performed. The Berendsen - de Galan and Sandoval equations are only valuable for the two first additions. Therefore we adapted the Berendsen - de Galan for the first addition to nitrogen (see Chapter 2.3).

## 3.3. Results and discussion

### 3.3.1. Synthesis of mixed-mode RP-WAX selector

The most significant results for the synthesis of the RP-WAX selector are given in Table 2.3.1. First of all, the product - solvent value is related to the product behavior. The N-(10-undecenoyl)-3-aminoquinuclidine hydrochloride combines a hydrophilic group and a lipophilic chain, which inhibits crystallization. Liquid - liquid extraction is also impossible because the molecule is amphiphile and leads to emulsions. Rheology of the product prevented also any filtration approach. The only possibility remained centrifugation: the product was obtained as a gel in toluene with a molar purity under 50 % (which corresponds to a mass purity of over 90 %). Only two species were present in solution, product and solvent, which was not disruptive for the grafting step (see Paragraph 3.3.2).

Looking at the second step of the reaction at first points out that the first method for the reaction with undecenoyl chloride remained unsuccessful (see Material 1, Table 2.3.1). The aim of this reaction consists in performing an hydrochloration of the product in parallel with the synthesis in order to obtain a solid salt as product. During the first reaction, the hydrochloride formed by the reaction reacts immediately with the free base in excess in the reactor, leading to an inhibition of the reactant. In order to avoid such phenomenon, we exchanged the reactants between reactor and dropping funnel which lead to a precipitation of the desired product. The free base preparation remained determinant for the overall purity and yield.

At first, 3-aminoquinuclidine dihydrochloride was dissolved in methanol before precipitating potassium chloride with potassium hydroxide. After evaporation of the solvent and dissolution in toluene, direct reaction lead to low yield (Material 2). Adding an evaporation and filtration step after obtention of the free base lead to a better yield (Material 3). As water is a little miscible with toluene, some potassium chloride solved in the mixture

Material number	Free base preparation <sup>a</sup>	Drying	Reaction with undecenoyl chloride <sup>b</sup>	Product - Solvent <sup>c</sup>	Yield <sup>d</sup>
1	1	<i>n.n.</i> <sup>e</sup>	1	-	-
2	1a	<i>n.n.</i> <sup>e</sup>	2	0.25	0.23
3	1b	<i>n.n.</i> <sup>e</sup>	2	0.33	0.29
4	2	yes	2	0.31	0.04
5	2	no	2	0.40	0.42

Table 2.3.1.: Synthesis of N-(10-undecenoyl)-3-aminoquinuclidine

<sup>a</sup>Reaction procedures corresponding to free base preparation number are given in section 3.2.3.2.

<sup>b</sup>Reaction procedures corresponding to reaction with undecenoyl chloride are given in section 3.2.3.2.

<sup>c</sup>Product – Solvent =  $\frac{I_{\text{Product}}}{I_{\text{Product}} + I_{\text{Solvent}}}$  where  $I_{\text{Product}}$  and  $I_{\text{Solvent}}$  are calculated from NMR integration value.

<sup>d</sup>Yield =  $\frac{m_{\text{total}} \times \text{Purity}}{m_{\text{theoretical}}}$  where  $m_{\text{total}}$  is the total amount of product after centrifugation and  $m_{\text{theoretical}}$  the theoretical calculated mass of product.

<sup>e</sup>*n.n.* stands for *not necessary*, when no water extraction was performed during free base preparation.

disturbed the following reaction. The yield remains very low for both materials and this method is not up-scalable because of the low solubility of the 3-aminoquinuclidine dihydrochloride in methanol (~ 20 g/L). The Material 4 was the first attempt to perform the free base preparation in water before extracting it with dichloromethane but almost no product was obtained. It seems, that sodium sulfate used as drying agent after the liquid - liquid extraction is fixing the free base and that the drying step is the reason for the very low yield. For Material 5, we directly evaporated the dichloromethane and remaining water was removed by azeotropic evaporation with toluene. The product obtained by this method was used for derivatizing the silica material prepared previously.

### 3.3.2. Selector grafting on mercaptopropyl modified silica surface

The addition of N-(10-undecenoyl)-3-aminoquinuclidine on thiol-modified silica occurs in methanol in the presence of AIBN. The impact of the temperature on the reaction is rather limited. Below 60°C, the reaction is very slow and above 65°C, reactivity remains constant. Therefore we fixed the reaction temperature at 65°C for the whole study.

No statistical optimization was performed but reducing the reaction time from 20 hours to 6 hours slightly reduces the ligand surface coverage (see Table 2.3.2). In order to avoid some regulatory issues, changing the radical initiator was envisaged. The use of V65 instead of AIBN brought not only some organization advantages but the surface coverage after a 6-hour reaction with V65 is similar to the ligand density after a 20-hour reaction in the presence of AIBN. We therefore chose V65 as radical initiator and we fixed the reaction time at 6 hours.

In order to verify the reproducibility of the reaction, some tests were performed at different number of equivalents (see Table 2.3.3). Below one equivalent, a significant diminution of the ligand density is observed. At 1.2 equivalents, reaction reached a sufficient value and is very reproducible. Further increase of the number of equivalents leads to a loss in reproducibility without meaningful improvement of the nitrogen surface coverage. The ligand density for the final RP-WAX material was therefore fixed at ca. 0.60  $\mu\text{mol}/\text{m}^2$ .

### 3. Synthesis of RP-WAX selector and grafting

Material number	Initiator	Reaction time	%N	Nitrogen surface coverage ( $\mu\text{mol}/\text{m}^2$ )
1	AIBN	20 h	0.50	0.61
2	AIBN	6 h	0.45	0.54
3	V65	6 h	0.51	0.62

Table 2.3.2.: Evaluation of the reaction time and of the radical initiator on the grafting reaction performed at 65°C.

Position	Number of equivalents	%N	Nitrogen surface coverage ( $\mu\text{mol}/\text{m}^2$ )
1	0.6	0.41	0.49
2	0.6	0.43	0.52
3	1.2	0.50	0.61
4	1.2	0.51	0.62
5	2.4	0.50	0.61
6	2.4	0.56	0.68

Table 2.3.3.: Evaluation of the impact of the RP-WAX selector amount and of the reproducibility of the grafting reaction.

### 3.4. Concluding remarks

A reproducible method was developed for the two-step synthesis of N-(10-undecenoyl)-3-aminoquinuclidine from 10-undecenoyl chloride and 3-aminoquinuclidine. Even if a single-step method was already established and worked in laboratory-scale, we chose a more reproducible, easier to implement procedure for production purposes. The selector could not be crystallized or filtrated. The liquid side products were therefore eliminated by centrifugation, which is not the best method at larger scales. Further study should be performed in order to get rid of the centrifugation.

Addition of the RP-WAX selector on the mercaptopropyl-modified silica was improved. Every parameter of the reactions was adjusted in order to be easily scaled-up to a production scale. Batches up to 500 g were already successfully prepared. Further scaling-up tests should be performed in order to attain production batches of 1 kg to 5 kg.

## 4. Improvement of the stability of mixed-mode phases: hypercrosslinking

### 4.1. Introduction

The notion of hypercrosslinking first appeared in the 1970's [78]. This term describes a method which should enhance the stability of the material through an increase of the number of covalent bonds between the surface and the ligands [79]. The first applications of such increase of the density of the bonding were achieved before the name "hypercrosslinking" was created. The first resins were ion exchange sorbents formed by condensation of formaldehyde with phenolic or aromatic amine derivatives [80]. Such ion exchange materials were further developed during the 20th century and were used extensively for water treatment, which became even more important over the years. In the field of HPLC, hypercrosslinking was first applied to the synthesis of polystyrenes particles to overcome the stability issues of silica material and to develop restricted access material [81].

Kirkland et al. started using such techniques in the late 1980's with the use of poly-functional silanes [82]. In this study, acid stability was improved by using poly-functional silanes which might react with the surface or among each others. Tsubokawa et al. chose similar approach by using highly branched polymer [83]. Their use of polyamidoamine dendrimer gave a stable dispersion of ultra-fine silica and it was not intended to increase the stability of the silica material, but the chemical techniques on the silica surface should have similar effects.

However, the cross-linking density on the surface remains low. Further improvement were achieved through performing a two-step hypercrosslinking by oligostyrene formation on the silica surface. Trammel et al. used a Friedel-Crafts crosslinking of chloromethyl-aromatic silanes with aromatic crosslinker (see Figure 2.4.1) [84].

Further improvement were achieved in the last years, but the basis of the hypercrosslinking remained mainly based on styrene derivates [79]. This technique was not only used to obtain reversed phase material but derivatizing on the styrene groups lead to sulfonate-modified mixed-mode reversed phase [85]. However, all the hypercrosslinking techniques

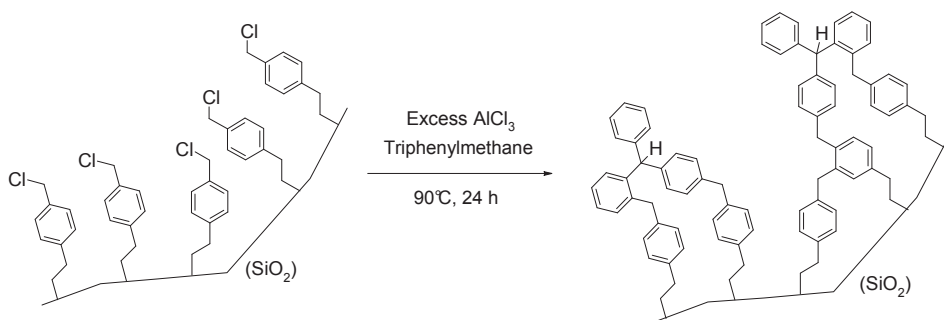


Figure 2.4.1.: Scheme of the Friedel-Craft hypercrosslinking developed by Trammel et al.

#### 4. Improvement of the stability of mixed-mode phases: hypercrosslinking

based on styrene derivatives, which lead to decrease of the pore size and to  $\Pi$ – $\Pi$  interactions.

Our work consisted in finding and evaluating different hypercrosslinking techniques, such as the use of polydentate silanes or hypercrosslinking of monodentate silanes with poly-functional molecules. One limitation for this study was the necessity to keep some free reactive thiol groups on the silica surface after the hypercrosslinking in order to graft the RP-WAX selector.

## 4.2. Experimental

### 4.2.1. Chemicals

Pharmprep Si 5  $\mu\text{m}$  was obtained from Merck (Darmstadt, Germany). The material exhibits a surface area of 300  $\text{m}^2/\text{g}$ .

3-Mercaptopropyltrimethoxymethylsilane (MPDMMS), trivinylchlorosilane (TVCS), vinyltrimethoxysilane (VTMS), 1,2,4-trivinylcyclohexane (TVCH), trimethyltrivinyltrisiloxane (TMTVS) and tetramethyltetravinyltetracyclosiloxane (TeMTeVTeS) were obtained from ABCR (Karlsruhe, Germany), (diethylamino)trimethylsilane (ATMS) from Bucher (Germany), dimethylaminopyridine (DMAP), imidazole and pentaerythritol tetrakis(mercaptoacetate) (PTMA) from AcrosOrganics (Geel, Belgium), and 1,3-propanedithiol, azobisisobutyronitrile (AIBN), acetic acid, hydrochloric acid, *p*-toluenesulfonic acid (PTSA), toluene and methanol from Merck.

The chemicals were used without any further purification.

### 4.2.2. Instrumentation

The elemental analyzes were carried out on an elemental (Hanau, Germany) vario EL III analyzer. The Berendsen - de Galan and Sandoval equations were used to calculate the surface coverages (see Part I, Chapter 2.4).

Some evaluations of reaction conditions were performed on a Radleys (Saffron Walden, United Kingdom) Tornado IS6 + Carousel 6, a 6-post reaction station equipped with heating plate, nitrogen inlet, water cooling and mechanical agitator. Material number in Table 2.4.3 are given by the position of the reactor flask on the station.

### 4.2.3. Reaction procedures

#### 4.2.3.1. Hypercrosslinking on tridentate silane

Addition of TVCS was performed on an apparatus flushed with nitrogen flux during the whole reaction process. The silica was slurried in toluene and heated at reflux for 1.5 h using a Dean-Stark trap in order to remove the water adsorbed on the silica surface. After cooling down to room temperature, TVCS and imidazole were added to the suspension and the mixture was heated for 20 h at 120°C.

Endcapping was performed by same procedure with parameters from chapter 2 (i.e. reagent ATMS, temperature 75°C and reaction time 6 h).

Hypercrosslinking on TVCS was then performed in methanol by addition of 1,3-propanedithiol and AIBN before heating at 65°C for 20 h.

Addition of RP-WAX selector (see chapter 3) was performed in methanol - acetic acid by addition of the RP-WAX selector and AIBN before heating at 65°C for 20 h.

For all reaction, the silica was washed with toluene and subsequently agitated three times in methanol at reflux for 20 min.



#### 4.2.3.2. Hypercrosslinking on monodentate silane

Optimized procedure described in chapter 1 was used to prepare mercaptopropyl modified silica. The apparatus was flushed with nitrogen flux during the whole reaction process. The silica was slurried in toluene and heated at reflux for 1.5 h using a Dean-Stark trap in order to remove the water adsorbed on the silica surface. After cooling down to room temperature, MPDMMS and DMAP were added and the suspension was heated up to 75°C.

Same procedure was used to add VTMS on the silica surface.

Endcapping was performed with same procedure as the mercaptopropyl addition with parameters from chapter 2 (i.e. reagent ATMS, temperature 75°C and reaction time 6 h).

Addition of pre-hypercrosslinkers TVCH and TMTVTS or hypercrosslinker pentaerythritol and 1,3-propanedithiol were then performed in methanol by addition of the corresponding reagent and AIBN before heating at 65°C for 20 h.

Addition of RP-WAX selector (see chapter 3) was performed in methanol - acetic acid by addition of the RP-WAX selector and AIBN before heating at 65°C for 20 h.

For all reaction, the silica was washed with toluene and subsequently agitated three times in methanol at reflux for 20 min.

#### 4.2.3.3. Hypercrosslinking on cyclosiloxane

The apparatus was flushed with nitrogen flux during the whole reaction process. Two different solvents were used: heptane and toluene. When the reaction was performed in heptane, the silica was only slurried in it before adding the reagents. When the reaction was performed in toluene, the silica was slurried and heated at reflux for 1.5 h using a Dean-Stark trap in order to remove the water adsorbed on the silica surface. After addition of the TeMTeVTeS and the acidic modifier given in Table 2.4.3, the mixture was agitated for fixed time ( $t_{RT}$ ) at room temperature before being heated for a different fixed time ( $t_{reflux}$ ) at reflux of the considered solvent.

Hypercrosslinking was then performed in methanol by addition of 1,3-propanedithiol and AIBN before heating at 65°C for 20 h.

Addition of RP-WAX selector (see chapter 3) was performed in methanol - acetic acid by addition of the RP-WAX selector and AIBN before heating at 65°C for 20 h.

For all reaction, the silica was washed with toluene and subsequently agitated three times in methanol at reflux for 20 min.

### 4.3. Results and discussion

#### 4.3.1. Hypercrosslinking on tridentate silane

The reaction scheme of the hypercrosslinking on the silica surface using a tridentate trivinylchlorosilane is given in Figure 2.4.2. The materials 1 to 4 described in Table 2.4.1 underwent exactly the same procedure, i.e. same amount of reagents, same temperature and reaction time. The surface coverage after the TVCS addition is already varying from 3.5 to 5  $\mu\text{mol}/\text{m}^2$ . The upper values are probably due to polymerization of the trivinylsilane on the silica surface. The lack of endcapping for material 3 confirms this inter-molecular bonding of the trivinyle group: the high ligand density after the first step leads to a shielding of the surface and therefore to a deactivation of the silanol groups. The further reaction steps for material 3 worked nice with high hypercrosslinking with propanedithiol and very high selector density in comparison with not hypercrosslinked

#### 4. Improvement of the stability of mixed-mode phases: hypercrosslinking

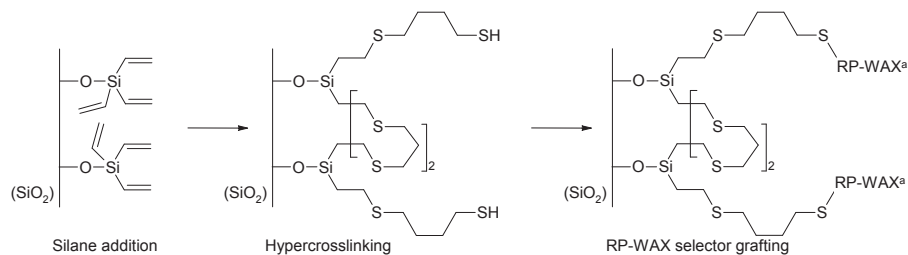


Figure 2.4.2.: Reaction scheme of the hypercrosslinking on the silica surface through a tridentate silane.

<sup>a</sup>RP-WAX group stands for the RP-WAX selector presented in the last chapter.

material (see Chapter 3). However, this method is too unreproducible to be implemented in production.

##### 4.3.2. Hypercrosslinking on monodentate silane

As we assume that the polymerization of the trivinylsilane on the silica surface presented in the last paragraph is the problematic step, mono-dentate silane was grafted to the surface silanols in a first step. An hypercrosslinker (i.e. trivinylcyclohexane or trimethoxytrivinylsiloxane) added after the endcapping can react with a multi-functional molecule (number of functionalities per molecule  $\geq 3$ ) on which the RP-WAX selector can be grafted during the last reaction or RP-WAX can directly react after the endcapping on a suitable hypercrosslinker (see Figure 2.4.3).

Table 2.4.2 contains the results for each step of the reaction described in Figure 2.4.3. The addition of mercaptopropylsilane gives similar values to those given in previous chapters. The value for material 1 is lower than expected because of the use of another silica material with less surface coverage. The addition of the mono-vinyl silane gives a slightly higher surface coverage, probably due to the better accessibility of the molecule to the silanol groups (steric effect). The following steps give high amount of hypercrosslinker fixed on the surface. Only the last step was totally unsuccessful, no RP-WAX selector grafted to the surface.

We can reasonably assume that each step increases the number of possible bonds between the brushes. During the penultimate step, a complete polymerization over the surface leads to high amounts of carbon and / or sulfur but no more reactive thiol groups remain accessible for the undecenoyl-aminoquinuclidine. Tentative to breach some disulfide bonds did not brought any measurable amelioration.

##### 4.3.3. Hypercrosslinking on cyclosiloxane

Hypercrosslinking on tridentate silane as well as reaction of a monodentate silane with a multi-functional hypercrosslinker lead to a cross-polymerization on the surface, which prevents the RP-WAX selector to graft on the surface. In order to circumvent the polymerization problem, we decided to use oligomers to graft on the surface silanols. Nawrocki and Dabrowska opened cyclosiloxanes in-situ in order to bridge between two silanols on the silica surface [86]. Instead of polymethylcyclosiloxanes, we used polymethylvinylcyclosiloxanes as basis for the further hypercrosslinking (see Figure 2.4.4). Our first tests consisted in evaluating the feasibility of the published reaction in heptane / hydrochloric

# Repetition	TVCS addition		Endcapping		Hypercrosslinking		RP-WAX selector	
	%C	Surface coverage <sup>a</sup> ( $\mu\text{mol}/\text{m}^2$ )	%C	Surface coverage <sup>b</sup> ( $\mu\text{mol}/\text{m}^2$ )	%S	Surface coverage <sup>c</sup> ( $\mu\text{mol}/\text{m}^2$ )	%N	Surface coverage <sup>d</sup> ( $\mu\text{mol}/\text{m}^2$ )
1	7.3	3.58	7.4	0.09	6.2	2.1	< 0.3	-
2	8.1	4.03	8.2	0.09	6.4	2.25	< 0.3	-
3	9.7	4.96	9.7	0.00	6.6	2.33	0.6	0.73
4	7.4	3.64	7.6	0.18	6.3	2.21	0.4	0.47

Table 2.4.1.: Characteristics of TVCS modified silica.

<sup>a</sup>Calculated from the Berendsen- de Galan's equation applied to the percentage of carbon.<sup>b</sup>Calculated from the Sandoval equation applied to the percentage of carbon.<sup>c</sup>Calculated from the Berendsen- de Galan's equation applied to the percentage of sulfur.<sup>d</sup>Calculated from the Berendsen- de Galan's equation applied to the percentage of nitrogen.

#### 4. Improvement of the stability of mixed-mode phases: hypercrosslinking

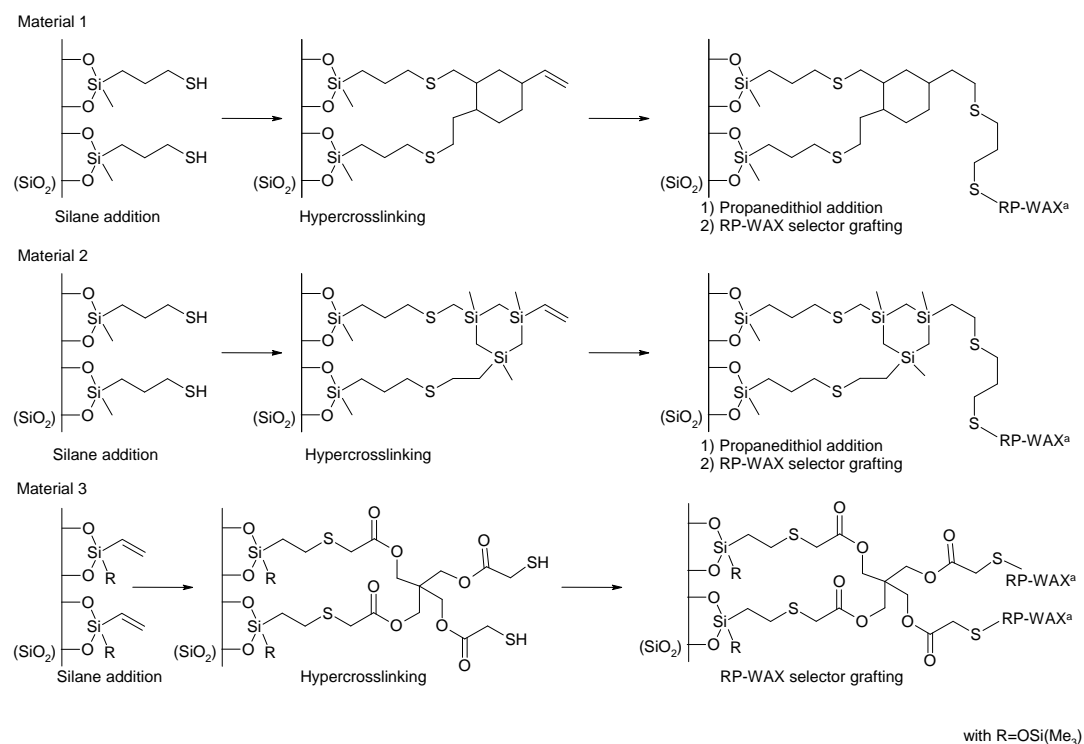


Figure 2.4.3.: Reaction scheme of the three types of hypercrosslinking on the silica surface through a monodentate silane.

<sup>a</sup>RP-WAX group stands for the RP-WAX selector presented in the last chapter.

# Material	Silane addition			Endcapping		Hypercrosslinking		Propane dithiol addition or hypercrosslinking			RP-WAX selector	
	Silane	%C	Surface coverage <sup>a</sup> ( $\mu\text{mol}/\text{m}^2$ )	%C	Surface coverage <sup>b</sup> ( $\mu\text{mol}/\text{m}^2$ )	Reagent	%C <sup>c</sup>	Reagent	%S	Surface coverage <sup>d</sup> ( $\mu\text{mol}/\text{m}^2$ )	%N	Surface coverage <sup>e</sup>
1	MPDMMS	4.4	2.91	5.2	0.67	TVCH	9.2	Propanedithiol	0.9	0.30	<	-
2	MPDMMS	5.7	4.01	6.7	0.86	TMTVTS	11.7	Propanedithiol	5.0	1.99	<0.3	-
3	VTMS	8.3	4.14	8.5	0.18	-	-	PTMA	10.6	4.04	<	-
											0.3	

Table 2.4.2.: Characteristics of monodentate modified silica.

<sup>a</sup>Calculated from the Berendsen - de Galan's equation applied to the percentage of carbon. The average value is given to facilitate the evaluation.

<sup>b</sup>Calculated from the Sandoval equation applied to the percentage of carbon.

<sup>c</sup>The surface coverage cannot be calculated because no equation is applicable for the third level of modification.

<sup>d</sup>Calculated from the Berendsen - de Galan's equation applied to the percentage of sulfur.

<sup>e</sup>Calculated from the Berendsen - de Galan's equation applied to the percentage of nitrogen.

#### 4. Improvement of the stability of mixed-mode phases: hypercrosslinking

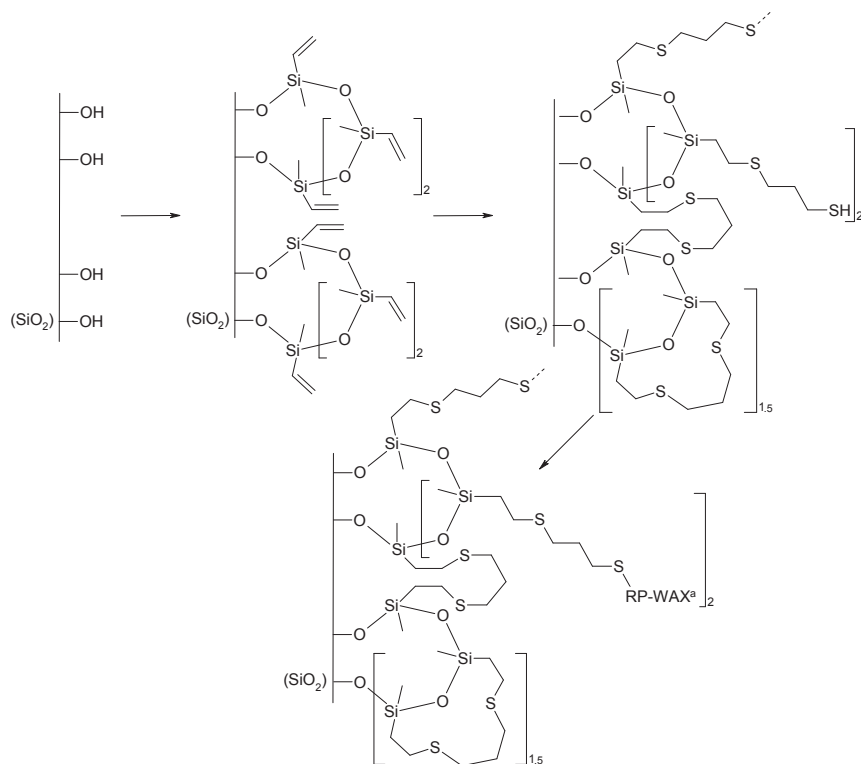


Figure 2.4.4.: Reaction scheme of the hypercrosslinking on the silica surface after tetramethyltetravinyldisiloxane opening.

<sup>a</sup>RP-WAX group stands for the RP-WAX selector presented in the last chapter.

acid with agitation during 48 h at room temperature followed by 5 h at reflux for tri- and tetra-cyclosiloxane. The results with tetra-cyclosiloxanes was much better and we therefore performed the rest of the study with this molecule.

Material 1 in Table 2.4.3 was prepared according to the protocol from the literature and lead to a surface coverage slightly above 1  $\mu\text{mol}/\text{m}^2$ . A visual representation of results from the different evaluated reactions can be found in Figure 2.4.5. Changing the reactive system from heptane / hydrochloric acid to toluene / PTSA lead to much better surface coverage. Even if the time at reflux influences the vinyl density, it is worth noticing that the most important parameter is the agitation time at room temperature. The bulky reagent must diffuse in the porous system and an equilibrium silica / siloxane / acidic modifier must be attained. Further increase of agitation time at room temperature and at reflux did not lead to better surface coverages. In order to keep the overall reaction time in acceptable limit, the material 3 was chosen for further study.

The next step consisted in grafting propanedithiol to the vinyl-modified silica in order to hypercrosslink the vinylsiloxanes with each other. We tested different quantity of propanedithiol (see Table 2.4.4). The addition of high amounts of hypercrosslinker lead to a large density of propanedithiol on the surface but surface coverage of RP-WAX selector is rather lower. This is probably due to worse accessibility of the surface by high hypercrosslinking grade. The reaction of material 3 with 2 equivalents of 1,3-propanedithiol followed by the addition of N-(10-undecenoyl)-3-aminoquinuclidine leads to the most promising material.

# Material	Solvent	Acidic modifier	Time at room temperature $t_{RT}$ (h)	Time at reflux $t_{reflux}$ (h)	%C	Surface coverage <sup>a</sup> ( $\mu\text{mol}/\text{m}^2$ )	Vinyl surface coverage <sup>b</sup> ( $\mu\text{mol}/\text{m}^2$ )
1	Heptane	Hydrochloric acid	48	5	5.6	1.07	4.28
2	Heptane	Hydrochloric acid	2	20	5.1	0.98	3.92
3	Toluene	PTSA	48	5	6.9	1.32	5.28
4	Toluene	PTSA	2	20	6.5	1.25	5.00
5	Toluene	PTSA	72	20	7.1	1.36	5.44
6	Toluene	PTSA	96	5	7.3	1.39	5.56

Table 2.4.3.: Characteristics of silica materials modified with TeMTeVTeS in different solvents in the presence of different acidic modifiers within different reaction times.

<sup>a</sup> Corresponding to the number of molecules linked to the surface.

<sup>b</sup> Corresponding to the number of vinyl groups present on the surface.

#### 4. Improvement of the stability of mixed-mode phases: hypercrosslinking

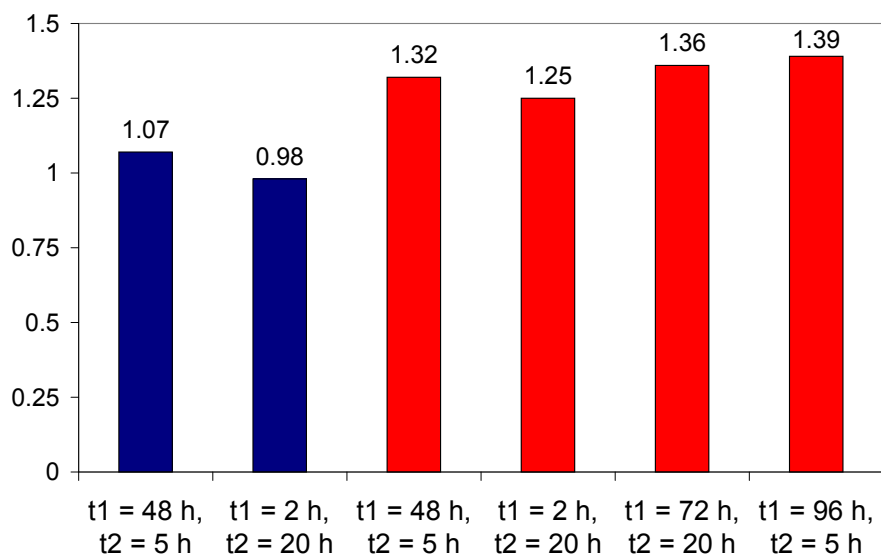


Figure 2.4.5.: Optimization of the TeMTeVTeS addition.

Blue bars stand for heptane / HCl reactions whereas red bars correspond to toluene / PTSA reactions.

t1 and t2 are respectively the reaction time at room temperature and the one at reflux.

Values are given in  $\mu\text{mol}/\text{m}^2$ .

Number of equivalent <sup>a</sup>	Hypercrosslinking		RP-WAX selector	
	%S	Surface coverage <sup>b</sup> ( $\mu\text{mol}/\text{m}^2$ )	%N	Surface coverage <sup>c</sup> ( $\mu\text{mol}/\text{m}^2$ )
1	4.3	1.48	0.5	0.60
2	5.3	1.84	0.5	0.60
10	13.4	5.14	0.4	0.47

Table 2.4.4.: Characteristics of TeMTeVTeS modified silica after endcapping, hypercrosslinking and grafting of the RP-WAX selector.

<sup>a</sup>Molar equivalent of 1,3-propanedithiol calculated from vinyl surface coverage given in Table 2.4.3.

<sup>b</sup>Calculated from the Berendsen - de Galan's equation applied to the percentage of sulfur.

<sup>c</sup>Calculated from the Berendsen - de Galan's equation applied to the percentage of nitrogen.



## 4.4. Concluding remarks

In order to gain in stability, protecting the surface through steric and hydrophobic shielding seems very promising. However, high reactive poly-functional reagents tend to overreact through inter- and / or intra-polymerization. Such material is very difficult to obtain in reproducible manner. Adding siloxane oligomers to the silica surface allows a better control of the degree of hypercrosslinking. We could even achieve reproducible hypercrosslinking of the silica surface.

The second aspect of those procedures is the number of free reactive sites remaining on the surface in order to add the RP-WAX selector. Once again, only the siloxane oligomer procedure allowed to keep enough thiol groups on the surface. The ligand density of the final product is then similar to that of the linear standard material. The selectivity of the hypercrosslinked RP-WAX phase in HPLC is evaluated elsewhere (see Part III Chapter 1).



## 5. Synthesis of other types of mixed-mode selectors

### 5.1. Introduction

Developing other types of selectors for mixed-mode chromatography consists in our case in synthesizing some molecules bearing a hydrocarbon chain for the reversed phase behavior and an ion exchange head group. Different types of functional groups for ion exchange chromatography are given in Table 2.5.1 [87]. Most of the developed material for ion exchange chromatography are based on these groups or some alkyl derivatives of it.

Type of exchanger	Functional group	Name
Strong anion (SAX)	$-CH_2 - N^+(CH_3)_3$	Quaternary ammonium
Weak anion (WAX)	See Chapter 3	Quinuclidine
Weak cation (WCX)	$-CH_2 - COO^-$	Carboxymethyl
Strong cation (SCX)	$-CH_2 - SO_3^-$	Sulphopropyl

Table 2.5.1.: Functional groups for ion exchange chromatography.

In this chapter, we will not deal with RP-WAX selectors but we will focus on the other ion exchanger in mixed-mode selectors.

Some commercially available mixed-mode materials are based on embedded ion exchangers, for example the SIELC Primesep product line [32]. We focused only on selectors where the ion exchange group is tipped on the reversed phase part of the molecule. Some mixed-mode HPLC material bearing other functionalities than WAX onto a RP chain were already published. Yang et al. as well as Auler et al. based their mixed-mode ligands on phenyl - ion exchange molecules (see Figure 2.5.1). Dionex already launched a RP-WCX column based on a linear hydrocarbon chain tipped by a carboxylic acid group on the market [33] and Interchim is commercializing two different mixed-mode columns, a RP-SAX and a RP-SCX [88]. Detailed structure thereof was not published yet.

In order to build up a coherent product line, to use the chemical knowledge from the RP-WAX product development as well as for obvious economical reason, we decided to construct the new RP-SAX and RP-WCX selectors the same way we worked for the RP-WAX material. Basis for the RP chain was built by the undecenyl chloride on which a

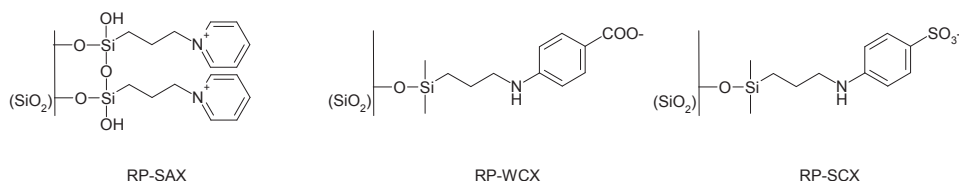


Figure 2.5.1.: Structures of some published mixed-mode reversed phase - ion exchange material (except RP-WAX).

## 5. Synthesis of other types of mixed-mode selectors



Figure 2.5.2.: Reaction scheme for the synthesis of a mixed-mode RP-SAX selector.

molecule containing the functional ion exchange group was linked through an amide bond (see Figure 2.5.4 and Figure 2.5.5 top).

For the RP-WCX selector, we also investigated a different approach with another ion exchange group. It is already known that tetrazole is an alternative to carboxylic acid groups in term of aqueous pKa [89]. Lei et al. showed that tetrazole groups were suitable for ion exchange chromatography [90]. We designed thus a new type of mixed-mode RP-WCX selectors. The RP-chain consists of an hexene chain, which leads to lower RP activity but still bears a double bond for the radical addition on a thiol group. The tetrazole group exhibits similar pKa values than COOH groups with different steric activities and  $\pi - \pi$  interactions.

For the RP-SCX selector, we grafted decanedithiol molecules on the silica surface previously modified with vinyl groups. The thiol group needed only to be oxidized by hydrogen peroxide to obtain the desired sulfone group.

## 5.2. Experimental

### 5.2.1. Chemicals

N-10-Undecenoyl chloride, ammonium chloride, hydrogen peroxide, 1,10-decanedithiol, dimethylformamide (DMF), dichloromethane, methanol and sodium sulfate were obtained from Merck (Darmstadt, Germany). Choline chloride, beta-alanine, 4-aminobutyric acid, 6-aminocaproic acid, sodium azide, 5-hexene nitrile and 1,2,4-trivinylcyclohexane (1,2,4-TVCH) were purchased by ArcosOrganics (Nidderau, Germany).

### 5.2.2. Selector synthesis

#### 5.2.2.1. Mixed-mode Reversed Phase - Strong Anion eXchanger

The reaction scheme is given in figure 2.5.2. Choline chloride and N-10-undecenoyl chloride were added in the reactor and heated for 24 h at 100°C. After cooling down to room temperature, the product is solved in dichloromethane before being filtrated. After evaporation of the solvent, the desired selector is obtained as a brown oil. The compound is extracted with dichloromethane / water. After drying of the organic phase on sodium sulfate, filtration and evaporation, crystallization was performed in methanol. The last filtration preceded the drying in vacuum drying oven. We obtained yellowish crystals. Compound identity was assessed by  $^1\text{H}$  and  $^{13}\text{C}$  NMR as well as by MS analyzes.

$^1\text{H}$  NMR (100 MHz, DMSO)  $\delta_{\text{H}}$  (ppm) 1.20-1.58 (m, 10 H, 8  $\text{CH}_2$ ), 1.65 (qt, 2 H,  $\text{CH}_2\text{-CO-O}$ ), 2.02 (q, 2 H,  $\text{CH}_2\text{-CH=}$ ), 2.34 (t, 2 H,  $\text{CH}_2\text{CO-O}$ ), 3.45 (s, 9 H,  $\text{N}^+(\text{CH}_3)_3$ ), 3.82 (t, 2 H,  $\text{N-CH}_2$ ), 4.44 (t, 2 H,  $\text{CH}_2\text{-OCO}$ ), 4.92 (q, 2 H,  $\text{CH}_2\text{=}$ ), 5.72 (qt, 1 H,  $\text{CH=}$ ).

$^{13}\text{C}$  NMR (100 MHz, DMSO)  $\delta_{\text{C}}$  (ppm) 23.6, 23.8, 24.5, 25.6, 27.8, 28.2, 32.8, 52.1, 54.2, 57.1, 58.9, 63.0, 113.9, 138.2, 171.9, 173.7.

MS (APCI)  $m/z$  256 ( $[\text{M} + \text{H}]^+$ ), 292 ( $[\text{M} + \text{HCl}]^+$ ), 302 ( $[\text{M} + \text{HCOOH}]^+$ ).

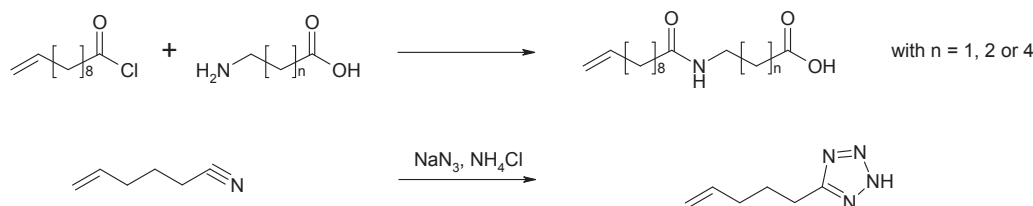


Figure 2.5.3.: Reaction scheme for the synthesis of mixed-mode RP-WCX selectors from undecenoyl chloride and from tetrazole.

#### 5.2.2.2. Mixed-mode Reversed Phase - Weak Cation eXchanger

The reaction scheme for both undecenoyl and tetrazole derivatives is given in figure 2.5.3.

**Undecenoyl derivatives** Beta-alanine ( $n = 1$ ), 4-aminobutyric acid ( $n = 2$ ) or 6-aminocaproic acid ( $n = 4$ ) and N-10-undecenoyl chloride were added in the reactor and heated for 24 h at 100°C. After cooling down to room temperature, the product is solved in dichloromethane before being filtrated. After evaporation of the solvent, the desired selector is obtained as a brown oil.

Beta-alanine derivate

$^1\text{H NMR}$  (400 MHz,  $\text{CDCl}_3$ )  $\delta_{\text{H}}$  (ppm) 1.22-1.52 (m, 16 H, 8  $\text{CH}_2$ ), 2.04 (q, 2 H,  $\text{CH}_2\text{NHCO}$ ), 2.33 (t, 1 H, NH), 3.50 (t, 2 H,  $\text{CH}_2\text{COOH}$ ), 4.95 (q, 2 H,  $\text{CH}_2=$ ), 5.81 (qt, 1 H,  $\text{CH}=$ ), 7.28 (s, 1 H, COOH).

4-Aminobutyric acid derivate

$^1\text{H NMR}$  (400 MHz,  $\text{DMSO}$ )  $\delta_{\text{H}}$  (ppm) 1.22-1.53 (m, 16 H, 8  $\text{CH}_2$ ), 2.51 (q, 2 H,  $\text{CH}_2\text{NHCO}$ ), 3.21 (t, 1 H, NH), 3.65 (t, 2 H,  $\text{CH}_2\text{COOH}$ ), 4.14 (qt, 2 H,  $\text{CH}_2\text{CH}_2\text{NHCO}$ ), 4.95 (q, 2 H,  $\text{CH}_2=$ ), 5.79 (qt, 1 H,  $\text{CH}=$ ), 7.50 (s, 1 H, COOH).

6-Aminocaproic acid derivate

$^1\text{H NMR}$  (400 MHz,  $\text{DMSO}$ )  $\delta_{\text{H}}$  (ppm) 1.09-1.58 (m, 16 H, 8  $\text{CH}_2$ ), 2.02 (qt, 2 H,  $\text{CH}_2$ ), 2.19 (q, 2 H,  $\text{CH}_2\text{NHCO}$ ), 2.21 (t, 1 H, NH), 2.72 (qt, 2 H,  $\text{CH}_2$ ), 3.01 (qt, 2 H,  $\text{CH}_2$ ), 3.81 (t, 2 H,  $\text{CH}_2\text{COOH}$ ), 4.98 (q, 2 H,  $\text{CH}_2=$ ), 5.79 (qt, 1 H,  $\text{CH}=$ ), 8.07 (s, 1 H, COOH).

**Tetrazole derivatives** Ammonium chloride and sodium azide are given in a three-neck-reactor. 5-Hexene nitrile solved in DMF is added to the reaction and the mixture is heated for 12 h at reflux. After filtration, the liquid phase is evaporated and extracted with dichloromethane / water. After drying of the organic phase on sodium sulfate, filtration and evaporation, the selector was isolated as yellowish crystals.

We verified the compound identity for the undecenoyl chloride derivatives by  $^1\text{H NMR}$  and for the tetrazole derivatives by  $^1\text{H NMR}$ , IR, and MS.

$^1\text{H NMR}$  (400 MHz,  $\text{DMSO}$ )  $\delta_{\text{H}}$  (ppm) 1.79 (qt, 2 H,  $\text{CH}_2$ ), 2.11 (q, 2 H,  $\text{CH}_2=\text{CH}$ ), 2.51 (t, 2 H,  $\text{CH}_2-\text{C}=\text{N}$ ), 5.02 (q, 2 H,  $\text{CH}_2=$ ), 5.82 (qt, 1 H,  $\text{CH}=$ ).

IR  $\nu_{\text{max}}$  ( $\text{cm}^{-1}$ ) 750 (C=C), 1405 (-NH), 1648 (N=N).

MS (EI)  $m/z$  138.0 ( $\text{M}^+$ ), 83.9, 81.0, 55.0, 41.0.

### 5.2.3. Surface modification

#### 5.2.3.1. Mixed-mode Reversed Phase - Strong Anion eXchanger

Mercaptopropyl modified and endcapped silica is prepared as presented in Chapters 1 and 2. It is slurried in methanol in the presence of 2 mmol acetic acid per gram of silica. The N-(10-undecenoyl)-choline is added to the slurry under nitrogen flow before adding the radical initiator. After heating at 65°C over night, the product is filtrated, washed three times with hot methanol, and dried at RT under vacuum until weight consistency (see Figure 2.5.4).

Evaluation of the surface coverage for the undecenoyl derivates could not be achieved regarding the nitrogen percentage because the presence of one single nitrogen atom on each molecule leads to percentages under the limit of quantification. The carbon percentage was then just used as indication for the success of the reaction but no quantification could be performed. A quantitative determination could be achieved by using the DPDS method (see Chapter 1). We performed the analysis before and after the addition of the selector and we could determine the surface coverage through the difference between both values.

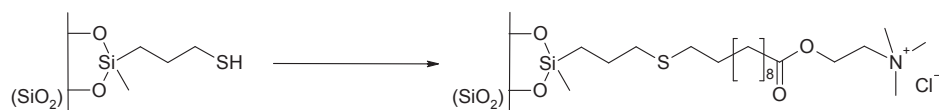


Figure 2.5.4.: Reaction scheme for the synthesis of mixed-mode RP-SAX silica phase.

#### 5.2.3.2. Mixed-mode Reversed Phase - Weak Cation eXchanger

The same procedure as before is used for the addition of undecenoyl chloride (see Figure 2.5.5). Evaluation of the ligand density encountered the same problems for the undecenoyl derivates as for the RP-SAX synthesis, and we therefore used the same analysis methods.

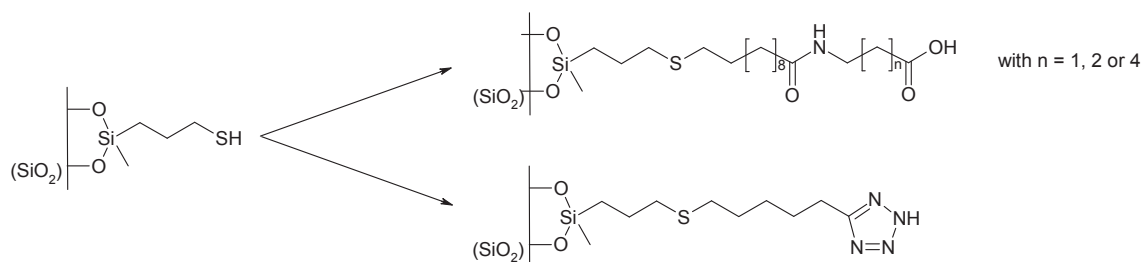


Figure 2.5.5.: Reaction scheme for the synthesis of mixed-mode RP-WCX silica phases.

#### 5.2.3.3. Mixed-mode Reversed Phase - Strong Cation eXchanger

The synthesis of linear RP-SCX material was performed on a previously vinyl-modified and endcapped silica (see Chapter 4). The silica is slurried in methanol and decanedithiol is added along with the radical initiator under nitrogen flow. After heating at 65°C over night, the product is filtrated, washed three times with hot methanol, and dried at RT under vacuum until weight consistency (see Figure 2.5.6 top).

The hypercrosslinked RP-SCX material was synthesized from the mercaptopropyl modified and endcapped silica prepared as presented in Chapters 1 and 2. A first step consists

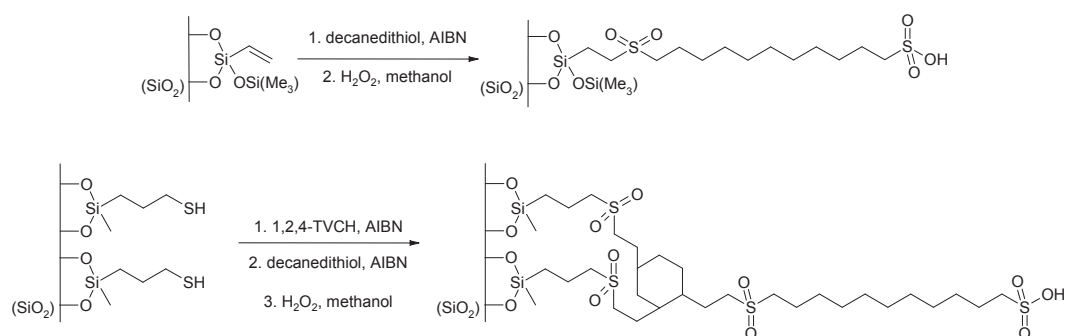


Figure 2.5.6.: Reaction scheme for the synthesis of mixed-mode RP-SCX silica phases.

in adding 1,2,4-trivinylcyclohexane and the radical initiator on the silica suspended in methanol under nitrogen flow. The reaction mixture is heated at 65°C over night, the product is filtrated, washed three times with hot methanol, and dried at RT under vacuum until weight consistency. The procedure is repeated with decanedithiol (see Figure 2.5.6 bottom).

The thiol groups of both materials are then oxidized with hydrogen peroxide in methanol during 24 h at room temperature. After washing with water, and with sulfonic acid, the material is washed sulfate-free before being washed in acetone. The silica is then dried at RT under vacuum until weight consistency.

## 5.3. Results and discussion

### 5.3.1. Mixed-mode Reversed Phase - Strong Anion eXchanger

We decided to base the reversed phase chain on the undecenoyl chloride starting block. The easiest way to form mixed-mode selector consisted thus in finding a molecule bearing the strong anion exchanger on one side and an amine group on the other side in order to form an amide bond like for the RP-WAX selector. We decided to use the easy-available cheap choline chloride as SAX group. We encountered some problems because of the difference in solubility between both compounds. On one hand, choline chloride is only soluble in water and in alcohol. On the other hand, undecenoyl chloride is hydrolyzed in the presence of water and alcohol lead to esterification reactions. Renshaw and Ware showed in the 1920's that such reactions with choline derivatives could be performed without solvent [91].

The product was obtained as a brownish oil with 81 % yield. After recrystallization of the product in methanol, we obtained whitish-yellowish crystals. The identity and the purity of the product were confirmed through NMR and MS and the overall yield reached 68 % for a 5 g synthesis. The reproducibility of the process was tested at different scales. The overall yield increased at higher scales and it attained 79 % for a 50 g synthesis.

After addition on the thiol-modified silica, we cannot evaluate the density of the SAX group regarding the nitrogen percentage because of the limit of quantification. Using the DPDS method, we obtained a surface coverage of 0.48  $\mu\text{mol}/\text{m}^2$ , which is similar to the results obtained for the RP-WAX material.

## 5. Synthesis of other types of mixed-mode selectors

WCX molecule	Selector synthesis		Silica modification
	Number of equivalent <sup>a</sup>	Yield	Surface coverage <sup>b</sup> ( $\mu\text{mol}/\text{m}^2$ )
Undecenoyl-beta-alanine	1.5	0.57	0.52
	2	0.69	
Undecenoyl-aminobutyric acid	1.5	0.71	0.46
	2	0.82	
Undecenoyl-aminocaproic acid	1.5	0.67	0.43
	2	0.75	
Undecenoic acid			0.51

Table 2.5.2.: Synthesis of weak cation exchangers based on undecenoyl chloride derivatives.

<sup>a</sup>Number of equivalent of carboxylic acid.

<sup>b</sup>Calculated from the DPDS method.

### 5.3.2. Mixed-mode Reversed Phase - Weak Cation eXchanger

The same approach was chosen at first for the synthesis of RP-WCX material, i.e. the RP chain is given by the undecenoyl chloride. We evaluated three different molecules bearing both amine and acidic groups. The yields are given in Table 2.5.2. The reaction on mercaptopropyl-modified silica lead to good results, similar for the carbon contents to those of the RP-WAX material but no quantitative data can be stated. The presence of carboxylic acid on the surface was confirmed by IR analysis. The strong absorption band between 2300 and 2400  $\text{cm}^{-1}$  is typical for COOH groups. The surface coverages determined by the DPDS method are similar to those obtained for the RP-WAX and RP-SAX materials. It is worth mentioning that the bigger the molecule, the higher the surface coverage.

An even easier way to obtain an undecenoyl chloride-based material consists in adding the undecenoyl chloride on the mercaptopropyl-modified silica before hydrolyzing the selector to a carboxylic acid with water. The surface coverage was also obtained through the DPDS method and exhibits comparable values to those obtained with beta-alanine.

The synthesis of the tetrazole-based selector lead to a crystalline product with 67 % overall yield. The reproducibility of the reaction was also verified. Even if the reaction lead to the desired compound in high purity and with acceptable yield, we decided not to perform the silica modification because some safety issues would inhibit the implementation on industrial scale. However, evaluating the advantages of using a selector bearing a tetrazole group instead of an usual carboxylic acid groups in chromatographic conditions could be interesting.

### 5.3.3. Mixed-mode Reversed Phase - Strong Cation eXchanger

We decided to synthesize RP-SCX materials without previous selector synthesis. As the typical SCX group consists of a sulfone group, we directly oxidized thiol groups in situ. The first step consisting in adding decanedithiol on vinyl-modified silica lead to sulfur percentage of  $\sim 3\%$  which corresponds to surface coverage around  $1.8\ \mu\text{mol}/\text{m}^2$ . We also evaluated the amount of reactive thiol groups remaining on the surface by the DPDS method. Before the oxidation,  $0.5\ \mu\text{mol SH}/\text{m}^2$  could be determined. After the oxida-



tion, no mercapto group could be identified on the surface, which indicates a quantitative reaction. The strong absorption band at  $1080\text{ cm}^{-1}$  is typical for  $\text{SO}_3^-$  groups.

The second approach consisted in adding the decanedithiol onto a hypercrosslinked surface. Even if the sulfur density on the surface is around  $0.3\text{ }\mu\text{mol/m}^2$ , no SCX group could be pointed out. Before the oxidation, no reactive SH groups were revealed by the DPDS method and after the oxidation, the IR analyzes only showed the presence of  $\text{SO}_2$  groups. The results are similar to those obtained in Chapter 4, the hypercrosslinking of the surface is total and no functional group is accessible. The first linear method should therefore be privileged for the obtention of RP-SCX material.

## 5.4. Concluding remarks

Mixed-mode selectors and silica-based materials are now available for each type of reversed phase - ion exchange mechanism. Some of the selectors were designed in a very typical manner, based on either undecenoyl chloride or decanedithiol. The hexene tetrazole molecule is less common and would need more investigations on its RP-WCX HPLC behavior.

Those molecules were synthesized in reproducible way, so that an implementation on production scale should be easy to carry out. However, no column was packed and we did not test the HPLC characteristics of those materials. The focus of our work was the development of the RP-WAX product for a market launch. The evaluation of the chromatographic behavior and the development of HPLC methods were therefore performed only on reversed phase - weak anion exchange columns.



## **Part III.**

# **HPLC method development on mixed-mode stationary phases**



# 1. Performance test and stability evaluation

## 1.1. Introduction

Several standard mixtures of analytes were developed over the last 25 years. Most of the well-known test systems were developed for the classification of reversed phase material, such as the methods from Walters [92], Tanaka [93], or Engelhardt [94]. Those tests allow comprehensive analysis of the quality of the modification through evaluation of the hydrophobicity, shape selectivity and silanol activity at different pH [95]. Comparisons of the results can be performed through one-to-one comparison of the specified data for each column, for example in order to determine the column with the largest hydrophobicity with the  $\alpha_{ethylbenzene/toluene}$  from the Engelhardt test. Tanaka used a more visual method by drawing a hexagram for an easier comparison. A standard hexagram for a RP18 column is given in Figure 3.1.1.

Hoogmartens et al. scouted 36 test parameters from eight different standard methods. They evaluated the significance of each parameter for the main properties: efficiency, hydrophobicity, silanol activity, ion-exchange capacity, steric selectivity, and metal impurity [96]. They identified some relevant parameters and ended up with four parameters sufficient to fully characterize any column. The retention factor of amylbenzene (or pentylbenzene)  $k'_{amylbenzene}$  ( $k'_{amb}$ ) is specific for the hydrophobicity, the silanol activity is expressed through the relative retention factor benzylamine / phenol at pH 2.7  $\alpha_{benzylamine/phenol}$  ( $rk'_{ba/pH\,2.7}$ ), the retention factor of 2,2'-dipyridyl  $k'_{2,2'-dipyridyl}$  ( $k'_{2,2'-dip}$ ) is related to the metal impurities and the relative retention factor triphenylene / o-terphenyl  $\alpha_{triphenylene/o-terphenyl}$  ( $rk'_{tri/ter}$ ) is the only parameter within the 36 ones which stands for steric selectivity. They defined then a ranking system based on a single F-value in order to easily compare columns amongst each other:

$$F = (k'_{amb,ref} - k'_{amb,i})^2 + (rk'_{ba/pH\,2.7,ref} - rk'_{ba/pH\,2.7,i})^2 + (rk'_{tri/ter,ref} - rk'_{tri/ter,i})^2 + (k'_{2,2'-dip,ref} - k'_{2,2'-dip,i})^2 \quad (1.1.1)$$

The lower the F-value between the column  $i$  and the reference column  $ref$ , the more similar the columns with each other [97]. An on-line freeware can be used in order to compare the data gathered from experimental value with the data generated for 69 different columns.

Lämmerhofer et al. designed a performance test specifically for the mixed-mode RP-WAX material with acidic compounds for the evaluation of the WAX behavior. The mixture is composed of two hydrophobic compounds, butylbenzene and pentylbenzene, as well as two acidic compounds with different lipophilicity, diethylthiophosphate and the more lipophilic tri-peptide Boc-Pro-Phe [98]. Different mixed-mode columns were evaluated in RP and in HILIC modes. The aim of our work consisted in defining a test mixture with smaller molecules for the comprehensive analysis of RP-WAX columns. The benzene derivatives from Hoogmartens and Lämmerhofer were kept and extended to other

## 1. Performance test and stability evaluation

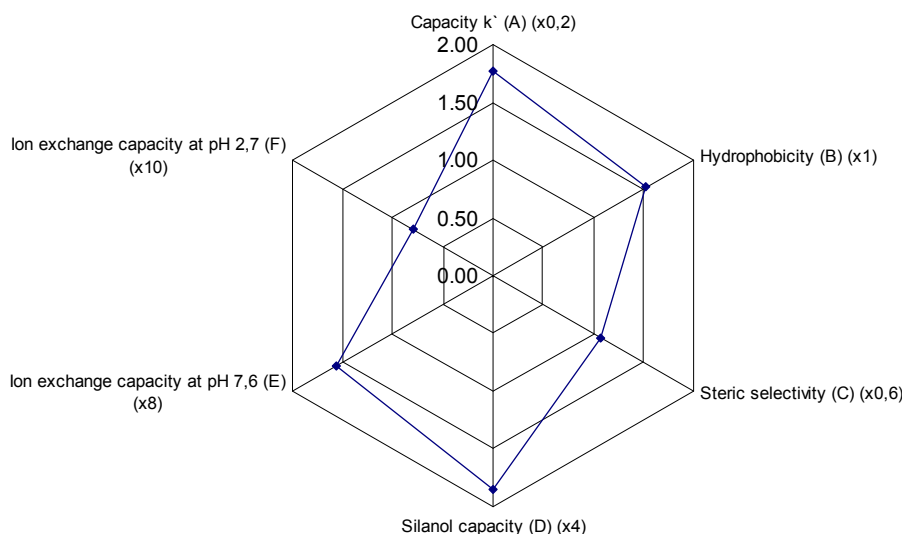


Figure 3.1.1.: Hexagram from the Tanaka test for a standard RP18 column.

small benzene-based analytes in order to evaluate the hydrophobicity ( $k'_{phenol}$ ,  $k'_{toluene}$ ,  $k'_{pentylbenzene}$ ), the methylene selectivity ( $\alpha_{pentylbenzene/butylbenzene}$ ) as well as the ionic selectivity ( $k'_{benzoic\ acid}$ ).

The stability of HPLC columns is a well-known issue. Most of the silica-based material are not stable at high and low pH [99]. The silica particles tend to dissolve in alkaline solutions. pH above 8 to 9 should be avoided. At lower pH the bonding becomes unstable and pH 2 seem to be the lower limit for silica-based bonded material. The columns bearing amine groups (for example aminopropyl ligands) are also known for their instability due to the local increase of the pH which attacks the silica itself [100].

The methods to evaluate how stable a sorbent is are numerous. The technique for evaluating the stability of chromatographic materials is quite simple. At first, the column is evaluated by injection of a standard mixture. Afterwards, a stress mixture at defined pH is pumped through the column. This process is repeated until the desired time is achieved or until the destruction of the column, or at least a dramatic decrease of the column performance. Some of the published test are performed at different basic pH to evaluate the silica protection [101]. Luo et al. evaluated the stability of the bonding by submitting the column to acidic non-buffered solution [79]. A more systematic method consists in evaluating the stability of the material at different acidic and basic pH. Ye et al. investigated the stability of HPLC materials at 9 different pH from pH 2 to pH 11. Such procedure is very time consuming.

We therefore designed a specific fast stability evaluation in acidic and basic conditions. Working at pH 2 is sufficient for separating most of the compounds, but the separation of basic compounds sometimes needs to work at higher pH. We investigated therefore the stability of the RP-WAX packing at pH 2 and at pH 10. The aim of the evaluation was a comparison of both Merck materials with the Dionex column. No long-term high-temperature study was therefore performed. We designed an easy-to-implement method which could be performed on a standard HPLC machine within a week-end.

## 1.2. Experimental

### 1.2.1. Chemicals

RP-WAX modified silica material was prepared according to the methods described in the last part from 5µm silica material. Three different materials were evaluated. The standard RP-WAX material corresponds to the material #3 in Table 2.3.2, the fully optimized material to the material #3 in Table 2.2.4 modified with the RP-WAX selector (see Part II Chapter 3) and the hypercrosslinked RP-WAX material to the material #2 in Table 2.4.4. All columns were packed in Hibar columns (125 × 4 mm) at 700 bar in iso-propanol after slurring the material in methanol - acetic acid (19:1, v/v).

The Acclaim Mixed-Mode WAX-1 column was purchased by Dionex in 150 × 4.6 mm and 5 µm particle size.

The mobile phases for chromatography were prepared from HPLC grade methanol and acetonitrile, di-sodium hydrogen phosphate, sodium di-hydrogen phosphate (Merck). The benzene derivates presented in Table 3.1.1 as well as benzylamine, phenol, 2,2'-dipyridyl, uracil, o-terphenyl, and triphenylene were purchased from Merck.

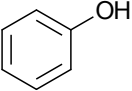
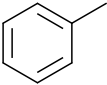
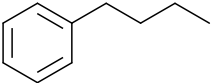
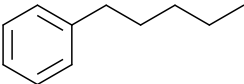
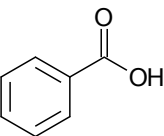
Chemical name	Structure	log P <sub>octanol/water</sub>	pKa
Phenol		1.42 [102]	10.00 [102]
Toluene		2.73 [102, 103]	
Butylbenzene		4.26 [102, 103]	
Pentylbenzene		4.90 [103]	
Benzoic acid		1.85 [102]	4.21 [102]

Table 3.1.1.: Structure and parameters of the benzene derivates used for the performance and stability tests.

### 1.2.2. Instrumentation

The measurements for the column classification system were performed on a VWR (Darmstadt, Germany) Hitachi LaChrom Elite HPLC system (three channels pump L-2130 with degasser, autosampler L 2200, oven L-2350, diode array detection (DAD) system L-2455). The chromatographic experiments for the specific RP-WAX test were carried out on a VWR (Darmstadt, Germany) Hitachi LaChrom Elite HPLC system (three channels pump L-2130 with degasser, autosampler L 2200, ultraviolet - visible (UV-Vis) detector L-2420).

## 1. Performance test and stability evaluation

Method	Mobile phase composition
A	Methanol - water - 0.2 M potassium phosphate buffer pH 2.7 (34:90:10, v/v)
B	Methanol - water - 0.2 M potassium phosphate buffer pH 6.5 (34:90:10, v/v)
C	Methanol - water (317:100, v/v)

(a)

Method	Sample composition
A	5 mg benzylamine and 5 mg phenol in 10.0 ml mobile phase A
B	3 mg 2,2'-dipyridyl in 10.0 ml mobile phase B
C	0.1 mg uracil, 7 mg amylbenzene, 0.2 mg o-terphenyl and 0.02 mg triphenylene in 10.0 ml mobile phase C

(b)

Table 3.1.2.: Mobile phase composition (a) and sample composition (b) for the measurement of the 4 parameters for the column classification system.

The data were processed using the Agilent (Waldbronn, Germany) EZChrom Elite version 3.21 software.

### 1.2.3. Column classification system

Three different samples analyzed each with a specific method lead to the four parameters needed for this classification system. These parameters are then inputted in the freeware for the column comparison [104]. Mobile phases and sample composition are given in Table 3.1.2. The chromatographic measurements shall be performed at 1.0 ml/min with 20  $\mu$ l injection volume and a column temperature at  $40^{\circ}\text{C} \pm 0.5^{\circ}\text{C}$ . The detection is performed at 254 nm.

### 1.2.4. Sample preparation and chromatographic conditions for the specific RP-WAX test

The analytes were solved in methanol / water (50:50, v/v). After ultrasonication and filtration of the samples, the mixture was directly injected on the column. For the peak identification, each compound was separately injected.

The injection volume was 10  $\mu$ l and the flow rate was set to 1.0 ml/min. The detection was performed at 215 nm at room temperature. The run was performed in isocratic mode with 0.01 M phosphate buffer pH 4.45 and acetonitrile (50:50, v/v). Methanol was used as  $t_0$  marker.

### 1.2.5. Stress test

Each column used in the test was new at the beginning. First of all, we conditioned the column with 30 column volumes (CV) at the chromatographic conditions. We then performed 5 injections in a row. This series (conditioning + 5 measures) is performed after each step of the stress procedure given in Table 3.1.3. The flow rate is maintained to 1 ml/min during the whole experiment except before the injection series where the flow is stopped for 30 minutes in order to add pressure change to the stress mechanism.



# Step	Stress solution	Step duration		
		Column volumes	Time (h)	Cumulated time (h)
1	Phosphate buffer pH 2 + 50 % acetonitrile	40	1	1
2		40	1	2
3		80	2	4
4		80	2	6
5		160	4	10
6		1600	40	50
7	Phosphate buffer pH 10 + 50 % acetonitrile	40	1	51
8		40	1	52
9		80	2	54
10		80	2	56
11		160	4	60
Total column volumes		2320		

Table 3.1.3.: Stress procedure for the evaluation of the stability of RP-WAX material.

## 1.3. Results and discussion

### 1.3.1. Column classification system

The standard methods for column evaluation cannot be used directly for the characterization of RP-WAX material. Even if most of the compounds are retarded on the column and capacity factors can be calculated, the characteristics corresponding to the parameters are not relevant. For example, the silanol activity is determined in the Walters test by the relative retention factor  $\alpha_{N,N\text{-diethyltoluamide/anthracene}}$  for RP material. On RP-WAX sorbent, the amide group will not only interact with the silanol groups on the surface but the quinuclidine group will also repulse the molecule. Therefore, no comprehensive assumption can be arisen. However, the classification system from Hoogmartens calculates a single parameter from different data and compares RP-18 columns as well as other types thereof. This system can then be applied to our work, not in a comprehensive approach, but only as an evaluation of the singularity of the column.

We calculated the four different parameters after performing the three intended runs with three replications for a standard RP-WAX column. Similar columns should have F-value close to 0. For example, the 4 C18 columns Purospher and Purospher STAR from Merck, Nucleodur from Macherey-Nagel and Omnispher from Varian have F-value below 1. For our material, the value of each parameter as well as the F-value is given in Table 3.1.2. The columns depicted underneath are the most similar ones regarding the F-value. With a smallest F-value over 6, we can conclude that the RP-WAX material is very different from any of the 69 columns from this system. Even some Amide or Polaris columns are not close to the mixed-mode material.

## 1. Performance test and stability evaluation

Column	F	k'amb	rk'ba/pH2.7	rk'tri/ter	k'2,2'-d
RP-WAX	0.000	1.90	-0.100	2.96	5.00
Apex Basic, 250 x 4.6 mm ID, 5 µm, Jones Chrom.	6.189	2.15	0.001	2.32	7.66
Prevail Select, 250 x 4.6 mm ID, 5 µm, Alltech	6.615	2.88	-0.057	2.27	4.33
Prevail Amide, 250 x 4.6 mm ID, 5 µm, Alltech	12.477	1.47	-0.112	1.99	3.45
HyPurity Advance, 250 x 4.6 mm, 5 µm, ThermoQuest	12.525	0.42	-0.263	2.09	0.92
HyPurity Aquastar, 250 x 4.6 mm, 5 µm, ThermoQuest	12.987	1.58	0.097	2.12	11.94
Nucleosil Nautilus, 250 x 4.6 mm, 5 µm, Macherey-Nagel	14.633	3.22	0.014	1.95	6.38
XTerra RP C18, 250 x 4.6 mm, 5 µm, Waters	17.100	2.26	0.076	1.88	4.41
Purospher, 250 x 4.6 mm ID, 5 µm, Merck	18.322	4.50	0.001	1.90	11.30
Prontosil 120-5-C18-ace-EPS, 250 x 4.6 mm, 5 µm	18.398	4.99	0.020	1.89	6.54
Nucleodur C18 Isis, 250 x 4.6 mm, 5 µm, Macherey-Nagel	20.483	6.88	0.030	2.00	10.58
Polaris C18-A, 250 x 4.6 mm ID, 5 µm, Varian	23.231	2.92	0.078	1.69	4.57
Prevail C18, 250 x 4.6 mm ID, 5 µm, Alltech	25.743	4.84	0.067	1.92	20.71
MP-Gel ODS-5, 250 x 4.0 mm, YMC/Omnichrom	25.943	5.82	0.038	1.73	10.69
HyPurity Elite, 150 x 4.6 mm ID, 5 µm, ThermoQuest	27.225	3.16	0.079	1.58	4.35
Altima AQ, 250 x 4.6 mm ID, 5 µm, Alltech	27.769	4.87	0.066	1.93	22.87
Everest, 250 x 4.6 mm ID, 5 µm, Grace	27.816	1.41	0.056	1.55	1.95
HyPurity Elite, 150 x 4.6 mm ID, 3 µm, ThermoQuest	28.370	3.11	0.083	1.55	4.43
Prontosil 120-5-C18 AQ PLUS, 250 x 4.6 mm, 5 µm	28.472	5.66	0.022	1.68	13.85
Nucleosil MN, 250 x 4.6 mm, 5 µm, Macherey-Nagel	28.565	4.40	0.111	1.66	13.47
Inertsil ODS-2, 250 x 4.6 mm ID, 5 µm, GL Sciences Inc.	28.809	5.92	0.054	1.65	9.87
Platinum EPS 3, 150 x 4.6 mm ID, 3 µm, Alltech	29.386	0.95	0.379	1.87	9.33
Hypersil BDS, 250 x 4.6 mm ID, 5 µm, ThermoQuest	29.531	3.56	0.131	1.56	6.59
HyPurity C18, 250 x 4.6 mm, 5 µm, ThermoQuest	29.924	3.16	0.084	1.51	4.45
Kromasil MN, 250 x 4.6 mm, 5 µm, Macherey-Nagel	30.126	6.20	0.063	1.63	9.37
Discovery C18, 250 x 4.6 mm ID, 5 µm, Supelco	30.213	3.04	0.083	1.50	4.36
Platinum EPS 5, 250 x 4.6 mm ID, 5 µm, Alltech	30.507	0.97	0.401	1.88	10.00
Brava BDS 5, 250 x 4.6 mm ID, 5 µm, Alltech	30.912	3.01	0.114	1.50	6.04
TSKgel Super ODS, 100 x 4.6 mm, 2 µm, TosoHaas	31.154	2.28	0.067	1.46	4.24

Figure 3.1.2.: Results from the column classification system.

### 1.3.2. Specific mixed-mode HPLC test

The aim of designing a new test for the mixed-mode RP-WAX material was the necessity to show the possibility to separate different types of molecules within a single fast isocratic run for comprehensive as well as for marketing purposes. Both hydrophobic compounds from the Lämmerhofer standard test, butylbenzene and propylbenzene, were used in our test to show the possibility to differentiate two molecules varying through a single methylene group. On this basis, we chose the benzene ring as common chromophore group for all the analytes. The anion exchange capacity was evaluated by separating benzoic acid. Phenol was injected as a polar, non-ionic compound and toluene was used as a reference molecule.

The first HPLC runs were performed theoretically using ChromSword for a RP18 material and the elution order followed the log P value, as can be expected from a reversed-phase material (see Figure 3.1.3).

The first mixed-mode test were performed on RP-WAX material at pH between 5.0 and 6.0. At this pH, the benzoic acid is deprotonated and we expected a high retention time with a  $\alpha_{benzoic\ acid/toluene}$  value large enough to differentiate it from the non ionic material. However, the retention of the benzoic acid between 10 and 20 minutes was too high at this pH. We therefore reduced the pH to 4.45 in order to obtain a fast separation.

The retention order for the non-ionic analytes remains similar to that obtained in reversed-phase mode but the benzoic acid is eluting last instead of eluting between the phenol and the toluene (see Figure 3.1.4). Both RP and WAX modes are then illustrated with this test mixture. We designed a very fast isocratic method in which both hydrophobic and anionic compounds can be separated. This method is not only a marketing tool or a first approach to understand what is mixed-mode chromatography. We designed a standard test which can be used on a regular basis in quality control laboratories in order

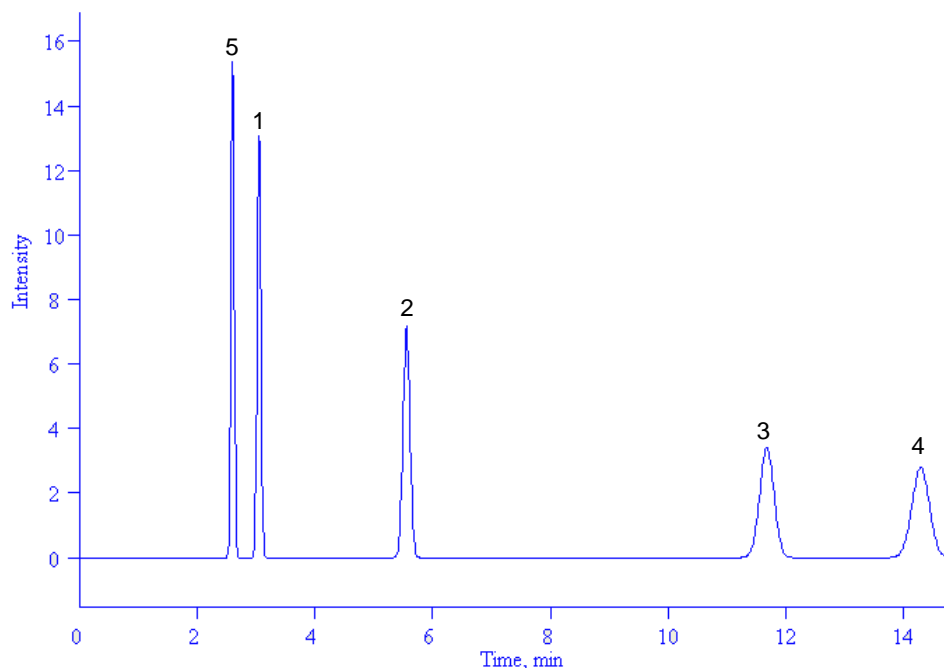


Figure 3.1.3.: Theoretical separation estimated through ChromSword on a Purospher STAR RP18-e 5 $\mu$ m.

*Mobile phase:* 25 % water, 75 % ACN

*Analytes:* phenol (1), toluene (2), butylbenzene (3), pentylbenzene (4) and benzoic acid (5).

to verify the quality of the production process of RP-WAX material before delivering the columns to the client.

We compared on the same figure the three most promising mixed-mode materials from Part II. In the middle of the Figure 3.1.4, good separation of polar, hydrophobic, and acidic compounds is observed on the chromatogram of the standard RP-WAX material. The red chromatogram at the bottom corresponds to the hypercrosslinked material. Even if the value from elemental analyzes were promising, the performance of the column is rather low, probably due to some pore sealing. This material will therefore be disregarded for the rest of the study. The first chromatogram on the top was generated on the fully optimized material. It is quite similar to the middle one even if the retention times are slightly higher. Both materials will therefore be investigated in terms of stability.

### 1. Performance test and stability evaluation

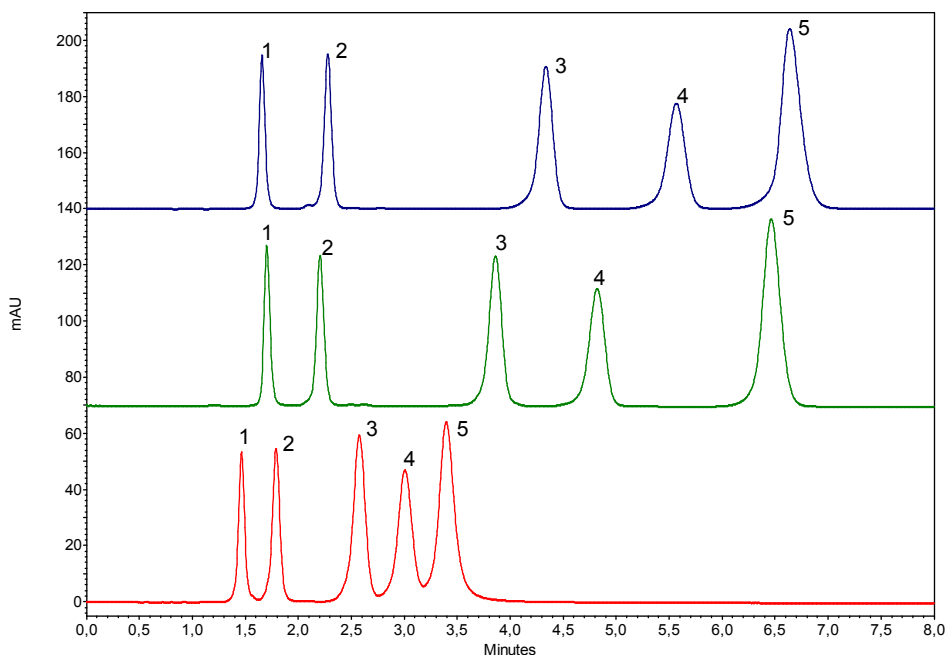


Figure 3.1.4.: Comparison of the separation of benzene derivatives on hypercrosslinked RP-WAX (red), standard RP-WAX (green) and fully optimized RP-WAX (blue).

*Mobile phase:* isocratic 0.01M phosphate buffer pH 4.45, 50 % ACN

*Temperature:* 25°C, *Flow rate:* 1 ml/min, *Injection volume:* 10µl, *Detection:* 215 nm.

*Analytes:* phenol (1), toluene (2), butylbenzene (3), pentylbenzene (4) and benzoic acid (5).

The most similar sorbent on the market is the Acclaim WAX-1 material from Dionex. Even if no detailed structure of the ligand was published until now, the silica-based material is modified with a ligand bearing a hydrocarbon chain with a WAX group bonded at the opposite from the surface. Such a column was then selected to perform a small benchmark. The chromatograms given in Figure 3.1.5 corresponds to the same mixture injected on both Merck and Dionex columns. A time correction was applied to the Dionex chromatogram because of the difference in the column dimensions. The elution on both materials is alike even if both hydrophobicity and anion exchange capacity are higher on the Merck material than on the Dionex one. This concurrence column was then selected for the upcoming stability evaluation.

#### 1.3.3. Stability evaluation and benchmark comparison

The three investigated columns were submitted to the same test procedure described before. The capacity factors are plotted in Figure 3.1.6. The standard RP-WAX material exhibits already first changes for both hydrophobic and ionic compounds in acidic conditions. After 400 CV at pH 2, the capacity factor for pentylbenzene already decreased by 2.60 %. In the same period, the  $k'_{\text{pentylbenzene}}$  for the optimized material only decreased by 0.64 %. Between 400 CV and 2000 CV, the  $k'$  value for hydrophobic compounds remains constant for both materials, which indicates a slowly washing of the ligand in acidic conditions before a stabilization. The anionic exchange capacity given by the capacity factor of benzoic acid evolves quite similarly for both Merck materials. The decrease for

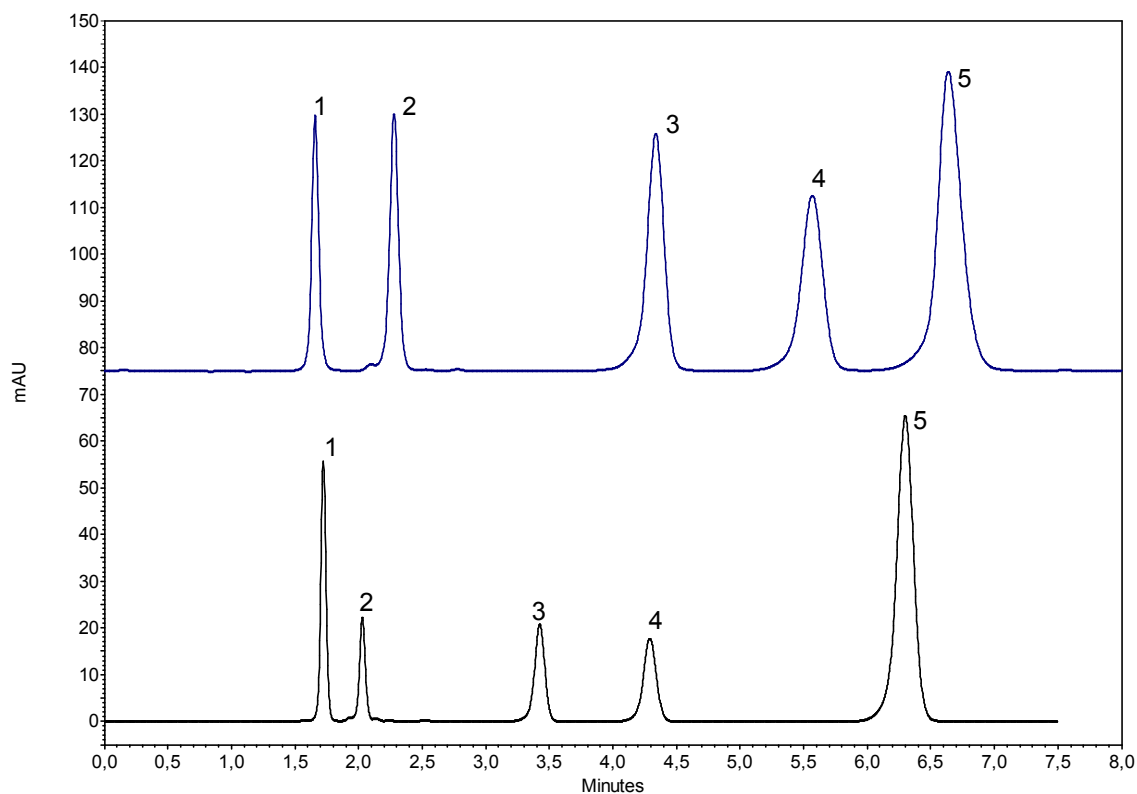


Figure 3.1.5.: Comparison of the separation of benzene derivatives on Merck fully optimized RP-WAX (blue) and on Dionex Acclaim Mixed-Mode WAX-1 (black) columns.

*Mobile phase*:: isocratic 0.01M phosphate buffer pH 4.45, 50 % ACN

*Temperature*: 25°C, *Flow rate*: 1 ml/min, *Injection volume*: 10µl, *Detection*: 215 nm.

*Analytes*: phenol (1), toluene (2), butylbenzene (3), pentylbenzene (4) and benzoic acid (5).

## 1. Performance test and stability evaluation

the standard column is by 2.6 % after 400 CV and by 2.8 % after 2000 CV <sup>1</sup>. For the optimized material, the evolution of  $k'_{benzoic\ acid}$  is even more slow-going with - 0.55 % after 400 CV and - 0.58 % after 2000 CV. As both  $k'$  for ionic and hydrophobic compounds are decreasing at the same rate, we can assume that the whole ligand is affected by the instability. The silane addition in water and the optimization of the endcapping lead to an amelioration of the stability of the material in water, such low variation can be also linked to the measurement imprecision.

The Dionex column encounters other behaviors in acidic conditions. After 400 CV at pH 2, the  $k'_{pentylbenzene}$  increased by 0.75 % and after 2000 CV, the increase is only by 0.5 %. Such variations are not significant. The capacity factor of benzoic acid delivers really significant value in comparison. The  $k'_{benzoic\ acid}$  is increasing by 5.2 % after 400 CV and the increase reaches 13.3 % after 2000 CV. If the whole selector was washed off the surface, the retention time of the hydrophobic molecules would decrease too. If only the WAX part of the selector was washed out of the column, the overall hydrophobicity of the material would increase whereas the benzoic acid would be less retarded. A possible reason for such variations could be an improper endcapping. The increase of the retention time of the acidic molecule is potentially due to an increase of the surface density of free silanol groups through a washing of the endcapper.

The stability of the material in basic conditions is getting rapidly worse, as can be expected from a silica-based material. However, both Merck material remain relatively efficient. The standard column is losing 5 % of its hydrophobic capacity after 10 hours at pH 10 and 13 % of its anionic capacity within the same period. Once again, the optimized material is better protected against the pH aggressions. The  $k'_{pentylbenzene}$  is only 1.5 % lower than at the beginning of the stability evaluation and the  $k'_{benzoic\ acid}$  is 8 % under its starting value. However, the methylene selectivity is not affected by the stress conditions and the  $\alpha_{pentylbenzene/butylbenzene}$  remained unaffected during the whole evaluation (see Figure 3.1.7). This indicates that the endcapping and the RP part of the molecule is quite stable after the optimization, whereas the WAX head group is probably washed off the selector in basic conditions.

The Dionex material is getting even worse at basic pH. After 6 h, the  $k'_{pentylbenzene}$  has increased by 1.1 % and the  $k'_{benzoic\ acid}$  by 28 %. The maximum was achieved after only 2 hours for the pentylbenzene and after 4 hours for the benzoic acid whose capacity factors reached respectively 5 % and 33 %. This increase - decrease phenomenon for the retention on Dionex RP-WAX material indicates a degradation process occurring on the surface as well as at the selector.

The symmetry factors  $A_S$  for the optimized Merck material are between 0.89 and 1.05 ( $\Delta A_S = 0.16$ ), see Figure 3.1.8). The symmetry factor range is much narrower for the Dionex material with asymmetry for all compounds between 0.91 and 0.99 ( $\Delta A_S = 0.08$ ). Submitting the columns to the stress conditions leads to the apparition of fronting on the Dionex material with a symmetry factor down to 0.83 for toluene and benzoic acid. The symmetry range is also getting worse with a  $\Delta A_S$  up to 0.13. The symmetry factors on the Merck material are not affected by the stress conditions, which is a good indication of a good protection of the structure of the silica-based particle by our modification.

A last aspect of the stability evaluation can already be suspected by looking onto the capacity, relative capacity, and symmetry factors. No data is given at the last measure for the Dionex column. Explanation of it is given in Figure 3.1.9. The back pressure remained

---

<sup>1</sup>The percentages are always given between the value at the given run and the value before the beginning of the stress test.

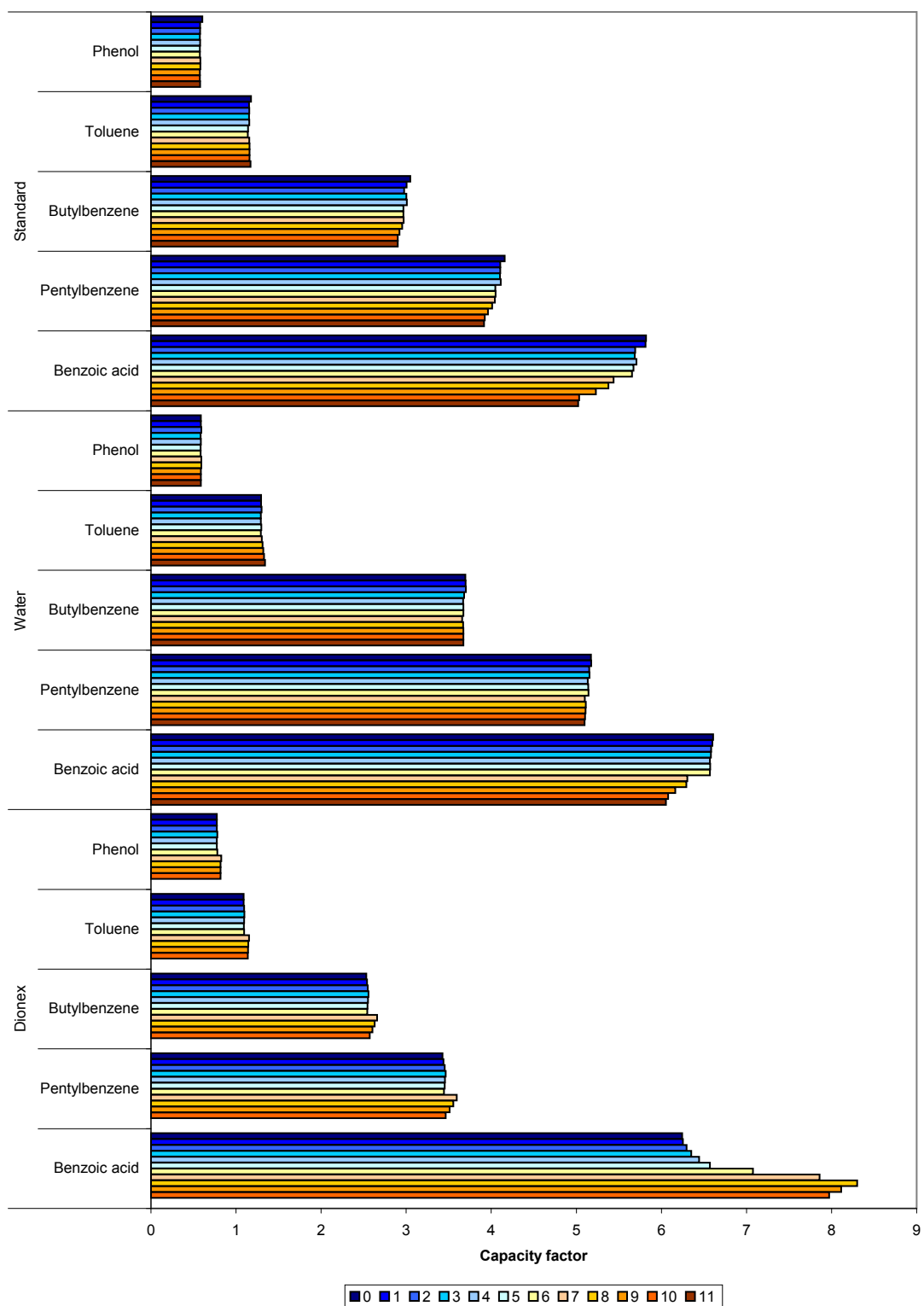


Figure 3.1.6.: Evolution of the capacity factor of benzene derivatives in acidic and in basic conditions.

# 1. Performance test and stability evaluation

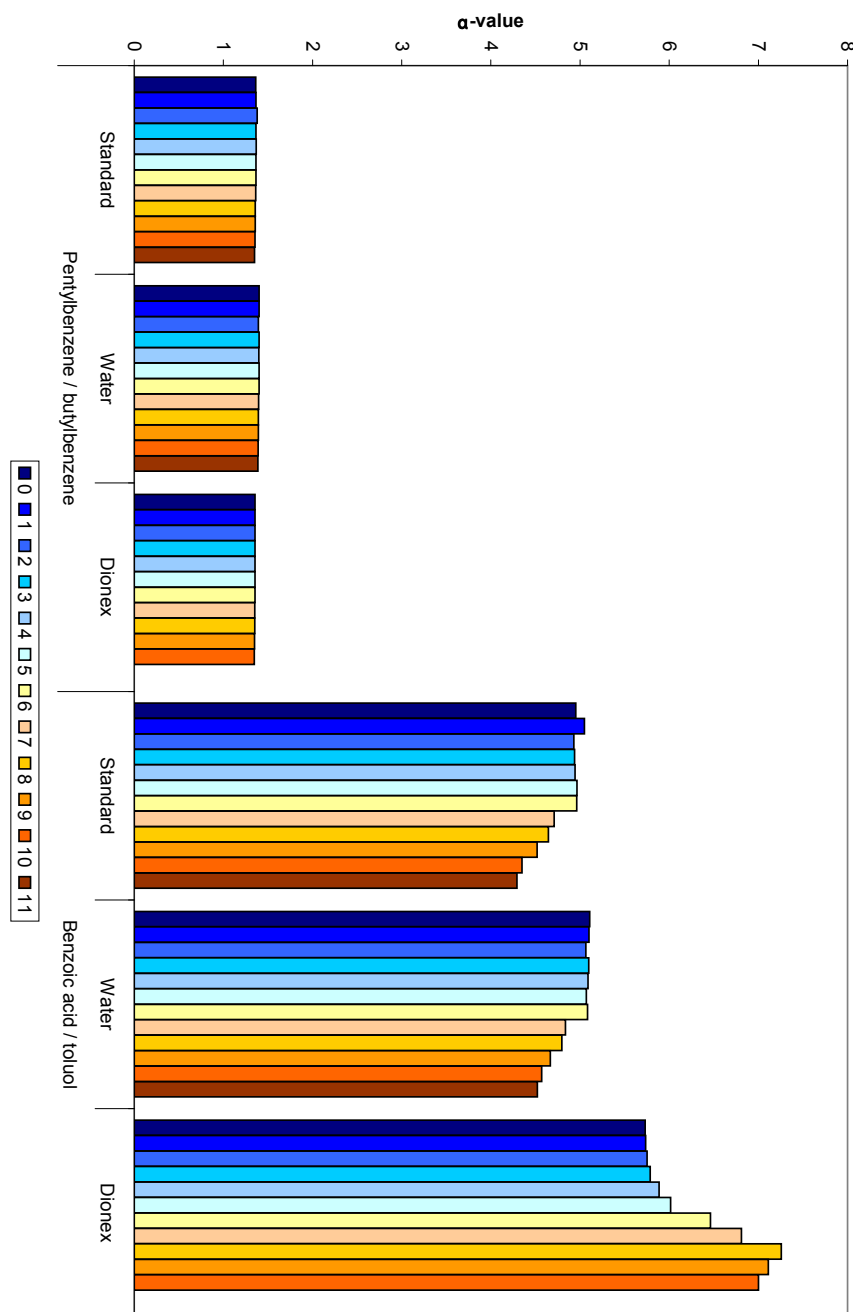
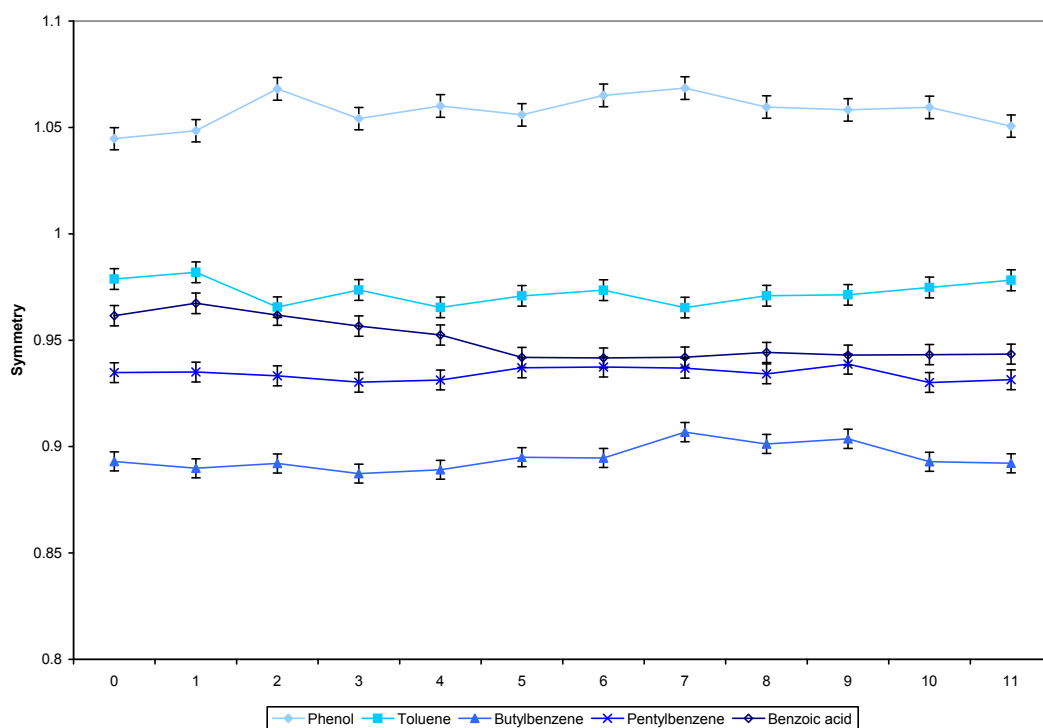
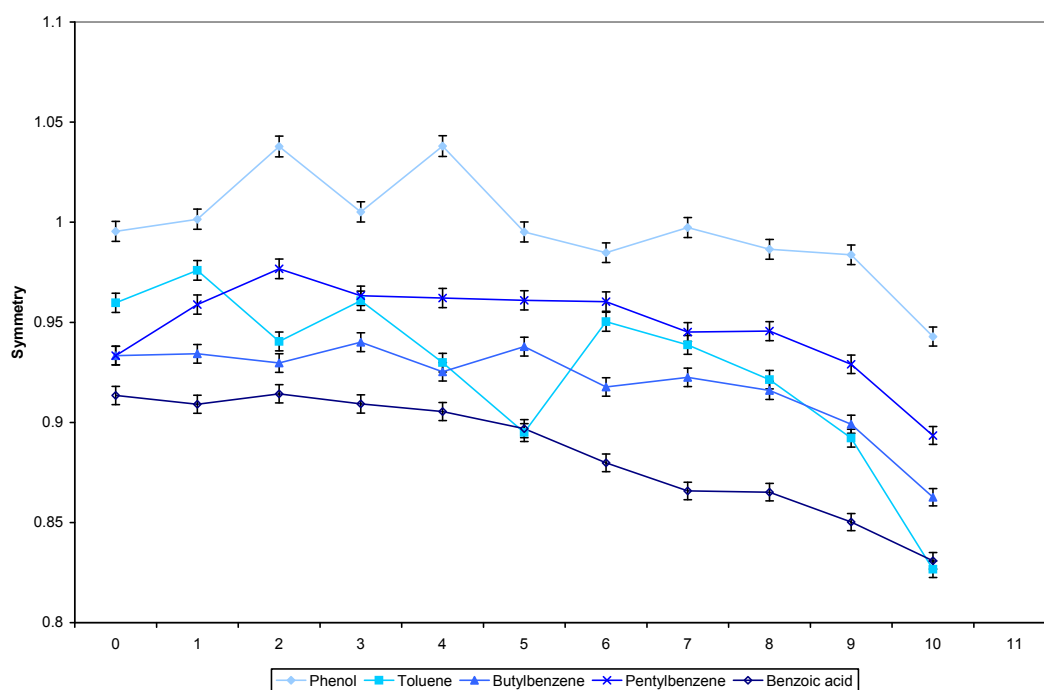


Figure 3.1.7.: Evolution of the relative capacity factors of pentylbenzene / butylbenzene and benzoic acid / toluene in acidic and in basic conditions.





(a) Merck optimized RP-WAX material



(b) Dionex RP-WAX material

Figure 3.1.8.: Comparison of the symmetry factor for the benzene derivatives on the Dionex column and on the Merck optimized material during the basic and acidic stability evaluation.

## 1. Performance test and stability evaluation

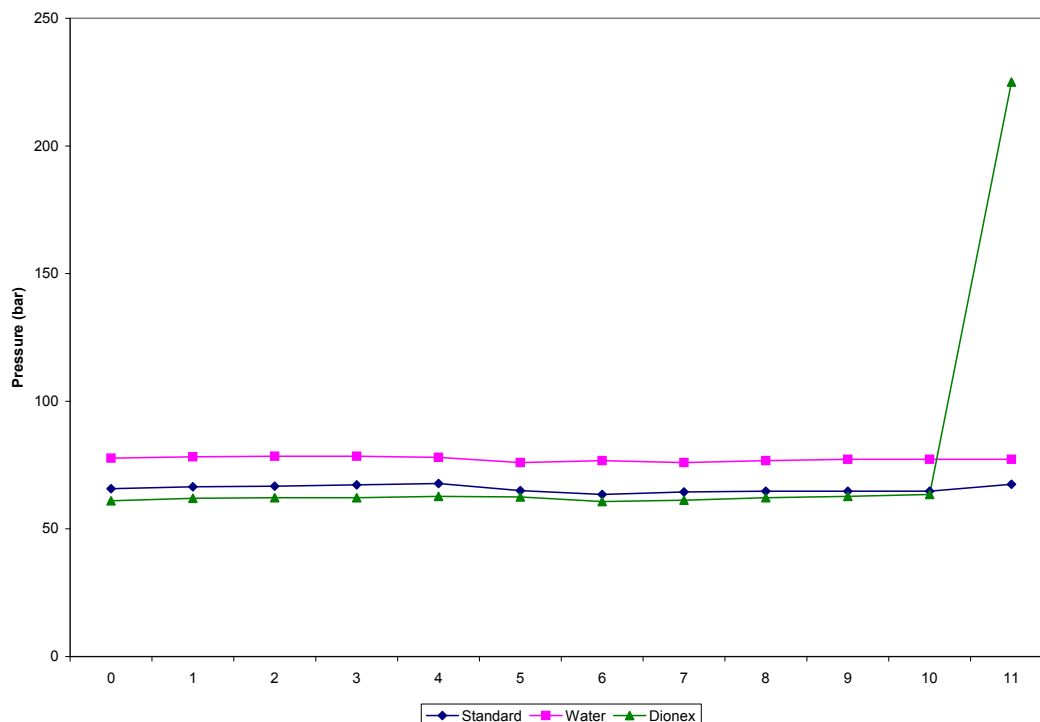


Figure 3.1.9.: Evolution of the column back pressure during the stability evaluation.

stable for every column. The back pressure measured by a standard Merck column with 50 % acetonitrile is around 65 bar and working with the Dionex material leads to a pressure of 60 bar. The optimized Merck material exhibits much higher back pressure with 75 bar. However, the back pressure with both Merck columns remained constant during the whole stability evaluation. The pressure by Dionex also remained constant until the last measurement step where the pressure rose within one minute to 225 bar. The column became definitely destroyed after the complete stress procedure.

## 1.4. Concluding remarks

Even if no comprehensive conclusions could be drawn from the classification system designed by Hoogmartens et al., we could rapidly find out that the mixed-mode RP-WAX materials exhibit no similar HPLC characteristics with any other silica-based sorbents. We could however demonstrate that the Merck and the Dionex materials are very similar in their selectivity.

Designing a specific standard mixture for the evaluation of the selectivity of the RP-WAX bonding is a really good educational tool as well as an easy-to-understand marketing example, and for quality control HPLC analysis. Furthermore, the stability evaluation could not have been performed without a dedicated selectivity test.

The stability evaluation was intended to serve as benchmark study to compare the acidic and basic stability between both Merck and Dionex materials. Both Merck materials are quite similar in this short time study, even if the standard column exhibits a slightly lower stability at lower pH. The Dionex column is similar to the optimized Merck material at low pH. However, at higher pH, the Dionex material is less stable than the Merck columns. The Merck material is very stable in an usual pH range. This was not tested during a specific stability test, but the whole validation depicted in Chapter 2 was performed at

pH 4.4 on a single column. Being able to fully validate a HPLC method is already an indication of good stability. The  $\beta$ -blocker analysis from Chapter 3 was also performed on a single column at pH between 7.25 and 8.75. During the whole study, at least 15000 column volumes were pumped through the column.



## **2. Simultaneous separation and analysis of water- and fat- soluble vitamins on multi-modal reversed phase – weak anion exchange material by HPLC-UV**

### **2.1. Introduction**

Vitamins are organic compounds that are essential in small amounts for cell metabolism. Vitamins cannot be synthesized by the organism and must therefore be regularly absorbed to the body via nutrition in order to avoid deficiency. The relationship between vitamin deficiencies and their symptoms are well-known since the beginning of the twentieth century although the impact of vitamin-rich food on the general health has been identified a long time before vitamins were identified. Eijkman received the Nobel price in 1929 for identifying the relationship between the lack of vitamin B1 and beriberi, which is endemic in Eastern Asia [105]. Scurvy as a consequence of vitamin C deficiency was identified by Szent-Györgyi Nagrapolt and he received also the Nobel Prize in 1937 for his discovery [106].

The first attempt to cure such deficiencies consisted in adapting the diet to prevent the emergence of diseases. A well-balanced diet is sufficient to cover the daily vitamin requirements. Multi-vitamin supplements were however developed in order to prevent and cure deficiencies of individuals being at risk for hypovitaminoses due to absorption failures, pregnancy, stress, bad food habits, and acute or chronic diseases.

It became therefore necessary to develop analysis methods in order to evaluate the quality of such dietary supplements. One challenge for vitamin analyzes is caused by the fact that vitamins are very different in their chemical properties. Vitamins of the B family for example are water-soluble whereas K vitamins are fat-soluble. Most of the validated methods are proposed for the quantitation of either hydrophilic [107, 108, 109, 110, 111] or lipophilic vitamins [112, 113], just to cite the latest publications. The first attempt to characterize both vitamin groups by HPLC on a single column consisted of a solid phase extraction followed by an HPLC separation [114, 115]. The first step consisted in separating the water- and the fat-soluble vitamins from each other by RP solid-phase extraction whereas in the second step the vitamins of each group were resolved from each other on RP silica-based material. The water soluble vitamins were separated using a methanol – buffer gradient, whereas the fat-soluble ones were separated using a methanol – acetonitrile or methanol - chloroform isocratic mobile phase. Buszewski and Zbanyszek overcame this challenge by performing a single-run analysis on two different C18 columns with low and high ligand density through a column switching valve [116]. Only very few single-run single-column analyzes of water- and fat-soluble vitamins were published. For example, the method of Li and Chen involved a multi-step gradient with a salting-desalting process on a C18 column [117]. Klejdus et al. developed a positive-negative gradient method on a Polaris C18 column [118].

The scope of our study consists in optimizing and validating a method for the simulta-

## 2. Simultaneous determination of fat- and water-soluble vitamins

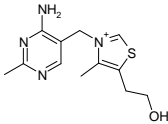
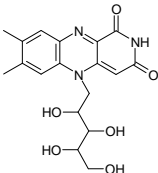
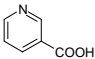
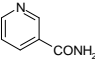
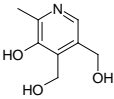
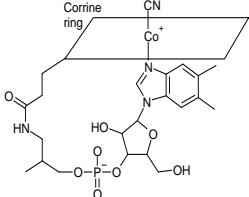
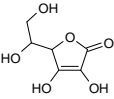
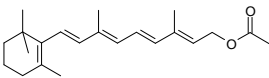
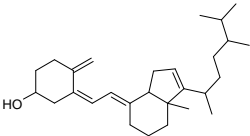
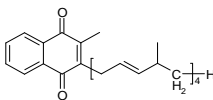
Generic name	Chemical name	Structure	Predominant deficiency disease	Recommended dietary allowances
<i>Water solubles</i>				
Vitamin B1	Thiamine		Beriberi	1.2 mg
Vitamin B2	Riboflavin		Ariboflavinois	1.3 mg
Vitamin B3	Nicotinic acid		Pellagra	16.0 mg
Vitamin B3-amide	Niacin amide		id.	id.
Vitamin B6	Pyridoxine		Anemia	1.3 - 1.7 mg
Vitamin B12	Cyanocobalamin		Megaloblastic anemia	2.4 µg
Vitamin C	Ascorbic acid		Scurvy	90.0 mg
<i>Fat soluble</i>				
Vitamin A-acetate	Retinol acetate		Keratomalcia	900 µg
Vitamin D3	Cholecalciferol		Osteomalcia	5.0 - 10.0 µg
Vitamin K1	Phyllochinon		Bleeding diathesis	120 µg

Table 3.2.1.: Names and structures of the considered vitamins, their main deficiency diseases and the recommended dietary allowances.

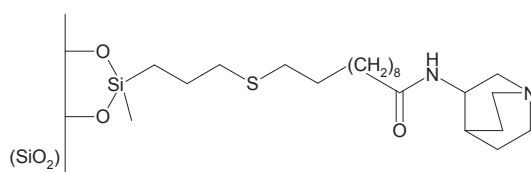


Figure 3.2.1.: Structure of the developed mixed-mode reversed phase - weak anion exchange (RP-WAX) separation material.

neous separation of eleven hydrophilic and lipophilic vitamins on a mixed-mode RP-WAX stationary phase. Names, structure, predominant deficiency disease, and recommended dietary allowances for the considered vitamins are given in Table 3.2.1 [119].

RP-WAX chromatography combines both reversed phase (RP) and weak anion exchange (WAX) groups, which leads to a high versatility in usage [98]. The structure of the mixed-mode ligand is given in Figure 3.2.1. The vitamins are either hydrophobic and interact therefore with the RP chain. The retention of the water-soluble ones is influenced by the presence of positively-charged, negatively-charged, or neutral polar groups which can interact with polar binding sites of the stationary phase. After optimization and validation of the method for simultaneous baseline separation of all vitamins, we determined the vitamin contents in commercially available supplement to demonstrate the applicability of the method.

## 2.2. Material and methods

### 2.2.1. Chemicals

RP-WAX modified silica material was prepared in our laboratory using an optimized proprietary manufacturing process which was partly published [1, 77].

Mobile phases for chromatography were prepared from HPLC grade acetonitrile, disodium hydrogen phosphate, sodium dihydrogen phosphate (Merck). Vitamins were purchased from Sigma-Aldrich (Steinheim, Germany). Log D values were calculated for pH 4.4 with ACD/Labs 7.00 software from Advanced Chemistry Development (Toronto, Canada).

### 2.2.2. Instrumentation

The chromatographic experiments were carried out on a VWR (Darmstadt, Germany) Hitachi LaChrom Elite HPLC system (three channels pump L-2130 with degasser, autosampler L 2200, oven L-2350, diode array detection (DAD) system L-2455). The data were processed using the Agilent (Waldbronn, Germany) EZChrom Elite version 3.21 software.

The gradient optimization was performed on a VWR Hitachi LaChrom Ultra HPLC system (two single-channel pumps L-2160U, autosampler L-2200U, oven L-2300, DAD system L-2455U). The optimization data were processed using ChromSword Auto version 4.0.1.

### 2.2.3. Sample preparation

Stock solutions of single vitamins were prepared in methanol at concentrations up to 3 mg/L or up to the limit of solubility. The working solutions with single vitamins were

## 2. Simultaneous determination of fat- and water-soluble vitamins

prepared at the desired concentrations by dilution of the stock solutions. The vitamin mixtures were prepared at the desired concentration directly from pure compounds. All solutions were stored at -20 °C after sonicating and filtered on a 0.2 µm PTFE syringe filter before being placed in the autosampler. The solutions were freshly prepared every two days except for the sample stability study.

The vitamin tablets (see Table 3.2.2 for ingredients) were dissolved in 20 ml water. After sonication and filtration on a 0.2 µm PTFE syringe filter, the mixture was directly injected on the column.

### 2.2.4. Chromatographic conditions

A column filled with the RP-WAX material described previously [77] (125 x 4 mm, 5 µm particle size, 100 Å) was used for the analysis. The injection volume was 10 µl and the flow rate was set to 1.0 ml/min. Four different wavelengths (260 nm, 270 nm, 300 nm, and 310 nm) were evaluated. The best results were obtained at 270 nm for almost every vitamin. Vitamin A acetate exhibits very low absorbance at this wavelength and the validation was therefore performed at 310 nm for this molecule. The simultaneous determination was performed at both wavelengths.

Mobile phase composition, pH, temperature, and gradient were optimized (see Section 2.3.1). Best results were obtained with a mobile phase containing water and acetonitrile in the presence of phosphate buffer (see Table 3.2.3). Dead volume  $t_0$  was determined by injecting pure methanol ( $t_0 = 1.70$ ).

### 2.2.5. Method validation

The method validation was performed according to the guidelines of the International Conference on Harmonization of Technical Requirements for Registration of Pharmaceuticals for Human Use (ICH).

#### 2.2.5.1. Selectivity

Standard vitamin solutions were first injected onto the column and the evaluation of the obtained chromatogram allowed us to ensure the purity of the stock solutions. The selectivity of the method was then demonstrated by comparison of the chromatogram of the vitamin mixture and of the real samples with chromatograms monitored for each vitamin standard solution.

#### 2.2.5.2. Robustness

The robustness of the vitamins quantification must be assessed through small deliberate variations of the method parameters [120]. We investigated the effect of small variations of the temperature, the pH, the buffer concentration and the slope of the gradient, which we identified as critical parameters. The relative standard deviation of the retention time was then calculated for each vitamin and the limit of deviation was set up to 5 %.

#### 2.2.5.3. Linearity

Evaluating the linearity of the method consists in verifying that the peak area for each vitamin in the chromatogram is directly proportional to the concentration in the mixture within a given range [121]. We evaluated the linearity for each vitamin within the mixture from 25 µg/L up to the limit of solubility. Ten measurements were performed between



Supplier	Rossmann	Penny
Brand	ALTRAPHARMA	Omni VIT
Name	A-Z Depot + Multivitamin Mineral	A-Z
	Biotin	Biotin
	Calcium carbonate	Calcium-D-Pantothenate
	Calcium-D-pantothenate	Calciumhydrogenphospahte
	Calciumhydrogenphosphate	Chromium(III) chloride
	Chromium(III) chloride	Iron(II) fumarate
	Iron(II) fumarate	Folic acid
	Iron oxide and iron hydroxide	Cellulose
	Polysorbate 80	Gum arabic
	Folic acid	Hydroxypropylmethylcellulose
	Cellulose	Sodium-carboxymethylcellulose
	Potassium chloride	Potassium chloride
	Potassium iodide	Potassium iodide
	Copper-(II) sulfate	Copper-(II) sulfate
	Magnesium oxide	Lutein
	Mangan-(II) sulfate	Magnesium oxide
	Sodium molybdate	Mangan-(II) sulfate
	Sodium selenate	Sodium molybdate
	Nicotinamide	Sodium selenate
	Titan dioxide	Titan dioxide
	Silicium dioxide	Silicium dioxide
	Talc	Talc
	Vitamin A	Vitamin A
	Vitamin B1	Vitamin B1
	Vitamin B12	Vitamin B12
	Vitamin B2	Vitamin B2
	Vitamin B6	Vitamin B6
	Vitamin C	Vitamin C
	Vitamin D3	Vitamin D3
	Vitamin E	Vitamin E
	Vitamin K1	Vitamin K1
	Zinc oxide	Zinc oxide

Table 3.2.2.: Composition of the vitamin tablets analyzed in this study.

## 2. Simultaneous determination of fat- and water-soluble vitamins

Time (min)	%B
0	0
2	0
7	12
22	82
30	97
33	97
34	0
40	0

Table 3.2.3.: Mobile phase composition for the optimal simultaneous separation of fat- and water- soluble vitamins.

Solvent A: 85 % water, 10 % 100 mM phosphate buffer pH 4.4, 5% acetonitrile

Solvent B: 18 % water, 2 % 100mM phosphate buffer pH 4.4, 80 % acetonitrile

the lower concentrations and the limit of linearity (tantamount to the upper limit of quantitation, ULOQ) of each molecule in order to obtain more accurate measurements. If calibration curves were observed to be non-linear, the upper limit of linearity ULOQ was stepwise reduced until the calibration curve for the resultant data set became linear. The slope and intercept were calculated using the least-square regression method.

The residual standard deviation is calculated as follows:

$$s = \sqrt{\frac{\text{RSS}}{n - 2}} \quad (2.2.1)$$

where RSS is the residual sum of squares and n the number of data for validation.

The relative residual standard deviation can then be calculated:

$$V_0 = 100 \times \frac{s}{b\bar{x}}[\%] \quad (2.2.2)$$

where  $b$  is the slope and  $\bar{x}$  the means of the concentrations.

For the two-tailed Fisher's exact test, we calculated at first the residual standard deviation with a quadratic function  $sy_2$ , which allowed us to determine the  $F_{\text{calc}}$  value [122]:

$$F = (n - 2)sy_2^2 - (n - 3)sy_2^2 \quad (2.2.3)$$

The  $F_{\text{table}}$  is given by the  $F_{\text{table}}$  data set at 99 % confidence. It depends for each vitamin on the number of measured data. The  $F_{\text{table}}$  is read with  $f_1=1$  and  $f_2=N-3$  where  $N$  is the number of measurements. If  $F_{\text{calc}} \leq F_{\text{table}}$ , the data set is linear in the chosen range[123].

### 2.2.5.4. Detection and quantitation limit

The limit of detection (LOD) for each vitamin is the lowest amount of analyte which can be detected and the limit of quantitation is the lowest concentration for quantitative determination with sufficient precision and accuracy [124]. We calculated both values from the calibration line at low concentration.

$$\text{LOD; LOQ} = \frac{F \cdot \text{SD}}{b} \times 100[\mu\text{g/ml}] \quad (2.2.4)$$

where  $F$  is a factor of 3.3 and 10 for LOD and LOQ respectively,  $\text{SD}$  the standard deviation of the blank calculated after ten repetitions of a blank injection and  $b$  the slope of the regression line.

#### 2.2.5.5. Precision and accuracy

Intraday ( $n = 6$ ) and interday ( $n = 6$ ) precisions are expressed as standard deviation percentage of the calculated concentration. They correspond to the degree of scatter between the series of measurements, respectively measured six times consecutively within a single day or measured once a day during six consecutive days [125]. The accuracy given in percentage corresponds to the closeness of agreement between the measured concentration and the theoretical value. Precision and accuracy were determined for six different theoretical concentrations (see Table 3.2.4) [126].

#### 2.2.5.6. Range

The range is given in mg/L as interval of concentrations for which precision is under 2 %, accuracy is in the 95 – 105 % range, recovery is stable and between the LLOQ and the ULOQ [127].

#### 2.2.5.7. Storage stability

To assess storage stability the evolution of the peak area was compared for each vitamin within the mixture during 15 hours at room temperature and during five days in four different conditions. For the 15-hour measurements, the mixture remained in the autosampler at RT. For the 5-day measurements, the mixture was prepared at day 0 and it was aliquoted in autosampler vials. One set of vial was stored at  $-28^{\circ}\text{C}$  in the absence of light and another one was stored in the dark at  $+4^{\circ}\text{C}$ . The two last set of vials were stored at room temperature, with and without light respectively. For each measurement, the vial was put in the autosampler shortly before injection.

## 2.3. Results and discussion

### 2.3.1. Method development

The difficulty of the separation of both water- and fat-soluble vitamins in a single chromatographic run is due to the fact that some vitamins are very polar (for example vitamin B1 or vitamin B6) whereas vitamins D3 and K1 were the most lipophilic in our study. The use of mixed-mode chromatography lead to a good separation of all species: the presence of both functionalities (apolar RP chain and polar neutral as well as polar ionic group) on a single ligand allows a bi-modal gradient which lead to baseline separation of all vitamins (see Figure 3.2.2).

#### 2.3.1.1. Effect of pH

First the impact of pH on the retention of the water-soluble vitamins was evaluated with a very simple acetonitrile gradient. The data presented in the figure 3.2.3 were generated with the optimum gradient (see paragraph 2.3.1.3).

Six different pHs were studied from pH 3 to pH 8. The basic molecules bearing a proton-acceptor nitrogen group (vitamins B1, B3-amide, and B6) exhibit very low retention on the RP-WAX material, and baseline separation was only obtained around pH 4 (see Figure 3.2.3 top). In order to find the optimum separation, a narrower pH range was investigated with 6 buffer systems from pH 4 to pH 5. Even minor pH variations in this range change the selectivity of the RP-WAX material for the investigated vitamins dramatically. It turned out that best separation was obtained at pH 4.4.

## 2. Simultaneous determination of fat- and water-soluble vitamins

	Vitamin B <sub>1</sub> [mg/ml]	Vitamin B <sub>2</sub> [mg/ml]	Vitamin B <sub>3</sub> [mg/ml]	Vitamin B <sub>3</sub> -amide [mg/ml]	Vitamin B <sub>6</sub> [mg/ml]	Vitamin B <sub>12</sub> [mg/ml]	Vitamin C [mg/ml]	Vitamin A - acetate [mg/ml]	Vitamin D <sub>3</sub> [mg/ml]	Vitamin K <sub>1</sub> [mg/ml]
Solution 1	0,8	0,016	2,4	1,2	1,2	3	0,8	2	2	2,5
Solution 2	0,64	0,0128	1,92	0,96	0,96	2,4	0,64	1,6	1,6	2
Solution 3	0,48	0,096	1,44	0,72	0,72	1,8	0,48	1,2	1,2	1,5
Solution 4	0,32	0,064	0,96	0,48	0,48	1,2	0,32	0,8	0,8	1
Solution 5	0,16	0,0032	0,48	0,24	0,24	0,6	0,16	0,4	0,4	0,5
Solution 6	0,008	0,003	0,0096	0,0048	0,0072	0,024	0,008	0,008	0,004	0,0025

Table 3.2.4.: Concentration of the vitamins in each solution for the determination of accuracy and precision.

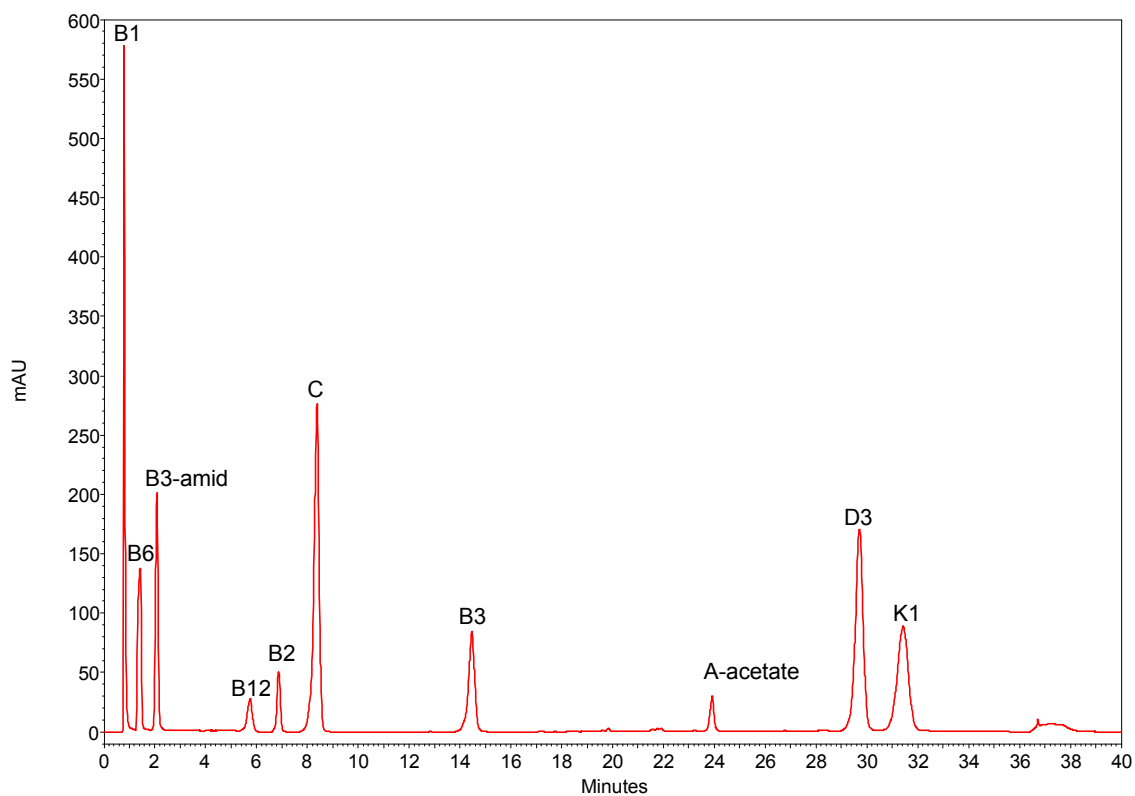


Figure 3.2.2.: HPLC-UV chromatogram of a standard mixture of 10 water- and fat-soluble vitamins under optimized gradient elution conditions.

Conditions: water / 100 mM phosphate buffer pH 4.4 / acetonitrile (85:10:5, v/v/v) (A) and water / 100 mM phosphate buffer pH 4.4 / acetonitrile (18:2:80, v/v/v), (B), 0' – 0 % B, 2' – 0 % B, 7' – 12 % B, 22' – 82 % B, 30' – 97 % B, 33' – 97 % B, 34' – 0 % B, 40' – 0 % B, temperature = 25°C, flowrate = 1 ml/min, injection volume = 10µl, detection at 280 nm.

## 2. Simultaneous determination of fat- and water-soluble vitamins

Most of the pH values lead to a baseline separation of polar and acidic vitamins B2, B3, B12, and C although the best resolution is obtained between pH 4 and 5. Retention times of these vitamins are higher than for the basic compounds B1, B3-amide and B6. The pH value of 4.4 is suitable for the separation of the nitrogen-rich vitamins and can therefore be used for the simultaneous separation of all the water-soluble vitamins.

The effect of the pH on the net retention time (i.e. retention time minus  $t_0$ ) of the fat-soluble vitamins A-acetate, D3, and K1 is due to their non-ionogenic nature almost negligible, as expected (see Figure 3.2.3 top panel). A slight increase with pH and a minor maximum around pH 4.4, respectively, may be noticed. Yet baseline separation is maintained over the entire pH range with significantly higher retention times in comparison to the water soluble vitamins. A simultaneous separation of all vitamins is possible at pH 4.4.

The plot of symmetry factors against pH under the same conditions reveals better symmetries at pH 4.4 (see Figure 3.2.3 bottom). The pH remained therefore fixed at pH 4.4 for further optimization and for the validation of the method.

### 2.3.1.2. Effect of temperature

The separation was evaluated at 25°C (Figure 3.2.3 a) and at 35 °C (Figure 3.2.3 b). Both retention times and symmetry factors were little affected by the temperature variation (see Figure 3.2.3). The optimization of the gradient was therefore performed at 25°C.

### 2.3.1.3. Adjustment of the gradient

The buffer and acetonitrile gradient were automatically optimized with ChromSword at the pH and temperature set previously. The idea was to combine a salt gradient along with an acetonitrile gradient. While the buffer concentration was decreased during the run, the organic modifier concentration was increased in the same time.

To get started, some isocratic runs were performed first to evaluate the lower and higher acetonitrile concentration at a fixed salt concentration of 10 mM. We found out, that 5 % acetonitrile was a suitable starting amount of organic modifier. Next, the effect of the starting salt concentration was evaluated between 2.5 mM and 15 mM, with a modifier percentage of 5 % acetonitrile in the mobile phase at the beginning of the gradient run. The resolution between the first two eluting peaks (vitamin B1 and B6) increased gradually when the buffer strength at the beginning of the gradient run was increased from 2.5 mM up to 10 mM. Above this value, no change in the resolution was observed. We therefore fixed the starting buffer concentration at 10 mM. However, at higher acetonitrile content, the salt precipitated and an elution of the most hydrophobic vitamins with 80 % acetonitrile was only possible with very low buffer concentration (< 3 mM) to avoid precipitation. After a few optimization runs, we set up the minimum at 2 mM. The optimized gradient profile is shown in Figure 3.2.4 resulting a separation as depicted in Figure 3.2.2.

Performing the whole separation with a decreasing buffer gradient is not only important for efficient separation of the water-soluble vitamins. It also avoids the risk of phosphate precipitation at higher acetonitrile concentration.

### 2.3.2. Elution order and mechanism

Within the first two minutes of the separation, vitamins bearing a protonated nitrogen group are separated on the RP-WAX material in the order of their polarity (B1,  $\log D_{4.4} = -2.19$ ; B6,  $\log D_{4.4} = -1.88$ ; B3-amide,  $\log D_{4.4} = -0.17$ ) and eluted very quickly

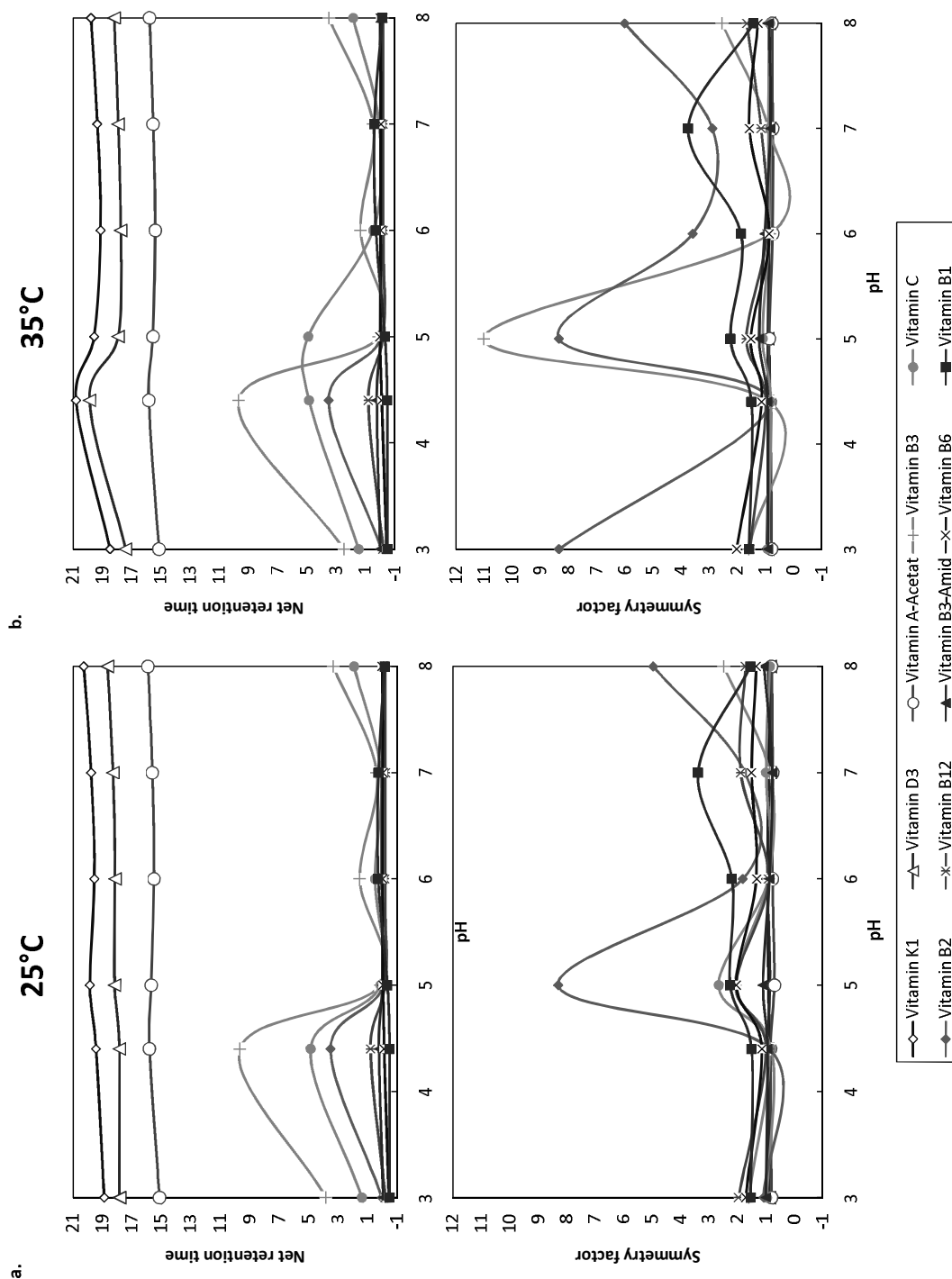


Figure 3.2.3.: Effect of the pH and of the temperature on the retention factor (a) and on the symmetry factor (b) of the vitamins.

The symmetry factor was calculated at 10 % of the peak height:  $A_S = \frac{t_p}{t_p}$  where  $t_p$  and  $f_p$  represent the width of respectively the tail and the front of the peak at the considered height.

## 2. Simultaneous determination of fat- and water-soluble vitamins

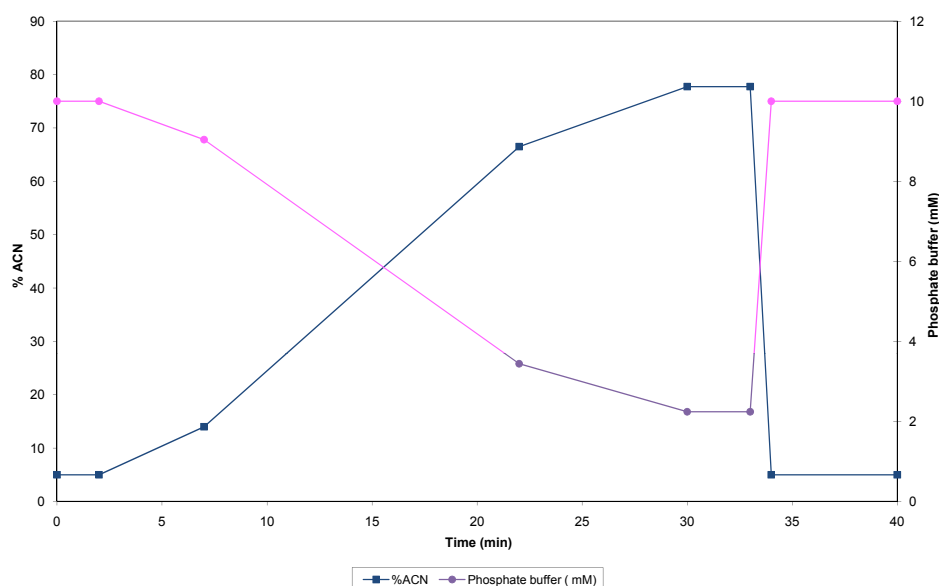


Figure 3.2.4.: Optimized gradient profile with respect to acetonitrile content and phosphate buffer concentration as obtained by automatic gradient profile optimization with ChromSword.

due to electrostatic repulsion at very low acetonitrile concentration. Vitamins B1 and B6 elute even before void volume, denoting an elution in ion-exclusion mode, also known as electrostatic repulsion mode [128, 129]. Other polar molecules such as vitamins B12 (log  $D_{4.4}$  cannot be calculated with ACD due to Co(II) and too many ionization states) and B2 (log  $D_{4.4}$  = -2.31) are eluted within the next 8 minutes by increasing the acetonitrile amount. During the increase of the concentration of organic modifier, the buffer concentration is slowly reduced, which leads to a longer retention time of acidic vitamins such as vitamins C (log  $D_{4.4}$  = -2.73) and B3 (log  $D_{4.4}$  = -1.31), which elute between 8 and 15 minutes. All the fat-soluble vitamins are eluted from 20 to 32 minutes through an increase of the acetonitrile concentration with a low gradient slope in the order A-acetate (log  $D_{4.4}$  = 7.39), D3 (log  $D_{4.4}$  = 9.72) and K1 (log  $D_{4.4}$  = 12.25) (see Figure 3.2.4). It is striking that within each group (hydrophilic cationic vitamins B1, B6, B3-amide; hydrophilic neutral or zwitterionic B12, B2; hydrophilic acidic C, B3; lipophilic neutral A-acetate, D3, K1) the solutes eluted in order of decreasing polarity, yet the ionic character plays a more dominant role for the general elution pattern as expected. In this method, the different vitamin clusters are eluted under different chromatographic modes, following an ion exclusion and ion repulsion mechanism, respectively, for vitamin B1, B6, and B3-amide, then switching to an ion exchange mode for vitamin B3 and C, and finally shifting to a reversed phase mode for neutral and hydrophobic compounds, respectively (e.g. vitamin A-acetate, D3, K1).

### 2.3.3. Method validation

#### 2.3.3.1. Selectivity and robustness

The selectivity of the method was evaluated by injections of single vitamin standards as well as of mixtures of vitamin standards. All the vitamins were baseline separated and selectivity between distinct solutes was satisfactory. From the single component injections



it was evident, that the purity of the reference compounds was sufficient for all vitamins to perform a validation. Individual vitamin standard solutions were allowed to stand at room temperature for controlled degradation. No interferences from degradation products were observed.

Robustness was evaluated for buffer molarity in the eluent ( $10 \text{ mM} \pm 0.5 \text{ mM}$ ), gradient time ( $30 \text{ min} \pm 2 \text{ min}$ ), temperature ( $25^\circ\text{C} \pm 1^\circ\text{C}$ ), and pH ( $4.4 \pm 0.2$ ). Mean relative standard deviations of retention time are given in Figure 3.2.5. For most of the vitamins, the deviation remains below 5 %, which is sufficient to ensure the robustness of the method. Molarity and gradient slope have a more pronounced effect on vitamin retention. The small temperature difference has almost no effect on the retention time and the pH has only little effect except for vitamin B12. The relative standard deviation reaches almost 20 % for this compound, which means that the method pH has to be controlled with utmost care i.e. to  $\text{pH } 4.4 \pm 0.05$ .

### 2.3.3.2. Linearity and assay sensitivity

The linearity was evaluated for each vitamin within the concentration range  $5 \text{ }\mu\text{g/ml}$  – limit of solubility. For vitamins with even higher limit of solubility, we arbitrary fixed the upper limit at  $3000 \text{ }\mu\text{g/ml}$ . After having measured more than eleven concentration levels for each compound, the data set was reduced until a linear calibration function was obtained. Decision on the validity of the linear calibration function was based on the F-test value (see Table 3.2.5). The upper limit of linearity ULOL was set to the value corresponding to a range in which the confidence of the model is better than 99 %. The limits of detection and quantitation for each vitamin were calculated from the calibration curve.

### 2.3.3.3. Accuracy and precision

The values of accuracy and precision are given in Table 3.2.6. Both intra-assay and inter-day precisions remain below 5 % for all vitamins over the entire range except for inter-day precisions of vitamin C. For this vitamin, the worse inter-day precisions may be ascribed to limited stability of this compound.

Likewise, intra-assay and inter-day accuracies are also in an acceptable range for all vitamins except for the lowest tested concentration level and vitamin C. The latter is again a result of the stability problem.

### 2.3.3.4. Range

Considering all the data described in the last paragraphs, we could determine a suitable range in which the quantitation of the vitamins can be performed due to satisfactory assay validity. The range was fixed to concentrations between the LLOQ and ULOQ, for which recovery was stable, precision better than 5%, and accuracy within 90 – 110 %. The adapted ranges are given in Table 3.2.7.

### 2.3.3.5. Storage stability

The stability of the vitamin mixture stored in the autosampler was evaluated over 15 hours. The deviation of the peak area is given in Figure 3.2.6. The least stable vitamins are the vitamins A-acetate and C. The peak area is continuously slightly decreasing for both vitamins during the whole time range, however, no additional interfering peaks were observed

## 2. Simultaneous determination of fat- and water-soluble vitamins

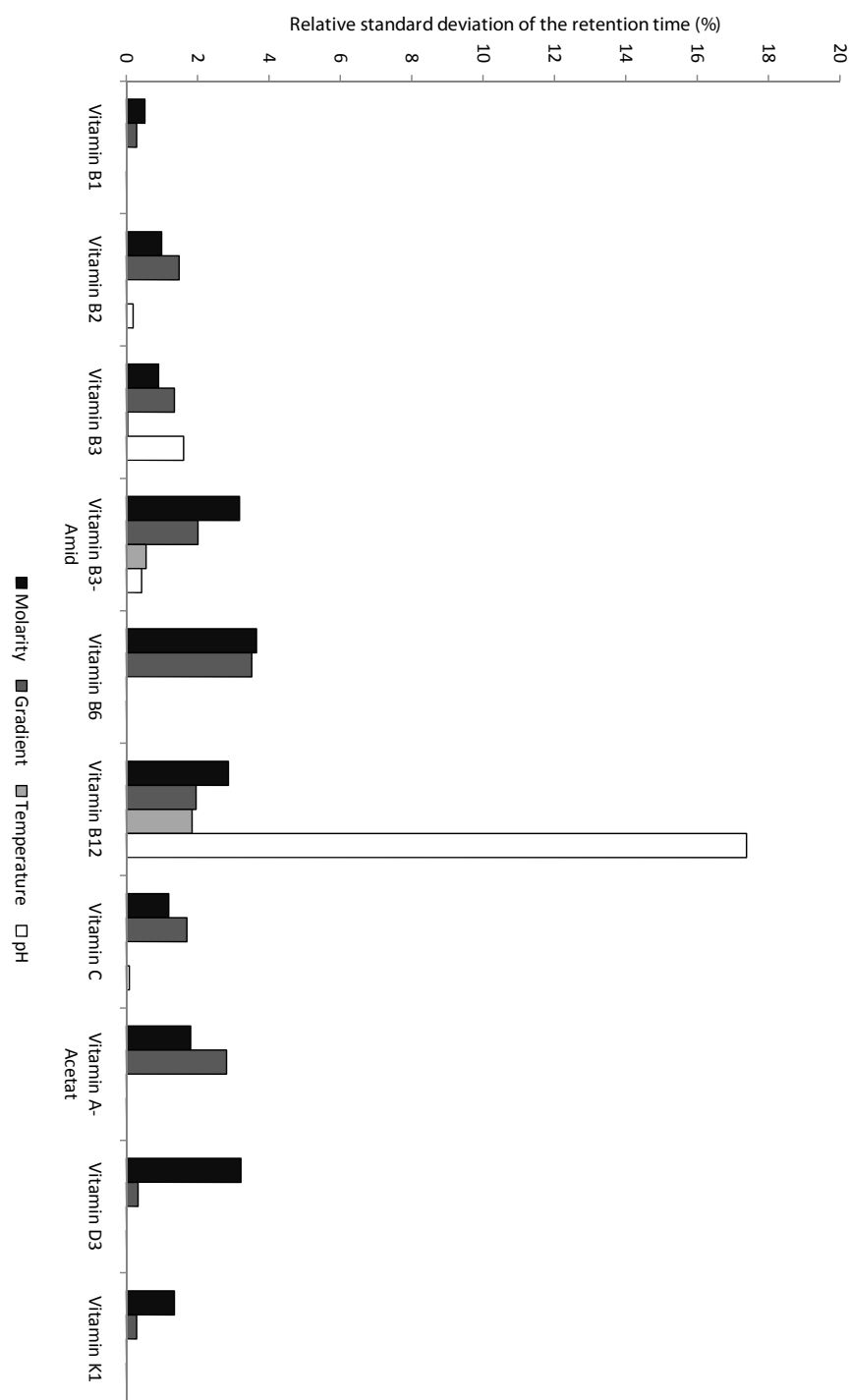


Figure 3.2.5.: Evaluation of the robustness of the method by plotting the relative standard deviation of the retention time for four different parameters (buffer molarity, gradient slope, temperature, and pH).

	Number of data points	Linearity					Analytical measurement limits		
		Slope	Intercept	r <sup>2</sup>	Residual standard deviation	Relative residual standard deviation (%)	F <sub>table</sub> (99 %)	F <sub>calc</sub>	ULOQ <sup>a</sup> (µg/ml)    LOD (µg/ml)    LOQ (µg/ml)
B1	10	49290833	268756	0,9992	407292	1,98	12,25	7,00	800    0,937    2,840
B6	7	29027381	474145	0,9999	135624	0,78	21,20	4,00	1200    1,591    4,822
B3-amide	7	33727937	284614	0,9996	326490	1,61	21,20	4,00	1200    1,370    4,150
B12	11	6874945	-204839	0,9978	336909	3,26	11,26	8,00	3000 <sup>b</sup> 6,719    20,360
B2	5	137747691	-22777	0,9957	49815	4,02	34,10	2,00	150 <sup>b</sup> 0,335    1,016
C	9	133338589	517540	0,9992	1063851	1,99	13,75	6,00	800    0,346    1,050
B3	9	30316561	-985550	0,9972	1410992	3,88	13,75	6,00	2400    1,524    4,617
A-acetate	11	61964118	-96734	0,9990	1484536	2,39	11,26	8,00	2000    0,745    2,259
D3	8	94336619	466515	0,9997	1228751	1,24	16,26	5,00	2100    0,490    1,484
K1	11	78237454	-4342720	0,9970	3723830	3,81	11,26	8,00	2500    0,590    1,789

Table 3.2.5.: Linearity and analytical measurement limits for the different vitamins.

<sup>a</sup> ULOQ stands for Upper Limit of Quantitation.<sup>b</sup> Limit of solubility.

## 2. Simultaneous determination of fat- and water-soluble vitamins

Solution	Precision									
	B1	B6	B3-amide	B12	B2	C	B3	A-acetate	D3	K1
Intraday (n=6)										
1	0,23	0,90	0,53	1,46	1,05	1,72	0,39	1,39	1,64	1,42
2	0,39	0,37	0,47	0,73	0,99	0,37	0,04	0,29	0,28	0,14
3	0,50	0,58	0,44	1,17	0,28	0,26	0,49	0,39	0,28	0,46
4	0,75	0,33	0,27	0,19	0,34	1,04	0,30	0,44	0,44	0,42
5	0,16	0,20	0,14	1,01	0,26	0,62	0,75	1,28	0,59	0,09
6	0,57	0,30	0,22	0,59	0,29	0,17	0,15	0,07	0,17	0,19
Interday (n=6)										
1	1,32	1,37	0,72	2,07	1,26	27,13	0,20	2,85	2,24	1,02
2	1,36	0,24	1,09	4,85	1,06	19,73	0,12	1,97	1,66	0,22
3	1,54	0,83	0,60	2,21	1,56	15,86	0,70	1,68	0,69	0,21
4	1,15	3,63	0,53	2,27	1,14	41,99	0,68	0,20	1,00	0,99
5	0,99	0,62	0,74	0,24	1,47	2,87	1,26	1,00	0,79	0,53
6	1,26	0,33	0,53	2,73	1,30	22,73	0,64	1,12	10,12	0,34

(a)

Solution	Accuracy									
	B1	B6	B3-amide	B12	B2	C	B3	A-acetate	D3	K1
Intraday (n=6)										
1	97,45	99,41	99,69	95,13	102,05	94,23	100,60	97,93	102,16	101,77
2	99,24	98,64	99,68	101,15	97,13	94,99	95,06	96,33	99,34	96,13
3	103,97	101,02	99,79	91,79	97,28	90,60	97,04	97,47	101,90	96,59
4	103,13	91,43	95,80	90,37	98,20	51,87	94,04	86,34	98,36	95,71
5	98,26	104,56	99,95	95,23	102,56	64,53	92,49	86,65	98,16	104,08
6	18,75	77,23	75,35	218,90	103,54	7,17	93,49	152,92	125,27	230,58
Interday (n=6)										
1	97,35	99,22	99,02	94,37	101,81	68,81	100,18	77,37	100,99	101,15
2	98,55	98,67	99,01	98,69	95,08	81,22	95,05	95,93	97,95	96,25
3	103,08	100,20	99,69	90,85	96,20	84,82	96,74	95,52	101,58	97,03
4	102,38	97,82	96,44	91,28	98,80	68,00	96,86	95,91	98,42	94,69
5	104,05	104,46	100,62	97,22	99,80	79,91	96,51	95,91	98,44	104,19
6	19,74	77,34	74,06	223,40	100,80	33,50	95,46	95,91	114,81	230,75

(b)

Table 3.2.6.: Intraday (n=6) and interday (n=6) precision and accuracy data for all the validated vitamins.

	Range ( $\mu\text{g/ml}$ )	
	Lower limit	Upper limit
B1	160	800
B6	240	1200
B3-amide	240	1200
B12	600	2400
B2	3	150
C	stability problem <sup>a</sup>	
B3	5	2400
A-acetate	400	1600
D3	400	2100
K1	500	2500

Table 3.2.7.: Measurement range of various vitamins.

<sup>a</sup>See Table 3.2.6, specially inter-day precision and accuracy.

in the chromatogram. However, within the first five hours, the deviation decreased gradually by less than 5 % and the mixture should be allowed to be used five hours long before preparing a fresh one. The stability of the mixture in a Peltier-autosampler thermostated to 6°C was not evaluated but the stability of the mixture should be improved.

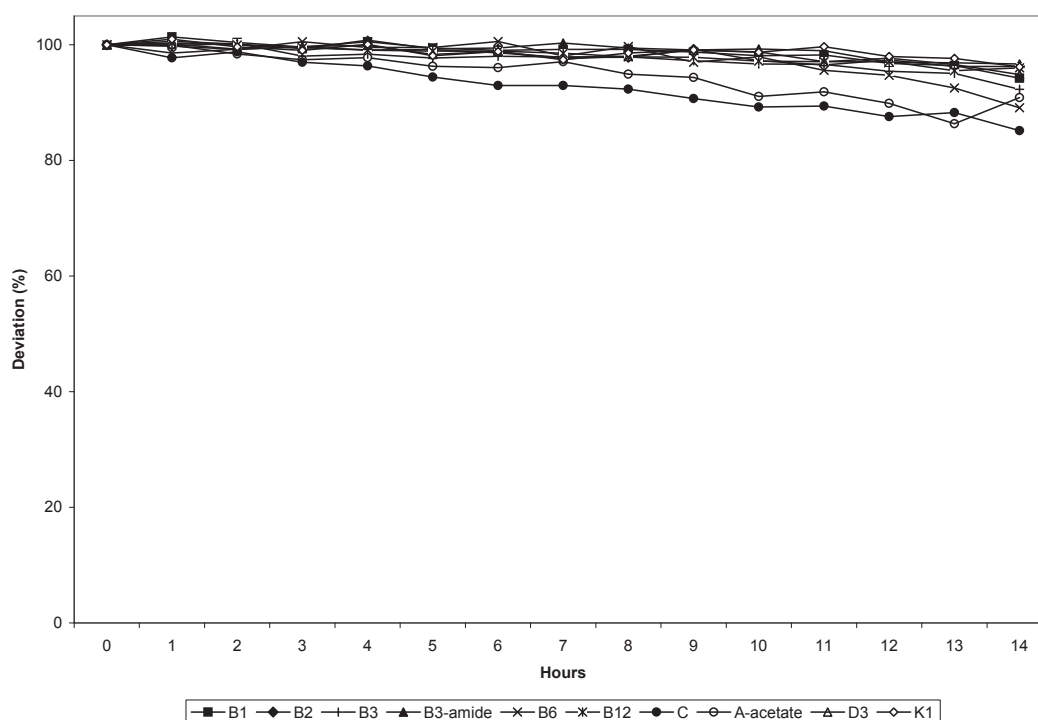


Figure 3.2.6.: Evolution of the stability of the vitamin mixture considering the peak area over 15 hours of storage in the autosampler at 25°C.

In Figure 3.2.7, the stability of the mixture at four different conditions within six days is compared. In the freezer, at  $-28^{\circ}\text{C}$ , all the vitamins within the mixture are stable over the whole period. The less stable vitamin remains the vitamin C, even if the deviation by less than 10 % is not dramatic. However, in order to maintain a deviation as low as

## *2. Simultaneous determination of fat- and water-soluble vitamins*

possible, a fresh solution should be prepared every two days if the mixture is freeze-stored.

At + 4°C, the stability is quite similar for most of the vitamins. For the two vitamins A-acetate and C, even one day of storage is sufficient for the peak area to decrease significantly.

At room temperature in the absence of light, both vitamins A-acetate and C are even less stable. The peak area of the vitamin B12 is also decreasing rapidly.

In the presence of light, most of the vitamins are decomposing rapidly, even if some of them are still stable, like vitamins B3-amide and B6. The deviation of the peak area for vitamin B2, which was quite stable at every previous storage conditions, is decreasing very fast in this case. The decomposition of riboflavin to peroxides and tryptophan derivatives due to light reaction is well known [130].

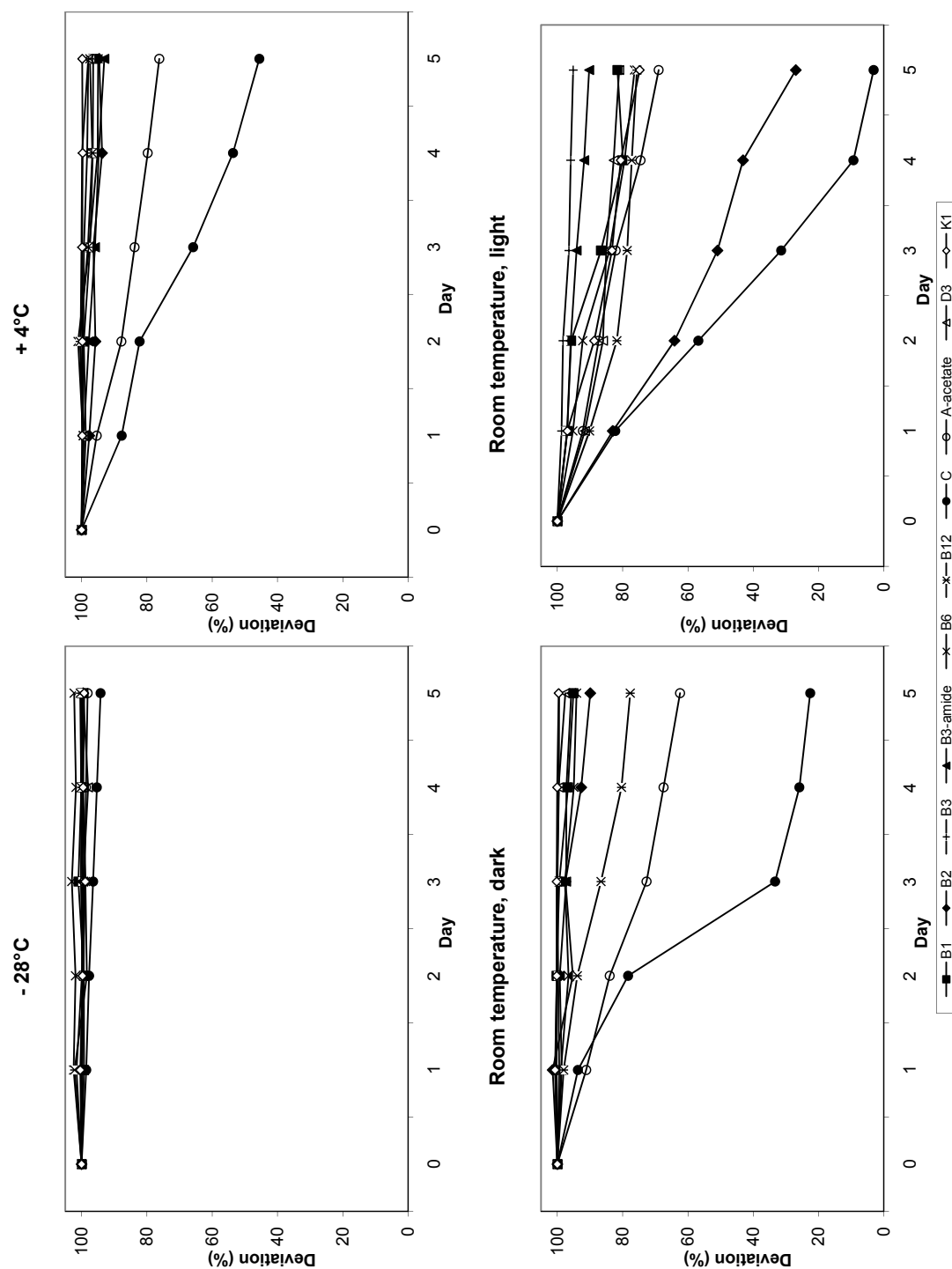


Figure 3.2.7.: Deviation of the peak area for each vitamin at 4 different storage conditions.

### 2.3.4. Identification and determination of vitamins in multivitamin tablets

Vitamin levels in both multivitamin tablets were determined using this new validated method. Chromatogram corresponding to analysis of one of the tablets is given in Figure . A reasonable agreement was found between specified and experimentally determined values i.e. recoveries were quite acceptable (see Table 3.2.8). Only the very hydrophobic compounds could not be quantified accurately because the concentrations in the tablet were below LLOQs. In order to reach the LLOQs for these compounds the tablets have to be dissolved in a smaller volume, which was however, impossible due to solubility limitations of vitamins and/or excipients. Sample preparation has therefore to be adapted to include an enrichment step which however was beyond the primary focus of the present study.

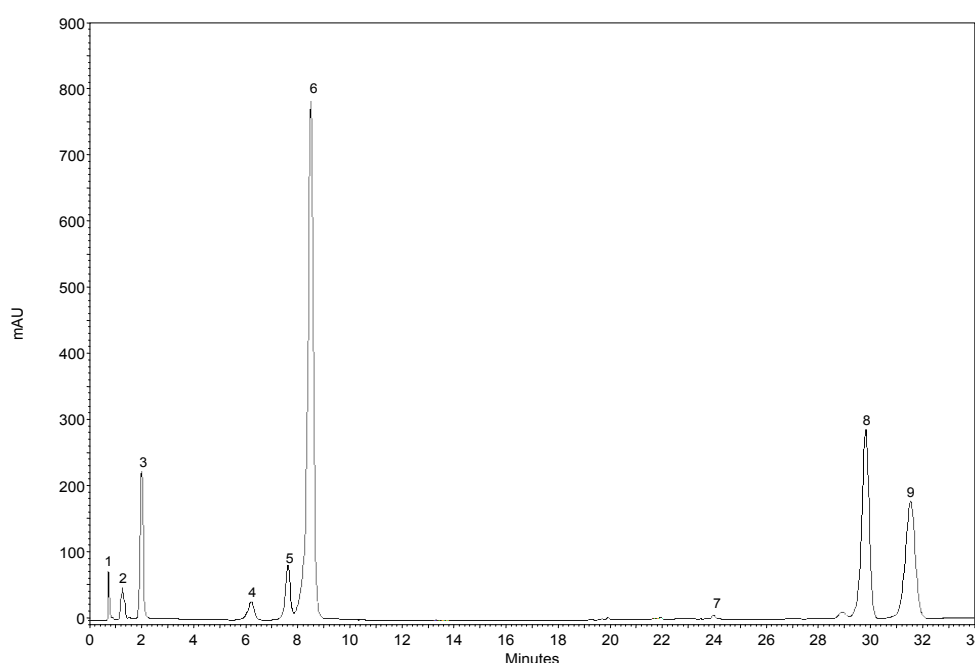


Figure 3.2.8.: HPLC-UV chromatogramm of the Rossmann tablet under optimized gradient elution conditions.

Conditions: water / 100 mM phosphate buffer pH 4.4 / acetonitrile (85:10:5, v/v/v) (A) and water / 100 mM phosphate buffer pH 4.4 / acetonitrile (18:2:80, v/v/v), (B), 0' – 0 % B, 2' – 0 % B, 7' – 12 % B, 22' – 82 % B, 30' – 97 % B, 33' – 97 % B, 34' – 0 % B, 40' – 0 % B, temperature = 25°C, flowrate = 1 ml/min, injection volume = 10µl, detection at 280 nm. 1: Vitamin B1, 2: Vitamin B6, 3: Vitamin B3-Amid, 4: Vitamin B12 , 5: Vitamin B2, 6: Vitamin C, 7: Vitamin A-Acetat, 8: Vitamin D3, and 9: Vitamin K1.

## 2.4. Conclusion

The current method for the simultaneous separation of water- and fat-soluble vitamins on RP-WAX material offers an alternative selectivity to the one on C18 columns. A challenge for the simultaneous quantitative analysis remains, however, the limited compound stability of vitamins which may be associated with poor method validation results as well as



	Altapharma				Omnivit			
	Labeled amount [mg/tablet]	Spiking level [mg/tablet]	Experimental amount including spiking [mg/tablet]	Accuracy (determined as recovery) (%)	Labeled amount [mg/tablet]	Spiking level [mg/tablet]	Experimental amount including spiking [mg/tablet]	Accuracy (determined as recovery) (%)
B1	1.4	0	1.51±0.02	108	1.4	0	1.40±0.02	100
B2	1.6	0	1.68±0.02	105	1.6	0	1.78±0.02	111
B3-amide	18	0	19.10±0.02	106	18	0	18.00±0.03	100
B6	2	0	2.16±0.01	108	2	0	2.00±0.01	100
A-acetate	0.8	2	2.95±0.06	105	0.8	1.2	1.82±0.06	91
D3	0.005	1.2	1.30±0.02	108	0.005	1.0	1.02±0.03	101
K1	0.03	1	1.04±0.01	101	0.03	0.7	0.74±0.01	101

Table 3.2.8.: Real sample analysis of two different commercially available tablets.

## *2. Simultaneous determination of fat- and water-soluble vitamins*

the huge concentration differences of vitamins in formulations. However, the use of mixed-mode chromatography for the analysis of mixtures containing compounds with different chemical properties could lead to faster one-step methods for specific applications.

### 3. Simultaneous separation of seven $\beta$ -blockers on multi-modal reversed phase – weak anion exchange material

#### 3.1. Introduction

$\beta$ -Adrenoceptor antagonists, better known as  $\beta$ -blockers, are widely used in the treatment of several cardiovascular, neurological and neuropsychiatric diseases, such as hypertension, cardiac arrhythmia, coronary insufficiency, glaucoma, anxiety and migraine. The International Olympic Committee (IOC) also added this class of compounds to the list of forbidden drugs because of their blood pressure regulatory and tremor decreasing effects [131]. Presence of these molecules in waste water and surface water has also been demonstrated, as well as their exotoxicity [132, 133]. Rapid determination of these molecules by High Performance Liquid Chromatography (HPLC) has therefore to be ensured. Seven different  $\beta$ -blockers amongst most popular ones have been chosen for our method development using our new RP-WAX materials (see Figure 3.3.1).

Standard HPLC separation of  $\beta$ -blockers is usually performed on Reversed Phase (RP) C18 and C8 columns [134]. On conventional C18 material, the separation of some  $\beta$ -blockers is rather difficult. For instance, sotalol and atenolol are extremely difficult to separate, even with complex method development [135]. With C8 columns, a slightly better resolution can be observed but the  $\alpha$  value remains low [136]. As expected significant separation enhancement was achieved with smaller particle diameters [134].

Different reversed phase – weak anion exchange (RP-WAX) materials have been developed in the last years. Their broad range of use includes the analysis of pharmaceuticals, food and beverage constituents, as well as fine chemicals. It provides also a complementary method to conventional RP columns leading to orthogonal selectivity [137]. Mixed-mode RP-WAX phases have been recently proposed for several applications, such as peptide separations, organophosphate metabolism studies, ethanol consumption marker analysis in urine, and chromatographic profiling of mycotoxins [98].

RP-WAX chromatography was developed to combine RP and anion-exchange retention and selectivity principles for separation of very different compounds. It can be operated in different modes, such as classical RP mode (e.g. for neutral molecules), WAX mode (for negatively charged solutes), ion exclusion chromatographic mode (cationic solutes), HILIC mode (polar neutral, basic, amphoteric, and acidic compounds), and hydrophobic interaction chromatography mode (for e.g. larger peptides). To our knowledge, no application of such RP-WAX phases was developed in combined reversed phase – weak cation repulsion mode. In order to evaluate the feasibility of the separation of weak cations by a mixed gradient, we studied the separation of seven different  $\beta$ -blockers in isocratic mode on a RP-WAX material developed in our laboratory (see Figure 3.3.2), considering organic modifier amount, pH, buffer type and buffer concentration as experimental variables to adjust retention and selectivity. Finally a gradient HPLC method was developed for the simultaneous separation of those seven compounds on RP, HILIC and RP-WAX materials.

### 3. Simultaneous separation of seven $\beta$ -blockers

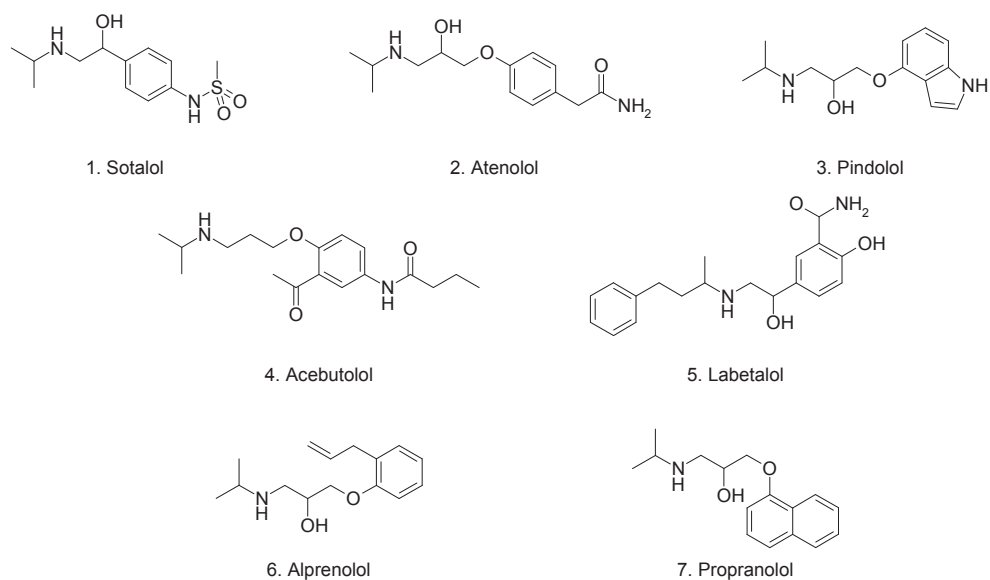


Figure 3.3.1.: Structure of the  $\beta$ -blockers investigated in present study.

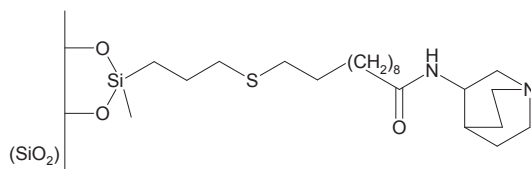


Figure 3.3.2.: Structure of the developed mixed-mode reversed phase - weak anion exchange (RP-WAX) separation material.

## 3.2. Material and methods

### 3.2.1. Chemicals

RP-WAX modified silica material was prepared in our laboratory using an optimized proprietary manufacturing process which was partly published [1, 77]. Purospher STAR RP-18e and ZIC-HILIC columns were obtained from Merck (Darmstadt, Germany). Mobile phases for chromatography were prepared from HPLC grade acetonitrile, tris(hydroxymethyl)aminomethane (TRIS), disodium hydrogen phosphate, sodium dihydrogen phosphate, analytical grade hydrochloric acid, acetic acid and trifluoroacetic acid (Merck).  $\beta$ -Blockers were purchased from Sigma-Aldrich (Steinheim, Germany).

### 3.2.2. Instrumentation

The chromatographic experiments were carried out on a VWR (Darmstadt, Germany) Hitachi LaChrom Elite HPLC system (three channels pump L-2130 with degasser, autosampler L 2200, oven L-2350, diode array detection (DAD) system L-2455). The data were processed using the Agilent (Waldbronn, Germany) EZChrom Elite version 3.21 software.

Gradient optimization was performed on a VWR Hitachi LaChrom Ultra HPLC system (two single-channel pumps L-2160U, autosampler L-2200U, oven L-2300, DAD system L-2455U).

### 3.2.3. Determination of retention factors

The retention factor of each analyte was determined at 10 different acetonitrile concentrations, 3 different pH, 2 different salt concentrations and 2 different buffer types, leading to 840 data points. Retention times higher than 30 minutes were not recorded in order to keep the retention times within reasonable length. At lower pH and higher acetonitrile concentration, some  $\beta$ -blockers eluted at void volume or even before because of complete cation exclusion mechanisms. For 20 mM TRIS buffer pH 7.25, a significant number of  $\beta$ -blockers eluted before  $t_0$  (ion-exclusion). Since retention factors are not defined for compounds eluting in this regime, they were not included in the further data processing so that the data matrix was reduced to 525 points (see Tables 3.3.1, 3.3.2, 3.3.3, and 3.3.4).

In order to facilitate comparison of different chromatographic conditions, salt concentration had to remain constant. To ensure this, we used therefore a ternary gradient pump (A – water; B – acetonitrile; C – 200 mM buffer). B was varied from 5 to 50 % with 5 % increments, C remained always constant at 5% for 20 mM measurements and at 50% for 100 mM measurements.

### 3.2.4. Method optimization

Optimization was performed and data were processed using ChromSword Auto version 4.0.1. ChromSword is a software tool that is able to automatically find the optimum conditions for HPLC [138]. The on-line rapid method screening used for gradient optimization in this study performs two different gradients before determining the best conditions for separation. Both gradients are multi-point non-linear gradients with same %B at start and end of gradient. The optimized method is then used to perform the last run. ChromSword is supposed to be used for binary gradient systems, which requires the pre-selection of two different mobile phases composition (for the beginning and the end of the gradient). At the beginning, the mobile phase which leads to a good resolution in isocratic mode for the

### 3. Simultaneous separation of seven $\beta$ -blockers

100 mM		pH 7.25								
Phosphate-	% acetonitrile									
buffer	5	10	15	20	25	30	35	40	45	50
Atenolol	0.46	0.23	0.09	-	-	-	-	-	-	-
Sotalol	1.07	0.61	0.36	0.20	0.10	-	-	-	-	-
Acebutolol	5.39	2.61	1.40	0.80	0.47	0.25	0.14	0.08	-	-
Pindolol	10.14	4.90	2.66	1.66	1.02	0.86	0.44	0.30	0.23	0.20
Labetalol	-	-	12.67	6.05	3.17	1.82	1.14	0.78	0.58	0.48
Alprenolol	-	-	11.09	5.68	2.83	1.79	1.10	0.74	0.54	0.42
Propranolol	-	-	19.57	9.16	4.68	2.61	1.61	1.08	0.80	0.70
100 mM		pH 8.00								
Phosphate-	% acetonitrile									
buffer	5	10	15	20	25	30	35	40	45	50
Atenolol	0.70	0.35	0.21	-	-	-	-	-	-	-
Sotalol	1.40	0.75	0.46	0.29	0.18	-	-	-	-	-
Acebutolol	11.78	4.91	2.52	1.39	0.82	0.50	0.31	0.20	0.13	-
Pindolol	-	9.05	4.88	2.90	1.82	1.22	0.85	0.63	0.50	0.42
Labetalol	-	-	12.10	5.95	3.18	1.88	1.18	0.80	0.59	0.45
Alprenolol	-	-	-	10.14	5.54	3.31	2.04	1.38	1.00	0.77
Propranolol	-	-	-	16.62	8.49	4.84	2.95	1.97	1.44	1.12
100 mM		pH 8.75								
Phosphate-	% acetonitrile									
buffer	5	10	15	20	25	30	35	40	45	50
Atenolol	2.20	1.02	0.56	0.34	0.20	0.11	0.05	-	-	-
Sotalol	1.56	0.90	0.55	0.37	0.25	0.18	0.12	-	-	-
Acebutolol	-	10.60	5.22	2.90	1.76	1.12	0.78	0.56	0.42	0.33
Pindolol	-	19.80	10.14	6.00	3.79	2.54	1.77	1.30	0.99	0.78
Labetalol	-	-	9.53	4.65	2.40	1.33	0.76	0.46	0.31	0.21
Alprenolol	-	-	-	-	11.24	6.40	3.89	2.50	1.73	1.25
Propranolol	-	-	-	-	16.92	9.20	5.39	3.38	2.32	1.67

Table 3.3.1.: Capacity factor of seven  $\beta$ -blockers determined at 100 mM phosphate buffer, three different pH and ten different acetonitrile concentrations.

*Conditions:* column Purospher STAR RP-WAX 5 $\mu$ m 125 x 4 mm, tris- or phosphate-buffer at given concentration (A) and acetonitrile (B), isocratic at given acetonitrile concentration, *Temperature* = 25°C, *Flow rate* = 1 ml/min, *Injection volume* = 10 $\mu$ l, *Detection* at 225 nm.

Data is not given for retention time lower than void volume (i.e. ion exclusion) or for retention time higher than 30 minutes.

20 mM		pH 7.25									
Phosphate-		% acetonitrile									
buffer		5	10	15	20	25	30	35	40	45	50
Atenolol		0.72	0.13	-	-	-	-	-	-	-	-
Sotalol		1.26	0.47	0.28	0.17	-	-	-	-	-	-
Acebutolol		7.46	3.29	1.67	0.89	0.49	0.27	0.14	-	-	-
Pindolol		11.04	5.14	2.84	1.74	1.13	0.72	0.50	0.38	0.28	0.24
Labetalol		-	-	11.91	6.06	3.33	1.93	1.26	0.87	0.64	0.50
Alprenolol		-	-	12.12	6.46	3.62	2.13	1.38	0.94	0.87	0.51
Propranolol		-	-	-	10.98	5.70	3.26	2.07	1.42	1.27	0.80
20 mM		pH 8.00									
Phosphate-		% acetonitrile									
buffer		5	10	15	20	25	30	35	40	45	50
Atenolol		0.99	0.48	0.16	0.06	-	-	-	-	-	-
Sotalol		1.82	0.94	0.47	0.30	0.20	0.14	-	-	-	-
Acebutolol		15.06	6.36	2.62	1.48	0.92	0.60	0.41	0.29	0.20	0.15
Pindolol		-	14.49	6.18	3.59	2.32	1.60	1.17	0.88	0.69	0.56
Labetalol		-	-	12.74	6.29	3.43	2.04	1.31	0.90	0.64	0.48
Alprenolol		-	-	-	13.67	7.56	4.50	2.92	1.98	1.40	1.04
Propranolol		-	-	-	-	12.00	6.82	4.30	2.89	2.04	1.52
20 mM		pH 8.75									
Phosphate-		% acetonitrile									
buffer		5	10	15	20	25	30	35	40	45	50
Atenolol		5.33	2.69	1.90	1.41	1.00	0.76	0.66	0.46	0.37	0.31
Sotalol		2.77	1.59	1.14	0.85	0.68	0.56	0.40	0.40	0.33	-
Acebutolol		-	19.81	10.75	6.54	4.03	2.66	1.84	1.33	1.00	0.78
Pindolol		-	14.94	10.10	7.21	4.88	3.40	2.39	1.78	1.34	1.04
Labetalol		-	-	11.12	5.40	2.96	1.67	1.03	0.71	0.48	0.36
Alprenolol		-	-	-	-	13.64	8.37	5.35	3.50	2.40	1.71
Propranolol		-	-	-	-	19.34	11.29	6.98	4.44	3.01	2.13

Table 3.3.2.: Capacity factor of seven  $\beta$ -blockers determined at 20 mM phosphate buffer, three different pH and ten different acetonitrile concentrations.

*Conditions:* column Purospher STAR RP-WAX 5 $\mu$ m 125 x 4 mm, tris- or phosphate-buffer at given concentration (A) and acetonitrile (B), isocratic at given acetonitrile concentration, *Temperature* = 25°C, *Flow rate* = 1 ml/min, *Injection volume* = 10 $\mu$ l, *Detection* at 225 nm.

Data is not given for retention time lower than void volume (i.e. ion exclusion) or for retention time higher than 30 minutes.

### 3. Simultaneous separation of seven $\beta$ -blockers

100 mM	pH 7.25									
Tris-	% acetonitrile									
buffer	5	10	15	20	25	30	35	40	45	50
Atenolol	-	-	-	-	-	-	-	-	-	-
Sotalol	-	-	-	-	-	-	-	-	-	-
Acebutolol	4.20	1.49	0.61	0.23	-	-	-	-	-	-
Pindolol	2.56	1.21	0.59	0.27	-	-	-	-	-	-
Labetalol	-	12.81	5.49	2.44	1.12	0.53	0.24	-	-	-
Alprenolol	10.15	5.25	2.70	1.34	0.64	0.29	-	-	-	-
Propranolol	-	9.59	4.43	2.05	0.97	0.45	-	-	-	-
100 mM	pH 8.00									
Tris-	% acetonitrile									
buffer	5	10	15	20	25	30	35	40	45	50
Atenolol	0.76	0.31	0.19	-	-	-	-	-	-	-
Sotalol	0.98	0.50	0.25	-	-	-	-	-	-	-
Acebutolol	8.48	3.45	1.51	0.72	0.32	-	-	-	-	-
Pindolol	5.49	2.80	1.46	0.80	0.41	0.20	-	-	-	-
Labetalol	-	21.87	10.33	5.03	2.55	1.38	0.79	0.46	0.29	0.18
Alprenolol	-	11.35	5.81	3.01	1.56	0.83	0.43	-	-	-
Propranolol	-	21.08	9.78	4.65	2.29	1.19	0.64	0.35	-	-
100 mM	pH 8.75									
Tris-	% acetonitrile									
buffer	5	10	15	20	25	30	35	40	45	50
Atenolol	1.76	0.99	0.53	0.23	0.17	-	-	-	-	-
Sotalol	1.69	1.02	0.65	0.42	0.26	-	-	-	-	-
Acebutolol	23.02	9.30	4.24	2.06	1.09	0.61	0.37	-	-	-
Pindolol	15.96	8.03	4.38	2.43	1.42	0.86	0.53	0.33	-	-
Labetalol	-	-	14.69	7.59	4.13	2.45	1.52	1.04	0.88	0.56
Alprenolol	-	-	16.88	8.67	4.60	2.56	1.48	0.91	0.58	0.38
Propranolol	-	-	-	13.59	6.74	3.63	2.06	1.26	0.82	0.55

Table 3.3.3.: Capacity factor of seven  $\beta$ -blockers determined at 100 mM tris buffer, three different pH and ten different acetonitrile concentrations.

*Conditions:* column Purospher STAR RP-WAX 5 $\mu$ m 125 x 4 mm, tris- or phosphate-buffer at given concentration (A) and acetonitrile (B), isocratic at given acetonitrile concentration, *Temperature* = 25°C, *Flow rate* = 1 ml/min, *Injection volume* = 10 $\mu$ l, *Detection* at 225 nm.

Data is not given for retention time lower than void volume (i.e. ion exclusion) or for retention time higher than 30 minutes.



20 mM	pH 7.25									
Tris-	% acetonitrile									
buffer	5	10	15	20	25	30	35	40	45	50
Atenolol										
Sotalol										
Acebutolol										
Pindolol	Number of elutions above $t_0$ too low to be significant									
Labetalol										
Alprenolol										
Propranolol										
20 mM	pH 8.00									
Tris-	% acetonitrile									
buffer	5	10	15	20	25	30	35	40	45	50
Atenolol	-	-	-	-	-	-	-	-	-	-
Sotalol	-	-	-	-	-	-	-	-	-	-
Acebutolol	5.72	2.24	0.83	0.26	-	-	-	-	-	-
Pindolol	4.06	1.94	0.89	0.35	0.15	-	-	-	-	-
Labetalol	-	-	12.74	6.05	2.98	1.55	0.82	0.45	0.23	-
Alprenolol	18.09	9.03	4.40	2.05	0.93	0.38	-	-	-	-
Propranolol	-	16.32	7.80	3.47	1.52	0.89	0.26	-	-	-
20 mM	pH 8.75									
Tris-	% acetonitrile									
buffer	5	10	15	20	25	30	35	40	45	50
Atenolol	3.36	1.97	1.08	0.59	0.33	0.19	-	-	-	-
Sotalol	2.16	1.44	0.98	0.66	0.45	0.31	-	-	-	-
Acebutolol	-	12.55	5.84	3.08	1.72	1.05	0.65	0.41	0.27	-
Pindolol	16.52	9.67	5.26	3.12	1.88	1.22	0.77	0.49	0.32	-
Labetalol	-	-	13.61	7.41	4.19	2.55	1.68	1.15	0.82	0.61
Alprenolol	-	-	18.97	10.10	5.51	3.16	1.97	1.26	0.77	0.51
Propranolol	-	-	-	15.89	8.11	4.49	2.70	1.68	1.14	0.72

Table 3.3.4.: Capacity factor of seven  $\beta$ -blockers determined at 20 mM tris buffer, three different pH and ten different acetonitrile concentrations.

*Conditions:* column Purospher STAR RP-WAX 5 $\mu$ m 125 x 4 mm, tris- or phosphate-buffer at given concentration (A) and acetonitrile (B), isocratic at given acetonitrile concentration, *Temperature* = 25°C, *Flow rate* = 1 ml/min, *Injection volume* = 10 $\mu$ l, *Detection* at 225 nm.

Data is not given for retention time lower than void volume (i.e. ion exclusion) or for retention time higher than 30 minutes.

### 3. Simultaneous separation of seven $\beta$ -blockers

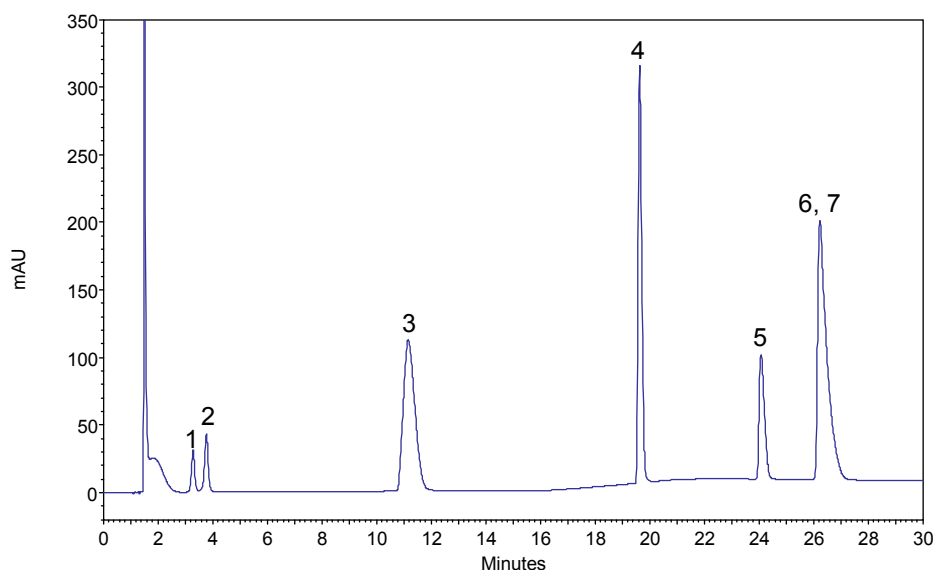


Figure 3.3.3.: Chromatogram of seven  $\beta$ -blockers separated on a C18 column (5  $\mu$ m, 125 x 4 mm).

*Analytes:* sotalol (1), atenolol (2), pindolol (3), acebutolol (4), labetalol (5), alprenolol (6), propranolol (7).

*Conditions:* water containing 0.03 % TFA (A) and water – acetonitrile (50:50, v/v) containing 0.3 % TFA (B), 0' – 19 % B, 1.4' – 21 % B, 13.3' – 24 % B, 18.5' – 51 % B, 30' – 51 % B, *Temperature* = 25°C, *Flow rate* = 1 ml/min, *Injection volume* = 10  $\mu$ l, *Detection* at 225 nm.

first eluting compounds is chosen as solvent A. The solvent B is the mobile phase which leads to the best resolution for the last eluted compounds within a short time.

## 3.3. Results and discussion

### 3.3.1. Separation of 7 $\beta$ -blockers on conventional HPLC materials

As basis for the study of the gradient separation of  $\beta$ -blockers by HPLC, we optimized the gradient separation on conventional HPLC stationary phases using buffer concentration and organic modifier found in the literature. Ranta et al. showed that separation of  $\beta$ -blockers on RP material could be achieved using water containing 0.03 % trifluoroacetic acid for solution A and water – acetonitrile (50:50, v/v) containing 0.03 % trifluoroacetic acid for solution B [136]. The chromatogram for the optimized RP method is given in Figure 3.3.3. As described in the literature, alprenolol and propranolol could not be separated on reversed phase material, even after extensive method optimization.

Besides standard RP chromatography, HILIC was used as complementary method. We evaluated different buffer combinations and we obtained best results using a mobile phase containing 89% to 56% acetonitrile and an aqueous 20 mM dipotassium phosphate buffer adjusted to pH 7.6 with acetic acid (see Figure 3.3.4). With this method, the analysis time could be speed-up by a factor 3. Separation of critical peak pairs in RP mode could be achieved. However, labetalol - alprenolol, and pindolol - acebutolol could not be baseline separated.

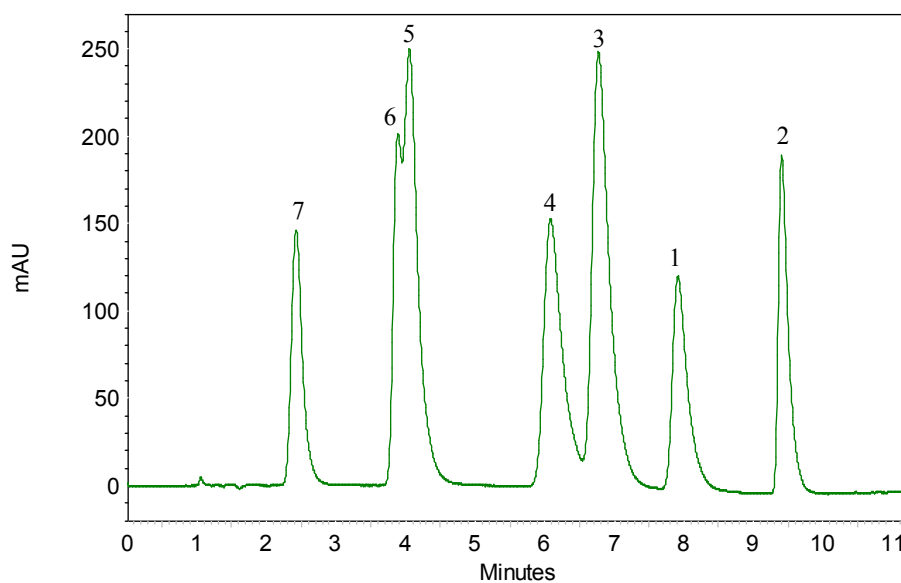


Figure 3.3.4.: Chromatogram of seven  $\beta$ -blockers separated on ZIC-HILIC column (5  $\mu$ m, 100 x 4.6 mm).

*Analytes:* sotalol (1), atenolol (2), pindolol (3), acebutolol (4), labetalol (5), alprenolol (6), propranolol (7).

*Conditions:* acetonitrile (A) and 20 mM di-potassium phosphate buffer adjusted to pH 7.6 with acetic acid (B), 0' – 11 % B, 4' – 12 % B, 11.2' – 44 % B, *Temperature* = 25°C, *Flowrate* = 1 ml/min, *Injection volume* = 10  $\mu$ l, *Detection* at 225 nm.

### 3. Simultaneous separation of seven $\beta$ -blockers

Conceptually the combination of complementary materials should lead to a complete separation of the compound mixtures, however with the necessity of on-line or off-line two-dimensional (2D) method development. 2D-chromatography can be cost-intensive and time-consuming.

Due to the intrinsic mixed-mode RP-WAX material characteristics they offer a wider potential for method optimization than classical single mode RP, ion exchange or HILIC chromatography. We investigated therefore the possibility of separating basic  $\beta$ -blockers at isocratic and optimized gradient modes.

#### 3.3.2. Effect of several parameters on the retention of 7 $\beta$ -blockers in isocratic mode

##### 3.3.2.1. Impact of acetonitrile concentration

For reversed-phase HPLC, the effect of the organic modifier on the retention time is well known: increasing the amount of organic modifier leads to diminution of the retention time through increase of the interactions between solvent and sample.

The RP-WAX function (see Figure 3.3.2) bears a C<sub>10</sub> hydrocarbon chain and has as consequence a similar behavior to RP materials regarding the effect of acetonitrile: hydrophilic  $\beta$ -blockers (i.e. atenolol) elute first whereas lipophilic  $\beta$ -blockers (i.e. alprenolol, propranolol) elute later not accounting any other increment responsible for retention. Increasing the concentration of acetonitrile in the mobile phase generally leads to shorter retention times. Thus an acetonitrile gradient can be used for a gradient optimization.

##### 3.3.2.2. Impact of pH

RP-WAX material is bearing a basic group ( $pK_a = 9.9$ ) and all  $\beta$ -blockers are also bearing basic groups. Depending on the pH the protonated WAX group will repel the protonated (ionized) amino group of the  $\beta$ -blockers at lower pH. Increasing the pH of the mobile phase will therefore lead to higher retention times as the repellent tendency will decrease (see Tables 3.3.1 to 3.3.4). To avoid too strong repulsive interactions, the separations were performed in the pH range between 7.25 to 8.75. Below 7.25, cation exclusion becomes predominant and retention disappears. At higher pH, ionization of both WAX group and solutes is gradually reduced, and hydrophobic interactions may become stronger, thus contributing in a relatively more significant extent to the net retention. Above 8.75, the retention is too high to allow fast analyzes. Even if the impact of the pH cannot be described mathematically due to the very narrow pH range, using the pH as a fine tuning parameter is a solution to improve the gradient separation.

##### 3.3.2.3. Impact of buffer type and concentration

The impact of the buffer type on the separation of  $\beta$ -blockers on RP materials was investigated by Gagliardi et al. They found out that retention times of  $\beta$ -blockers on RP sorbent were 1.5 to 4 times higher using TRIS rather than phosphate buffer [139]. In a further study they extended their work to 4 different RP columns with similar results: the retention of  $\beta$ -blockers in TRIS buffer is much higher at pH 7.84 and 8.78 even at very low salt concentrations[140]. With RP-WAX sorbent, the effect of TRIS and phosphate buffer is opposite (see Figure 3.3.5 for pindolol).

However, even with intensive molecular dynamic to study the interaction between the basic  $\beta$ -blockers and the ligands on the surface of the chromatographic materials in different salt types, no correlation could be established. Several interactions are taking place,

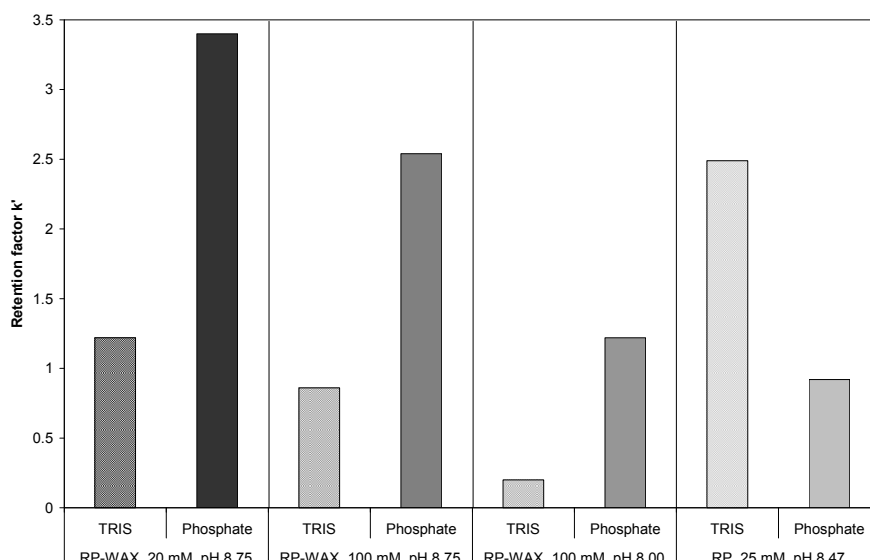


Figure 3.3.5.: Capacity factors for pindolol at 30% acetonitrile at different pH and TRIS / phosphate buffer concentrations on RP-WAX and RP columns (RP data from Ref. [139]).

such as cation repulsion and anion exchange as well with the ligand as with the buffer salts. Therefore, no general guideline for the method development can be stated, and preliminary isocratic tests should be done to determine the most suitable buffer system for each problematic.

The buffer concentration has a more general effect on the separation, which is similar for both buffers: increasing the buffer concentration leads to an ionic saturation of the system and therefore to a decrease of the retention factor for both buffers. In order to speed up the analysis and to avoid complex interactions analyte / buffer / surface modification, we performed the optimization of the gradient separation in 100 mM TRIS buffer.

### 3.3.3. Simultaneous separation of 7 $\beta$ -blockers on RP-WAX material

We investigated separation at isocratic conditions. This allowed us to get a better empirical understanding of the interactions between sample / stationary phase / mobile phase. This first step allowed us to verify the possibility to separate basic molecules on RP-WAX in reversed phase – cation repulsion mode. However, for faster method development, performing the whole isocratic runs would not have been necessary. In order to reduce the number of experiments to set up the general conditions, the use of a design of experiment would be advantageous for screening purposes. Injecting the sample at a few different conditions (i.e. by variation of pH, salt concentration, and acetonitrile content) would then have been sufficient. Nevertheless, an intensive study has to be performed because of the variety of parameters influencing the separation on mixed-mode materials.

As mentioned before, we used 100 mM Tris as a buffer. We performed automatic optimizations with three different gradients. The first one was an acetonitrile gradient from 5 to 50% with pH fixed at 8.75. The second one was a pH gradient from pH 8.75 to pH 7.25 with acetonitrile concentration fixed at 10%. The last one was a mixed gradient from pH 8.75 to pH 7.25 and from 5 to 50% acetonitrile. The retention time of the last peak and the critical resolution i.e. of the least separated adjacent peak pairs are given

### 3. Simultaneous separation of seven $\beta$ -blockers

	RP	HILIC	RP-WAX		
			ACN gradient	pH gradient	Combined gradient
Retention time of last peak	26.4	9.4	22.5	31.4	26.1
Rs min.	0	0.4	1.34	1.85	1.98

Table 3.3.5.: Resolution factor calculated from the Unite States Pharmacopoeia calculation method of the less resolved peak for each column and each RP-WAX gradient.

in Table 3.3.5 for the three optimized gradients on RP-WAX as well as for the methods developed on conventional HPLC columns.

Looking at the RP-WAX results, a simple ACN gradient method according to a common RP mode already gives a good resolution within a short time. Switching to pH gradient enhances the resolution but analysis time becomes longer. Combining both gradients in a mixed-mode method leads to an acceptable time of analysis with an excellent resolution. The best chromatogram obtained by optimization with a mixed-mode gradient is given in Figure 3.3.6.

If we compare the separation on RP-WAX material with the separations obtained on conventional phases, the advantage of using such multimodal material for separating basic compounds is obvious.

## 3.4. Conclusion

Studying isocratic separation of  $\beta$ -blockers on RP-WAX column allowed us to better understand interactions of analytes with the surface of chromatography material on both RP and RP-WAX materials. Organic modifier, pH and buffer effects have an effect on the retention of basic compounds on RP-WAX material. Hydrophilic compounds elute before lipophilic ones and increasing the concentration of acetonitrile in the mobile phase leads to shorter retention times because of the RP behavior of the mixed-mode phase. Furthermore, for those compounds, the separation is RP-driven and the elution order is similar to that observed on RP phases.

Automatic method optimization based on starting conditions defined by preliminary isocratic runs lead to complete baseline separation with nearly equal band spacing of seven  $\beta$ -blockers within a short time and with high resolution (resolution of the two worst separated compounds  $R_{s \text{ min.}} \sim 2$ ). The pH of the elution buffer has a direct impact on the retention time, as well as the buffer type, which allows a fine tuning of the separation to improve the critical resolutions and the speed of the analysis. Mixed-mode RP-WAX material provides an efficient tool for rapid separation of  $\beta$ -blockers and other solute mixtures. A new scope of application for RP-WAX material (i.e. separation of cationic compounds) could be illustrated.

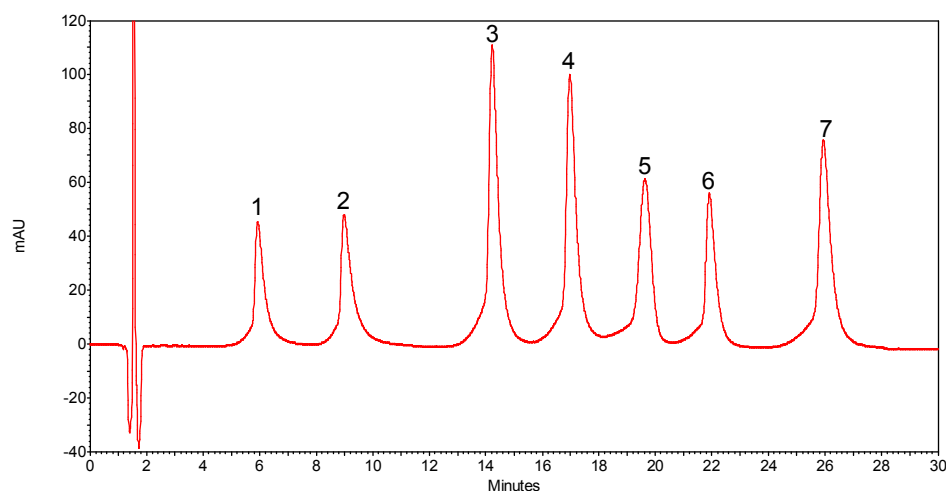


Figure 3.3.6.: Chromatogram of seven  $\beta$ -blockers separated on RP-WAX column (5  $\mu$ m, 125 x 4 mm).

*Analytes:* sotalol (1), atenolol (2), pindolol (3), acebutolol (4), labetalol (5), alprenolol (6), propranolol (7).

*Conditions:* 100 mM TRIS buffer adjusted to pH 8.75 with acetic acid / acetonitrile (95:5, v/v) (A) and 100 mM TRIS buffer adjusted to pH 7.25 with acetic acid / acetonitrile (80:20, v/v) (B), 0' – 0 % B, 4.2' – 22 % B, 16.5' – 72 % B, 22.7' – 86 % B, 30' – 86 % B, *Temperature* = 25°C, *Flow rate* = 1 ml/min, *Injection volume* = 10  $\mu$ l, *Detection* at 225 nm.

Method development was performed before optimization of the packing, which lead to poor asymmetry.





## 4. Further applications of RP-WAX mixed-mode material

### 4.1. Introduction

The last chapter of this introduction part is intended to give an overview of the variety of compounds which can be advantageously separated on a mixed-mode HPLC column. Other applications were already presented in the last chapters, not only from our work but also from other research groups. Each of the following application will therefore be presented briefly and each corresponding subsection in Section 4.3 contains the theoretical background in term of physiological applicability and importance of the HPLC for those compounds as well as the experimental results. The scope of those molecules is covering a very large chemical range. Some of them are synthetic small molecules with different characteristics, like the amphoteric antibiotics, the acidic anti-inflammatory drugs, and the acidic and neutral dermatological molecules. The isoprenoide derivatives belong to the synthetic peptide family whereas the human insulin is a biosimilar peptidic hormone.

### 4.2. Experimental

#### 4.2.1. Chemical

All the HPLC solvents were gradient grade quality from Merck (Darmstadt, Germany). The buffer salts and acidic and basic modifier were provided by the same supplier.

The norfloxacin and the norfloxacin CRS were obtained by the European Pharmacopoeia, the ciprofloxacin by Applichem (Darmstadt, Germany) and the danofloxacin by Dr. Ehrenstorfer GmbH (Augsburg, Germany). AcrosChemicals (Geel, Belgium) delivered the anti-inflammatory drugs naproxen, ibuprofen, ketoprofen, bezafibrat, and diclofenac. FPP and GGPP were purchased by Sigma Aldrich (Schnelldorf, Germany).

The human insulin and its impurities, and the Tri-Luma compounds belong to the stock of research samples in our laboratory.

#### 4.2.2. Instrumentation

The measurements at room temperature were performed on a VWR (Darmstadt, Germany) Hitachi LaChrom Elite HPLC system (three channels pump L-2130 with degasser, autosampler L 2200, oven L-2350, diode array detection (DAD) system L-2455). The chromatographic experiments at fixed temperature were carried out on a VWR (Darmstadt, Germany) Hitachi LaChrom Elite HPLC system (three channels pump L-2130 with degasser, autosampler L 2200, ultraviolet - visible (UV-Vis) detector L-2420). Gradient optimization was performed on a VWR Hitachi LaChrom Ultra HPLC system (two single-channel pumps L-2160U, autosampler L-2200U, oven L-2300, DAD system L-2455U). The experiments with fluorescence detection were carried out on a Jasco (Gross-Umstadt, Germany) system consisting of a PU-980 pump equipped with degasser DG-1580-53, tertiary

#### 4. Further applications of RP-WAX mixed-mode material

gradient unit LG-980-02 and autosampler AS-950 and the detector was a Gilson (Middleton, WI, USA) Fluorometer 122.

The data were processed using the Agilent (Waldbronn, Germany) EZChrom Elite version 3.21 software and the gradient optimization were performed using ChromSword Auto version 4.0.1 from VWR.

### 4.3. Synthetic and biosimilar neutral, amphoteric, acidic, and basic active compounds

#### 4.3.1. Amphoteric compounds: fluoroquinolone antibiotics

##### 4.3.1.1. Antibiotics mixture

The separation of three amphoteric antibiotics was evaluated at first. The structure thereof is given in Table 3.4.1. Norfloxacin and ciprofloxacin are human antibiotics of the second generation. Ciprofloxacin is used against many different bacteria infections such as cystitis, prostatitis, sinusitis and typhoid fever among others. In the USA, 12 licensed uses were approved by the FDA. Norfloxacin is mainly used as a treatment of complicated urinary tract infections but its prescription is limited due to a large number of side effects. Danofloxacin is not used for human medicine and it is classified in the veterinary drugs. Contamination or mixing of those substances should therefore be avoided and a proper fast HPLC method can be useful for quality control and regulatory purposes.

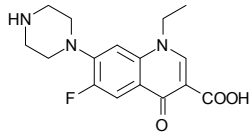
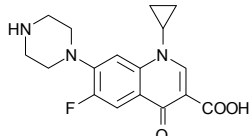
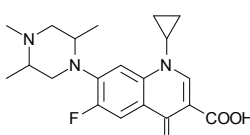
Abbreviation	Name	Structure
N	Norfloxacin	
C	Ciprofloxacin	
D	Danofloxacin	

Table 3.4.1.: Structure of the three amphoteric fluoroquinolone antibiotics.

We compared the separation on a RP18 column and on a mixed mode RP-WAX material (see Figure 3.4.1). Both separations were optimized using ChromSword Auto and several buffer type, pH and concentrations were tested. The best separation (i.e. optimum chromatogram identified by the software because of different parameters like resolution or speed of analysis) was obtained within 7 minutes in acidic conditions for the RP18 material. On the RP-WAX material, working at pH 8.0 and performing a mixed-mode gradient combining increase of the acetonitrile concentration and decrease of the pH lead to a separation as good as with the RP18 material considering the peak shape and the resolution but within only half the time needed on the RP material, i.e. 3.5 minutes.

#### 4.3. Synthetic and biosimilar neutral, amphoteric, acidic, and basic active compounds

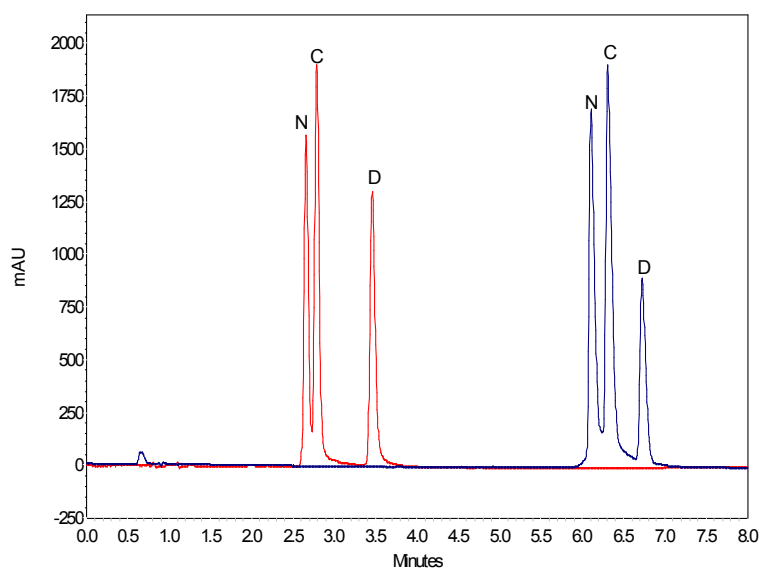


Figure 3.4.1.: Comparison of both chromatograms for the separation of norfloxacin (N), ciprofloxacin (C) and danofloxacin (D) after smart screening on RP18 (blue) and on RP-WAX (red) columns.

*Temperature:* 30 °C, *Flow rate:* 1 ml/min, *Injection:* 10 µl, *Detection:* UV 280 nm.

- *Column a:* Purospher STAR RP-18e column (125 x 4 mm), *Mobile phase:* A: Water pH 2.0, B: Acetonitrile, 0', 4 % B - 5'1, 17 % B - 10', 100 % B.

- *Column b:* Purospher STAR RP-WAX research sample column (125 x 4 mm), *Mobile phase:* A: Tris-buffer pH 8.0, B: Acetonitrile, 0.1 % acetic acid, 0', 13 % B - 6'4, 100 % B.

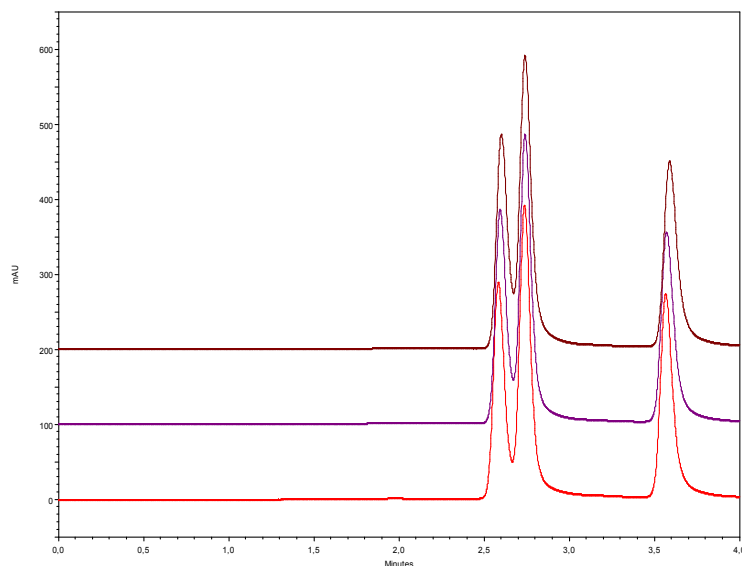


Figure 3.4.2.: Evaluation of the reproducibility of the separation of the 3 fluoroquinolone antibiotics (bottom: 1st injection, middle: 50th injection, top: 100th injection).

*Column:* Purospher STAR RP-WAX research sample column (125 x 4 mm), *Temperature:* RT, *Mobile phase:* A: Tris-buffer pH 8.0, B: Acetonitrile, 0.1 % acetic acid, 0', 13 % B - 6'4, 100 % B, *Flow rate:* 1 ml/min, *Injection:* 10 µl, *Detection:* UV 280 nm.

#### 4. Further applications of RP-WAX mixed-mode material

We did not perform a fully validation of the method but we just repeated the injection 100<sup>th</sup> times over several weeks on a single column and with different probe preparations and the chromatograms presented in figure 3.4.2 reveal only minimal changes in the peak areas. Only a low shifting of the danofloxacin is observed, which does not prohibit any peak identification. However, a proper method validation should be performed in order to evaluate the accuracy, specificity, sensitivity and precision of the method.

##### 4.3.1.2. Norfloxacin CRS

During the synthesis of norfloxacin, some impurities can be carried out in the final product because of production issues. Those side products must therefore be specifically identified and HPLC methods are the most suitable techniques for the quality control and the reaction monitoring of this synthesis [141]. To our knowledge, the separation of norfloxacin from its impurities was only performed using C18 columns [142, 143]. The chromatogram in Figure 3.4.3 is given in the leaflet of the European Pharmacopoeia delivered with the Norfloxacin CRS, a mixture for system suitability [144]. This is composed of norfloxacin in large excess along with three impurities in very low quantities (see Table 3.4.2). The validated method takes 30 minutes and the impurity E is problematic because of its proximity with the main norfloxacin peak.

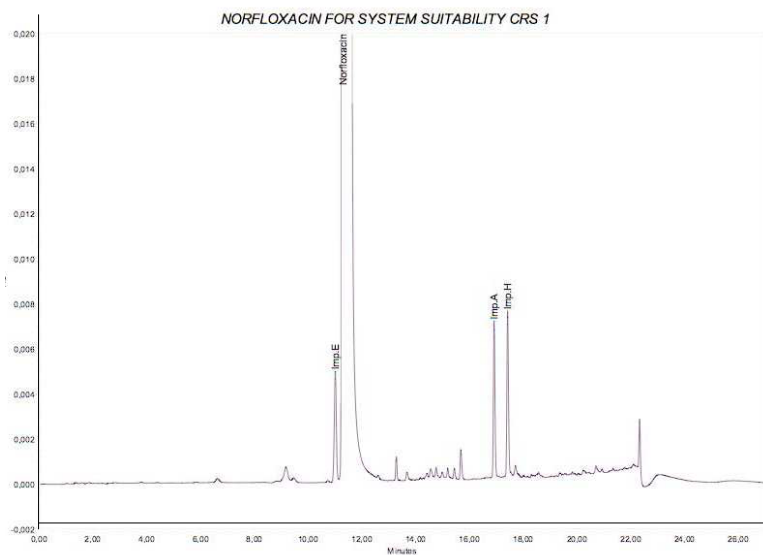


Figure 3.4.3.: European Pharmacopoeia validated method for the separation of norfloxacin from its three main impurities.

*Column:* Polar-embedded RP-18 column (250 x 4.6 mm), *Temperature:* 60 °C, *Mobile phase:* A: Water adjusted to pH 2.0 with phosphoric acid, B: Acetonitrile, 0', 5 % B - 5', 5 % B - 7', 7 % B - 10', 13 % B, 15', 53 % B - 20', 90 % B, *Flow rate:* 1 ml/min, *Injection:* 20 µl, *Detection:* UV 265 nm.

### 4.3. Synthetic and biosimilar neutral, amphoteric, acidic, and basic active compounds

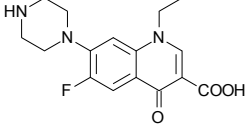
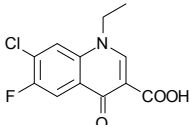
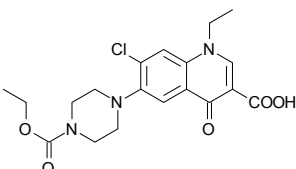
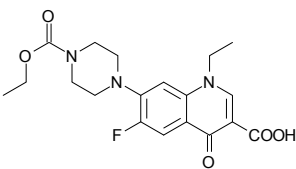
Abbreviation	Name	Structure
N	Norfloxacin	
A	Impurity A	
E	Impurity E	
H	Impurity H	

Table 3.4.2.: The norfloxacin antibiotic and its three main impurities.

We optimized at first the separation onto a C18 column and we could separate all the impurities contained in the mixture from the main compound within 13 minutes (see Figure 3.4.4). However, as we did not have the impurities as pure product and as we could not perform any MS experiments, we cannot assign each peak to its corresponding impurity. However, the use of a DAD detector allowed an area and UV-spectrum tracking of the peaks. When we performed the optimization on the RP-WAX material, the resolution decreased but remained sufficient (see Figure 3.4.5). However, as the order of elution for the impurities changed between the RP and the RP-WAX column, the mixed-mode material can be used as a complementary method to standard RP. Such complementary methods are always more needed to obtain a FDA agreement.

#### 4. Further applications of RP-WAX mixed-mode material

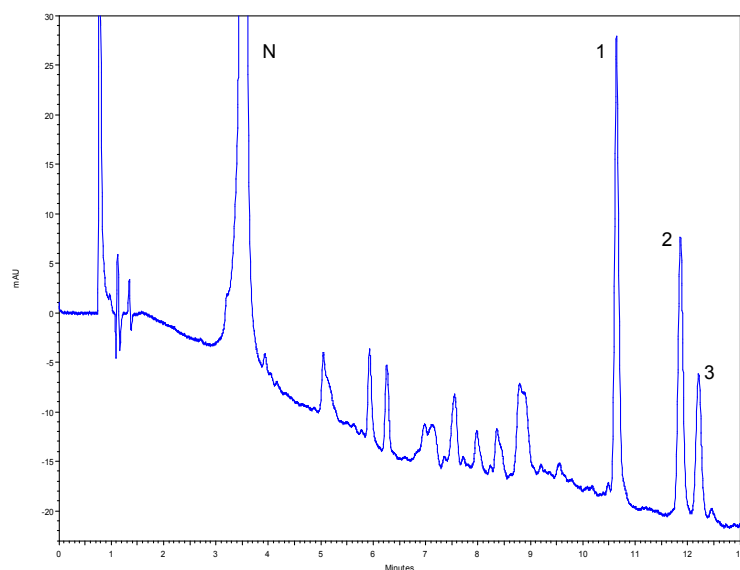


Figure 3.4.4.: Separation of norfloxacin (N) from its three main impurities (1, 2, and 3) after fine optimization on RP18 material.

*Temperature:* 30 °C, *Flow rate:* 1 ml/min, *Injection:* 10 µl, *Detection:* UV 265 nm

*Column:* Purospher STAR RP-18e column (125 x 4 mm), *Mobile phase RP18:* A: Water pH 2.0 (acetic acid), B: Acetonitrile, 0', 9 % B - 3'7, 33 % B - 8'6, 65 % B - 14'4, 69 % B

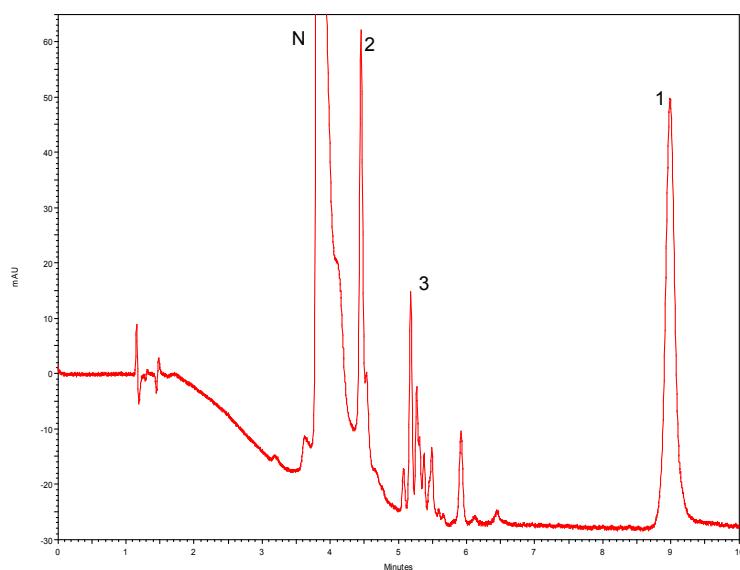


Figure 3.4.5.: Chromatogram of the separation of norfloxacin (N) from its three main impurities (1, 2, and 3) after fine optimization on a RP-WAX column.

*Temperature:* 30 °C, *Flow rate:* 1 ml/min, *Injection:* 10 µl, *Detection:* UV 265 nm

*Column:* Purospher STAR RP-WAX research sample column (125 x 4 mm), *Mobile phase RP-WAX:* A: Water pH 2.0 (acetic acid), B: Acetonitrile, 0', 9 % B - 3'7, 33 % B - 8'6, 65 % B - 14'4, 69 % B

### 4.3.2. Isoprenoides<sup>1</sup>

The mevalonate (MVA) pathway is the only source for cholesterol and isoprenoides in mammals. This pathway (see Figure 3.4.6) consists of several enzyme steps [145]. The initial enzymatic reaction takes place between Acetyl-CoA and Acetoacetyl-CoA forming HMG-CoA. The following reduction of HMG-CoA to MVA is catalyzed by HMG-CoA reductase. In the following, MVA gets converted into 3-isopentenyl pyrophosphate (IPP-C5 unit) and isomerization of IPP results in the formation of dimethylallyl pyrophosphate (DMAPP). Condensation of DMAPP and IPP forms long chain isoprenoides such as geranyl pyrophosphate (GPP), and farnesyl pyrophosphate (FPP). At this point, the pathway is further divided into two different routes, producing cholesterol and its products (bile acids, steroid hormones) through a multitude of enzymatic reactions on one side and on the other side geranylgeranyl pyrophosphate (GGPP). GGPP is the precursor of all longer chain isoprenoides. FPP and GGPP can covalently be attached to intracellular proteins, which is called isoprenylation. Isoprenylation of proteins is a post-translational modification (PTM) and has been shown to allow sub-cellular localization and intracellular trafficking of membrane associated proteins. PTMs are of vital importance for the cell due to their involvement in cell growth and survival, metabolism, differentiation and cytoskeletal organization. Perturbation of the mevalonate pathway appears to be associated with different diseases such as Alzheimer's disease, cardiovascular disease and different cancers.

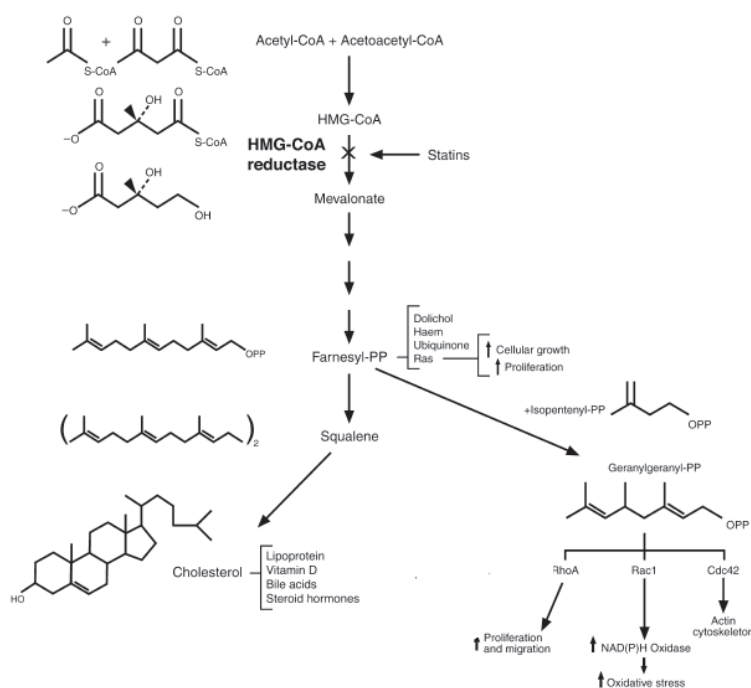


Figure 3.4.6.: Mevalonate (MVA) pathway resulting in the formation of isoprenoides and cholesterol.

Despite the great interest in isoprenoides, there are only few methods to evaluate FPP and GGPP level in different tissues [146, 147, 148]. Two methods are based on a derivatization procedure, coupling the two isoprenoides to dansyl-labeled pentapeptides (designated

<sup>1</sup>This study was achieved at the Department of Pharmacology of the University of Frankfurt in collaboration with Gero Hooff.

#### 4. Further applications of RP-WAX mixed-mode material

as FPP\* and GGPP\*, see Figure 3.4.7) which are fluorescent and can be detected in a second step by HPLC-fluorescence [149, 150].

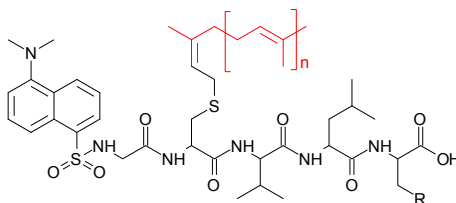


Figure 3.4.7.: Structure of the two isoprenoides coupled with the appropriate dansyl-labeled pentapeptides.

*FPP\**:  $n = 2$ ,  $R = -OH$ , *GGPP\**:  $n = 3$ ,  $R = \text{isopropyl}$ .

The chromatogram in Figure 3.4.8 corresponds to the validated separation method developed by Hooff et al [150]. The separation on RP18 column is achieved within 15 minutes. Because of the peptide-analog structure, RP-WAX HPLC was an alternative in order to achieve faster analyzes. The results given in Figure 3.4.9 confirm this assumption. Both markers are well separated from each other, from the matrix, and from the internal standards used for quantification purposes within 6 minutes. After a proper validation, the RP-WAX technique could be used as an alternative to the standard RP method with a speed up of the analysis time by a factor 2.5.

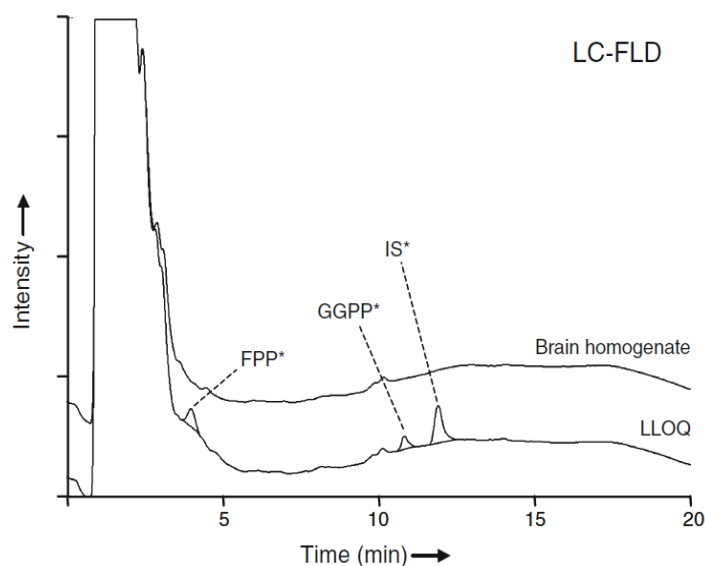


Figure 3.4.8.: Separation of both FPP\* and GGPP\* as well as an internal standard IS\* from a brain homogenate on a C18 column using a validated method.

*Column*: Supelco Ascentis Express C18 2.7 $\mu$ m fused core, *Mobile phase*: A: ACN-H<sub>2</sub>O 20mM ammonium acetate 40:60, B: acetonitrile - 20mM ammonium acetate 90:10, 0', 35 % B - 1.5', 35 % B - 8.5', 100 % B -14', 100 % B - 16', 35 %B - 20', 35 % B, *Flow rate*: 0.5 ml/min, *Temperature*: RT, *Injection*: 80 $\mu$ l, *Detection*: Fluorescence 340/525 nm.



#### 4.3. Synthetic and biosimilar neutral, amphoteric, acidic, and basic active compounds

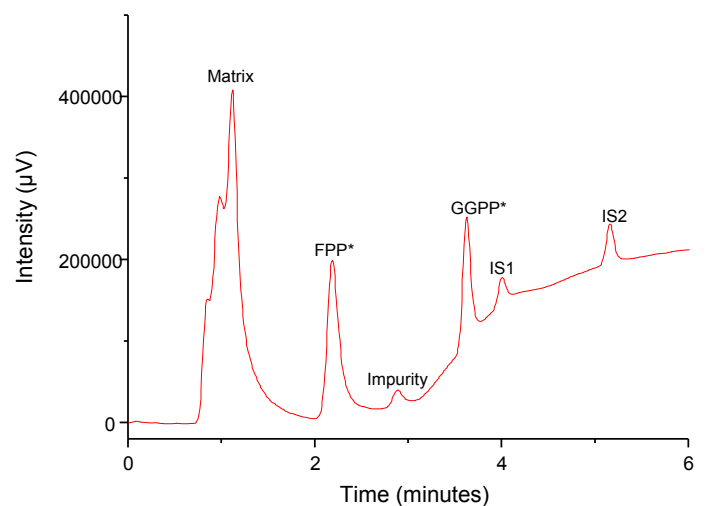


Figure 3.4.9.: Separation of both FPP\* and GGPP\* as well as two internal standard IS1 and IS2 in a brain matrix on a RP-WAX column.

*Column:* Purospher STAR RP-WAX research sample column, *Mobile phase:* A: 50 mM ammonium formate pH 3.5, B: acetonitrile - water 75:25, 0', 98 % B - 1.5', 98 % B - 15', 10 % B - 19', 10 % B - 19.5', 98 % B - 20', 98 % B, *Flow rate:* 1 ml/min, *Temperature:* RT, *Injection:* 60μl, *Detection:* Fluorescence 340/525 nm.

### 4.3.3. Acidic compounds: anti-inflammatory drugs

Non-steroidal anti-inflammatory compounds are widely used as treatment against rheumatoid arthritis or tendinitis for example [151]. Those drugs have similar action as steroid drugs without the side effects. Due to the increasing consumption of such drugs, the concern about their impact onto the environment is becoming more important. Acidic pharmaceutical drugs are widely present in sewage water and thus in the aquatic environment [152]. The five compounds described in Table 3.4.3 were detected in surface waters in concentrations up to several micrograms per liter [153]. The need of analytical methods for the identification and quantitation of those compounds is therefore increasing in order to investigate the effluents of the sewage treatment plants. Another reason for the need of an analytical method for such drugs is the incidence of poisoning, specially in Japan [154].

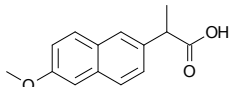
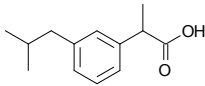
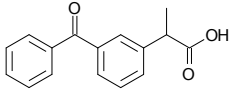
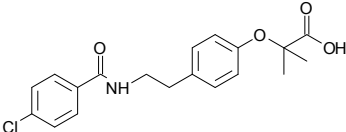
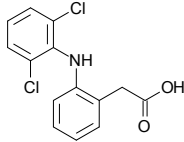
Abbreviation	Name	Structure	log P <sup>1</sup>	pKa <sup>2</sup>
N	Naproxen		1.22	4.15
I	Ibuprofen		3.97	4.41
K	Ketoprofen		3.12	4.45
B	Bezafibrat		4.25	3.29
D	Diclofenac		4.51	4.16

Table 3.4.3.: Schemes of the five acidic anti-inflammatory drugs.

<sup>1</sup>See Reference [155].

<sup>2</sup>See References [156] and [157].

The most common chromatography methods for the separation of non-steroidal anti-inflammatory drugs are performed on reversed-phase columns. Hirai et al. validated an isocratic method on C18 material using 50 mM phosphate buffer at pH 5.0 - acetonitrile [151]. In order to obtain alternative methods to the standard RP ones, some pH- and thermo-responsive techniques were developed to achieve separation in aqueous conditions [158].

The first part of our study consisted in optimizing the separation of the anti-inflammatory drugs on RP material. We used the same mobile phase composition as Hirai et al. at the beginning. An optimization of the separation in gradient mode using ChromSword Auto lead to even better separation of the five considered molecules (see Figure 3.4.10 a). The baseline separation was achieved within 21 minutes. The mixture was then injected onto a RP-WAX column. We started with low buffer concentration, low acetonitrile content and

#### 4.3. Synthetic and biosimilar neutral, amphoteric, acidic, and basic active compounds

increased both with a linear gradient over 30 minutes. The corresponding chromatogram is given in Figure 3.4.10 b. First of all, it is clear that the separation on the mixed-mode material is worse in term of resolution and peak shape. One explanation for the bad symmetry factor could be that working at a pH close to the pKa of the molecules leads to the presence of both protonated and neutral species in solution.

The separation of such compounds containing polar acidic, alkyl and aromatic groups is rather difficult to predict. On RP and on RP-WAX materials, the elution order is not following either the log P or the pKa values (see Table 3.4.3). Even if the separation is worse on the mixed-mode column, it is nevertheless interesting that the elution order is different between both materials. The FDA requires complementary methods for quality control and substance identification and this trend could extend for water purity assessment for example. The RP-WAX HPLC methods could therefore be used in the sewage analysis.

Another positive aspect of the separation on RP-WAX material is the consumption of organic modifier. Due to the anion exchange behavior which increases the retention of acidic compounds, we could reduce the amount of acetonitrile needed for the HPLC analysis by ~ 50 %.

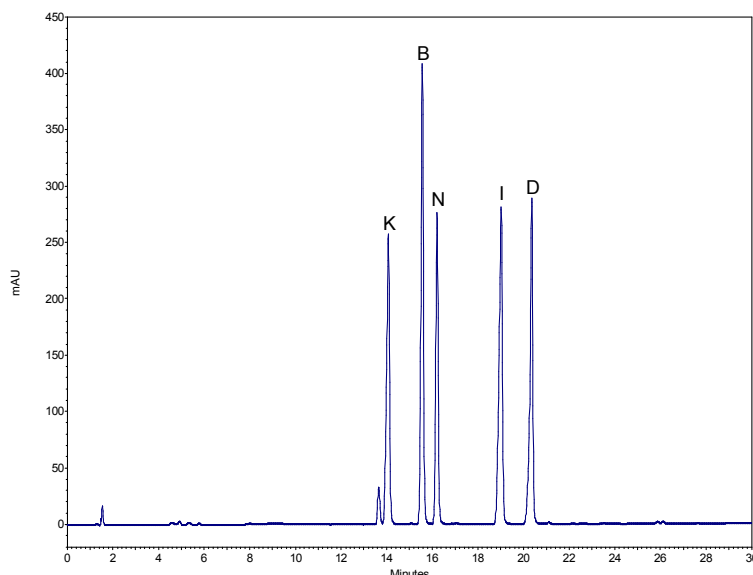


Figure 3.4.10.: Separation of five different acidic anti-inflammatory drugs on a RP column. *Temperature:* RT, *Flow rate:* 1 ml/min, *Injection:* 10  $\mu$ l, *Detection:* UV 225 nm, *Analytes:* naproxen (N), ketoprofen (K), ibuprofen (I), bezafibrat (B), diclofenac (D). *Column:* Purospher STAR RP-18e column (125 x 4 mm), *Mobile phase RP18:* A: 20 mM phosphate buff er adjusted to pH 5, B: acetonitrile, 0' – 40 % B, 30' – 90 % B.

#### 4. Further applications of RP-WAX mixed-mode material

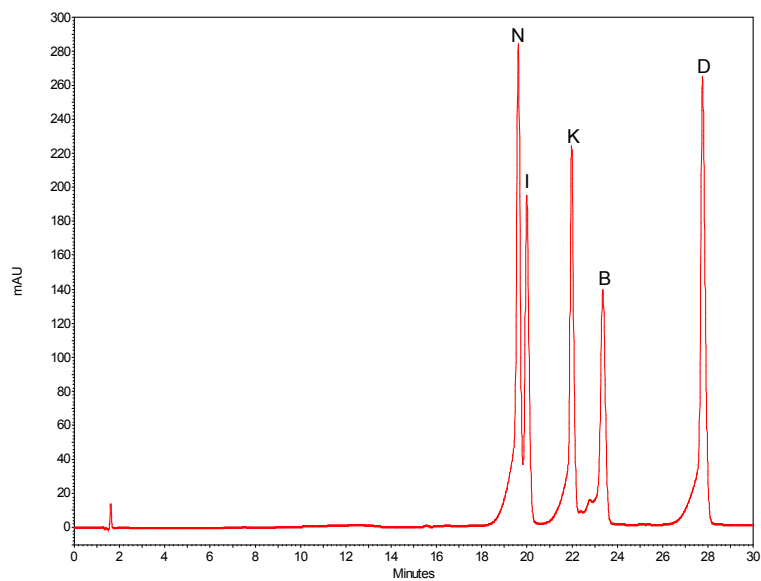


Figure 3.4.11.: Five different acidic anti-inflammatory drugs separated on a RP-WAX (b) columns.

*Temperature:* RT, *Flow rate:* 1 ml/min, *Injection:* 10  $\mu$ l, *Detection:* UV 225 nm, *Analytes:* naproxen (N), ketoprofen (K), ibuprofen (I), bezafibrat (B), diclofenac (D).

*Column:* Purospher STAR RP-WAX research sample column (125 x 4 mm), *Mobile phase RP-WAX:* A: 10 mM phosphate buffer pH 4.5, water / acetonitrile (70:30, v/v), B: 50 mM phosphate buffer pH 4.5, water / acetonitrile (50:50, v/v), 0' – 10 % B, 30' – 90 % B.

#### 4.3.4. Human insulin

Insulin is one of the most important hormone for the human metabolism. It assures the regulation of the glucose by enabling organs to stock it from blood as glycogen. Diabetes appears when insulin is depleted and the glucose regulation is not possible anymore. The type 1 diabetes mellitus involves the administration of bio-synthetic insulin in order to maintain the glucose homeostasis. Insulin is a peptidic compounds with 51 amino acids (molecular weight = 5808 Da) arranged in two helices linked by a disulfide bond (A-chain) and in a helical segment (B-chain). Banting and MacLeod obtained the Nobel Prize for Medicine in 1923 for the discovery of insulin [159]. The structure of the insulin was described by Blundell et al. in 1969 (see Figure 3.4.12) [160].

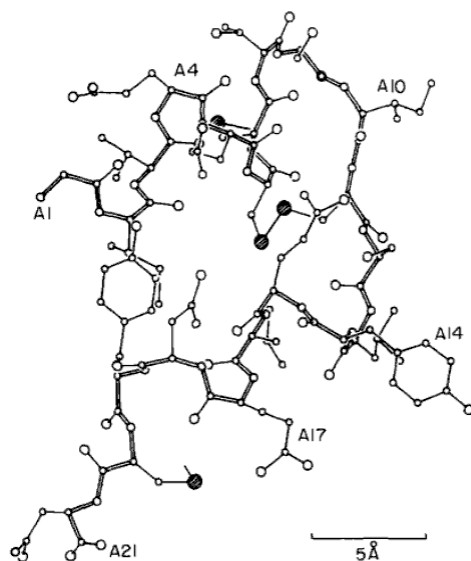


Figure 3.4.12.: Scheme of the human insulin as published by Hodgkin in 1969.

Porcine insulin, which derives from human one by only one single amino acid, was prescribed until the 1980's. Nowadays, the synthesis of bio-synthetic human insulin is performed using recombinant DNA techniques [161]. The first companies who commercialized synthetic insulin were Lilly and Novo. Two different methods were developed. The first one consists in inserting the nucleotide sequence coding for both A- and B- chains into *E. coli* before incubating both purified chains. For the second one, the recombinant *E. coli* is used to produce human pro-insulin which leads to insulin through proteolytic excision.

The resulting product is cleaned up on a C8 or C18 column at larger scale. The columns used for production purposes exhibit mostly an internal volume of at least 80 l and up to 1200 g of insulin can be loaded during a single run [162]. Typically, the method consists of gradient elution using mobile phases composed of acetonitrile - acidic buffer. This chromatographic process is known as "polishing step" and allows the purity to get from 92 to 99 %. It is therefore needed to assess purity through an analytical HPLC step. However, most of the methods described in the literature are based on RP-HPLC.

An optimized separation of the insulin from two impurities from the process was developed on a RP18 column (see Figure 3.4.13). The method is in accordance with the analyzes performed in the industry [163]. The resolution is rather low and probably not sufficient to validate the method. Switching to RP-WAX material not only increased the

#### 4. Further applications of RP-WAX mixed-mode material

resolution of the impurities but the developed method is also more simple than the mobile phase composition used on the RP column (see Figure 3.4.14). The increased resolution leads to more robust method for the validation. The RP-WAX sorbent has also the advantage to be a complementary material to the more common RP one. It could be therefore of great advantage for production monitoring, quality control, and regulatory issues to validate such method.

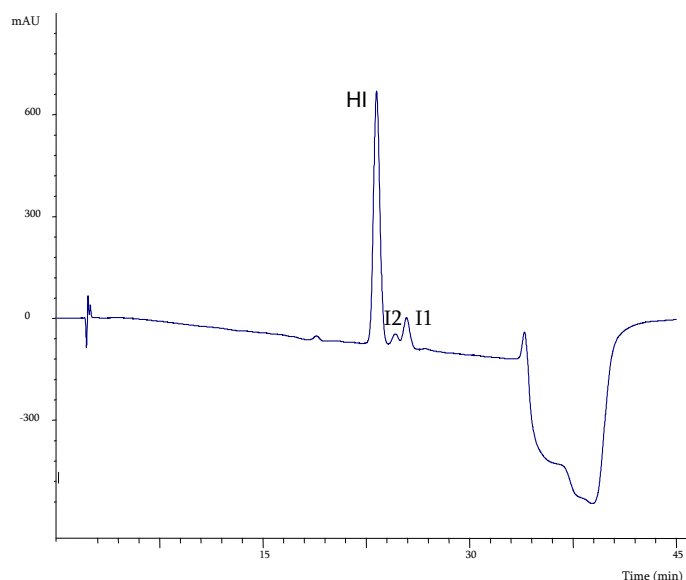


Figure 3.4.13.: Separation of human insulin (HI) from two impurities (I1 and I2) on RP18 material.

*Column:* Kromasil RP8 (250 x 4 mm), *Mobile phase RP18:* A: 140 mM sodium perchlorate, 34 mM triethylammoniumacetate, 60 mM sodium dihydrogen-phosphate, 5,5% acetonitrile pH 2.3, B: 70 mM sodium perchlorate, 17 mM triethylammonium-acetate, 110 mM sodium dihydrogen-phosphate, 50.3% acetonitrile pH 2.3, 45% to 55 % B in 30 min, 80%B at 30.1 min until 35 min, 45% B for 10 min, *Temperature:* 25 °C, *Flow rate:* 1 ml/min, *Injection:* 10 µl, *Detection:* UV 210 nm.

#### 4.3. Synthetic and biosimilar neutral, amphoteric, acidic, and basic active compounds

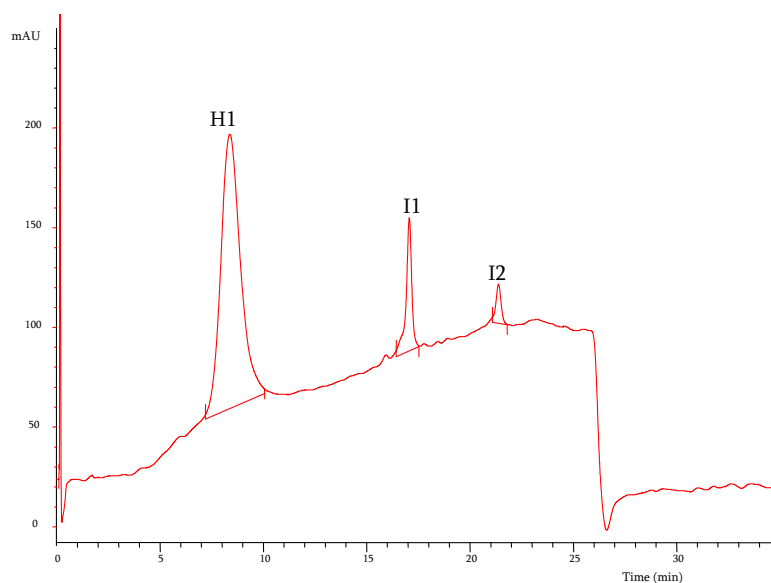


Figure 3.4.14.: Separation of human insulin (HI) from two impurities (I1 and I2) on a RP-WAX column.

*Column:* Purospher STAR RP-WAX research sample column (125 x 4 mm), *Mobile phase RP-WAX:* A: water, B: ACN, C: 500 mM triethylammonium phosphate pH 6.0, 1% to 50% B in 20 min and C constant at 10%, *Temperature:* 25 °C, *Flow rate:* 1 ml/min, *Injection:* 10 µl, *Detection:* UV 210 nm.

## 4.3.5. Tri-Luma

Tri-Luma is a dermatological preparation of the three different molecules presented in Table 3.4.4 along with other non-active products. The effect of the mixture is increased in comparison with the use of those 3 compounds alone [164]. This dermatological preparation was patented in 2006 as a treatment against hyper-pigmentation of pathological scars [165]. Other hyper-pigmentation diseases can be advantageously cured using Tri-Luma, Melasma for example [166]. It can only be ordered with a medical prescription.

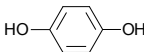
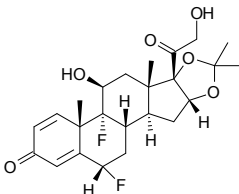
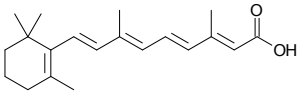
Name	Structure	Mass concentration in final preparation	Pharmaceutical class
Hydroquinone		4.00 %	Bleaching agent
Fluocinolone acetonide		0.01 %	Corticosteroid
Tretinoin		0.05 %	Vitamin A derivative

Table 3.4.4.: Three active molecules in the Tri-Luma product.

One derivation risk of this cream is the increasing use in skin whitening, which raises not only ethical problems. Indeed, Tri-Luma is getting very popular along the Internet in many forums dealing with cosmetological convenience skin whitening, where its effects were already discussed before the patent was published. The number of pages where you can buy Tri-Luma is tremendously increasing as described in Figure 3.4.15. A major issue in the next year will be the control of such preparations. Some of these cheaper prescription-free cream will be prepared in unauthorized way and the quality of the product will not be assessed. It is therefore important to be able to separate the active compounds from each other and to quantify them.



### 4.3. Synthetic and biosimilar neutral, amphoteric, acidic, and basic active compounds

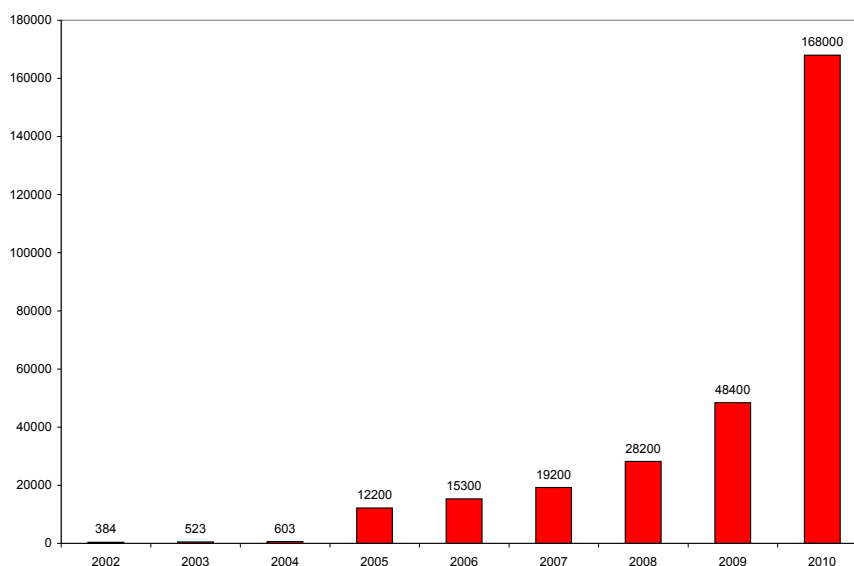


Figure 3.4.15.: Number of pages generated by Google with the key words “buy tri-luma” on the 1st of January of each year.

A method for the separation of those three different compounds was developed by an independent labor. They tested different methods and they obtained the best separation by a combination of both RP and HILIC columns (see Figure 3.4.16). The three compounds are baseline separated within 25 minutes. However, the use of two columns in series with a two solvents gradient at constant buffer concentration and varying flow rate is not a straightforward method and its applicability as an easy method for rapid evaluation of a preparation purity is rather low.

Considering the structure of the molecules, we can observe that the hydroquinone is a polar aromatic molecule, the tretinoin is composed of a hydrophobic chain tipped by an acidic group and the fluocinolone acetonide is a more complex molecule bearing polar groups. The mixed-mode RP-WAX material was designed to deal with mixtures containing molecules with different chemical activities. The method development was performed with ChromSword Auto for the gradient optimization. We investigated several buffer compositions and concentrations but the one used for the RP-HILIC method lead to the best results (see Figure 3.4.17). The three compounds were baseline separated within 10 minutes.

Even if we demonstrated the possibility to easily separate the three active compounds of the Tri-Luma cream on RP-WAX material, the method should be validated and applied to the whole matrix in order to ensure the applicability of the method in real conditions. This could become an essential method in the future due to the increasing demand of cheap non-prescribed Tri-Luma.

#### 4. Further applications of RP-WAX mixed-mode material

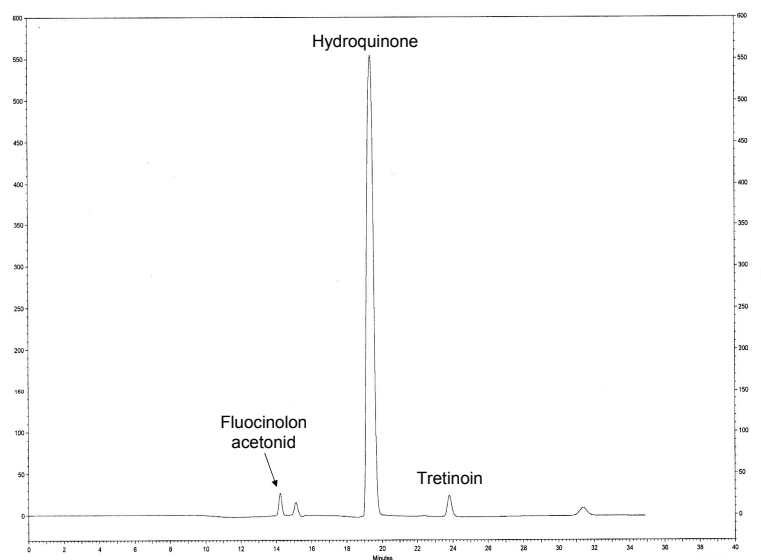


Figure 3.4.16.: Separation of the three active molecules hydroquinone, fluocinolone acetone, and tretinoin of the Tri-Luma product on a two dimensional RP18/HILIC system.

*Column:* LiChrosphere RP18 (125x4mm) + ZIC HILIC (250x4.6mm), *Mobile phase:* A: 100 mM ammonium acetate buffer pH 4.5, B: methanol, C: acetonitrile, 3 % B constant, 0', 94 % C - 35', 87 % C, *Flow rate:* 0', 0.3 ml/min - 35', 0.5 ml/min, *Temperature:* RT, *Injection:* 20 $\mu$ l, *Detection:* UV 240 nm.

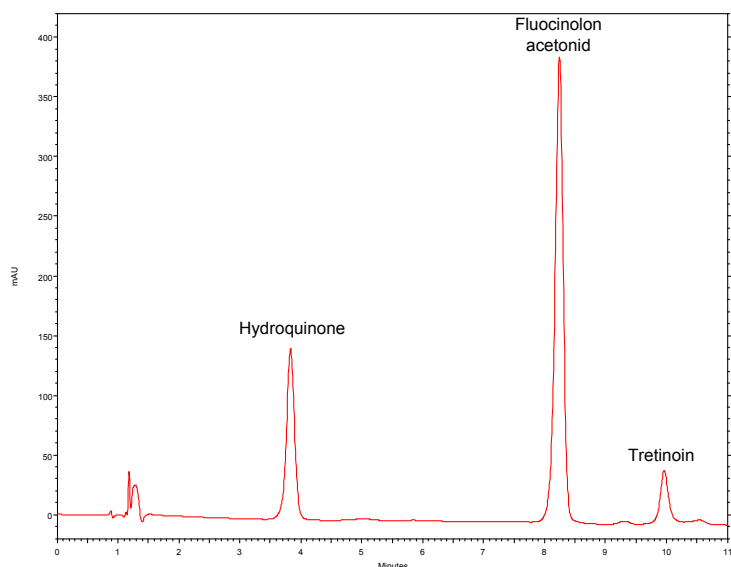


Figure 3.4.17.: Separation of the three active molecules hydroquinone, fluocinolone acetone, and tretinoin of the Tri-Luma product on a RP-WAX column.

*Column:* Purospher STAR RP-WAX research sample column (125 x 4 mm), *Mobile phase:* A: 100 mM ammonium acetate buffer pH 4.5, B: acetonitrile, 0', 5 % B - 2.1', 17 % B - 10', 56 % B - 12', 56 % B, *Flow rate:* 1ml/min, *Temperature:* RT, *Injection:* 10 $\mu$ l, *Detection:* UV 250 nm.

## 4.4. Conclusion

We described in this chapter several examples for the use of RP-WAX for the separation of chemicals and peptides. Identification of substances within a mixture, trace analysis of impurities, separation of markers from internal standards could be successfully achieved. Those are however only some of the possibilities of the RP-WAX material. Some of these methods should be further investigated and validated before use in every-day analysis. We demonstrated however the large range of application of such mixed-mode material. A more recent work by Lämmerhofer et al. confirmed the fully multi-modal behavior of this RP-WAX material by investigating the multiple separation patterns with peptide mixtures [167].



**Part IV.**

**Conclusion**



The aim of this PhD work was to develop a commercializable mixed-mode reversed phase - weak anion exchange chromatography product based on a patented chemistry. Even if the first studies already showed the feasibility and the applicability of the project, the production process had to be implemented in a larger scale. Increasing the lot size to a pre-production scale not only lead to adapt the quantities and concentrations. Safety and economical aspects had to be taken in consideration. Therefore, every production step was examined, the reagents were adapted to reduce costs and hazards, the critical procedures were optimized, and the overall reproducibility and robustness of the method was studied.

The grafting to the silica consists of at least three different steps for such a complex modification. At first a spacer bearing two reactive groups (one for silylation and one for ligand addition) is added to the surface. The non-reacted silanol groups are then capped in a second step. The last step consists in adding the ligand to the spacer. The bottle-neck of the method is not the grafting to the surface. The main issue remains the production of the RP-WAX ligand. We had to eliminate the use of organometallic reagent, and the purification of the ligand was also an issue. Even if a suitable method was developed, some work still remains to improve even more this part of the synthesis. However, the current process allows production up to 500 g scale.

Another aspect to be investigated when developing a commercializable chromatography resin is the stability of the material. Amine phases are well known for their leaching issue, and this aspect had to be kept in mind during this work. Even if some hypercrosslinking methods were promising, the lack of reproducibility and the increase in production costs because of additional steps lead to abandon those consideration for the first generation of RP-WAX material. The material we developed is stable enough, especially in comparison with concurrence resins. However, if the launch of this material on the market is successful, a more expensive and more stable resin could be put on the market in parallel with the current product. Furthermore, until now, the RP-WAX material was based on 5  $\mu\text{m}$  particles. It will be easy to go down to 3, 2, and 1.7  $\mu\text{m}$  particles to get some very fast complex separations on UPLC systems.

The same aspect was taken into account for the development of supplementary ligands. If the combination of reversed phase and weak anion exchange behavior is successful, the molecules described in this work could be further developed and the resulting resins could be put in the pipe line of the company to build up the mixed-mode chromatography product division. The build-up of a mixed-mode portfolio has to be linked to the growth of the market. There is a trend going onto such mixed-mode phases, but it is still not clear if there will be a long-lasting need for such products. We should not forget, that the majority of the sold columns are still some older RP ones. Another trend to follow is the reduction of the particle size.

However, developing a suitable product is not the only input to be achieved in order to successfully launch a new product. First of all, a quality control method has to be set up in order to be able to evaluate the quality of each production batch. The chemical methods on lose material is not sufficient, and column performances have to be evaluated. An easy and inexpensive chromatography method was developed to assess the quality of the packed columns. This method can be implemented in a routine QC laboratory between packing and shipping.

Furthermore, usefulness in every-day work-life has to be demonstrated through development of real applications. This was done with several analytes, in order to cover the entire application range. Indeed, we had to show the possibility to separate hydrophobic

#### *4. Further applications of RP-WAX mixed-mode material*

compounds with no charges as on standard RP phases, and charged compounds as on standard IEC gels. The most difficult part of the method development consisted in finding some operating conditions which allows separation in a single run of compounds with polarity, charges, and steric differences at the same time. We could even show, that it is possible to fully validate a method on such resins. This allows the material to be used for qualitative and quantitative analyzes.

The echoes of the first publications presented in scientific conferences were very promising. There is a real need of such material for the separation of complex mixtures. This need was even increased by the FDA requirements, which prescript the use of orthogonal chromatography methods for quality control of pharmaceuticals.

To sum-up the proposed product evolution, the first generation RP-WAX resin is ready to market and should be launched as soon as possible on 5  $\mu\text{m}$  silica particles in order to avoid a saturation of the emerging niche by concurrence materials. Shortly after, the smaller particles should be available. Subsequently, second generation RP-WAX with better stability should be launched in parallel with other kind of RP-IEC materials. The development of further real applications should be continued in order to support marketing activities.

Going out of the scope of this study, which consisted in developping a new phase for analytical purposes, some preparative applications in the domain of biochromatography could be developped. However, silica based materials are not stable enough for the purification of proteins in larger scale. Coupling the ligand to polymeric based particles would be feasible due to the presence of the reactive double bond, and it would offer an alternative to some newer mixed-mode purification resins.



# Bibliography

- [1] R. Dabre, A Schwämmle, M. Lämmerhofer, and W. Lindner. *J. Chromatogr. A*, 1216:3473, 2009.
- [2] R. Dabre, N. Azad, A. Schwämmle, M. Lämmerhofer, and W. Lindner. *J. Sep. Sci.*, 34:761, 2011.
- [3] M. Schulte and A. Epping. *Preparative chromatography*, chapter 2, page 13. Wiley-VCH, 2005.
- [4] U.D. Neue. *HPLC columns: Theory, Technology, and Practice*, chapter 2, page 11. Wiley-VCH, 1997.
- [5] U.D. Neue. *HPLC columns: Theory, Technology, and Practice*, chapter 2, page 13. Wiley-VCH, 1997.
- [6] U.D. Neue. *HPLC columns: Theory, Technology, and Practice*, chapter 6, page 109. Wiley-VCH, 1997.
- [7] R. K. Iler. *The chemistry of silica*. Wiley-Interscience, 1979.
- [8] G. E. Kellum and R. C. Smith. *Anal. Chem.*, 39:341, 1967.
- [9] K. K. Unger, N. Becker, and P. Roumeliotis. *J. Chromatogr. A*, 125:115, 1976.
- [10] <http://www.separations.eu.tosohbioscience.com/products/hplccolumns/bymode/reversedphase/polymerbasedcolumns/tskgeloctadecyl-npr.htm>. March 2011.
- [11] <http://www.phenomenex.com/phen/em/ws63990808/images/pdf/po70580809.pdf>. January 2011.
- [12] <http://www.merck-chemicals.com/food-analytics/chromolith-hplc-columns>. March 2011.
- [13] <http://eetd.lbl.gov/ecs/aerogels/sa-pore.html>. January 2011.
- [14] de Galan L. Berendsen, G.E. *J. Liq. Chromatogr.*, 1:561, 1978.
- [15] J. E. Sandoval. *J. Chromatogr. A*, 852:375, 1999.
- [16] A.J. Alpert. *J. Chromatogr.*, 499:177, 1990.
- [17] D. V. McCalley and U. D. Neue. *J. Chromatogr. A*, 1192:225, 2008.
- [18] P. Hemstroem and K. Irgum. *J. Sep. Sci.*, 29:1784, 2006.
- [19] P. Hemström, A. Nordborg, K. Irgum, F. Svec, and J.M.J. Fréchet. *J. Sep. Sci.*, 29:25, 2006.
- [20] J. Lee, J. Kim, and T. Hyeon. *Advanced Materials*, 18:2073, 2006.

- [21] L. R. Snyder, J. J. Kirkland, and J. W. Dolan, editors. *Introduction to Modern Liquid Chromatography*. Wiley, 2010.
- [22] U.D. Neue. *HPLC columns: Theory, Technology, and Practice*, chapter 10, page 183. Wiley-VCH, 1997.
- [23] Y. Kato, K. Nakamura, T. Kitamura, H. Moriyama, M. Hasegawa, and H. Sasaki. *J. Chromatogr. A*, 971:143, 2002.
- [24] J. H. Knox and R. A. Hartwick. *J. Chromatogr.*, 204:3, 1981.
- [25] [www.poplc.de](http://www.poplc.de). December 2010.
- [26] Y.-F. Maa, F. D. Antia, Z. El Rassi, and C. Horváth. *J. Chromatogr.*, 452:331, 1988.
- [27] P. J. Davis, R. J. Ruane, and I. D. Wilson. *Chromatographia*, 37:60, 1993.
- [28] W. S. Hancock and J. T. Sparrow. *J. Chromatogr. A*, 206:71, 1981.
- [29] K.-S. Boos and C. H. Grimm. *Trends Anal. Chem.*, 18:175, 1999.
- [30] P. Chiap, O. Rbeida, B. Christiaens, Ph. Hubert, D. Lubda, K. S. Boos, and J. Crommen. *J. Chromatogr. A*, 975:145, 2002.
- [31] J. L. Rafferty, J. I. Siepmann, and M. R. Schure. *Analytical Chemistry*, 80:6214, 2008.
- [32] [www.sielc.com](http://www.sielc.com). *Products -> Primesep*, March 2010.
- [33] [www.dionex.com/en-us/products/columns/lc/mixed-mode/acclaim-mixed-mode-wcx-1/lp-71738.html](http://www.dionex.com/en-us/products/columns/lc/mixed-mode/acclaim-mixed-mode-wcx-1/lp-71738.html). March 2010.
- [34] [http://www.gelifesciences.com/aptrix/upp01077.nsf/content/bioprocess\\_media\\_multimodal+chromatography](http://www.gelifesciences.com/aptrix/upp01077.nsf/content/bioprocess_media_multimodal+chromatography). March 2011.
- [35] M. Gilar, Y.-Q. Yu, J. Ahn, J. Fournier, and J. C. Gebler. *J. Chromatogr. A*, 1191:162, 2008.
- [36] Z. Guo, Y. Jin, T. Liang, Y. Liu, Q. Xu, X. Liang, and A. Lei. *J. Chromatogr. A*, 1216, 2009.
- [37] H. Hinterwirth, M. Lämmerhofer, B. Preinerstorfer, A. Gargano, R. Reischl, W. Bicker, O. Trapp, L. Brecker, and W. Lindner. *J. Sep. Science*, 33:3273, 2010.
- [38] E. Peachey, K. Cook, A. Castles, C. Hopley, and H. Goenaga-Infante. *J. of Chromatogr. A*, 1216:7001, 2009.
- [39] K. Zhang, L. Dai, and N. P. Chetwyn. *J. Chromatogr. A*, 1217:5776, 2010.
- [40] H. L. Phillips, J. C. Williamson, K. A. van Elburg, A. P. L. Snijders, P. C. Wright, and M. J. Dickman. *Proteomics*, 10:2950, 2010.
- [41] <http://www.dionex.com/en-us/products/columns/lc/specialty/acclaim-trinity/lp-81754.html>. March 2011.
- [42] B. N. Tran, R. Okoniewski, R. Storm, R. Jansing, and K. M. Aldous. *J. Agricultural and Food Chem.*, 58:101, 2010.

- [43] X. Liu and C. A. Pohl. *J. Sep. Sci.*, 33:779, 2010.
- [44] W. Lindner and M. Lämmerhofer. *US Patent 2008/0164211, Mixed-Modal Anion-Exchanged Type Separation Material*, 2008.
- [45] M. Lämmerhofer and W. Lindner. *J. Chromatogr. A*, 741:33, 1996.
- [46] E. Zarbl, M. Lämmerhofer, A. Woschek, F. Hammerschmidt, C. Parenti, G. Cannazza, and W. Lindner. *J. Sep. Sci.*, 25:1269, 2002.
- [47] R. Nogueira, M. Lämmerhofer, and W. Lindner. *J. Chromatogr. A*, 1089:158, 2005.
- [48] G. Göktürk, M. Delzendeh, and M. Volkan. *Spectrochim. Acta B*, 55:1063, 2000.
- [49] T. Djekic, A. G. J. van der Ham, and A. B. de Haan. *J. Chromatogr. A*, 1142:32, 2007.
- [50] B. B. Wheals. *J. Chromatogr. A*, 177:263, 1979.
- [51] A. Heckel and D. Seebach. *Chem. Eur. J.*, 8:559, 2002.
- [52] K. J. Welch and N. E. Hoffman. *J. High Resol. Chromatogr.*, 9:417, 1986.
- [53] A. Ruderisch, W. Iwanek, J. Pfeiffer, G. Fischer, K. Albert, and V. Schurig. *J. Chromatogr. A*, 1095:40, 2005.
- [54] C. M. Crudden, M. Sateesh, and R. Lewis. *J. Am. Chem. Soc.*, 127:10045, 2005.
- [55] J. N. Kinkel and K. K. Unger. *J. Chromatogr. A*, 316:193, 1984.
- [56] H. Engelhardt and P. Orth. *J. Liq. Chromatogr. Relat. Technol.*, 10:1999, 1987.
- [57] N. M. Scully, G. P. O’Sullivan, L. O. Healy, J. D. Glennon, B. Dietrich, and K. Albert. *J. Chromatogr. A*, 1156:68, 2007.
- [58] K. K. Unger. *Adsorbents in column liquid chromatography*, volume 47, chapter 6, pages 331–470. Marcel Dekker, 1990.
- [59] P. Van Der Voort and E. F. Vansant. *J. Liq. Chromatogr. Relat. Technol.*, 19:2723, 1996.
- [60] R. Nogueira, M. Lämmerhofer, N. M. Maier, and W. Lindner. *Anal. Chim. Acta*, 533:179, 2005.
- [61] B. Buszewski, M. Jezierska, M. Welniak, and D. Berek. *J. High Resol. Chromatogr.*, 21:267, 1998.
- [62] B. Pfeleiderer, K. Albert, and E. Bayer. *J. Chromatogr.*, 506:343, 1990.
- [63] K. Albert and E. Bayer. *J. Chromatogr.*, 544:345, 1991.
- [64] A. B. Scholten, J. W. de Haan, H. A. Claessens, L. J. M. van de Ven, and C. A. Cramers. *Langmuir*, 12:4741, 1996.
- [65] M. Pursch, L. C. Sander, and K. Albert. *Anal. Chem.*, 68:4107, 1996.
- [66] C. Hellriegel, U. Skogsberg, K. Albert, M. Lämmerhofer, N. M. Maier, and W. Lindner. *J. Am. Chem. Soc.*, 126:3809, 2004.

- [67] C. Yang, T. Ikegami, T. Hara, and N. Tanaka. *J. Chromatogr. A*, 1130:175, 2006.
- [68] C. C. Sweeley, R. Bentley, M. Makita, and W. W. Wells. *J. Am. Chem. Soc.*, 85:2497, 1963.
- [69] C. Cao, A. Y. Fadeev, and T. J. McCarthy. *Langmuir*, 17:757, 2001.
- [70] E. A. Smith and W. Chen. *Langmuir*, 24:12405, 2008.
- [71] S. M. Kanan, W. T. Y. Tze, and C. P. Tripp. *Langmuir*, 18:6623, 2002.
- [72] J. L. McCallum, R. Yang, J. C. Young, J. N. Strommer, and R. Tsao. *J. Chromatogr. A*, 1148:38, 2007.
- [73] X. Liu and C. Pohl. *LC-GC North America*, FEV:65, 2007.
- [74] H. Parnes and E. J. Shelton. *J. Label Compd. Radiopharm.*, 38:19, 1996.
- [75] B. R. de Costa, X.-S. He, J. T. M. Linders, C. Dominguez, Z. Q. Gu, W. Williams, and W. D. Bowen. *J. Med. Chem.*, 36:2311, 1993.
- [76] E. E. Mikhлина, A. D. Yanina, L. N. Yakhontov, K. A. Zaitseva, L. F. Roshchina, and M. D. Mashkovskii. *Pharmaceutical Chemistry Journal*, 5:590, 1971.
- [77] R. Nogueira, D. Lubda, A. Leitner, W. Bicker, N. M. Maier, M. Lämmerhofer, and W. Lindner. *J. Sep. Sci.*, 29:966, 2006.
- [78] S.V. Rogozhin, V.A. Davankov, and M.P. Tsyurupa. *Patent USSR 299165*, 1969.
- [79] H. Luo and P.W. Carr. *Anal. Bioanal. Chem.*, 391:919, 2008.
- [80] I.M. Abrams and J.R. Millar. *Reactive & Functional Polymers*, 35:7, 1997.
- [81] M. Beth, K. K. Unger, M.P. Tsyurupa, and V.A. Davankov. *Chromatographia*, 36:351, 1993.
- [82] J. J. Kirkland, J. L. Glajch, and R. D. Farlee. *Anal. Chem.*, 61:2, 1989.
- [83] N. Tsubokawa, H. Ichioka, T. Satoh, S. Hayashi, and K. Fujiki. *Reactive & Functional Polymers*, 37:75, 1998.
- [84] B.C. Trammel. *Novel Stationary Phases on Silica and Zirconia for the Reversed Phase High Performance Liquid Chromatographic Separation of Acidic and Basic Analytes*. PhD thesis, University of Minnesota, 2002.
- [85] H. Luo, L. Ma, and P.W. Carr. *J. Chromatogr. A*, 1182:41, 2008.
- [86] J. Nawrocki and A. Dabrowska. *J. Chromatogr. A*, 868:1, 2000.
- [87] P. Stanton. *Ion-exchange chromatography*, chapter 3, page 27. Humana Press, 2004.
- [88] [www.interchim.com/interchim/](http://www.interchim.com/interchim/). *Interchrom -> HPLC -> Uptisphere specialty columns : Mixed mode, DNAP*, March 2010.
- [89] J. S. Morley. *J. Chem. Soc. C*, page 809, 1969.
- [90] G. Lei, X. Xiong, Y. Wei, X. Zheng, and J. Zheng. *J. Chromatogr. A*, 1187:197, 2008.

- [91] R.R. Renshaw and J.C. Ware. *J. Am. Chem. Soc.*, 47:2989, 1925.
- [92] M.J. Walters. *J. Assoc. Off. Anal. Chem.*, 70:465, 1987.
- [93] K. Kimata, K. Iwaguchi, S. Onishi, K. Jinno, R. Eksteen, K. Hosoya, M. Araki, and N. Tanaka. *J. Chromatogr. Sci.*, 27:721, 1989.
- [94] H. Engelhardt and M. Jungheim. *Chromatographia*, 29:59, 1990.
- [95] H. A. Claessens, M.A. van Straten, C.A. Cramers, M. Jezierka, and B. Buszewski. *J. Chromatogr. A*, 826:135, 1998.
- [96] D. Visky, Y. Vander Heyden, T. Iványi, P. Baten, J. De Beer, Z. Kovács, B. Noszál, E. Roets, D.L. Massart, and J. Hoogmartens. *J. Chromatogr. A*, 977:39, 2002.
- [97] K. Kóczyán, E. Haghedooren, S. Dragovic, B. Noszál, J. Hoogmartens, and E. Adams. *J. Pharm. Biomed. Anal.*, 44:894, 2007.
- [98] M. Lämmerhofer, M. Richter, J. Wu, R. Nogueira, W. Bicker, and W. Lindner. *J. Sep. Sci.*, 31:2572, 2008.
- [99] U.D. Neue. *HPLC columns: Theory, Technology, and Practice*, chapter 6, page 107. Wiley-VCH, 1997.
- [100] U.D. Neue. *HPLC columns: Theory, Technology, and Practice*, chapter 6, page 219. Wiley-VCH, 1997.
- [101] D.A. Fonsesca, H.R. Gutiérrez, K.E. Collins, and C.H. Collins. *J. Chromatogr. A*, 1030:149, 2004.
- [102] S. J. Gluck, M. H. Benkö, R. K. Hallberg, and K. P. Steele. *J. Chromatogr. A*, 744:141, 1996.
- [103] R. G. Fischer and K. Ballschmiter. *J. Anal. Chem.*, 360:769, 1998.
- [104] [pharm.kuleuven.be/pharmchem/pages/ccs.html](http://pharm.kuleuven.be/pharmchem/pages/ccs.html). March 2010.
- [105] C. Eijkman. Nobel lecture in physiology or medicine 1929. *Elsevier Publishing Company, Amsterdam*, 1965.
- [106] A. von Szent-Györgyi Nagrapolt. Nobel lecture in physiology or medicine 1937. *Elsevier Publishing Company, Amsterdam*, 1965.
- [107] P. Chen, R. Atkinson, and W. R. Wolf. *Journal of AOAC International*, 92:680, 2009.
- [108] R. Amidzic, J. Brboric, O. Cudina, and S. Vladimirov. *J. Serb. Chem. Soc.*, 70:1229, 2005.
- [109] Z. Chen, B. Chen, and S. Yao. *Analytica Chimica Acta*, 569:169, 2006.
- [110] S. Perveen, A. Yasmin, and K. M. Khan. *The Open Analytical Chemistry Journal*, 3:1, 2009.
- [111] S. Vidovic, B. Stojanovic, J. Veljkovic, L. Prazic-Arsic, G. Roglic, and D. Manojlovic. *J. Chromatogr. A*, 1202:155, 2008.

- [112] M. Ake, H. Fabre, A. K. Malan, and B. Mandrou. *J. Chromatogr. A*, 826:183, 1998.
- [113] P. F. Chatzimichalakis, V. F. Samanidou, and I. N. Papadoyannis. *J. Chromatogr. B*, 805:289, 2004.
- [114] I. N. Papadoyannis, G. K. Tsioni, and V. F. Samanidou. *Journal of Liquid Chromatography & Related Technologies*, 20:3203, 1997.
- [115] P. Moreno and V. Salvadó. *J. Chromatogr. A*, 870:207, 2000.
- [116] B. Buszewski and W. Zbanyszek. *Journal of Liquid Chromatography & Related Technologies*, 25:1229, 2005.
- [117] H. B. Li and F. Chen. *Chromatographia*, 54:270, 2001.
- [118] B. Klejdus, J. Petrlova, D. Potesil, V. Adam, R. Mikelova, J. Vacek, R. Kizek, and V. Kuban. *Analytica Chimica Acta*, 520:57, 2004.
- [119] The Merck Manual of Medical Information, <http://www.merck.com/mmhe/sec12/ch154/ch154a.html>, March 2010.
- [120] G. Kleinschmidt. *Method Validation in Pharmaceutical Analysis: A Guide to Best Practice*, chapter 2.7, page 120. WILEY-VCH, Weinheim, 2005.
- [121] J. Ermer. *Method Validation in Pharmaceutical Analysis: A Guide to Best Practice*, chapter 2.4, page 80. WILEY-VCH, Weinheim, 2005.
- [122] P. Steliopoulos, E. Stickel, and S. Haas, H. andKranz. *Analytica Chimica Acta*, 572:121, 2006.
- [123] S. Kromidas. page 139. WILEY-VCH, Weinheim, 2000.
- [124] J. Ermer and C. Burgess. *Method Validation in Pharmaceutical Analysis: A Guide to Best Practice*, chapter 2.6, page 101. WILEY-VCH, Weinheim, 2005.
- [125] J. Ermer. *Method Validation in Pharmaceutical Analysis: A Guide to Best Practice*, chapter 2.1, page 21. WILEY-VCH, Weinheim, 2005.
- [126] J. Ermer. *Method Validation in Pharmaceutical Analysis: A Guide to Best Practice*, chapter 2.3, page 63. WILEY-VCH, Weinheim, 2005.
- [127] J. Ermer. *Method Validation in Pharmaceutical Analysis: A Guide to Best Practice*, chapter 2.5, page 99. WILEY-VCH, Weinheim, 2005.
- [128] G. Yang, S. Feng, H. Liu, Yin J., L. Zhang, and L. Cai. *J. Chromatogr. B*, 854:85, 2007.
- [129] C. V. Hofmann, R. Reischl, N. M. Maier, M. Lämmerhofer, and W. Lindner. *J. Chromatogr. A*, 1216:1157, 2009.
- [130] E. Silva, M. Salim-Hanna, A.M. Edwards, Becker, and A.E. De Ioannes. *Adv. Exp. Med. Biol.*, 289:33, 1991.
- [131] S. Carda-Broch and A. Berthod. *J. Chromatogr. A*, 995:55, 2003.
- [132] K. Fent, A.A. Weston, and D. Caminada. *Aquatic. Toxicol.*, 76:122, 2006.

- [133] H.-B. Lee, K. Sarafin, and T.E. Peart. *J. Chromatogr. A*, 1148:158, 2007.
- [134] D. Hernando, J. Gómez, A. Agüera, and A.R. Fernández-Alba. *Trends in Analytical Chemistry*, 26:581, 2007.
- [135] G. Vivó-Truyols, J.R. Torres-Lapasió, and M.C. García-Alvarez-Coque. *J. Chromatogr. A*, 1018:183, 2003.
- [136] V.-P. Ranta, E. Toropainen, A. Talvitie, S. Auriola, and A. Urtti. *J. Chromatogr. B*, 772:81, 2002.
- [137] X. Liu and C. Pohl. *LC-GC Europe*, 33, 2007.
- [138] S. S. Galushko, I. Tanchuk, V. and Shishkina, O. Pylypchenko, and W. D. Beiner. *HPLC Made to Measure: A Practical Handbook for Optimization*, chapter ChromSword Software for automated and computer-assisted development of HPLC methods. Number 9. WILEY-VCH Verlag GmbH & Co. KGaA, Weinheim (Germany).
- [139] G. Gagliardi, C.B. Castells, C. Ràfols, M. Rosés, and E. Bosch. *J. Sep. Sci.*, 31:969, 2008.
- [140] X. Subirats, J. Gotta, L.G. Gagliardi, C.B. Castells, C. Ràfols, M. Rosés, and E. Bosch. Anomalous chromatographic retention of betablockers in mobile phases buffered by tri(hydroxymethyl)aminomethane. Poster presented at HPLC 2009, Dresden (Germany).
- [141] R. Nageswara Rao and V. Nagaraju. *J. Pharm. Biomed. Anal.*, 33:335, 2003.
- [142] R. Nageswara Rao and V. Nagaraju. *J. Pharm. Biomed. Anal.*, 34:1049, 2004.
- [143] B. Miseljic, G. Popovic, and D. Agbaba. *J. AOAC Int.*, 91:332, 2008.
- [144] Council of Europe Strasbourg (France). *European Pharmacopoeia 6.2*, page 1248, 2008.
- [145] J.K. Liao. *J. Clin. Invest.*, 110:285, 2002.
- [146] E. Bruenger and H.C. Rilling. *Anal. Biochem.*, 173:321, 1988.
- [147] Y. Saisho, A. Morimoto, and T. Umeda. *Anal. Biochem.*, 252:89, 1997.
- [148] H. Tong, S.A. Holstein, and R.J. Hohl. *Anal. Biochem.*, 336:51, 2005.
- [149] H. Tong, A.J. Wiemer, J.D. Neighbors, and R.J. Hohl. *Anal. Biochem.*, 378:138, 2008.
- [150] G.P. Hooff, D.A. Volmer, W.G. Wood, W.E. Müller, and G.P. Eckert. *Anal. Biochem.*, 392:673, 2008.
- [151] T. Hirai, S. Matsumoto, and I. Kishi. *J. Chromatogr. B*, 692:375, 1997.
- [152] X.-S. Miao, B. G. Koenig, and C. D. Metcalfe. *J. Chrom. A*, 952:139, 2002.
- [153] N. M. Vieno, T. Tuhkanen, and L. Kronberg. *Environ. Sci. Technol.*, 39:8220, 2005.

- [154] T. Shinozuka and R. Nakajima. *Drugs and poisons in humans: a handbook of practical analysis*, chapter 2, page 325. Springer-Verlag, 2005.
- [155] [www.syrres.com/what-we-do/databaseforms.aspx?id=386](http://www.syrres.com/what-we-do/databaseforms.aspx?id=386). April 2010.
- [156] C. Zwiener. *Heil-Lasten: Arzneimittelrückstände in Gewässern*, page 210. Springer-Verlag, 2006.
- [157] C. Ràfols, M. Rosés, and E. Bosch. *Anal. Chim. Acta*, 338:127, 1997.
- [158] E. Ayano, K. Nambu, C. Sakamoto, H. Kanazawa, A. Kikuchi, and T. Okano. *J. Chromatogr. A*, 119:58, 2006.
- [159] J. Sjöquist. *Nobel Lectures, Physiology or Medicine 1922-1941*, 1923, 1965.
- [160] T. Blundell, G. Dodson, D. Hodgkin, and D. Mercola. *Advances in protein chemistry, Volume 26*, page 284. Elsevier, 1972.
- [161] T.A. Brown. *Gene Cloning an DNA Analysis: an introduction*, chapter 14, page 246. Wiley-Blackwell, 2010.
- [162] G. Walsh. *Pharmaceutical biotechnology: concepts and applications*, chapter 11, page 297. John Wiley & Sons Ltd., 2007.
- [163] D.R. Owens. *Human insulin: clinical pharm studies in normal man*, chapter 4, page 56. Kluwer, 1986.
- [164] A.M. Kligman and I. Willis. *Arch. Dermatol.*, 54:272, 2006.
- [165] I. Pelisson and A. Jomard. *Organisation mondiale de la Propriété Intellectuelle*, WO 2007/125262, 2007.
- [166] R. Chan, K.C. Park, M.H. Lee, E.-S. Lee, S.E. Chang, Y.H. Leow, Y-K. Tay, F. Legarda-Montinola, R-Y. Tsai, T-H. Tsai, S. Shek, N. Kerrouche, G. Thomas, and V. Verallo-Rowell. *British Journal of Dermatology*, 159:697, 2008.
- [167] M. Lämmerhofer, R. Nogueira, and W. Lindner. *Analytical and Bioanalytical Chemistry*, 10.1007/s00216-011-4755-3:1, 2011.



# List of Figures

1.1.1.	Principle of chromatography. . . . .	5
1.1.2.	Chromatogram of three components and corresponding parameters for the calculation of different chromatographic data [3]. . . . .	6
1.2.1.	Postulated types of hydroxyl groups on the surface of amorphous silica. . . .	10
1.2.2.	Reactive silanols on silica surfaces. . . . .	11
1.2.3.	Scanning electron microscopy of Merck in-house produced silica-based research sample. . . . .	11
1.2.4.	Pore size distribution of silica material measured by nitrogen desorption [13].	12
1.3.1.	Schematic illustration of the partitioning mechanism on the surface of HILIC modified silica. . . . .	16
1.3.2.	Schematic illustration of the partitioning mechanism on the surface of RP modified silica. . . . .	17
1.3.3.	Synthesis of different types of mixed-mode materials . . . . .	19
2.1.1.	Response surface illustrating the dependency of surface coverage (SC) on reaction time and temperature. . . . .	28
2.1.2.	<sup>29</sup> Si CP-MAS NMR spectra of thiopropyl-modified silica particles prepared from 3-mercaptopropyltrimethoxymethylsilane. . . . .	30
2.1.3.	SH activity ( $\alpha_{\text{caffeine/benzylamine}}$ ) and silanol activity ( $\alpha_{\text{acetophenone/caffeine}}$ ) of five different modified silica particles. . . . .	33
2.1.4.	Chromatograms of the developed HPLC test for columns packed with mercaptopropyl modified silica material synthesized at two different temperatures.	34
2.1.5.	Change of SH and silanol activity for two materials synthesized at two different temperatures in the course of the stability testing. . . . .	35
2.1.6.	Evolution of the $m/z = 166.32$ Da response during ESI/MS runs. . . . .	36
2.2.1.	Investigation of the bleeding of the RP-WAX material through LC-MS. . . .	40
2.3.1.	Structure of the RP-WAX selector and proton numbering. . . . .	47
2.3.2.	Spatial representation of the RP-WAX selector. . . . .	48
2.4.1.	Scheme of the Friedel-Craft hypercrosslinking developed by Trammel et al. .	51
2.4.2.	Reaction scheme of the hypercrosslinking on the silica surface through a tridentate silane. . . . .	54
2.4.3.	Reaction scheme of the hypercrosslinking on the silica surface through a monodentate silane. . . . .	56
2.4.4.	Reaction scheme of the hypercrosslinking on the silica surface after tetramethyltetravinylcyclsiloxane opening. . . . .	58
2.4.5.	Optimization of the TeMTeVTeS addition. . . . .	60
2.5.1.	Structures of some published mixed-mode reversed phase - ion exchange material. . . . .	63

2.5.2.	Reaction scheme for the synthesis of a mixed-mode RP-SAX selector. . . . .	64
2.5.3.	Reaction scheme for the synthesis of mixed-mode RP-WCX selectors. . . . .	65
2.5.4.	Reaction scheme for the synthesis of mixed-mode RP-SAX silica phase. . . . .	66
2.5.5.	Reaction scheme for the synthesis of mixed-mode RP-WCX silica phases. . . . .	66
2.5.6.	Reaction scheme for the synthesis of mixed-mode RP-SCX silica phases. . . . .	67
3.1.1.	Hexagram from the Tanaka test for a standard RP18 column. . . . .	74
3.1.2.	Results from the column classification system. . . . .	78
3.1.3.	Theoretical separation estimated through ChromSword on a Purospher STAR RP18-e 5µm. . . . .	79
3.1.4.	Comparison of the separation of benzene derivates on hypercrosslinked RP-WAX (red), standard RP-WAX (green) and fully optimized RP-WAX (blue) columns. . . . .	80
3.1.5.	Comparison of the separation of benzene derivates on Merck fully optimized RP-WAX (blue) and on Dionex Acclaim Mixed-Mode WAX-1 (black) columns. . . . .	81
3.1.6.	Evolution of the capacity factor of benzene derivates in acidic and in basic conditions. . . . .	83
3.1.7.	Evolution of the relative capacity factors of pentylbenzene / butylbenzene and benzoic acid / toluene in acidic and in basic conditions. . . . .	84
3.1.8.	Comparison of the symmetry factor for the benzene derivates on the Dionex column and on the Merck optimized material during the basic and acidic stability evaluation. . . . .	85
3.1.9.	Evolution of the column back pressure during the stability evaluation. . . . .	86
3.2.1.	Structure of the developed mixed-mode reversed phase - weak anion exchange (RP-WAX) separation material. . . . .	91
3.2.2.	HPLC-UV chromatogram of a standard mixture of 10 water- and fat-soluble vitamins under optimized gradient elution conditions. . . . .	97
3.2.3.	Effect of the pH and of the temperature on the retention factor and on the symmetry factor of the vitamins. . . . .	99
3.2.4.	Optimized gradient profile with respect to acetonitrile content and phosphate buffer concentration as obtained by automatic gradient profile optimization with ChromSword. . . . .	100
3.2.5.	Evaluation of the robustness of the method by plotting the relative standard deviation of the retention time for four different parameters (buffer molarity, gradient slope, temperature, and pH). . . . .	102
3.2.6.	Evolution of the stability of the vitamin mixture considering the peak area over 15 hours of storage in the autosampler at 25°C. . . . .	105
3.2.7.	Deviation of the peak area for each vitamin at 4 different storage conditions. . . . .	107
3.2.8.	HPLC-UV chromatogram of the Rossmann tablet under optimized gradient elution conditions. . . . .	108
3.3.1.	Structure of the $\beta$ -blockers investigated in present study. . . . .	112
3.3.2.	Structure of the developed mixed-mode reversed phase - weak anion exchange (RP-WAX) separation material. . . . .	112
3.3.3.	Chromatogram of seven $\beta$ -blockers separated on a C18 column. . . . .	118
3.3.4.	Chromatogram of seven $\beta$ -blockers separated on ZIC-HILIC column. . . . .	119
3.3.5.	Capacity factors for pindolol at 30% acetonitrile at different pH and TRIS / phosphate buffer concentrations on RP-WAX and RP columns . . . . .	121
3.3.6.	Chromatogram of seven $\beta$ -blockers separated on a RP-WAX column. . . . .	123

3.4.1. Comparison of both chromatograms for the separation of norfloxacin, ciprofloxacin and danofloxacin after smart screening on RP18 and on RP-WAX columns. .	127
3.4.2. Evaluation of the reproducibility of the separation of the 3 fluoroquinolone antibiotics. . . . .	127
3.4.3. European Pharmacopoeia validated method for the separation of norfloxacin from its three main impurities. . . . .	128
3.4.4. Separation of norfloxacin from its three main impurities after fine optimization on RP18 material. . . . .	130
3.4.5. Chromatogram of the separation of norfloxacin from its three main impurities after fine optimization on a RP-WAX column. . . . .	130
3.4.6. Mevalonate (MVA) pathway resulting in the formation of isoprenoides and cholesterol. . . . .	131
3.4.7. Structure of the two isoprenoides coupled with the appropriate dansyl-labeled pentapeptides. . . . .	132
3.4.8. Separation of both FPP* and GGPP* as well as an internal standard IS* from a brain homogenate on a C18 column using a validated method. . . . .	132
3.4.9. Separation of both FPP* and GGPP* as well as two internal standard IS1 and IS2 in a brain matrix on a RP-WAX column. . . . .	133
3.4.10. Separation of five different acidic anti-inflammatory drugs on a RP column. .	135
3.4.11. Five different acidic anti-inflammatory drugs separated on a RP-WAX column.	136
3.4.12. Scheme of the human insulin as published by Hodgkin in 1969. . . . .	137
3.4.13. Separation of human insulin (HI) from two impurities (I1 and I2) on RP18 material. . . . .	138
3.4.14. Separation of human insulin (HI) from two impurities (I1 and I2) on a RP-WAX column. . . . .	139
3.4.15. Number of pages generated by Google with the key words “buy tri-luma” on the 1st of January of each year. . . . .	141
3.4.16. Separation of the three active molecules hydroquinone, fluocinolone acetonide, and tretinoin of the Tri-Luma product on a two dimensional RP18/HILIC system. . . . .	142
3.4.17. Separation of the three active molecules hydroquinone, fluocinolone acetonide, and tretinoin of the Tri-Luma product on a RP-WAX column. . . . .	142



## List of Tables

2.1.1. Characteristics of synthesized thiol-modified particles. . . . .	25
2.1.2. Estimated coefficient values, standard errors and significance after model fitting from surface coverage determined for active sulfhydryls. . . . .	29
2.1.3. Relative signal intensities (%) as obtained by deconvolution of the <sup>29</sup> Si CP-MAS NMR spectra. . . . .	31
2.1.4. Modified silica materials with different surface modifications and corresponding surface coverages employed for the development of a specific chromatographic test. . . . .	32
2.2.1. Characteristics of endcapped thiol-modified particles from 4 different endcapper compositions. . . . .	42
2.2.2. Comparison of endcapping surface coverage with ATMS at 120°C and 75°C for 20 h. . . . .	42
2.2.3. Verification of reproducibility of the endcapping reaction after 6 h and 20 h of reaction at 75°C. . . . .	42
2.2.4. Impact of hydrolysis on both mercaptopropyl and endcapping carbon surface coverage. . . . .	43
2.3.1. Synthesis of N-(10-undecenoyl)-3-aminoquinuclidine . . . . .	49
2.3.2. Evaluation of the reaction time and of the radical initiator on the grafting reaction. . . . .	50
2.3.3. Evaluation of the impact of the RP-WAX selector amount and of the reproducibility of the grafting reaction. . . . .	50
2.4.1. Characteristics of TVCS modified silica. . . . .	55
2.4.2. Characteristics of monodentate modified silica. . . . .	57
2.4.3. Characteristics of silica materials modified with TeMTeVTeS in different solvents in the presence of different acidic modifiers within different reaction times. . . . .	59
2.4.4. Characteristics of TeMTeVTeS modified silica after endcapping, hypercrosslinking and grafting of the RP-WAX selector. . . . .	60
2.5.1. Functional groups for ion exchange chromatography. . . . .	63
2.5.2. Synthesis of weak cation exchangers based on undecenoyl chloride derivatives. . . . .	68
3.1.1. Structure and parameters of the benzene derivates used for the performance and stability tests. . . . .	75
3.1.2. Mobile phase composition and sample composition for measurement of the 4 parameters from the column classification system. . . . .	76
3.1.3. Stress procedure for the evaluation of the stability of RP-WAX material. . . . .	77
3.2.1. Names and structures of the considered vitamins, their main deficiency diseases and the recommended dietary allowances. . . . .	90
3.2.2. Composition of the vitamin tablets analyzed in this study. . . . .	93

3.2.3. Mobile phase composition for the optimal simultaneous separation of fat- and water- soluble vitamins. . . . .	94
3.2.4. Concentration of the vitamins in each solution for the determination of accuracy and precision. . . . .	96
3.2.5. Linearity and analytical measurement limits for the different vitamins. . . . .	103
3.2.6. Intraday and interday precision and accuracy data for all the validated vitamins. . . . .	104
3.2.7. Measurement range of various vitamins. . . . .	105
3.2.8. Real sample analysis of two different commercially available tablets. . . . .	109
3.3.1. Capacity factor of seven $\beta$ -blockers determined at 100 mM phosphate buffer, three different pH and ten different acetonitrile concentrations. . . . .	114
3.3.2. Capacity factor of seven $\beta$ -blockers determined at 20 mM phosphate buffer, three different pH and ten different acetonitrile concentrations. . . . .	115
3.3.3. Capacity factor of seven $\beta$ -blockers determined at 100 mM tris buffer, three different pH and ten different acetonitrile concentrations. . . . .	116
3.3.4. Capacity factor of seven $\beta$ -blockers determined at 20 mM tris buffer, three different pH and ten different acetonitrile concentrations. . . . .	117
3.3.5. Resolution factor calculated from the Unite States Pharmacopoeia calculation method of the less resolved peak for each column and each RP-WAX gradient. . . . .	122
3.4.1. Structure of the three amphoteric fluoroquinolone antibiotics. . . . .	126
3.4.2. The norfloxacin antibiotic and its three main impurities. . . . .	129
3.4.3. Schemes of the five acidic anti-inflammatory drugs. . . . .	134
3.4.4. Three active molecules in the Tri-Luma product. . . . .	140

# Index

- Anti-inflammatory drugs, 134
- Antibiotics, 126
- Application, 89, 111, 125
- Asymmetry, 8
  
- Backpressure, 11
- Berendsen and de Galan, 12
- Betablockers, 111
  - Retention factors, 113
  - Separation on conventional materials, 118
  - Separation on RP-WAX material, 121
- Bonding density, 12
  
- Carbon content, 12
- Column classification system, 77
  
- Design of Experiment, 27
- Design of experiment, 23
  
- Efficiency, 7
  
- HETP, 7
- Hydrophilic Interaction Chromatography, 16
- Hydrophobic Interaction Chromatography, 17
- Hypercrosslinking, 52–54
  
- Insulin, 137
- Ion exchange chromatography, 17
- Isoprenoides, 131
  
- Mixed-mode chromatography, 18
  
- Normal Phase Chromatography, 15
  
- Packings, 9
- Particle size, 10
  
- Resolution, 8
- Retention time, 6
- Reversed Phase, 17
  
- RP-SAX
  - Grafting, 66
  - Selector Synthesis, 64
- RP-SCX
  - Grafting, 66
- RP-WAX
  - Endcapping, 41
  - Grafting, 47, 49
  - Hydrolysis, 42
  - Selector synthesis, 46, 48
  - Spacer addition, 23
- RP-WCX
  - Grafting, 66
  - Selector Synthesis, 65
  
- Sandoval, 13
- Selectivity, 7, 15
- Selector, 63
- Silica surface, 9
- Solid state NMR, 29
- Specific mixed-mode HPLC test, 78
- Stability, 34, 39, 51, 73, 80
- Surface area, 11
- Surface coverage, 13, 27, 41, 49, 53, 68
  
- Tri-Luma, 140
  
- Vitamins, 89
  - Real sample analysis, 108
  - Validation, 92, 100
  
- ZIC-HILIC, 16





## **Addenda**



# Papers

Both following papers were included within corpus of the PhD thesis, respectively in Part II, Chapter 1, and in Part III, Chapter 2.



Contents lists available at ScienceDirect

Journal of Chromatography A

journal homepage: [www.elsevier.com/locate/chroma](http://www.elsevier.com/locate/chroma)

## Statistical optimization of the silylation reaction of a mercaptosilane with silanol groups on the surface of silica gel

Romain Dabre<sup>a,b</sup>, Achim Schwämmle<sup>a</sup>, Michael Lämmerhofer<sup>b</sup>, Wolfgang Lindner<sup>b,\*</sup><sup>a</sup> Merck KGaA, Performance and Life Science Chemicals, Frankfurter Strasse 250, D-64293 Darmstadt, Germany<sup>b</sup> Christian Doppler Laboratory for Molecular Recognition Materials, Department of Analytical Chemistry & Food Chemistry, University of Vienna, Währinger Strasse 38, A-1090 Vienna, Austria

### ARTICLE INFO

Article history:  
Available online 15 January 2009

Keywords:  
Silylation  
Mercaptopropyl-bonded silica  
Design of experiment  
Optimization  
Stability  
Mono-functional bonding  
Di-functional bonding  
<sup>29</sup>Si CP-MAS NMR

### ABSTRACT

Thiol-modified silica is often used as an intermediate product for further synthesis of modified stationary phases for chromatography or purification processes. Different conditions were used to synthesize such thiol-modified particles, but systematic optimizations remained scarce. In this study the reaction conditions for the synthesis of mercaptopropyl-modified silica were optimized. The general synthetic method consists in slurrying the silica gel in toluene before adding 3-mercaptopropyltrimethoxymethylsilane together with a tertiary amine as catalyst (here dimethylaminopyridine). Reaction time and temperature were optimized using a full factorial design of experiment (DoE) from 3 to 25 h with temperature varying between 45 and 105 °C. The surface coverage of the silica with mercaptopropyl-groups was analyzed by two different ways (elemental analysis and chemical surface reaction with 2,2'-dipyridyl disulfide followed by HPLC-UV analysis of stoichiometrically liberated pyridyl-2-thione). We obtained a three-dimensional (3D) plot of the surface coverage as a function of reaction time and temperature. The arch-shaped hyperplane allowed us to determine an optimum with regard to time and temperature, which yields to the highest surface coverage possible. We also verified that the increase of the surface coverage does not lead to a decrease of the stability of the surface modification by subjecting the gels to treatment with high temperature and acidic conditions. The stability was monitored by different chromatographic methods. Moreover, <sup>29</sup>Si cross-polarization-magic angle spinning (CP-MAS) NMR spectra of materials prepared by different conditions allowed to confirm that the Si species on the surface were essentially the same, while there was only a minute difference in signal intensities for the individual Si species for materials obtained by distinct temperatures.

© 2009 Elsevier B.V. All rights reserved.

### 1. Introduction

Thiol-modified silica is often used as an intermediate product for further synthesis of modified stationary phases for chromatography, amongst others chiral phases [1,2], or mixed-mode reversed-phase/weak anion-exchange phases [3]. Many other uses of thiol-modified silica itself can be found in the literature, for example to analyze the very low amount of germanium in natural waters [4] or to recover homogenous catalysts from the reaction mixture by interaction between the thiol-group and the metal centre of the catalyst [5].

The study of mercaptopropylsilanes as silylating agent has started in the late seventies and the first synthesis route involved 3-mercaptopropyltrimethoxysilane (MPTMS) heated with silica gel at reflux for 1 h in the presence of hexane and water [6]. Less common is the synthesis by heating the silica gel with MPTMS in dimethyl-

formamide (DMF) with imidazole as a catalyst at 100 °C for 20 h [7]. The surface coverage obtained by the latter was between 1.30 and 1.64 μmol/m<sup>2</sup>. In most of the publications, the general synthetic method consisted in slurrying the silica gel in toluene before adding MPTMS. Heating this suspension for 24 h leads to surface coverage between 1.8 and 2.6 μmol/m<sup>2</sup> [8]. Further study showed that adding a tertiary amine such as pyridine or its derivatives enhances the surface coverage. Heated at 80 °C for 28 h, the mercaptopropylsilica reaches a surface coverage of 2.0 μmol/m<sup>2</sup> [9]. Lewis et al. obtained a surface coverage of 4.37 μmol/m<sup>2</sup> by heating the suspension at 115 °C for 24 h [10]. Different studies with other small silanes such as trimethylchlorosilane or trimethylalkoxysilanes which had been performed over the years show that surface coverage up to the average limit of 4.5–4.75 μmol/m<sup>2</sup> is principally possible [11,12]. Scully et al. have performed an optimization of the silylation reaction with mercaptopropyl silane in supercritical carbon dioxide leading to surface coverage up to 6.0 μmol/m<sup>2</sup> [13]. Different conditions were used to synthesize thiol-modified stationary phases, but were seldom optimized by a systematic approach in which temperature and reaction time were both investigated over a wide range.

\* Corresponding author.  
E-mail address: [wolfgang.lindner@univie.ac.at](mailto:wolfgang.lindner@univie.ac.at) (W. Lindner).

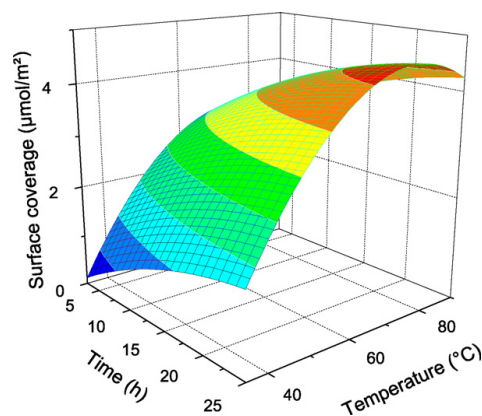


**Fig. 1.** Response surface illustrating the dependency of surface coverage (SC) from sulfur content determined by DPDS-method on reaction time (h) and temperature (°C)  $SC = A + B \times t + C \times T + D \times t^2 + E \times T^2 + F \times t \times T$  with adj.  $R^2 = 0.987976$ , RMS-error = 0.09498 and  $n = 13$ . For coefficient values and standard errors, see Table 2.

In our study, a design of experiment (DoE) has therefore been performed in order to optimize the reaction time and temperature. Commonly, silylations with tri-functional silanes induce much more silanol activity than di-functional silanes without improving the surface coverage. Tri-functional silanes yield an average linkage number of 1.6 which means that the third reactive leaving group of the silane (usually a methoxy substituent) remains always unreacted and enhances the silanol activity of the resulting silica gel [14,15]. In preliminary experiments for this study, we compared the surface coverage after reaction of silica gel with MPTMS and with 3-mercaptopropyltrimethoxymethylsilane (MPDMS) in toluene with addition of dimethylaminopyridine at different temperatures and reaction time. It turned out that the surface coverage is exactly the same for both reagents at given temperature,

time and concentrations. The following study has therefore been performed with MPDMS (see Fig. 1), because it was deemed beneficial in terms of its chromatographic performance and stability. Selected thiol-modified particles were characterized by solid-state NMR.

## 2. Experimental

### 2.1. Chemicals

Pharmprep Si 100 10 μm obtained from Merck, Darmstadt, Germany. The material exhibits a surface area of 300 m<sup>2</sup>/g and a specific pore volume of 0.81 ml/g. Dimethylaminopyridine (DMAP) was obtained from AcrosOrganics (Geel, Belgium), MPDMS, hexamethyldisilazane (HMDS) and *n*-propylmethyldimethoxysilane (PMDMS) from ABCR (Karlsruhe, Germany), azobisisobutyronitrile (AIBN), 1-tetradecene, toluene and 25% sulfuric acid from Merck, 2,2'-dipyridyl disulfide (DPDS) and 2-mercaptoethanol from Sigma-Aldrich (Steinheim, Germany). The chemicals were used without any further purification.

Mobile phases for chromatography were prepared from HPLC grade solvents (i.e. water, acetonitrile and methanol LiChrosolv from Merck) and analytical grade formic acid (FA) and trifluoroacetic acid (TFA) (Merck).

### 2.2. Silica pretreatment

The raw silica has been rehydroxylated in 25% sulfuric acid over 20 h at room temperature before being washed with deionized water and dried at 90 °C under vacuum for at least 24 h until weight constancy.

### 2.3. Instrumentation

The elemental analyses were carried out on an Elementar (Hanau, Germany) vario EL III analyzer. The Berendsen-de Galan's equation was used to calculate the surface coverages [16] and the results are given in Table 1.

**Table 1**  
Characteristics of synthesized thiol-modified particles.

Material number	Temperature (°C)	Reaction time (h)	%C	%S	Surface coverage S (μmol/m <sup>2</sup> )		Reactive sulfhydryls by DPDS (μmol/m <sup>2</sup> )
					Low <sup>a</sup>	High <sup>b</sup>	
1	45	3.0	1.8	1.0	1.08	1.09	1.09
2		8.0	2.8	1.5	1.66	1.68	1.70
3		25.0	4.0	2.5	2.87	2.95	2.88
4	60	3.0	4.0	2.2	2.50	2.56	2.54
5		5.5	4.4	2.4	2.75	2.82	2.81
6		8.0	4.6	2.6	3.00	3.09	3.10
7		15.0	5.0	3.0	3.52	3.64	3.56
8		25.0	5.8	3.4	4.06	4.21	4.15
9	75	3.0	4.7	2.6	3.00	3.09	3.09
10		5.5	5.0	2.9	3.39	3.50	3.35
11		8.0	5.2	3.0	3.52	3.64	3.64
12		15.0	5.6	3.4	4.06	4.21	4.20
13		25.0	5.7	3.5	4.20	4.36	4.35
14	90	3.0	4.0	2.4	2.75	2.82	2.77
15		5.5	4.2	2.6	3.00	3.09	3.01
16		8.0	4.5	2.8	3.26	3.36	3.25
17		15.0	4.8	3.1	3.66	3.78	3.76
18		25.0	5.3	3.5	4.20	4.36	4.31
19	105	3.0	3.8	2.3	2.62	2.69	2.71
20		8.0	4.5	2.7	3.13	3.22	3.21
21		25.0	5.4	3.5	4.20	4.36	4.30

<sup>a</sup> As calculated for di-functionally bonded silane from %S of elemental analysis data.

<sup>b</sup> As calculated for mono-functionally bonded silane from %S of elemental analysis data.

The chromatographic experiments were carried out on a VWR (Darmstadt, Germany) Hitachi LaChrom Elite HPLC system (three channels pump L-2130 with degasser, autosampler L-2200, oven L-2300, diode array detection (DAD) system L-2455). The data were processed using the Agilent (Waldbronn, Germany) EZChrom Elite version 3.21 software.

For the liquid chromatography–mass spectrometry (LC–MS) analysis, the chromatographic system was an Agilent 1100 Series equipment comprising a pump, a degasser, a column oven and an autosampler. MS-detection has been performed on a Bruker Daltonics (Bremen, Germany) Esquire 3000 plus device and the data were processed using the Esquire Control version 5.0 software from the same company.

#### 2.4. Determination of reactive surface thiols

This method is based on a thiol–disulfide exchange reaction in acetonitrile with 2,2'-dipyridyl disulfide (DPDS) as reagent and HPLC–UV analysis of pyridyl-2-thione which is liberated in equimolar amounts to reactive sulphydryls as validated and described in detail in ref. [17]. 2-Mercaptoethanol solutions in acetonitrile served as standards for calibration and the detailed procedure can be found elsewhere [17]. The experimental results along with the corresponding elemental analysis data are given in Table 1.

#### 2.5. Reaction procedure

The apparatus was flushed with nitrogen flux during the whole reaction process. The silica was slurried in toluene and heated at reflux for 1.5 h using a Dean–Stark trap in order to remove the water adsorbed on the silica surface. After cooling down to room temperature, the reagents were added and the suspension was heated up to the temperature given by the DoE. After the predetermined time of reaction, the silica was directly washed with toluene and subsequently agitated three times in methanol at reflux for 20 min.

For preparation of mercaptopropyl-modified silica, the reagent was MPDMMS and for preparation of propyl-modified silica, PMDMMS was used as reagent. For endcapping, the reagent was HMDS.

For C14-S-C3-e-silica, mercaptosilica ( $2.16 \mu\text{mol}/\text{m}^2$ ) endcapped with HMDS ( $0.32 \mu\text{mol}/\text{m}^2$ ) was heated at  $60^\circ\text{C}$  in presence of AIBN and 1-tetradecene in methanol before being washed as before.

#### 2.6. Statistical method

The different surface modification experiments were planned using the statistical software Cornerstone (Applied Materials, Santa Clara, CA, USA). This DoE software was used to calculate the three-dimensional (3D) model whereas the Origin software (OriginLab, Northampton, MA, USA) has been used to plot the 3D arch-shape plane of the surface coverage and to perform the two-dimensional modeling on the whole range.

#### 2.7. NMR spectroscopy

The NMR experiments were performed on Bruker AV 400 MHz spectrometer.

All spectra were acquired at 300 K. XWINNMR software version 3.5 (Bruker) was used for data acquisition and processing. Four millimeters zirconia spinners were used.

The solid-state CP-MAS NMR experiments were performed at 400.13 MHz using TPPM25 and a spinning rate of 5000 Hz. A total of 1188 data points were recorded and 4 k scans were performed. The relaxation delay was set at 5 s and the contact time was set at 7 ms.

#### 2.8. Conditions for the chromatographic test

The chromatographic conditions were optimized to achieve base-line separation for the test mixture (see below) in less than 10 min. The mobile phase was composed of a mixture of 0.1% TFA in water (A) and 0.1% TFA in methanol (B). A linear gradient was run from 20 to 80% B in 6 min followed by elution with 80% B for another 4 min. The temperature was maintained at  $25^\circ\text{C}$  and the flow rate was 1 ml/min. Ten microliters of the analyte mixture (benzylamine:  $0.76 \mu\text{l}/\text{ml}$ , caffeine:  $0.26 \mu\text{l}/\text{ml}$  and acetophenone:  $0.98 \mu\text{l}/\text{ml}$  dissolved in methanol–water–TFA, 50:50:0.1%, v/v/v) were injected. Peaks were detected at 212 nm. The methanol in the sample solution appeared as a solution peak and was used as  $t_0$  marker.

#### 2.9. Stress treatment

Before each chromatographic test run using the method described above the column was rinsed with an acidic eluent (methanol–water, 80:20, v/v, pH 2.0 by addition of TFA) at a flow rate of 1 ml/min for 2 h at  $45^\circ\text{C}$ .

#### 2.10. LC–MS bleeding test

The bleeding of the material was tested with a linear gradient of acetonitrile, 0.1% FA (A) and water, 0.1% FA (B) from 10 to 90% A in 5 min, 90% A for 3 min and 10% A for 10 min. The column was kept at RT and the flow rate was 1 ml/min. The ionization was carried out in electrospray ionization in the positive ion mode (ESI(+) mode) and the extracted ion chromatogram was monitored. The column was flushed between each measurement run with 2-propanol, 0.1% FA for 60 min at a flow rate of 0.5 ml/min.

### 3. Results and discussion

#### 3.1. Optimization of the silylation reaction

A systematic approach employing a DoE strategy was utilized to optimize the surface coverage of the thiol-modified particles. The parameter range for optimization was fixed from 3 to 25 h for the reaction time and for  $45$ – $105^\circ\text{C}$  for the reaction temperature. After a first screening, we found that the response was quadratic between  $45$  and  $90^\circ\text{C}$ . To reduce the number of experiments without losing information, a full factorial DoE was automatically generated between  $60$  and  $90^\circ\text{C}$ . The individual experiments and the results in terms of carbon and sulfur contents, surface coverages and active sulphydryl concentrations are given in Table 1.

The statistical software was then used to derive the coefficients for the subsequent model which describes the surface coverage (SC) as analyzed by elemental analysis and the DPDS test for active sulphydryls, respectively, in dependence of temperature ( $T$ ) and reaction time ( $t$ ):

$$\text{SC} = A + B \times t + C \times T + D \times t^2 + E \times T^2 + F \times t \times T \quad (1)$$

where  $A$ ,  $B$ ,  $C$ ,  $D$ ,  $E$  and  $F$  are the coefficients of the model. A second-order polynomial model has been chosen in order to study the impact of time and temperature. Interrelation of both effects (last term in the equation) has been excluded from the model after statistical fitting because of lack of statistical significance.

While the model fitted well to the experimental data in the  $T$  range between  $45$  and  $90^\circ\text{C}$ , larger deviations between experimental and calculated surface coverages were observed between  $90$  and  $105^\circ\text{C}$ . Therefore, only the temperature range up to  $90^\circ\text{C}$  was considered in the 3D model (Fig. 1). The estimated coefficients and their standard errors are given in Table 2 whereas adjusted  $R^2$ , root mean square error (RMS-error) and residual degrees of freedom ( $n$ ) are given in the caption of Fig. 1.

**Table 2**

Estimated coefficient values, standard errors and significance after model fitting from surface coverage determined for active sulphydryls.

Coefficient	Coefficient value	Std. error	P-value <sup>a</sup>
A	−810,355	0.468337	2.34E−10
B	0.281336	0.0141719	4.17E−11
C	0.127002	0.0142075	6.50E−07
D	−0.0018327	0.000102393	1.53E−10
E	−0.00204266	0.000487857	1.06E−03
F	−	−	0.07

<sup>a</sup> P-value of <0.05 was set as statistical significance criterium for a term to be kept in model.

As can be seen from Fig. 1, the surface coverage is increasing slowly as a function of reaction time at any temperature before reaching a pseudo-plateau above 20 h. We can also conclude that the surface coverage cannot exceed the value of SC = 4.4  $\mu\text{mol}/\text{m}^2$  with the given reaction mixture, which corresponds to the maximum surface coverage. This value for the maximal surface coverage is in agreement with literature data [11,18].

Concerning temperature dependency, a few aspects are noteworthy to be briefly outlined here. Below 45 °C, barely any reaction could be observed. Between 45 and 75 °C, surface coverage increases whereas above 75 °C, the surface coverage slowly decreases.

Further surface coverage data have been monitored at higher temperatures not covered by the depicted temperature range of Fig. 1 (i.e. 90–105 °C). Combining these data with the former allows to derive information on the entire available reaction temperature range (i.e. 45–105 °C). It is seen that above 90 °C, surface coverage slowly reaches a plateau, which means that within high temperature range (i.e. 90–105 °C), the amount of silane bonded to the surface remains constant. A maximum in the surface coverage at 75 °C could be read out, which corresponds to the overall temperature optimum at any reaction time.

Overall, performing a design of experiment to optimize the reaction conditions is a very efficient tool to obtain optimum surface coverage on silica material. Moreover, it is easier to find the most reasonable compromise in terms of high surface coverage, low energy input and short reaction time. For example, a surface coverage of more than 3  $\mu\text{mol}/\text{m}^2$  can be reached after only 3 h of reaction at 75 °C, whereas the same degree of coverage at 105 °C is obtained only after 6 h.

### 3.2. Characterization of thiol-modified particles by <sup>29</sup>Si CP-MAS NMR

Solid-state NMR was shown to be a powerful tool to investigate the bonding chemistry of modified silica surfaces [19–22]. Herein, we utilized <sup>29</sup>Si cross-polarization-magic angle spinning NMR (<sup>29</sup>Si

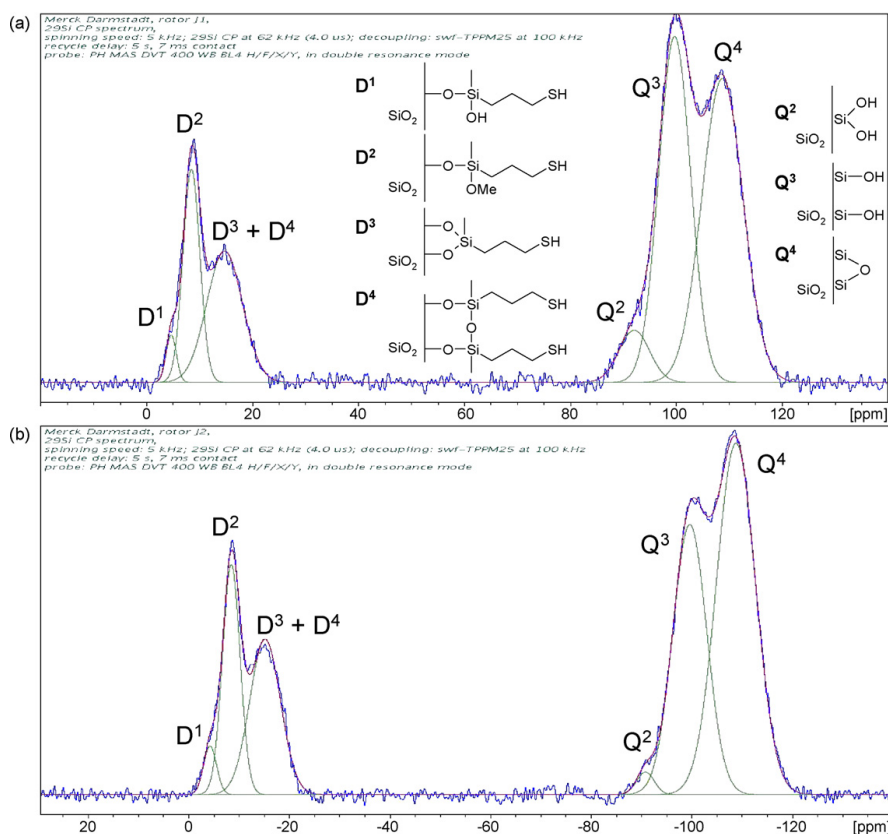


**Fig. 2.** <sup>29</sup>Si CP-MAS NMR spectra of thiolpropyl-modified silica particles prepared from 3-mercaptopropyltrimethoxymethylsilane at 60 °C (a) and 90 °C (b) for 3 h.

**Table 3**  
Relative signal intensities (%) as obtained by deconvolution of the  $^{29}\text{Si}$  CP-MAS NMR spectra.

Conditions	SC ( $\mu\text{mol}/\text{m}^2$ )	$D^1 + D^2$ , –4 and –8 ppm	$D^3 + D^4$ , –15 ppm	$Q^2$ , –92 ppm	$Q^3$ , –100 ppm	$Q^4$ , –109 ppm	$(D^1 + D^2)/(D^3 + D^4)$	$Q^3/Q^4$
60 °C for 3 h	2.54	12	14	4	33	37	0.86	0.89
75 °C for 3 h	3.09	14	14	1	31	40	0.97	0.78
90 °C for 3 h	2.77	14	15	1	28	42	0.99	0.67
90 °C for 5.5 h	3.01	16	16	1	31	36	0.98	0.86

CP-MAS NMR) to derive information on the type of linkages that do exist on the surface of the modified particles. Representative  $^{29}\text{Si}$  CP-MAS NMR spectra of two distinct materials, prepared by silylation at 60 °C for 3 h (top) and 90 °C for 3 h (bottom) are shown in Fig. 2. Corresponding spectra of materials prepared with different reaction temperature and reaction time do feature similar signal patterns with slightly distinct signal intensities which are given for four different modified particles. Those four different materials are described in Table 2.

As can be seen from Fig. 2 two different groups of signals are found in the spectra. The signals denoted with  $Q^2$ ,  $Q^3$ ,  $Q^4$  come from the silica matrix and correspond to geminal silanol (–92 ppm,  $Q^2$ ), isolated silanol (–100 ppm,  $Q^3$ ) and siloxane (–109 ppm,  $Q^4$ ), respectively. Further, there are signals that can be assigned to the surface-bonded silanes. The signals at –4 and –8 ppm (respectively  $D^1$  and  $D^2$ ) corresponds to the mono-functionally bonded silanes. The signal denoted with  $D^3 + D^4$  corresponds to the di-functionally bonded silane species. Although the individual signals are partly overlapping, Gaussian decomposition allows to derive their individual signal intensities (Table 3). While the  $^{29}\text{Si}$  CP-MAS NMR spectra suggest a similar surface structure of the materials prepared by different temperatures and reaction times, a closer inspection of the individual signal intensities may provide some minor peculiarities of the distinct materials. While the  $(D^1 + D^2)/(D^3 + D^4)$  ratio remained largely constant with higher temperatures and longer reaction time, some minor though characteristic alterations in relative signal intensities of the Q-species were noticed.  $Q^2$  intensity diminishes and the  $Q^4$  signal intensity grows relative to the  $Q^3$  signal when the reaction temperature is raised from 60 to 75–90 °C, as indicated by the  $Q^3/Q^4$  ratio. Both geminal and isolated silanol concentrations are reduced in favor of siloxane species. This would indicate a slightly lower silanol activity of the latter materials. However, when the reaction time is increased (90 °C, for 5.5 h), the  $Q^3/Q^4$  ratio drops back to the initial value which is hard to explain.

It is worth noting, however, that the present materials which are prepared from the di-functional silane appear to have less silanol groups stemming from the bonded silane as compared to previously described thiol-modified silica particles obtained from

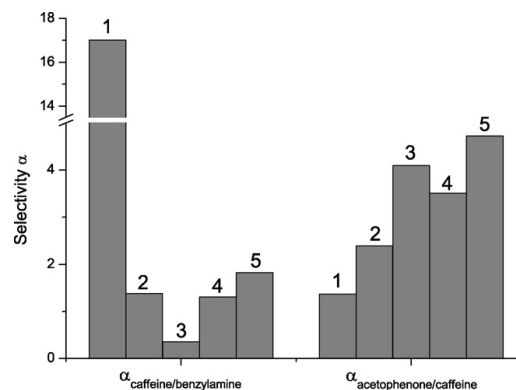


**Fig. 3.** SH activity ( $\alpha_{\text{caffeine/benzylamine}}$ ) and silanol activity ( $\alpha_{\text{acetophenone/caffeine}}$ ) of five different modified silica particles: 1, propyl; 2, mercaptopropyl LC; 3, mercaptopropyl HC; 4, mercaptopropyl LC + endcapping; 5, C14-S-C3 LC (see Table 3). In order to facilitate the readability of the figure the y-axis has been discontinued between 5 and 13.5. Note that decreasing  $\alpha_{\text{caffeine/benzylamine}}$  values indicates increasing SH activities, while increasing  $\alpha_{\text{acetophenone/caffeine}}$  values are indicative for decreasing silanol activities.

tri-functional silanes which showed  $T^1$ ,  $T^2$ ,  $T^3$  signals corresponding to mono-functionally bonded species ( $T^1$ ) leading to two free silanols, di-functionally bonded silane with single silanol ( $T^2$ ) and surface crosslinked siloxane ( $T^3$ ) [13,23].  $T^1$  and  $T^2$  signals together are strongly dominating with regards to intensities as compared to  $T^3$  which may be regarded as tantamount to a higher silanol number. Hence, the present developed silica particles may also be expected to be more stable than corresponding former particles prepared from tri-functional silanes, because the number of silanol groups ( $D^1 + D^2$ ) remaining on the surface of our material (prepared from dialkoxysilane) is lower than that of material prepared from trialkoxysilane ( $T^1 + T^2$ ).

**Table 4**  
Modified silica materials with different surface modifications and corresponding surface coverages employed for the development of a specific chromatographic test.

# Material	Modification	%C	%S	SH (DPDS) <sup>a</sup> ( $\mu\text{mol}/\text{m}^2$ )	Added ligand	Surface coverage of added ligand ( $\mu\text{mol}/\text{m}^2$ )
						%C
1	Propyl (C3)	3.1	<0.3	–	Propyl	1.87/2.33 <sup>b</sup>
2	Mercaptopropyl LC <sup>c</sup> (S-C3)	3.2	1.9	2.16	Mercaptopropyl	1.93/2.41 <sup>b</sup>
3	Mercaptopropyl HC <sup>d</sup> (S-C3)	6	3.5	4.39	Mercaptopropyl	3.92/4.89 <sup>b</sup>
4 <sup>e</sup>	Mercaptopropyl LC + endcapping (S-C3-e)	3.5	1.9	2.15	TMS-endcapping	0.32 <sup>f</sup>
5 <sup>g</sup>	Mercaptopropyl LC + endcapping + C14 (C14-S-C3-e)	11.9	2	1.14	C14-residue	n.d. <sup>h</sup>
						DPDS <sup>a</sup>
						–
						2.16
						4.39
						–
						1.11 <sup>i</sup>

<sup>a</sup> Reactive sulfhydryls by DPDS.

<sup>b</sup> Calculated for mono-functionally (low) and di-functionally (high) bonded silane from %C of elemental analysis data.

<sup>c</sup> LC: low coverage.

<sup>d</sup> HC: high coverage.

<sup>e</sup> Synthesized from material # 2.

<sup>f</sup> Surface coverage from %C of elemental analysis calculated by extended Berendsen-de Galan's equation [16].

<sup>g</sup> Synthesized from material # 4.

<sup>h</sup> n.d., not determined.

<sup>i</sup> Calculated from the difference of reactive sulfhydryls before and after adding C14 chain.



### 3.3. Chromatographic characterization of the mercaptopropyl-modified silica particles

In order to characterize the effect of the modification on the silica surface, we developed a specific chromatographic test. The purpose of this test was to describe chromatographically the SH activity and the silanol activity. Five different chromatographic materials have been synthesized with well-defined thiol modifications (see Table 4).

After having tested about 20 different compounds, we were able to pick out three analytes, which may be adequate to probe the two parameters, i.e. SH activity and silanol activity (see Fig. 3).

When the SH activity of considered material is increasing (material 1, 2 and 3 for example), the  $\alpha_{\text{caffeine/benzylamine}}$  value is decreasing. Decrease of silanol activity (material 2, 4 and 3) leads to an increase of the  $\alpha_{\text{acetophenone/caffeine}}$  value. These two parameters are regarded as sufficient to describe the material in a first approach: SH activity to verify the extent of surface modification and silanol activity to assess chromatographically the existence of residual silanols and their accessibility. This test is employed hereafter for testing the stability of the prepared bonded particles.

### 3.4. Stability of the phases

The surface coverage of a silica material is only one of the important parameters to look at during an optimization. The corresponding stability of the material has also to be considered and must be investigated. The chromatographic test described in the experimental part (see Section 2.6) was therefore established and the stability was studied by submitting the material to the specific stress treatment described in Section 2.9. Two different materials were selected for the test: the first one was a material synthesized at 4 h/75 °C and the second one at 8 h/90 °C. The surface coverage of both materials was 3.2  $\mu\text{mol}/\text{m}^2$ . By selecting materials with the same surface coverage yet obtained at distinct reaction conditions for the chromatographic characterization and stress test, respectively, it was hoped that some information on possibly existing differences of the surface structure of the bonding can be derived. The chromatograms that were furnished for the two materials are illustrated in Fig. 4. The retention times for each analyte were essentially identical except for acetophenone for which a minor retention time shift was observed.

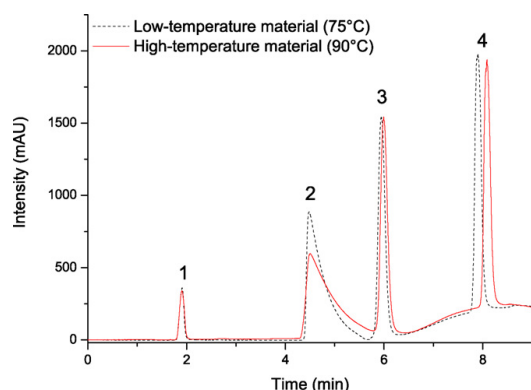


**Fig. 4.** Chromatograms of the developed HPLC test for columns packed with mercaptopropyl modified silica material synthesized at two different temperatures (75 °C/4 h and 90 °C/8 h) (see Section 2.6). Conditions: water, 0.1% TFA (A) and methanol, 0.1% TFA (B), 20% to 80% B in 6 min, 80% B for 4 min, temperature = 25 °C, flowrate = 1 ml/min, injection volume = 10  $\mu\text{l}$ , detection at 212 nm. Analytes: 1, methanol; 2, benzylamine; 3, caffeine; 4, acetophenone.

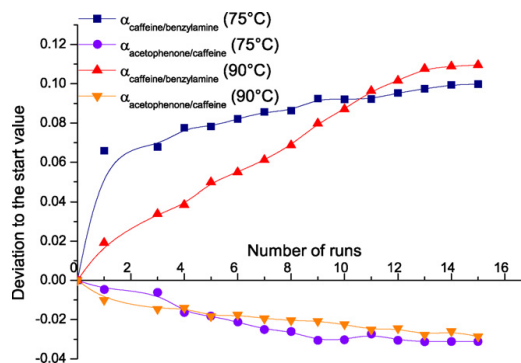


**Fig. 5.** Change of SH and silanol activity for two materials synthesized at two different temperatures in the course of the stability testing. SH activity:  $\alpha_{\text{caffeine/benzylamine}}$  and silanol activity:  $\alpha_{\text{acetophenone/caffeine}}$ . The deviation  $\Delta\alpha$  has been calculated as follows:  $\Delta\alpha = (\alpha - \alpha_0)/\alpha_0$  where  $\alpha$  is the selectivity at the respective run and  $\alpha_0$  the selectivity at the first measurement after packing the column. Note, that both  $\alpha$ -values are inversely proportional to the real activity.

Next, the stabilities of these two mercaptopropyl-bonded silica particles were examined (see Fig. 5). Both materials were submitted to the stress treatment described in the Section 2.7. The reproducibility of the test has been investigated by replicating each measurement two times.

At the beginning the material synthesized by a 75 °C reaction shows a faster increase in  $\alpha_{\text{caffeine/benzylamine}}$  being indicative for a stronger loss of thiol-ligand and thus of SH activity when compared to the material synthesized by a 90 °C reaction. After a few cycles of stress treatment, however, the SH loss leveled off and became largely comparable to that of the 90 °C material. On the other hand, the increase in silanol activity as indicated by a drop of  $\alpha_{\text{acetophenone/caffeine}}$  became less significant with increasing number of stress cycles and was largely comparable for the two tested materials.

It is striking that the optimum-temperature material exhibits a strong loss of SH activity during the first stress run whereas its silanol activity is not increasing proportionally. That is due to the fact that the first loss of SH activity involves probably the cleavage of

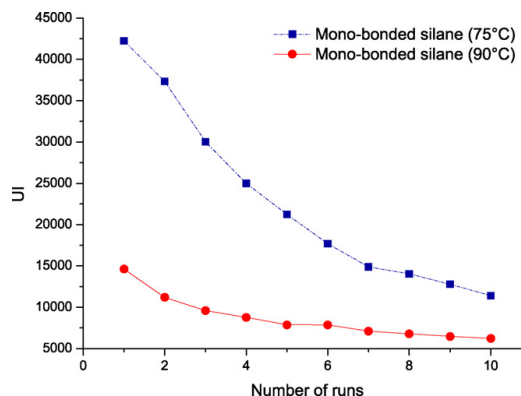


**Fig. 6.** Evolution of the  $m/z = 166.32$  Da response during ESI/MS runs (acetonitrile, 0.1% FA (A) and water, 0.1% FA (B) from 10 to 90% A in 5 min, 90% A for 3 min and 10% A for 10 min, column kept at RT and flow rate 1 ml/min) monitored between washing runs (2-isopropanol, 0.1% FA for 60 min, 0.5 ml/min). The  $m/z$  value corresponds to the cleavage of mono-bonded silane (3-mercaptopropylmethoxymethylsilanol) from the silica surface.

mono-functionally bonded silane groups, the unreacted methoxy-groups of which were already hydrolysed, so that one silane–silanol is replaced by one surface silanol. As a comparison, the evolution of the SH and silanol activity for the high-temperature material is much more equivalent.

To ensure these results, both materials were tested for bleeding by LC-MS as described in Section 2.9. Submitted to acidic conditions, the silane moieties are partially cleaved off the surface. The dihydroxy-silane originating from the cleavage of a di-functionally bonded silane is not ionizable in the positive mode whereas the hydroxy-methoxy-silane resulting from the cleavage of a mono-functionally bonded silane is ionizable and therefore easily detectable by ESI/MS detection ( $m/z = 166.32$  Da). As can be seen from the plot of the amount of this fragment against the number of stress runs, an almost three times higher amount of mono-bonded silane is released from the optimum-temperature material compared to the high-temperature material (see Fig. 6).

As a conclusion for the stability study we can assume that material prepared at lower temperature does not necessarily exhibit lower stability because after excessive initial washing the change in thiol- and silanol activity is largely equivalent for the two materials. Initially, however, the low-temperature (75 °C) material shows a stronger bleeding of mono-functionally bonded silane and in general, the silanol activity of the low-temperature material seems to be slightly higher.

#### 4. Concluding remarks

A new approach to thiol-modified silica particles is presented in which the formerly common trifunctional 3-mercaptopropyltrimethoxysilane was replaced by the di-functional 3-mercaptopropyltrimethoxymethylsilane. Such di-functional silane should lead to more stable bonding as compared to the trifunctional one. A systematic optimization of the silylation reaction by a design of experiment with reaction temperature and time was employed which revealed that optimal surface coverage can be accomplished at 75 °C. Materials with same surface coverage but prepared at 75 and 90 °C, respectively, revealed differences in initial bleeding behavior. The low temperature material showed a stronger loss of ligand especially at the beginning of the stress test and a stronger mono-functional silane bleeding than the high temperature material. After a while the change in both thiol and silanol activity became insignificant for both of the materials suggesting that they show similar stability after excessive initial washings. The slightly higher silanol activity of material obtained at a lower reaction temperature could be seen as a disadvantage of the method, but a proper endcapping of the material should prevent the resulting material from a problematic silanol activity. The  $^{29}\text{Si}$  CP-MAS NMR spectra acquired for low and high temperature materials were qualitatively the same and showed only minute differences regarding relative signal intensities of the individual Si species. While the ratio of  $\text{D}^1$  to  $\text{D}^2$  (mono-functional to di-functional

silane bonding) was relatively constant for different temperature materials, the  $^{29}\text{Si}$  CP-MAS NMR spectra suggested that the surface silanol activity should be lower for the high-temperature material as indicated by a decrease of the  $\text{Q}^2$ -to- $\text{Q}^3$  ratio (ratio of isolated silanols versus siloxanes).

The fact that the optimum in terms of surface coverage is observed at 75 °C has some other benefits. It should facilitate the on-column modification, because working at 75 °C is much easier than running an in-line modification equipment at the reflux of toluene. This point is perhaps not so important for particulate material but in the case of monolithic columns, the implementation of an in-line modification becomes a relevant challenge.

Finally, this study has shown the usefulness of performing a statistical design of experiment for the optimization of chemical reactions, even if the reaction is already well described in the literature.

#### Acknowledgments

The authors wish to thank Flavie Nowatzki (student of ENSI-CAEN, France) for some experimental work and Markus Knoth (Merck KGaA) for valuable support concerning NMR experiments, as well as Michael Schulz (Merck KGaA) for introducing us to Cornerstone software.

#### References

- [1] M. Lämmerhofer, W. Lindner, J. Chromatogr. A 741 (1996) 33.
- [2] E. Zarbl, M. Lämmerhofer, A. Woschek, F. Hammerschmidt, C. Parenti, G. Cannazza, W. Lindner, J. Sep. Sci. 25 (2002) 1269.
- [3] R. Nogueira, M. Lämmerhofer, W. Lindner, J. Chromatogr. A 1089 (2005) 158.
- [4] G. Göktürk, M. Delzendeh, M. Volkan, Spectrochim. Acta B 55 (2000) 1063.
- [5] T. Djekic, A. van der Ham, A. de Haan, J. Chromatogr. A 1142 (2007) 32.
- [6] B.B. Wheals, J. Chromatogr. 177 (1979) 263.
- [7] A. Heckel, D. Seebach, Chem. Eur. J. 8 (2002) 559.
- [8] K.J. Welch, N.E. Hoffman, J. High Resol. Chromatogr. 9 (1986) 417.
- [9] A. Ruderisch, W. Iwanek, J. Pfeiffer, G. Fischer, K. Albert, V. Schurig, J. Chromatogr. A 1095 (2005) 40.
- [10] C.M. Crudden, M. Sateesh, R. Lewis, J. Am. Chem. Soc. 127 (2005) 10045.
- [11] J.N. Kinkel, K.K. Unger, J. Chromatogr. 316 (1984) 193.
- [12] H. Engelhardt, P. Orth, J. Liq. Chromatogr. Relat. Technol. 10 (1987) 1999.
- [13] N.M. Scully, G.P. O'Sullivan, L.O. Heal, J.D. Glennon, B. Dietrich, K. Albert, J. Chromatogr. A 1156 (2007) 68.
- [14] K.K. Unger, Adsorbents in Column Liquid Chromatography, 47, Marcel Dekker, 1990, Chapter 6, 331 pp.
- [15] P. van der Voort, E.F. Vansant, J. Liq. Chromatogr. Relat. Technol. 19 (1996) 2723.
- [16] J.E. Sandoval, J. Chromatogr. A 852 (1999) 375.
- [17] R. Nogueira, M. Lämmerhofer, N. Maier, W. Lindner, Anal. Chim. Acta 533 (2005) 179.
- [18] B. Buszewski, M. Jezierska, M. Welniak, D. Berek, J. High Resol. Chromatogr. 21 (1998) 267.
- [19] B. Pfeleiderer, K. Albert, E. Bayer, J. Chromatogr. 506 (1990) 343.
- [20] K. Albert, E. Bayer, J. Chromatogr. 544 (1991) 345.
- [21] A.B. Scholten, J.W. de Haan, H.A. Claessens, L.J.M. van de Ven, C.A. Cramers, Langmuir 12 (1996) 4741.
- [22] M. Pursch, L.C. Sander, K. Albert, Anal. Chem. 68 (1996) 4107.
- [23] C. Hellriegel, U. Skogsberg, K. Albert, M. Lämmerhofer, N.M. Maier, W. Lindner, J. Am. Chem. Soc. 126 (2004) 3809.

Romain Dabre<sup>1</sup>  
Nazanin Azad<sup>2</sup>  
Achim Schwämmle<sup>3</sup>  
Michael Lämmerhofer<sup>1</sup>  
Wolfgang Lindner<sup>1</sup>

<sup>1</sup>Department of Analytical  
Chemistry, University of Vienna,  
Vienna, Austria

<sup>2</sup>Europa Fachhochschule  
Fresenius, Idstein, Germany

<sup>3</sup>Merck KGaA, Performance and  
Life Science Chemicals,  
Darmstadt, Germany

Received November 12, 2010

Revised January 7, 2011

Accepted January 7, 2011

## Research Article

# Simultaneous separation and analysis of water- and fat-soluble vitamins on multi-modal reversed-phase weak anion exchange material by HPLC-UV

Several methods for the separation of vitamins on HPLC columns were already validated in the last 20 years. However, most of the techniques focus on separating either fat- or water-soluble vitamins and only few methods are intended to separate lipophilic and hydrophilic vitamins simultaneously. A mixed-mode reversed-phase weak anion exchange (RP-WAX) stationary phase was developed in our laboratory in order to address such mixture of analytes with different chemical characteristics, which are difficult to separate on standard columns. The high versatility in usage of the RP-WAX chromatographic material allowed a baseline separation of ten vitamins within a single run, seven water-soluble and three fat-soluble, using three different chromatographic modes: some positively charged vitamins are eluted in ion exclusion and ion repulsion modes whereas the negatively charged molecules are eluted in the ion exchange mechanism. The non-charged molecules are eluted in a classical reversed-phase mode, regarding their polarities. The method was validated for the vitamin analysis in tablets, evaluating selectivity, robustness, linearity, accuracy, and precision. The validated method was finally employed for the analysis of the vitamin content of some commercially available supplement tablets.

**Keywords:** Fat-soluble / Mixed-mode chromatography / Optimization / Reversed phase / Reversed-phase weak anion exchange / Validation / Vitamins / Water-soluble  
DOI 10.1002/jssc.201000793



## 1 Introduction

A well-balanced diet is usually sufficient to cover the daily vitamin requirements of the human organism [1, 2]. Multi-vitamin supplements were however developed in order to prevent and cure deficiencies of individuals being at risk for hypovitaminoses due to absorption failures, pregnancy, stress, bad food habits, and acute or chronic diseases.

It became therefore necessary to develop analysis methods in order to evaluate the quality of such dietary supplements. One challenge for vitamin analyses is caused by the fact that vitamins are very different in their chemical properties. Vitamins of the B family, for example, are water-soluble, whereas K vitamins are fat-soluble. Most of the validated methods are proposed for the quantitation of either hydrophilic [3–7] or lipophilic vitamins [8, 9], just to

cite the latest publications. The first attempt to characterize both vitamin groups by HPLC on a single column consisted of a solid-phase extraction followed by an HPLC separation [10, 11]. The first step consisted in separating the water- and the fat-soluble vitamins from each other by RP solid-phase extraction, whereas in the second step the vitamins of each group were resolved from each other on RP silica-based material. The water-soluble vitamins were separated using a methanol–buffer gradient, whereas the fat-soluble ones were separated using a methanol–acetonitrile or methanol–chloroform isocratic mobile phase. Buszewski and Zbanyszek overcame this challenge by performing a single-run analysis on two different C18 columns with low and high ligand density through a column-switching valve [12]. Only very few single-run single-column analyses of water- and fat-soluble vitamins were published. For example, the method of Li and Chen involved a multi-step gradient with a salting–desalting process on a C18 column [13]. Klejdus et al. developed a positive-negative gradient method on a Polaris C18 column [14].

The scope of our study consists in optimizing and validating a method for the simultaneous separation of 10 hydrophilic and lipophilic vitamins on a mixed-mode reversed-phase weak anion exchange (RP-WAX) stationary

**Correspondence:** Prof. Wolfgang Lindner, Währinger Straße 42, A-1090 Vienna, Austria  
**E-mail:** wolfgang.lindner@univie.ac.at  
**Fax:** +43-1315-1826

**Abbreviations:** LLOQ, lower LOQ; RP-WAX, reversed-phase weak anion exchange; ULOQ, upper LOQ

phase. Names, structure, predominant deficiency disease, and recommended dietary allowances for the considered vitamins are given in Table 1 ([15], <http://www.merck.com/mmhe/sec12/ch154/ch154a.html>, March 2010).

RP-WAX chromatography combines both reversed-phase (RP) and weak anion exchange (WAX) groups, which leads to a high versatility in usage [16]. The structure of the mixed-mode ligand is given in Fig. 1. If vitamins are hydrophobic, they interact with the RP chain. The retention of the water-soluble ones is influenced by the presence of positively charged, negatively charged, or neutral polar groups that can interact with polar binding sites of the stationary phase. After optimization and validation of the method for simultaneous baseline separation of all vitamins, we determined the vitamin contents in commercially available supplements to demonstrate the applicability of the method.

## 2 Materials and methods

### 2.1 Chemicals

RP-WAX-modified silica material was prepared in our laboratory using an optimized proprietary manufacturing process, which was partly published [17, 18].

Mobile phases for chromatography were prepared from HPLC grade acetonitrile, disodium hydrogen phosphate and sodium dihydrogen phosphate (Merck). Vitamins were purchased from Sigma-Aldrich (Steinheim, Germany).

Log *D* values were calculated for pH 4.4 with ACD/Labs 7.00 software from Advanced Chemistry Development (Toronto, ON, Canada).

### 2.2 Instrumentation

The chromatographic experiments were carried out on a VWR (Darmstadt, Germany) Hitachi LaChrom Elite HPLC system (three channels pump L-2130 with degasser, autosampler L-2200, oven L-2350, diode array detection (DAD) system L-2455). The data were processed using the Agilent (Waldbronn, Germany) EZChrom Elite version 3.21 software.

The gradient optimization was performed on a VWR Hitachi LaChrom Ultra HPLC system (two single-channel pumps L-2160U, autosampler L-2200U, oven L-2300, diode array detection system L-2455U). The optimization data were processed using ChromSword Auto version 4.0.1.

### 2.3 Sample preparation

Stock solutions of single vitamins were prepared in methanol at concentrations up to 3 mg/L or up to the limit of solubility. The working solutions with single vitamins were prepared at the desired concentrations by dilution of

the stock solutions. The vitamin mixtures were prepared at the desired concentration directly from pure compounds. All solutions were stored at  $-20^{\circ}\text{C}$  after sonicating and filtered on a 0.2- $\mu\text{m}$  PTFE syringe filter before being placed in the autosampler. The solutions were freshly prepared every 2 days except for the sample stability study.

The vitamin tablets (see Table 2 for ingredients) were dissolved in 20 mL water. After sonication and filtration on a 0.2- $\mu\text{m}$  PTFE syringe filter, the mixture was directly injected onto the column.

### 2.4 Chromatographic conditions

A column filled with the RP-WAX material described previously [17] (125  $\times$  4 mm, 5  $\mu\text{m}$  particle size, 100 Å) was used for the analysis. The injection volume was 10  $\mu\text{L}$  and the flow rate was set to 1.0 mL/min. Four different wavelengths (260, 270, 300, and 310 nm) were evaluated. The best results were obtained at 270 nm for almost every vitamin. Vitamin A-acetate exhibits very low absorbance at this wavelength and the validation was therefore performed at 310 nm for this molecule. The simultaneous determination was performed at both wavelengths.

Mobile phase composition, pH, temperature, and gradient were optimized (see Section 3.1). Best results were obtained with a mobile phase containing water and acetonitrile in the presence of phosphate buffer (see Table 3). Dead volume  $t_0$  was determined by injecting pure methanol ( $t_0 = 1.70$ ).

### 2.5 Method validation

The method validation was performed according to the guidelines of the International Conference on Harmonisation of Technical Requirements for Registration of Pharmaceuticals for Human Use (ICH).

#### 2.5.1 Selectivity

Standard vitamin solutions were first injected onto the column and the evaluation of the obtained chromatogram allowed us to ensure the purity of the stock solutions. The selectivity of the method was then demonstrated by comparison of the chromatograms of the vitamin mixture and of the real samples with chromatograms monitored for each vitamin standard solution.

#### 2.5.2 Robustness

The robustness of the vitamins quantification must be assessed through small deliberate variations of the method parameters [19]. We investigated the effect of small variations of the temperature, the pH, the buffer concentration, and the slope of the gradient, which we identified as critical parameters. The relative standard deviation of the

**Table 1.** Names and structures of the considered vitamins, their main deficiency diseases and the recommended dietary allowances

Generic name	Chemical name	Structure	Predominant deficiency disease	Recommended dietary allowances
<i>Water soluble</i>				
Vitamin B1	Thiamine		Beriberi	1.2 mg
Vitamin B2	Riboflavin		Ariboflavinois	1.3 mg
Vitamin B3	Nicotinic acid		Pellagra	16.0 mg
Vitamin B3-amide	Niacinamide		id.	id.
Vitamin B6	Pyridoxine		Anemia	1.3–1.7 mg
Vitamin B12	Cyanocobalamin		Megaloblastic anemia	2.4 µg
Vitamin C	Ascorbic acid		Scurvy	90.0 mg
<i>Fat soluble</i>				
Vitamin A-acetate	Retinol acetate		Keratomalcia	900 µg
Vitamin D3	Cholecalciferol		Osteomalcia	5.0–10.0 µg
Vitamin K1	Phyllochinon		Bleeding diathesis	120 µg

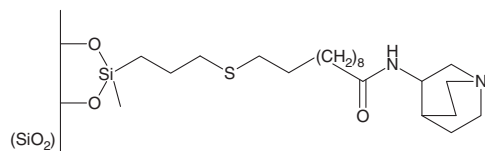


**Figure 1.** Structure of the developed mixed-mode reversed-phase weak anion exchange (RP-WAX) separation material.

**Table 2.** Composition of two vitamin tablets analyzed in this study

<i>Supplier:</i> Rossmann	<i>Supplier:</i> Penny
<i>Brand:</i> ALTRAPHARMA	<i>Brand:</i> Omni VIT
<i>Name:</i> A-Z Depot+Multivitamin Mineral	<i>Name:</i> A-Z
Biotin	Biotin
Calcium carbonate	Calcium-D-pantothenate
Calcium-D-pantothenate	Calciumhydrogenphosphate
Calciumhydrogenphosphate	Chromium(III) chloride
Chromium(III) chloride	Iron(II) fumarate
Iron(II) fumarate	Folic acid
Iron oxide and iron hydroxide	Cellulose
Polysorbate 80	Gum arabic
Folic acid	Hydroxypropylmethylcellulose
Cellulose	Sodium-carboxymethylcellulose
Potassium chloride	Potassium chloride
Potassium iodide	Potassium iodide
Copper(II) sulfate	Copper(II) sulfate
Magnesium oxide	Lutein
Mangan(II) sulfate	Magnesium oxide
Sodium molybdate	Mangan(II) sulfate
Sodium selenate	Sodium molybdate
Nicotinamide	Sodium selenate
Titan dioxide	Titan dioxide
Silicium dioxide	Silicium dioxide
Talc	Talc
Vitamin A	Vitamin A
Vitamin B <sub>1</sub>	Vitamin B <sub>1</sub>
Vitamin B <sub>12</sub>	Vitamin B <sub>12</sub>
Vitamin B <sub>2</sub>	Vitamin B <sub>2</sub>
Vitamin B <sub>6</sub>	Vitamin B <sub>6</sub>
Vitamin C	Vitamin C
Vitamin D <sub>3</sub>	Vitamin D <sub>3</sub>
Vitamin E	Vitamin E
Vitamin K <sub>1</sub>	Vitamin K <sub>1</sub>
Zinc oxide	Zinc oxide

retention time was then calculated for each vitamin and the limit of deviation was set up to 5%.

### 2.5.3 Linearity

Evaluating the linearity of the method consists in verifying that the peak area for each vitamin in the chromatogram is directly proportional to the concentration in the mixture within a given range [20]. We evaluated the linearity for each

**Table 3.** Mobile phase compositions for the optimal simultaneous separation of fat- and water- soluble vitamins

Time (min)	%B
0	0
2	0
7	12
22	82
30	97
33	97
34	0
40	0

Solvent A: 85% water, 10% 100 mM phosphate buffer, pH 4.4, 5% acetonitrile. Solvent B: 18% water, 2% 100 mM phosphate buffer, pH 4.4, 80% acetonitrile.

vitamin within the mixture from 25 µg/L up to the limit of solubility. Ten measurements were performed between the lower concentrations and the limit of linearity (tantamount to the upper limit of quantitation, ULOQ) of each molecule in order to obtain more accurate measurements. If calibration curves were observed to be non-linear, the upper limit of linearity ULOQ was stepwise reduced until the calibration curve for the resultant data set became linear. The slope and intercept were calculated using the least-square regression method.

The residual standard deviation is calculated as follows:

$$s_y = \sqrt{\frac{RSS}{n-2}}$$

where RSS is the residual sum of squares and  $n$  the number of data for validation.

The relative residual standard deviation can then be calculated:

$$V_{x0} = 100 \times \frac{s_y}{b\bar{x}} [\%]$$

where  $b$  is the slope and  $\bar{x}$  the means of the concentrations.

For the two-tailed Fisher's exact test, we calculated at first the residual standard deviation with a quadratic function  $sy_2$ , which allowed us to determine the  $F_{calc}$  value [21]:

$$F_{calc} = (n-2) \cdot sy^2 - (n-3) \cdot sy_2^2$$

The  $F_{table}$  is given by the  $F_{table}$  data set at 99% confidence. It depends for each vitamin on the number of measured data. The  $F_{table}$  is read with  $f_1 = 1$  and  $f_2 = N$  where  $N$  is the number of measurements. If  $F_{calc} \leq F_{table}$ , the data set is linear in the chosen range [22].

### 2.5.4 Detection and quantitation limit

The limit of detection (LOD) for each vitamin is the lowest amount of analyte that can be detected and the limit of quantitation is the lowest concentration for quantitative determination with sufficient precision and accuracy [23].

We calculated both values from the calibration line at low concentration.

$$\text{LOD; LOQ} = \frac{F \cdot \text{SD}}{b} \times 1000 \text{ (}\mu\text{g/mL)}$$

where  $F$  is a factor of 3.3 and 10 for LOD and LOQ, respectively, SD the standard deviation of the blank calculated after ten repetitions of a blank injection and  $b$  the slope of the regression line.

### 2.5.5 Precision and accuracy

Intra-day ( $n = 6$ ) and inter-day ( $n = 6$ ) precisions are expressed as standard deviation percentage of the calculated concentration. They correspond to the degree of scatter between the series of measurements, respectively, measured six times consecutively within a single day or measured once a day during six consecutive days [24]. The accuracy given in percentage corresponds to the closeness of agreement between the measured concentration and the theoretical value. Precision and accuracy were determined for six different theoretical concentrations (see Table 1 in Supporting Information) [25].

### 2.5.6 Range

The range is given in mg/L as interval of concentrations for which precision is under 2%, accuracy is in the 95–105% range, recovery is stable, and between the LLOQ and the ULOQ [26].

### 2.5.7 Storage stability

To assess storage stability, the evolution of the peak area was compared for each vitamin within the mixture during 15 h at room temperature and during 5 days in four different

conditions. For the 15-h measurements, the mixture remained in the autosampler at RT. For the 5-day measurements, the mixture was prepared at day 0 and it was aliquoted in autosampler vials. One set of vial was stored at  $-28^{\circ}\text{C}$  in the absence of light and another one was stored in the dark at  $+4^{\circ}\text{C}$ . The two last sets of vials were stored at room temperature, with and without light, respectively. For each measurement, the vial was put in the autosampler shortly before injection.

## 3 Results and discussion

### 3.1 Method development

The difficulty of the separation of both water- and fat-soluble vitamins in a single chromatographic run is due to the fact that some vitamins are very polar (for example, vitamin B<sub>1</sub> or vitamin B<sub>6</sub>), whereas vitamins D<sub>3</sub> and K<sub>1</sub> were the most lipophilic in our study. The use of mixed-mode chromatography leads to a good separation of all species: the presence of both functionalities (apolar RP chain and polar neutral as well as polar ionic groups) on a single ligand allows a bimodal gradient, which leads to baseline separation of all vitamins (see Fig. 2).

#### 3.1.1 Effect of pH

First, the impact of pH on the retention of the water-soluble vitamins was evaluated with a very simple acetonitrile gradient. The data presented in the Fig. 3 were generated with the optimum gradient (see Section 3.1.3.).

Six different pHs were studied from pH 3 to 8. The basic molecules bearing a proton-acceptor nitrogen group (vitamins B<sub>1</sub>, B<sub>3</sub>-amide, and B<sub>6</sub>) exhibit very low retention

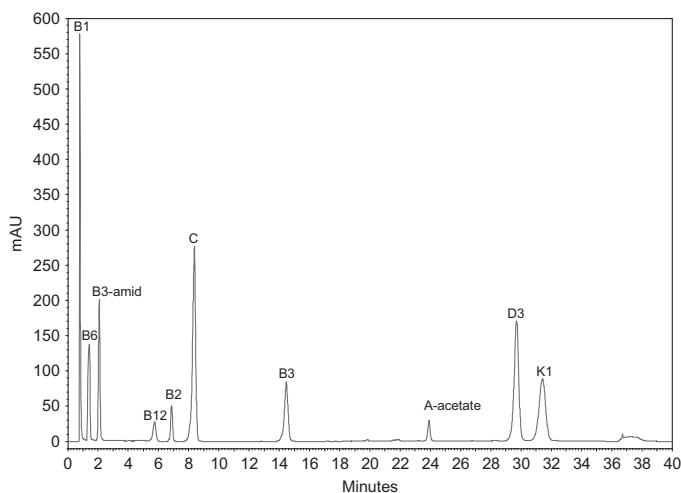


**Figure 2.** HPLC-UV chromatogram of a standard mixture of ten water- and fat-soluble vitamins under optimized gradient elution conditions. *Conditions:* water/100 mM phosphate buffer, pH 4.4/acetonitrile (85:10; v/v/v) (A) and water/100 mM phosphate buffer, pH 4.4/acetonitrile (18:2:80, v/v/v), (B) 0' – 0% B, 2' – 0% B, 7' – 12% B, 22' – 82% B, 30' – 97% B, 33' – 97% B, 34' – 0% B, 40' – 0% B, temperature =  $25^{\circ}\text{C}$ , flow rate = 1 mL/min, injection volume = 10  $\mu\text{L}$ , detection at 280 nm.

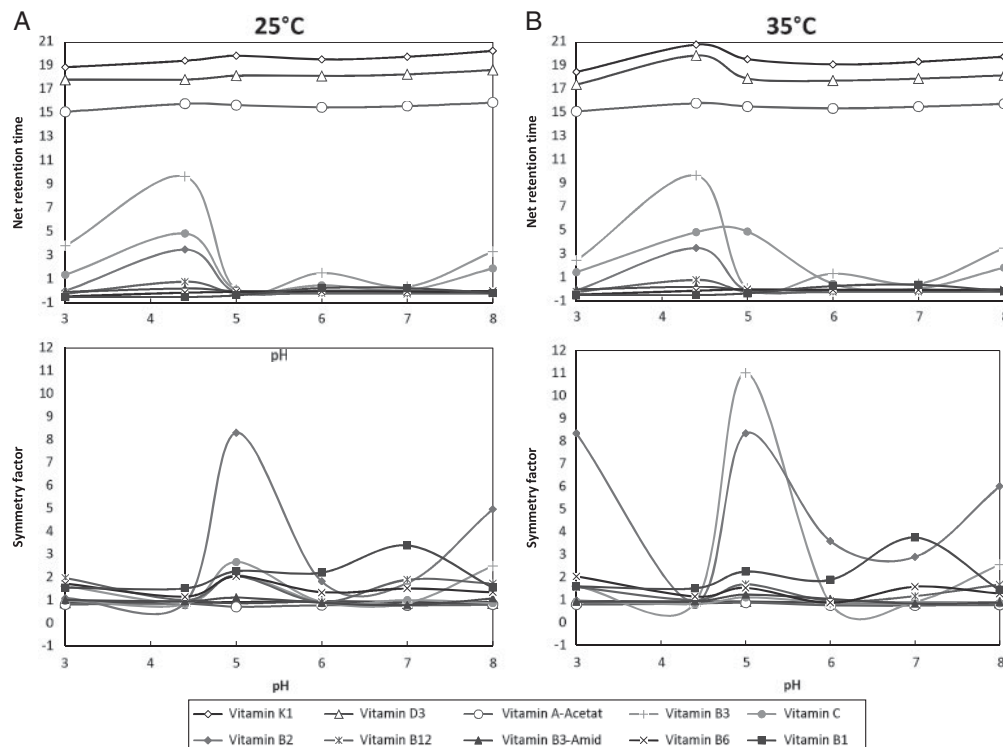


**Figure 3.** Effect of the pH and of the temperature on the retention factor (A) and on the symmetry factor (B) of the vitamins. The symmetry factor was calculated at 10% of the peak height:  $A_s = t_p/f_p$  where  $t_p$  and  $f_p$  represent the width of the tail and the front of the peak, respectively, at the considered height.

on the RP-WAX material, and baseline separation was only obtained around pH 4 (see Fig. 3, top panel). To find the optimum separation, a narrower pH range was investigated with six buffer systems from pH 4 to 5. Even minor pH variations in this range change the selectivity of the RP-WAX material for the investigated vitamins dramatically. It turned out that best separation was obtained at pH 4.4.

Most of the pH values lead to a baseline separation of polar and acidic vitamins B<sub>2</sub>, B<sub>3</sub>, B<sub>12</sub>, and C although the best resolution is obtained between pH 4 and 5. Retention times of these vitamins are higher than for the basic compounds B<sub>1</sub>, B<sub>3</sub>-amide, and B<sub>6</sub>. The pH value of 4.4 is suitable for the separation of the nitrogen-rich vitamins and can therefore be used for the simultaneous separation of all the water-soluble vitamins.

The effect of the pH on the net retention time (i.e. retention time minus  $t_0$ ) of the fat-soluble vitamins A-acetate, D<sub>3</sub>, and K<sub>1</sub> is almost negligible, due to their non-ionic nature, as expected (see Fig. 3, top panel). A slight increase with pH and a minor maximum around pH 4.4 may be noticed. Yet, baseline separation is maintained over the entire pH range with significantly higher retention

times in comparison to the water-soluble vitamins. A simultaneous separation of all vitamins is possible at pH 4.4.

The plot of symmetry factors against pH under the same conditions reveals better symmetries at pH 4.4 (see Fig. 3, bottom). The pH remained therefore fixed at pH 4.4 for further optimization and for the validation of the method.

### 3.1.2 Effect of temperature

The separation was evaluated at 25°C (Fig. 3A) and at 35°C (Fig. 3B). Both retention times and symmetry factors were little affected by the temperature variation (see Fig. 3). The optimization of the gradient was therefore performed at 25°C.

### 3.1.3 Adjustment of the gradient

The buffer and acetonitrile gradient were automatically optimized with ChromSword at the pH and temperature set previously. The idea was to combine a salt gradient along



with an acetonitrile gradient. While the buffer concentration was decreased during the run, the organic modifier concentration was increased at the same time.

To get started, some isocratic runs were performed first to evaluate the lower and higher acetonitrile concentration at a fixed salt concentration of 10 mM. We found out that 5% acetonitrile was a suitable starting amount of organic modifier. Next, the effect of the starting salt concentration was evaluated between 2.5 and 15 mM, with a modifier percentage of 5% acetonitrile in the mobile phase at the beginning of the gradient run. The resolution between the first two eluting peaks (vitamins B<sub>1</sub> and B<sub>6</sub>) increased gradually when the buffer strength at the beginning of the gradient run was increased from 2.5 up to 10 mM. Above this value, no change in the resolution was observed. We therefore fixed the starting buffer concentration at 10 mM. However, at higher acetonitrile content, the salt precipitated and an elution of the most hydrophobic vitamins with 80% acetonitrile was only possible with very low buffer concentration (<3 mM) to avoid precipitation. After a few optimization runs, we set up the minimum at 2 mM. The optimized gradient profile is shown in Fig. 4, resulting in a separation as depicted in Fig. 2.

Performing the whole separation with a decreasing buffer gradient is not only important for efficient separation of the water-soluble vitamins but it also avoids the risk of phosphate precipitation at higher acetonitrile concentration.

### 3.2 Elution order and mechanism

Within the first 2 min of the separation, vitamins bearing a protonated nitrogen group are separated on the RP-WAX material in the order of their polarity (B<sub>1</sub>, log  $D_{4,4}$  = −2.19; B<sub>6</sub>, log  $D_{4,4}$  = −1.88; B<sub>3</sub>-amide, log  $D_{4,4}$  = −0.17) and eluted very quickly due to electrostatic repulsion at very low acetonitrile concentration. Vitamins B<sub>1</sub> and B<sub>6</sub> elute even

before  $t_0$ , denoting an elution in ion-exclusion mode, also known as electrostatic repulsion mode [27, 28]. Other polar molecules such as vitamins B<sub>12</sub> (log  $D$  cannot be calculated with ACD due to Co(II) and too many ionization states) and B<sub>2</sub> (log  $D_{4,4}$  = −2.31) are eluted within the next 8 min by increasing the acetonitrile amount. During the increase in the concentration of organic modifier, the buffer concentration is slowly reduced, which leads to a longer retention time of acidic vitamins such as vitamins C (log  $D_{4,4}$  = −2.73) and B<sub>3</sub> (log  $D_{4,4}$  = −1.31), which elute between 8 and 15 min. All the fat-soluble vitamins are eluted from 20 to 32 min through an increase of the acetonitrile concentration with a low gradient slope in the order A-acetate (log  $D_{4,4}$  = 7.39), D<sub>3</sub> (log  $D_{4,4}$  = 9.72) and K<sub>1</sub> (log  $D_{4,4}$  = 12.25) (see Fig. 2). It is striking that within each group (hydrophilic cationic vitamins B<sub>1</sub>, B<sub>6</sub>, B<sub>3</sub>-amide; hydrophilic neutral or zwitterionic B<sub>12</sub>, B<sub>2</sub>; hydrophilic acidic C, B<sub>3</sub>; lipophilic neutral A-acetate, D<sub>3</sub>, K<sub>1</sub>), the solutes eluted in order of decreasing polarity, yet the ionic character plays a more dominant role for the general elution pattern as expected. In this method, the different vitamin clusters are eluted under different chromatographic modes, following an ion-exclusion and ion-repulsion mechanism, respectively, for vitamin B<sub>1</sub>, B<sub>6</sub>, and B<sub>3</sub>-amide, then switching to an ion-exchange mode for vitamin B<sub>3</sub> and C, and finally shifting to a reversed-phase mode for neutral and hydrophobic compounds, respectively (e.g. vitamin A-acetate, D<sub>3</sub>, and K<sub>1</sub>).

### 3.3 Method validation

#### 3.3.1 Selectivity and robustness

The selectivity of the method was evaluated by injections of single vitamin standards as well as of mixtures of vitamin standards. All the vitamins were baseline separated and selectivity between distinct solutes was satisfactory. From the single component injections it was evident that the purity of the reference compounds was sufficient for all vitamins to perform a validation. Individual vitamin standard solutions were allowed to stand at room temperature for controlled degradation. No interferences from degradation products were observed.

Robustness was evaluated for buffer molarity in the eluent ( $10 \pm 0.5$  mM), gradient time ( $30 \pm 2$  min), temperature ( $25 \pm 1^\circ\text{C}$ ), and pH ( $4.4 \pm 0.2$ ). Mean relative standard deviations of retention times are given in Fig. 5. For most of the vitamins, the deviation remains below 5%, which is sufficient to ensure the robustness of the method. Molarity and gradient slope have a more pronounced effect on vitamin retention. The small temperature difference has almost no effect on the retention time and the pH has only little effect except for vitamin B<sub>12</sub>. The relative standard deviation reaches almost 20% for this compound, which means that the method pH has to be controlled with utmost care, i.e. to pH  $4.4 \pm 0.05$ .

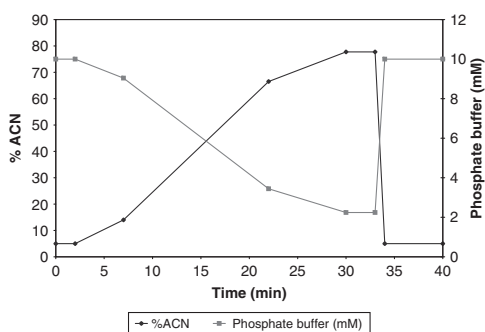


**Figure 4.** Optimized gradient profile with respect to acetonitrile content and phosphate buffer concentration as obtained by automatic gradient profile optimization with ChromSword.

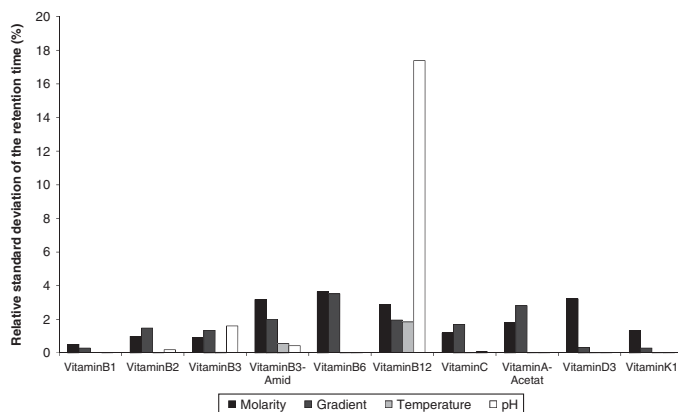


**Figure 5.** Evaluation of the robustness of the method by plotting the relative standard deviation of the retention time for four different parameters (buffer molarity, gradient slope, temperature, and pH).

**Table 4.** Linearity and analytical measurement limits for the different vitamins

	Number of data points	Linearity			Analytical measurement limits	
		Slope	$r^2$	ULOQ <sup>a)</sup> (µg/mL)	LOD (µg/mL)	LOQ (µg/mL)
B1	10	49 290 833	0.9992	800	0.937	2.840
B6	7	29 027 381	0.9999	1200	1.591	4.822
B3-amide	7	33 727 937	0.9996	1200	1.370	4.150
B12	11	6 874 945	0.9978	3000 <sup>b)</sup>	6.719	20.360
B2	5	137 747 691	0.9957	150 <sup>b)</sup>	0.335	1.016
C	9	133 338 589	0.9992	800	0.346	1.050
B3	9	30 316 561	0.9972	2400	1.524	4.617
A-acetate	11	61 964 118	0.9990	2000	0.745	2.259
D3	8	94 336 619	0.9997	2100	0.490	1.484
K1	11	78 237 454	0.9970	2500	0.590	1.789

a) ULOQ stands for upper limit of quantitation.

b) Limit of solubility.

### 3.3.2 Linearity and assay sensitivity

The linearity was evaluated for each vitamin within the concentration range 5 µg/mL – limit of solubility. For vitamins with even higher limit of solubility, we arbitrarily fixed the upper limit at 3000 µg/mL. After having measured more than 11 concentration levels for each compound, the data set was reduced until a linear calibration function was obtained. Decision on the validity of the linear calibration function was based on the *F*-test value. The upper limit of linearity (ULOL) was set to the value corresponding to a range in which the confidence of the model is better than 99%. The LOD and LOQ for each vitamin were calculated from the calibration curve (Table 4).

### 3.3.3 Accuracy and precision

The values of precision and some values of accuracy are given in Table 5. Extended data can be found in Table 2 of

the Supporting Information. Both intra-assay and inter-day precisions remain below 5% for all vitamins over the entire concentration range except for inter-day precisions of vitamin C. For this vitamin, the worse inter-day precisions may be ascribed to limited stability of this compound.

Likewise, intra-assay and inter-day accuracies are also in an acceptable range for all vitamins except for the lowest tested concentration level and vitamin C. The latter is again a result of the stability problem.

### 3.3.4 Range

Considering all the data described in the last paragraphs, we could determine a suitable range in which the quantitation of the vitamins can be performed due to satisfactory assay validity. The range was fixed to concentrations between the LLOQ and ULOQ, for which recovery was stable, precision better than 5%, and accuracy within 90–110%. The adapted ranges are given in Table 6.

**Table 5.** Intraday ( $n = 6$ ) and interday ( $n = 6$ ) precision and accuracy data for all the validated vitamins

Concentration range (mg/mL) <sup>a</sup>	B1	B6	B3-amide	B12	B2	C	B3	A-acetate	D3	K1
	0.008–0.8	0.0072–1.2	0.0048–1.2	0.024–3	0.003–0.016	0.008–0.8	0.0096–2.4	0.008–2	0.004–2	0.0025–2.5
<i>Precision</i>										
<i>Intraday (<math>n = 6</math>)</i>										
1	0.23	0.90	0.53	1.46	1.05	1.72	0.39	1.39	1.64	1.42
2	0.39	0.37	0.47	0.73	0.99	0.37	0.04	0.29	0.28	0.14
3	0.50	0.58	0.44	1.17	0.28	0.26	0.49	0.39	0.28	0.46
4	0.75	0.33	0.27	0.19	0.34	1.04	0.30	0.44	0.44	0.42
5	0.16	0.20	0.14	1.01	0.26	0.62	0.75	1.28	0.59	0.09
6	0.57	0.30	0.22	0.59	0.29	0.17	0.15	0.07	0.17	0.19
<i>Interday (<math>n = 6</math>)</i>										
1	1.32	1.37	0.72	2.07	1.26	27.13	0.20	2.85	2.24	1.02
2	1.36	0.24	1.09	4.85	1.06	19.73	0.12	1.97	1.66	0.22
3	1.54	0.83	0.60	2.21	1.56	15.86	0.70	1.68	0.69	0.21
4	1.15	3.63	0.53	2.27	1.14	41.99	0.68	0.20	1.00	0.99
5	0.99	0.62	0.74	0.24	1.47	2.87	1.26	1.00	0.79	0.53
6	1.26	0.33	0.53	2.73	1.30	22.73	0.64	1.12	10.12	0.34
<i>Accuracy<sup>a)</sup></i>										
1	97.45	99.41	99.69	95.13	102.05	94.23	100.60	97.93	102.16	101.77
1	97.35	99.22	99.02	94.37	101.81	68.81	100.18	77.37	100.99	101.15

a) The detailed concentrations as well as the accuracy at concentrations 2–6 can be found in Supporting Information.

**Table 6.** Measurement range of various vitamins

	Range (µg/mL)	
	Lower limit	Upper limit
B1	160	800
B6	240	1200
B3-amide	240	1200
B12	600	2400
B2	3	150
C	Stability problem <sup>a)</sup>	
B3	5	2400
A-acetate	400	1600
D3	400	2100
K1	500	2500

a) See Table 5, especially for interday precision.

### 3.3.5 Storage stability

The stability of the vitamin mixture stored in the autosampler was evaluated over 15 h. The deviation of the peak area is given in Fig. 6. The least stable vitamins are the vitamins A-acetate and C. The peak area is continuously slightly decreasing for both vitamins during the whole time range; however, no additional interfering peaks were observed in the chromatogram. Within the first 5 h, the deviation decreased gradually by less than 5% and the mixture should be allowed to be used 5 h long before preparing a fresh one. The stability of the mixture in a

Peltier-autosampler thermostated to 5°C was not evaluated but the stability of the mixture should be improved.

In Fig. 7, the stability of the mixture at four different conditions within 6 days is compared. In the freezer, at –28°C, all the vitamins within the mixture are stable over the whole period. The least stable vitamin remains the vitamin C, even if the deviation by less than 10% is not dramatic. However, to maintain a deviation as low as possible, a fresh solution should be prepared every 2 days if the mixture is freeze-stored.

At +4°C, the stability is quite similar for most of the vitamins. For the two vitamins A-acetate and C, even 1 day of storage is sufficient for the peak area to decrease significantly.

At room temperature in the absence of light, both vitamins A-acetate and C are even less stable. The peak area of the vitamin B<sub>12</sub> is also decreasing rapidly.

In the presence of light, most of the vitamins are decomposing rapidly, even if some of them are still stable, like vitamins B<sub>3</sub>-amide and B<sub>6</sub>. The deviation of the peak area for vitamin B<sub>2</sub>, which was quite stable at every previous storage conditions, is decreasing very fast in this case. The decomposition of riboflavin to peroxides and tryptophan derivatives due to light reaction is well known [29].

### 3.4 Identification and determination of vitamins in multivitamin tablets

Vitamin levels in both multivitamin tablets were determined using this new validated method. Chromatogram

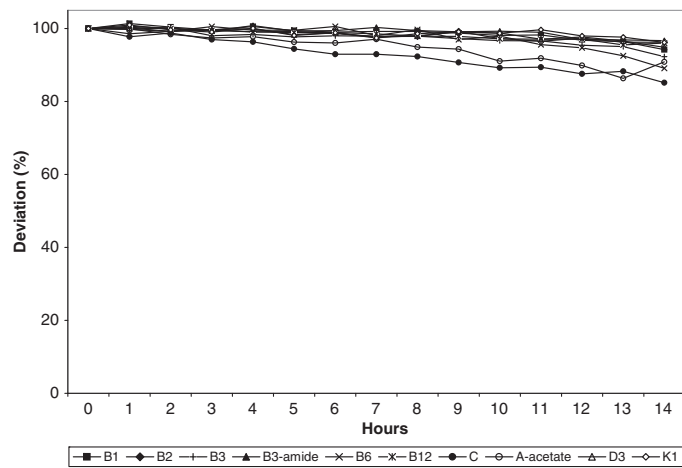


**Figure 6.** Evolution of the stability of the vitamin mixture considering the peak area over 15 h of storage in the autosampler at 25°C.

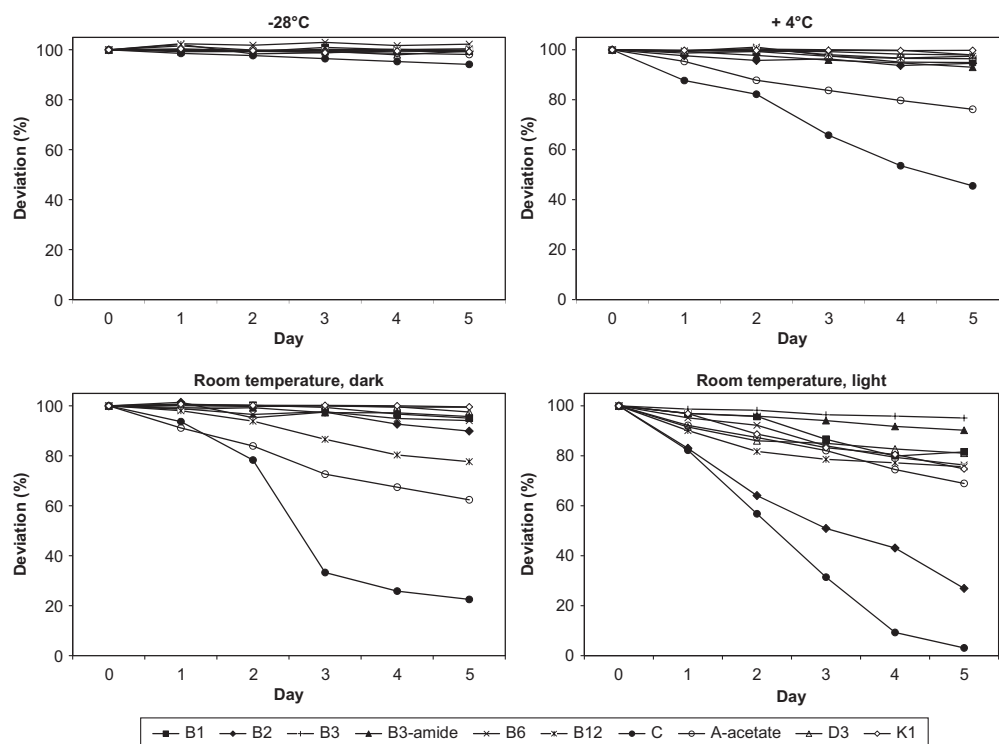


**Figure 7.** Deviation of the peak area for each vitamin at four different storage conditions.

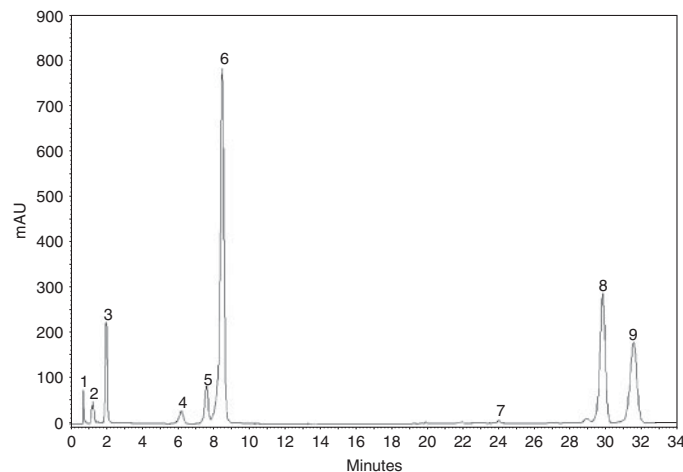


**Figure 8.** HPLC-UV chromatogram of the Rossmann tablet under optimized gradient elution conditions. Conditions: water/100 mM phosphate buffer, pH 4.4/acetonitrile (85:10:5, v/v/v) (A) and water/100 mM phosphate buffer, pH 4.4/acetonitrile (18:2:80, v/v/v) (B), 0' – 0% B, 2' – 0% B, 7' – 12% B, 22' – 82% B, 30' – 97% B, 33' – 97% B, 34' – 0% B, 40' – 0% B, temperature = 25°C, flow rate = 1 mL/min, injection volume = 10 µL, detection at 280 nm. 1: Vitamin B<sub>1</sub>, 2: vitamin B<sub>6</sub>, 3: vitamin B<sub>3</sub>-amide, 4: vitamin B<sub>12</sub>, 5: vitamin B<sub>2</sub>, 6: vitamin C, 7: vitamin A-acetate, 8: vitamin D<sub>3</sub>, and 9: vitamin K<sub>1</sub>.

**Table 7.** Real sample analysis of two different commercially available tablets

	Altapharma				OmniVIT			
	Labeled amount (mg/tablet)	Spiking level (mg/tablet)	Experimental amount including spiking (mg/tablet)	Relative error (%)	Labeled amount (mg/tablet)	Spiking level (mg/tablet)	Experimental amount including spiking (mg/tablet)	Relative error (%)
B1	1.4	0	1.51 ± 0.02	108	1.4	0	1.40 ± 0.02	100
B2	1.6	0	1.68 ± 0.02	105	1.6	0	1.78 ± 0.02	111
B3-amide	18	0	19.10 ± 0.02	106	18	0	18.00 ± 0.03	100
B6	2	0	2.16 ± 0.01	108	2	0	2.00 ± 0.01	100
A-acetate	0.8	2	2.95 ± 0.06	105	0.8	1.2	1.82 ± 0.06	91
D3	0.005	1.2	1.30 ± 0.02	108	0.005	1.0	1.02 ± 0.03	101
K1	0.03	1	1.04 ± 0.01	101	0.03	0.7	0.74 ± 0.01	101

corresponding to analysis of one of the tablets is given in Fig. 8. A reasonable agreement was found between specified and experimentally determined values, i.e. recoveries were quite acceptable (Table 7). Only the very hydrophobic compounds could not be quantified accurately because the concentrations in the tablet were below LLOQs. To reach the LLOQs for these compounds, the tablets have to be dissolved in a smaller volume, which was, however, impossible due to solubility limitations of vitamins and/or excipients. Sample preparation has therefore to be adapted, which however was beyond the primary focus of the present study.

#### 4 Concluding remarks

The current method for the simultaneous separation of water- and fat-soluble vitamins on RP-WAX material offers an alternative selectivity to the one on C18 columns. A

challenge for the simultaneous quantitative analysis, however, remains the limited compound stability of vitamins, which may be associated with poor method validation results as well as the huge concentration differences of vitamins in formulations. However, the use of mixed-mode chromatography for the analysis of mixtures containing compounds with different chemical properties could lead to faster one-step methods for specific applications.

*The authors have declared no conflict of interest.*

#### 5 References

- [1] Eijkman, C., *Nobel Lecture in Physiology or Medicine 1929*, Elsevier Publishing Company, Amsterdam 1965.

- [2] von Szent-Györgyi Nagyrapolt, A., *Nobel Lecture in Physiology or Medicine 1937*, Elsevier Publishing Company, Amsterdam 1965.
- [3] Chen, P., Atkinson, R., Wolf, W. R., *J. AOAC Int.* 2009, **92**, 680–688.
- [4] Amidzic, R., Brboric, J., Cudina, O., Vladimirov, S., *J. Serb. Chem. Soc.* 2005, **70**, 1229–1235.
- [5] Chen, Z., Chen, B., Yao, S., *Anal. Chim. Acta* 2006, **569**, 169–175.
- [6] Perveen, S., Yasmin, A., Khan, K. M., *Open Anal. Chem. J.* 2009, **3**, 1–5.
- [7] Vidovic, S., Stojanovic, B., Veljkovic, J., Prazic-Arsic, L., Roglic, G., Manojlovic, D., *J. Chromatogr. A* 2008, **1202**, 155–162.
- [8] Ake, M., Fabre, H., Malan, A. K., Mandrou, B., *J. Chromatogr. A* 1998, **826**, 183–189.
- [9] Chatzimichalakis, P. F., Samanidou, V. F., Papadoyannis, I. N., *J. Chromatogr. B* 2004, **805**, 289–296.
- [10] Papadoyannis, I. N., Tsioni, G. K., Samanidou, V. F., *J. Liq. Chromatogr. Relat. Technol.* 1997, **20**, 3203–3219.
- [11] Moreno, P., Salvadó, V., *J. Chromatogr. A* 2000, **870**, 207–215.
- [12] Buszewski, B., Zbanyszek, W., *J. Liq. Chromatogr. Relat. Technol.* 2005, **25**, 1229–1241.
- [13] Li, H. B., Chen, F., *Chromatographia* 2001, **54**, 270–273.
- [14] Klejdus, B., Petrlova, J., Potesil, D., Adam, V., Mikelova, R., Vacek, J., Kizek, R., Kuban, V., *Anal. Chim. Acta* 2004, **520**, 57–67.
- [15] The Merck Manual of Medical Information, [www.merck.com](http://www.merck.com).
- [16] Lämmerhofer, M., Richter, M., Wu, J., Nogueira, R., Bicker, W., Lindner, W., *J. Sep. Sci.* 2008, **31**, 2572–2588.
- [17] Nogueira, R., Lubda, D., Leitner, A., Bicker, W., Maier, N. M., Lämmerhofer, M., Lindner, W., *J. Sep. Sci.* 2006, **29**, 966–978.
- [18] Dabre, R., Schwämmle, A., Lämmerhofer, M., Lindner, W., *J. Chromatogr. A* 2009, **1216**, 3473–3479.
- [19] Kleinschmidt, G., *Method Validation in Pharmaceutical Analysis: A Guide to Best Practice*, WILEY-VCH, Weinheim 2005, p. 120.
- [20] Ermer, J., *Method Validation in Pharmaceutical Analysis: A Guide to Best Practice*, WILEY-VCH, Weinheim 2005, p. 80.
- [21] Steliopoulos, P., Stickel, E., Haas, H., Kranz, S., *Anal. Chim. Acta* 2006, **572**, 121–124.
- [22] Kromidas, S., *Handbuch Validierung in der Analytik*, WILEY-VCH, Weinheim 2000, p. 139.
- [23] Ermer, J., Burgess, C., *Method Validation in Pharmaceutical Analysis: A Guide to Best Practice*, WILEY-VCH, Weinheim 2005, p. 101.
- [24] Ermer, J., *Method Validation in Pharmaceutical Analysis: A Guide to Best Practice*, WILEY-VCH, Weinheim 2005, p. 21.
- [25] Ermer, J., *Method Validation in Pharmaceutical Analysis: A Guide to Best Practice*, WILEY-VCH, Weinheim 2005, p. 63.
- [26] Ermer, J., *Method Validation in Pharmaceutical Analysis: A Guide to Best Practice*, WILEY-VCH, Weinheim 2005, p. 99.
- [27] Yang, G., Feng, S., Liu, H., Yin, J., Zhang, L., Cai, L., *J. Chromatogr. B* 2007, **854**, 85–90.
- [28] Hofmann, C. V., Reischl, R., Maier, N. M., Lämmerhofer, M., Lindner, W., *J. Chromatogr. A* 2009, **1216**, 1157–1166.
- [29] Silva, E., Salim-Hanna, M., Edwards, A. M., Becker, M. I., De Ioannes, A. E., *Adv. Exp. Med. Biol.* 1991, **289**, 33–48.

# Lectures

## **28 th International Symposium & Exhibit on the Separation of Proteins, Peptides & Polynucleotides - Germany (D) - September 23, 2008**

### **Preparative separation of peptide mixture on a column containing a mixed-mode reversed-phase/ weak-anion exchange material**

Romain Dabre, Achim Schwämmle, Michael Lämmerhofer, and Wolfgang Lindner

Separation of peptides using liquid chromatography has prospered during the last years. Among others, proteomics, purity control or peptide purification are the major fields of activity for the use of HPLC in the separation of peptides. Reversed-phase HPLC combined with gradient optimization remains the most frequent method to achieve such separations, although new techniques are emerging, but ion-exchange chromatography is still rarely used in this context.

A new chromatographic material based on particulate silica material has been developed for highly effective preparative separations. It is modified with a ligand containing a long hydrophobic chain and a weak anion exchange group. This material is a derivative of a mixedmode phase, which has already been presented for different analytical applications. This kind of material shows a complementary mechanism compared to the conventional HPLC RP-gradient method for the separation of synthetic peptides.

A column packed with this material can exploit hydrophobic interaction, anion-exchange, ionexclusion, and hydrophilic interaction as retention and selectivity principles, depending on the employed conditions. As a consequence, the column can be operated in the RP mode (neutral compounds), anion-exchange mode (AEX) (acidic compounds), ion-exclusion chromatography mode, hydrophobic interaction chromatography (HIC) mode and hydrophilic interaction chromatography (HILIC) mode as well.

The first achievement was to perform typical reversed-phase preparative separation on the material we developed. Afterwards we have extended some of the techniques mentioned above to preparative scale chromatography of different synthetically or biotechnologically produced peptide mixtures of various chemical nature and sizes, which allows tuning the selectivity of our material by simply modifying the operating conditions.

## **29 th International Symposium & Exhibit on the Separation of Proteins, Peptides & Polynucleotides - Delray Beach (FL, USA) - October 27, 2009**

### **An alternative method for peptide mapping using mixed-mode stationary phases**

Romain Dabre, Achim Schwämmle, Michael Lämmerhofer, Wolfgang Lindner, Renato Froidevaux, Didier Guillochon, and Dominique Vercaigne-Marko

Pepsin-catalyzed hydrolysis of porcine haemoglobin revealed the presence of several interesting bioactive peptides in the mixture. A detailed knowledge of the different fragments is necessary in order to better understand bioactivity, and the separation steps must be optimized in order to ameliorate purification and quality control processes. In many cases the first chromatographic step for peptide separation is ion exchange chromatography, whereas reversed phase chromatography is usually applied for the last purification.

Mixed-mode silica-based chromatography materials developed in our laboratories combine both reversed phase (RP) and weak anion exchange (WAX) characteristics and offer a wide range of applicability for the separation of neutral, acidic, basic, or amphoteric compounds. Chromatographic runs can be performed in many different interaction modes such as reversed phase, hydrophilic and hydrophobic interaction, ion exclusion, ion exchange, or a combination of several of those modes.

In our study, we used the versatility of RP/WAX stationary phases to perform peptide separation in different modes just by varying modifier concentration and gradients. The use of different eluent systems on a single multimodal column lead to complementary elution profiles. Consequently, the use of such material for peptide mapping enables an increase in sequence resolution.



# Posters

32<sup>th</sup> HPLC, May 10 - 16, 2008, Baltimore, MA, USA



## Statistical optimization: silylation reaction of mercaptosilanes with silanol groups on silica surface

Romain Dabre<sup>1,2\*</sup>, Achim Schwämmle<sup>1</sup>, Michael Lämmerhofer<sup>2</sup> and Wolfgang Lindner<sup>2</sup>

<sup>1</sup>Merck KGaA, Darmstadt, Germany, <sup>2</sup>Christian Doppler Laboratory for Molecular Recognition Materials, Vienna, Austria | \* Corresponding author: romain.dabre@merck.de

### Introduction

Thiol-modified silica is commonly used as an intermediate product for further synthesis of modified stationary phases for chromatography. Different conditions were used to synthesize thiol-modified phases, but no systematic approach was made yet. The general synthetic method which has been established over the years consists in slurrying the silica gel in toluene before adding mercaptopropylsilane together with a tertiary amine as catalyst.

We followed two main objectives in this study:

- Optimizing the reaction conditions
- Understanding the mechanism of the silylation reaction.

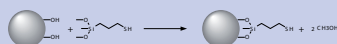
### Analytical methods

Two methods to evaluate the surface coverage of the silica were applied:

- Elemental analysis
- Chemical surface reaction with 2,2'-dipyridyl disulfide and HPLC-UV analysis of stoichiometrically liberated 2-pyridyl thione

### Reaction

Silylating agent: Dimethoxymethyl-mercaptopropylsilane



Constant parameter: Concentration of suspension and of silane  
Optimized parameters: Reaction time and temperature

Range of the optimization:

- 3 h – 60 h
- 35°C – 110°C

### Statistical design of experiment

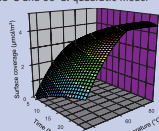
Computer-assisted design of experiment (DoE)

Screening:

- Quadratic model between 3 h and 60 h
  - Combination of different methods to cover the whole temperature range:
1. 60°C – 90°C: full factorial DoE → quadratic model
  2. 35°C – 60°C: verification of the validity of the quadratic model
  3. 90°C – 110°C: further experiments to extend the model

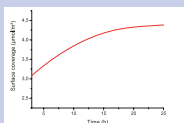
### Results

- Under 35°C, barely any reaction could be observed.
- Between 35°C and 90°C: quadratic model



#### Time effect

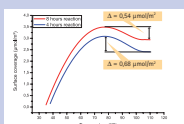
- Slow increase of the surface coverage as a function of the reaction time before reaching a pseudo-plateau after ~20h.



#### Temperature effect

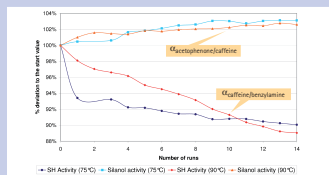
- Quadratic model up to 90°C, a plateau is reached slowly above.

- Difference between optimum and plateau decreases with increasing the reaction time.



- Maximum in the surface coverage at 75°C, which corresponds to the overall temperature optimum.
- Effect is reduced by increasing the reaction time.

### Stability tests



→ SH Activity (75°C) → Silanol activity (75°C) → SH Activity (90°C) → Silanol activity (90°C)

- α-acetophenone/caffeine → Silanol activity
- α-benzylamine/caffeine → SH-activity

Lowering the temperature to increase the surface coverage  
→ No disadvantage for the stability of the material

### Proposed reaction mechanism

Stability test between low- and high-temperature material:  
Optimum-temperature material → strong loss of SH-activity at the beginning of the stability test with small increase of silanol activity

Why?

- cleavage of mono-bonded silane

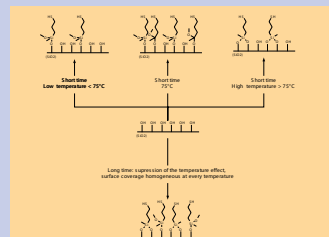
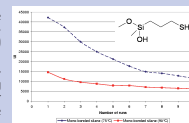
(replacement 1:1 silane silanol / surface silanol)

- more mono-functional reaction at lower temperatures

LC-MS bleeding:

Hydroxy-methoxy-silane (cleavage of a mono-functionally bonded silane)  
m/z=166.32g/mol

- 3 times more mono-bonded silane cleaving off the silica surface for the optimum-temperature material.



Presence of an optimum for the surface coverage at 75°C:

- Reduction of the number of hydrocarbon chains on the surface of the silica material at higher temperature by bi-functional modification.

### Conclusion

- Increasing the reaction temperature (bonding functionality) does not lead to an improvement of the stability but leads to a lower surface coverage, as long as the same time of reaction is considered.
- Controlling the reaction temperature allows choosing the privileged modification-type (i.e. mono- or bi-functional modification) and improving the surface coverage.
- Lowering the reaction temperature facilitates the on-column modification. This point is perhaps not so important for particulate material but in the case of monolithic columns, the implementation of an in-line modification becomes a relevant challenge.
- Finally, performing a statistical design of experiment for the optimization of chemical reactions should always be considered, even if the reaction is already well described in the literature.

# Recovery of Biological Products XII, June 22 – 27, 2008, Quebec City, Canada

## Purification of peptides and small proteins by means of reversed phase / weak anion exchange mixed mode chromatography

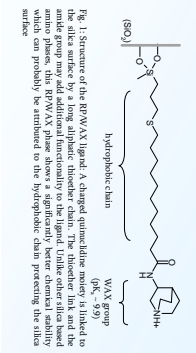
A. Schwämmle<sup>1</sup>, R. Dabre<sup>1,2</sup>, R. Nogueira<sup>1</sup>, M. Schulte<sup>1</sup>, M. Lämmerhofer<sup>2</sup>, W. Lindner<sup>2</sup>  
<sup>1</sup>Merck KGaA – Performance & Life Science Chemicals R&D, Frankfurter Str. 250, D-64293 Darmstadt, Germany  
<sup>2</sup>Christian Doppler Laboratory for Molecular Recognition Materials, Department of Analytical and Food Chemistry, University of Vienna, Währinger Strasse 38, A-1090 Vienna, Austria  
 Recovery of Biological Products XII, June 22 – 27, 2008, Quebec City, Canada

### Abstract

Peptides and small proteins such as insulin or erythropoietin are commonly purified by means of classical reversed-phase chromatography, using interactions between the hydrophobic and the stationary phase. To not always provide good selectivities. On the other hand, ion-exchange have been used as stationary phase with a high polarity which normally separate peptides and proteins. However, the separation of peptides and proteins with selectivities which would be supportive especially in the separation of peptides, proteins, or other biomolecules. To overcome these limitations new even ionic – along with hydrophobic interactions. These materials offer must greater flexibility in selectivity adjustment which frequently results in better separation. We report on applications of a novel reversed-phase material, the RP/WAX, on separation of insulin and erythropoietin with superior selectivities for the purification of peptides and small proteins in comparison with classical reversed-phase materials.

### Introduction

Multimodal separation mechanisms have already been described in the scientific literature more than 20 years ago<sup>1</sup>. With mixed-mode chromatography, analytes are separated from each other through two different interactions (for example reversed-phase and anion exchange interactions in our case). We developed a silica-based multimodal material which will be referred to in the following as RP/WAX (reversed phase / weak anion exchange) material. This material is characterized by a unique ligand with two distinct binding domains (see figure 1): a relatively hydrophilic, quaternary head group which bears the positive charge (WAX) is linked to the silica surface by a hydrophobic aliphatic hydrocarbon chain (RP).

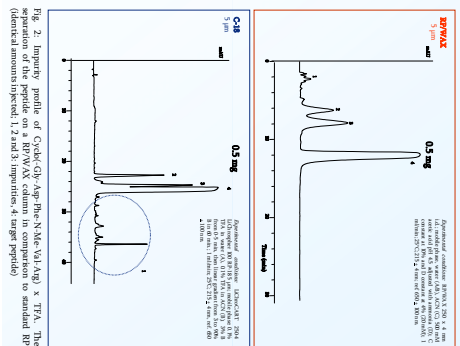


The silica-based particles used in this study have pore size of 100 Å. The reversed-phase and anion-exchange interactions are expected to be enhanced at cyclohexane and human insulin. Higher proteins would be excluded from the pore and size-exclusion mechanism would interfere with the multimodal selectivity. The range of each chromatographic material is the broader range of analyses which can be separated. Furthermore, with column packed with mixed-mode material, hydrophobic interaction, anion-exchange, ion exclusion and hydrophilic interaction can be exploited as retention and separation mechanisms. The RP/WAX material can be operated in the reversed phase (RP) mode, anion-exchange (AEX) mode, ion-exclusion (IE) chromatography mode and hydrophilic interaction (HILIC) mode as well. The separation of insulin and human insulin came directly from industrial processes, in order to assess the possibility of implementation.

### Application example: Purification of a synthetic cyclopeptide

The performance of a 250 x 4 mm I.D. RP/WAX column based on LiChrospher 100 Å (5 µm) silica was tested with a sample of a synthetic bioactive cyclopeptide (BIO11191). The compound is obtained as a TFA cyclopeptide shows an amphiphilic behavior due to basic and acidic residues. The pI is 8.2. There is also a lipophilic domain on another side of the molecule made up of different hydrophobic fragments.

In a series of preliminary chromatographic experiments the optimal separation conditions on a RP/WAX prototype based on LiChrospher 100 Å (5 µm) silica were determined. The separation of the synthetic cyclopeptide with a C18 column based on same LiChrospher 100 Å silica. Results of optimization showed an improvement of resolution for the target peptide with change of selectivity.



After having identified the appropriate separation conditions for both columns, a study was performed to establish the stability of the RP/WAX material for preparative separation (see figure 3). The stability is 40 times higher for the RP/WAX material than for the standard C18 and the higher productivity and a dramatic decrease of solvent consumption.

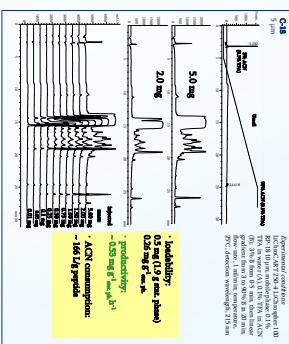
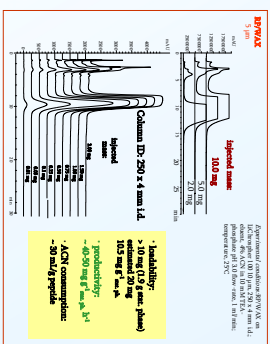
### Application example: Purification of human insulin

A 100 x 4 column based on same RP/WAX silica material was tested with a sample of human insulin (see figure 4). The insulin was freshly prepared by insulin synthesis and purified by reversed-phase chromatography. The column was compared to that of a C8 modified silica, which is considered to be one of the standard methods for insulin purification.

- Such increase in loadability, productivity and decrease in solvent consumption leads to different saving possibilities:
- less material (i.e. stationary phase, organic solvent)
- reduction of solvent recycling costs
- personal costs reduced
- smaller (and therefore cheaper) equipment needed

Financial savings are not the only benefits of such a productivity gain; the "green chemistry" aspect will be more and more important. Using RP/WAX environmental friendly through:

- reduction of organic phase consumption
- reduction of energy consumption



### Conclusion

The purification studies with cyclopeptide show that the loading capacity of the RP/WAX phase is significantly higher in comparison to a standard silica-based reversed-phase material. The higher productivity is not the only benefit of using multimodal material. Acetate consumption drops significantly, which reduces the environmental impact of the process. Separation of human insulin shows outstanding selectivity for multimodal material. Improvement of resolution allows working at higher flow rate and leads consequently to reduction of purification costs. The RP/WAX material should be considered in order to establish a new generation of purification materials not only to gain new selectivity but also to improve the profit ratio of a purification process.

### References

- 1: L.W. McLaughlin, *Chem. Rev.* **1989** 309-319
- 2: E. Apfleiderer, W. Bickel, M. Lämmerhofer, M. Sponke, R. Kisch, W. Lindner and R. Schimmler, *J. Chromatogr. A* **191** **2008** 171-181

# 34th HPLC conference, June 28 - July 2, 2009, Dresden, Germany



## A Rapid Method for the Optimization of Separation Conditions on Mixed-Mode Stationary Phases Using Automated Method Development Software

Romain Dabre<sup>1,2,\*</sup>, Achim Schwämme<sup>1</sup>, Adeline René<sup>1,3</sup>, Michael Lämmerhofer<sup>2</sup> and Wolfgang Lindner<sup>2</sup>

<sup>1</sup>Merck KGaA, Darmstadt, Germany, <sup>2</sup>Institute of Analytical Chemistry and Food Chemistry, Vienna, Austria, <sup>3</sup>ENSIACEN, Caen, France | \* Corresponding author: romain.dabre@merck.de

34<sup>th</sup> HPLC conference, June 28 - July 2, 2009, Dresden, Germany

### Introduction

**Silica-based mixed-mode chromatography materials** developed in our laboratories combine both **reversed phase (RP)** and **weak anion exchange (WAX)** characteristics, which offers a wide range of applicability for the separation of neutral, acidic, basic, or amphoteric compounds. Chromatographic runs can be performed in many different interaction modes such as reversed phase, hydrophilic and hydrophobic interaction, ion exclusion, ion exchange, or a combination of several of those modes<sup>1</sup>. Due to this high flexibility in usage it could be difficult and time consuming especially for less experienced users to identify the appropriate separation mode and to optimize the chromatographic conditions on such columns.

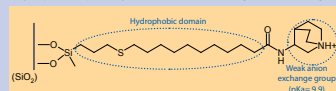
As a case study for such method development, we optimized the separation of **three fluoroquinolone-based antibiotics containing both acidic and basic functionalities** – ciprofloxacin, danofloxacin and norfloxacin – as well as the separation of **norfloxacin from the three main impurities** described in the European Pharmacopoeia.

The first step of our work included a **rapid screening** of the different separation modes in order to locate approximately promising chromatographic conditions. Then those preliminary methods were further optimized using **ChromSword® Auto** (CSA) which is known as a powerful tool for the automated HPLC method optimization.

### Multi-modal chromatography material

**Ultrapur high performance silica** was modified with a **unique ligand developed in our laboratory** containing two different binding domains<sup>1</sup>:

- Hydrophilic: quinuclidinyl head group bearing the positive charge
- Hydrophobic: aliphatic hydrocarbon chain containing a thioether bridge



### ChromSword® Auto: a powerful tool<sup>2</sup>

- Ability to optimize the separation of a sample mixture **without having pure product or impurity standards at disposal**
- Mixture with **unknown amounts of impurities** (< 0.05 area%) can be fully separated

➔ Possibility to develop sample separation HPLC methods and quality control HPLC methods

Two optimization modes can be used:

- **Smart screening** for easily separated compounds within 2 hours
- **Fine optimization** for more complicated mixtures within 9 hours

### Using ChromSword® with RP-WAX material

CSA was developed to **optimize HPLC conditions in reversed-phase, normal phase or ion pair** modes but not in combination of several modes!

CSA artificial intelligence is assuming that:

- **Eluent A has the smaller eluting strength**
- **Eluent B has the highest eluting strength**

Optimization on RP-WAX with CSA is feasible as long as two appropriate eluents have been identified

➔ Aim of first gradient pre-screening

### Gradient pre-screening

As aforementioned, **several eluent systems** can be used to perform separations on **RP-WAX columns**. Determination of the best suitable eluent system can be performed through a **rapid screening** on a 4-channel HPLC equipment.

In our case, separating compounds containing both acidic and basic groups led us to investigate different pH and salt systems:

- **Eluent 1:** Tris-buffer adjusted to pH 8.0 with acetic acid
- **Eluent 2:** Water pH 2.0 with phosphoric acid
- **Eluent 3:** Acetonitrile with 0.1 % acetic acid
- **Eluent 4:** Pure acetonitrile

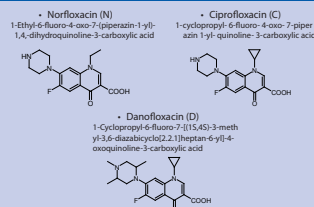
**RP-WAX conditions:**

**Eluent 1 and eluent 3** for antibiotic mixture and norfloxacin CRS separations

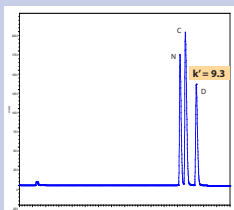
**RP conditions:**

**Eluent 2 and eluent 4** for both separations

### Antibiotic mixture



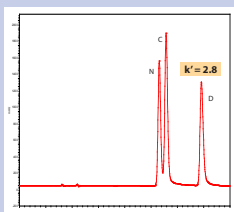
### Smart screening: RP18 silica



Optimized CSA method

- Column: Poragel STAR<sup>®</sup> RP18 150 column (125 x 4 mm)
- Temperature: 30 °C
- Mobile phase:
  - A: Water pH 2.0
  - B: Acetonitrile
- Gradient: 0: 4 % B - 17: 17 % B - 18: 100 % B
- Injection: 10 µl
- Detection: UV 280 nm

### Smart screening: RP-WAX silica



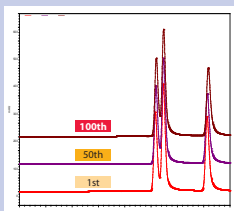
Optimized CSA method

- Column: Poragel STAR<sup>®</sup> RP-WAX research sample column (125 x 4 mm)
- Temperature: 30 °C
- Mobile phase:
  - A: Tris-buffer pH 8.0 (acetic acid)
  - B: Acetonitrile, 0.1 % acetic acid
- Gradient: 0: 13 % B - 6: 4 % B - 100 % B
- Injection: 10 µl
- Detection: UV 280 nm

Because of the **unique selectivity of RP-WAX material**, **analysis duration can be dramatically reduced** by using such material combined with a proper method development.

### Reproducibility test

**Stability of RP-WAX material** even after large number of runs allows **implementation in routine analysis**.



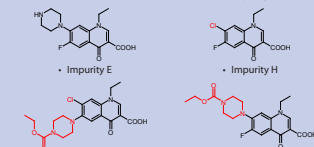
Optimized CSA method

- Column: Poragel STAR<sup>®</sup> RP-WAX research sample column (125 x 4 mm)
- Temperature: RT
- Mobile phase:
  - A: Tris-buffer pH 8.0 (acetic acid)
  - B: Acetonitrile, 0.1 % acetic acid
- Gradient: 0: 13 % B - 6: 4 % B - 100 % B
- Injection: 10 µl
- Detection: UV 280 nm

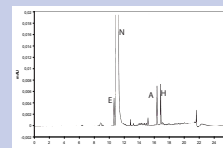
### Norfloxacin CRS

Norfloxacin for system suitability CRS is a mixture containing following compounds as well as many other impurities at lower amount:

- Norfloxacin (> 99 %) (N)
- Impurity A
- Impurity E
- Impurity H



### Standard HPLC-method for quality control

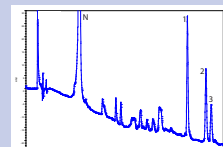


European Pharmacopoeia validated method<sup>3</sup>

- Column: Polar embedded RP18 column (250 x 4.6 mm)
- Temperature: 60 °C
- Mobile phase:
  - A: Water adjusted to pH 2.0 with phosphoric acid
  - B: Acetonitrile
- Gradient: 0: 5 % B - 5: 5 % B - 7: 7 % B - 10: 13 % B - 15: 53 % B - 20: 90 % B
- Injection: 20 µl
- Detection: UV 265 nm

Peaks have been identified by comparison from peak area and UV spectrum. We can assume that peaks 1, 2 and 3 in the following correspond respectively to impurities A, H and E. Peak assignment must be confirmed with LC/MS.

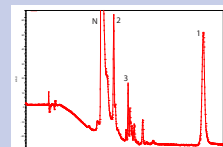
### Fine optimization: RP18 silica



Optimized CSA method

- Column: Poragel STAR<sup>®</sup> RP18 150 column (125 x 4 mm)
- Temperature: 30 °C
- Mobile phase:
  - A: Water pH 2.0 (acetic acid)
  - B: Acetonitrile
- Gradient: 0: 9 % B - 7: 7 % B - 13: 53 % B - 16: 65 % B - 18: 69 % B
- Injection: 10 µl
- Detection: UV 265 nm

### Fine optimization: RP-WAX silica



Optimized CSA method

- Column: Poragel STAR<sup>®</sup> RP-WAX research sample column (125 x 4 mm)
- Temperature: 30 °C
- Mobile phase:
  - A: Tris-buffer pH 8.0 (acetic acid)
  - B: Acetonitrile, 0.1 % acetic acid
- Gradient: 0: 3 % B - 4: 3 % B - 15: 76 % B - 15: 76 % B
- Injection: 10 µl
- Detection: UV 265 nm

### Conclusion

**Versatility of RP-WAX columns** can be used for mixture separation as well as for impurities determination (quality control). Drawback of complicated method development can be easily overcome by:

- **Good knowledge of chemical structures** to choose best possible eluent systems
- **Pre-screening** to determine 2-solvents elution system
- **Unattended method development** with ChromSword® Auto
  - **Rapid optimization** for simple compounds separation
  - **Fine optimization** for more complex mixtures

**RP-WAX chromatography can therefore be easily implemented as a complementary method to standard RP.**

### References

1. E. Apfelter, W. Bicker, M. Lämmerhofer, M. Sulyok, R. Krka, W. Lindner and R. Schumacher, J. Chromatogr. A, 1191 (2008) 171-181
2. S. Galichienko, V. Tanchuk, I. Shokina, O. Polyshchenko and W.D. Belner in HPLC method optimization, S. Kromidas, Wiley-VCH, 2006
3. European Pharmacopoeia 6.2, 07/2008: 1248



## A procedure for optimizing the separation of mixtures of pharmaceutical compounds on RP-WAX stationary phases

Romain Dabre<sup>1,3,\*</sup>, Achim Schwämmle<sup>1</sup>, Christian Jungfer<sup>1,2</sup>, Michael Lämmerhofer<sup>3</sup> and Wolfgang Lindner<sup>3</sup>

<sup>1</sup>Merck KGaA, Darmstadt, Germany, <sup>2</sup>Hochschule Mannheim, Germany, <sup>3</sup>Institute of Analytical Chemistry and Food Chemistry, Vienna, Austria | \* Corresponding author: romain.dabre@merck.de

Euroanalysis XV, September 06 - 10, 2009, Innsbruck, Austria

### Introduction

**Silica-based mixed-mode chromatography materials** developed in our laboratories combine both **reversed phase (RP)** and **weak anion exchange (WAX)** characteristics, which offers a wide range of applicability for the separation of neutral, acidic, basic, or amphoteric compounds. Chromatographic runs can be performed in many different interaction modes such as reversed phase, hydrophilic and hydrophobic interaction, ion exclusion, ion exchange, or a combination of several of those modes<sup>1</sup>.

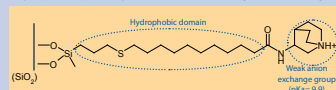
In order to demonstrate the versatility of our material, we studied the chromatographic properties of pharmaceutical compounds bearing acidic or basic moieties. We used therefore **fluoroquinolone antibiotics**, **betablockers**, and **non-steroidal anti-inflammatory** and **anti-hypercholesterolemia drugs**, respectively.

The first step of our work consisted in studying the separation on **standard RP** material. In a second step, the chromatographic behaviour of pharmaceutical compounds on **innovative RP-WAX** stationary phase was studied regarding **organic modifier**, **pH** and **salt concentration as variable**.

### Multi-modal chromatography material

**Ultrapure high performance silica** was modified with an **unique ligand developed in our laboratory** containing two different binding domains<sup>1</sup>:

- Hydrophilic quinuclidinyl head group bearing the positive charge
- Hydrophobic aliphatic hydrocarbon chain containing a thioether bridge



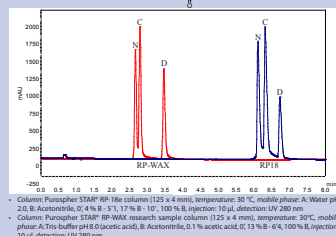
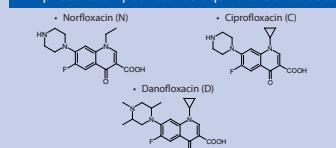
### ChromSword® Auto: RP-WAX optimization

- The first step of optimization consists in performing a few isocratic runs at different organic modifier concentrations and pH in order to define a range in which all compounds can be separated.

Determination of a mobile phase composition at which the first eluting compounds are well separated (solvent A) and of a second one at which the last eluted compounds are well separated within a short time (solvent B).

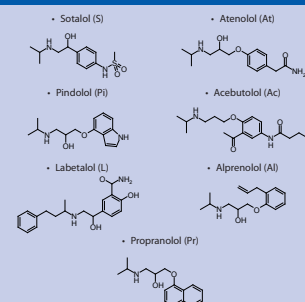
- In a second step, the separation gradient is optimized using ChromSword® Auto software in order to obtain the best separation within the shortest time possible.

### Amphoteric compounds: fluoroquinolone antibiotics

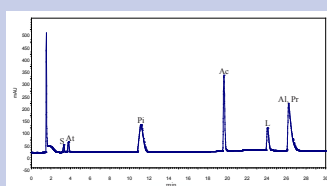


Separation of **amphoteric compounds** can be achieved on RP-WAX material using a **constant salt concentration** and **constant pH** combined with **increasing amount of organic modifier**. In this case, the RP-WAX stationary phase is used in standard RP mode. The shorter retention time in comparison with the standard C18 material is due to the smaller hydrophobicity of the surface modification which is comparable to that of an octyl phase.

### Basic compounds: beta-blockers



### Separation on RP-18 column

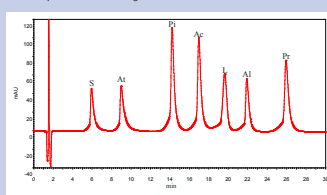


Column: PuruStar® RP-18 column (125 x 4 mm), temperature: 25 °C, mobile phase: A: water containing 0.03 % TFA, B: water - acetonitrile (50:50, v/v) containing 0.3 % TFA, 0 - 19 % B, 1.4 - 21 % B, 13.3 - 24 % B, 13.5 - 51 % B, 30 - 51 % B, injection: 10 µl, detection: UV 225 nm.

As already described in the literature, **some beta-blocker couples - sotalol / atenolol, or alprenolol / propranolol - are rather difficult to separate on standard RP-18 material<sup>1</sup>**.

### Separation on RP-WAX column

After isocratic pre-screening, we optimized the separation by varying acetonitrile and pH gradients in different combinations. The best separation - shown in the chromatogram below - was obtained using a gradient combining decreasing pH value and increasing organic modifier amount. Analysis time and peak resolution are given in table 1.



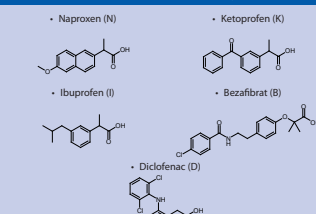
Column: PuruStar® RP-WAX research sample column (125 x 4 mm), temperature: 25 °C, mobile phase: A: 100 mM Tris buffer adjusted to pH 7.25 (acetic acid) / acetonitrile (80:20, v/v), 0 - 0 % B, 4.2 - 22 % B, 16.5 - 72 % B, 22.7 - 86 % B, 30 - 86 % B, injection: 10 µl, detection: UV 225 nm.

	Reversed Phase column		Reversed Phase - Weak Anion Exchange column	
	ACN gradient	ACN gradient	pH gradient	ACN and pH gradient
Retention time of last peak	26.4	22.5	31.4	26.1
Fastest peak resolution	0	1.85	1.34	1.98

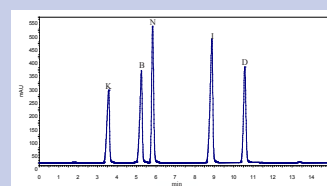
Table 1. Resolution factor of the less resolved peak and retention time of last peak in minutes for each column and each RP-WAX gradient. Resolution factor is calculated from the United States Pharmacopoeia calculation method.

The separation of **basic compounds** can be achieved efficiently using a combination of **increasing organic modifier** and **decreasing pH gradients - RP and weak cation exclusion (WCK) gradients - on RP-WAX material**. Even analytes which are **impossible to separate on RP columns** can be **baseline-separated with high resolution on RP-WAX columns**.

### Acidic compounds: anti-inflammatory drugs

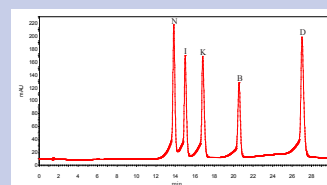


### Separation on RP-18 column



Column: PuruStar® RP-18 column (125 x 4 mm), temperature: 25 °C, mobile phase: A: 20 mM phosphate buffer adjusted to pH 4.5 (formic acid), B: acetonitrile, 0 - 40 % B, 30 - 90 % B, injection: 10 µl, detection: UV 225 nm.

### Separation on RP-WAX column



Column: PuruStar® RP-WAX research sample column (125 x 4 mm), temperature: 25 °C, mobile phase: A: 10 mM phosphate buffer pH 4.5, water / acetonitrile (70:30, v/v), B: 50 mM phosphate buffer pH 4.5, water / acetonitrile (50:50, v/v), 0 - 10 % B, 30 - 90 % B, injection: 10 µl, detection: UV 225 nm.

Even if peak shape and speed of analysis are better on the RP-18 column the five acidic analytes can be **efficiently separated with a completely different order of elution on the RP-WAX column** using a combination of **salt and organic modifier gradient**.

### Conclusion

Due to its **remarkable versatility**, the **RP-WAX stationary phase** allows for a perfect separation of different types of pharmaceutical compounds:

- Amphoteric compounds:** RP mode with a retention behaviour **similar to C8** stationary phases.
- Basic compounds:** perfect separation using a **combination of reversed phase and cation exclusion modes**
- Acidic compounds:** different elution order obtained through **reversed phase and anion exchange modes**

**RP-WAX chromatography** is a reasonable **alternative to standard RP methods** to separate analytes with different **acidic or basic properties**.

### References and remarks

- E. Apflethaler, W. Bickel, M. Lämmerhofer, M. Salyok, R. Kriks, W. Lindner and R. Schuhmacher, J. Chromatogr. A, 1191 (2008) 171-181
- G. Wolf-Trapp, J.R. Torres-Lapiedra, M.C. Garcia-Alvarez-Coque, J. Chromatogr. A 1018 (2003) 183

<sup>1</sup> Gradients were manually optimized because of technical problems.

In memory of Christian Jungfer († 25.07.09)

# 7th HIC/RPC bioseparation conference, March 21 -24, 2011, Estoril, Portugal



universität  
wien

## Procedures for optimizing the separation of mixtures of pharmaceutical compounds on RP-WAX stationary phases

Romain Dabre<sup>1,\*</sup>, Achim Schwämmle<sup>2</sup>, Michael Lämmerhofer<sup>1</sup> and Wolfgang Lindner<sup>1</sup>

<sup>1</sup>Institute of Analytical Chemistry, Vienna, Austria; <sup>2</sup>Merck KGaA, Darmstadt, Germany | \*Corresponding author: romain.dabre@gmail.com

7th HIC/RPC bioseparation conference, March 21 -24, 2011, Estoril, Portugal

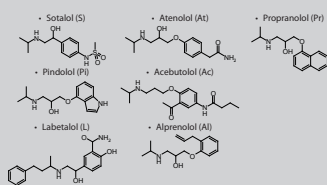
### Introduction

**Silica-based mixed-mode chromatography materials** developed in our laboratories combine both **reversed phase (RP)** and **weak anion exchange (WAX)** characteristics, which offers a wide range of applicability for the separation of neutral, acidic, basic, or amphoteric compounds. Chromatographic runs can be performed in many different interaction modes such as reversed phase, hydrophilic and hydrophobic interaction, ion exclusion, ion exchange, or a combination of several of those modes<sup>1</sup>.

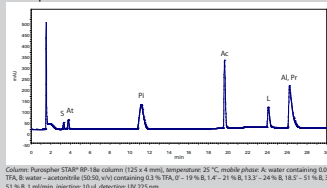
In order to demonstrate the versatility of our material, we studied the chromatographic properties of pharmaceutical compounds bearing zwitterionic, acidic or basic groups, or none of them. We used therefore different **beta-blockers**, **anti-inflammatory** as well as a **vitamin mixture**.

The first step of our work consisted in studying the separation on **standard RP or HILIC** material. In a second step, the chromatographic behaviour of pharmaceutical compounds on **innovative RP-WAX** stationary phase was studied regarding **organic modifier, pH and salt concentration** as variable.

### Basic compounds: beta-blockers



### Separation on RP-18 column

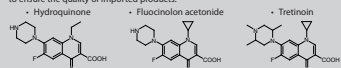


As already described in the literature, some **beta-blocker couples** – sotalol / atenolol, or alprenolol / propranolol – are **rather difficult to separate on standard RP-18 material**<sup>2</sup>.

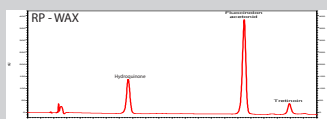
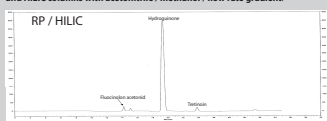
### Complex mixture: Tri-Luma

Tri-Luma is a dermatologic cream composed of 3 active compounds. It was first patented as a treatment against hyper-pigmentation of pathological scars. Further hyper-pigmentation diseases were successfully cured using same preparation, always under medical prescription.

Increased used by healthy people for skin whitening leading to the emergence of non-authorized suppliers. It is therefore necessary to develop some specific analytical method to ensure the quality of imported products.



A method for the separation of those three different compounds was developed by an independent labor. They obtained the best separation by a **combination of both RP and HILIC columns with acetonitrile / methanol / flow rate gradient**.

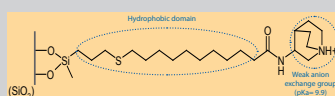


On **RP-WAX material**, a **fast and simple method** could easily be set up. The automated method development using ChromSword Auto allowed a **complete method development within 4 hours**.

### Multi-modal chromatography material

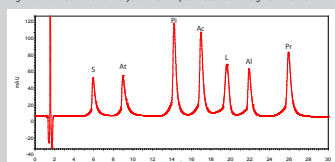
**Ultrapure high performance silica** was modified with an **unique ligand developed in our laboratory** containing two different binding domains<sup>3</sup>:

- Hydrophilic quinuclidinyl head group bearing the positive charge
- Hydrophobic aliphatic hydrocarbon chain containing a thioether bridge



### Separation on RP-WAX column

After isocratic pre-screening, we optimized the separation by varying acetonitrile and pH gradients in different combinations. Best separation – shown in the chromatogram below – was obtained using a gradient combining decreasing pH value and increasing organic modifier amount. Analysis time and peak resolution are given in table 1.



	Reversed Phase column	Reversed Phase column	Weak Anion Exchange column	Weak Anion Exchange column
	ACN gradient	ACN gradient	pH gradient	ACN and pH gradient
Retention time of last peak	36.4	22.5	31.4	26.1
Purest peak resolution	0	1.85	1.54	1.98

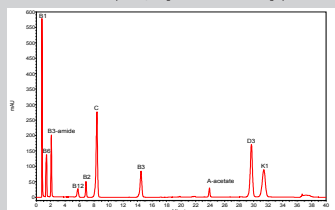
Table 1. Resolution factor of the last resolved peak and retention time of last peak in minutes for each column and each RP-WAX gradient. Resolution factor is calculated from the United States Pharmacopoeia calculation method.

The separation of **basic compounds** can be achieved efficiently using a combination of **increasing organic modifier and decreasing pH gradients** – **RP and weak repulsive electronic interaction gradients** – on **RP-WAX material**. Even analytes which are **impossible to separate on RP columns** can be **baseline-separated with high resolution on RP-WAX columns**.

<sup>1</sup>G. Wink-Troyer, J.R. Torres-Lapiedra, M.C. Garcia-Alvarez-Coque, J. Chromatogr. A 1018 (2003) 185.

### Complex mixture: fat- and water-soluble vitamins

Simultaneous separation of 10 vitamins with different chemical properties on RP-WAX material and validation thereof was recently published<sup>4</sup>. Seven water-soluble and three fat-soluble vitamins were separated, using three different chromatographic modes.



Some positively charged vitamins are eluted in **ion exclusion** and **ion repulsion** modes whereas the negatively charged molecules are undergoing **ion exchange** mechanism. The non-charged molecules are eluted on a **classical reversed-phase mode**, regarding their polarities. The method was validated, evaluating selectivity, robustness, linearity, accuracy and precision. The **validated method** was finally employed for the analysis of the vitamin content of some **commercially available supplement tablets** (see Table 2).

	Supplier 1				Supplier 2			
	Labelled amount (µg/tablet)	Spiking level (µg/tablet)	Experiment - total amount including spiking (recovery)	Accuracy (detected amount - spiked amount)	Labelled amount (µg/tablet)	Spiking level (µg/tablet)	Experiment - total amount including spiking (recovery)	Accuracy (detected amount - spiked amount)
B1	1.4	0	1.31±0.02	108	1.4	0	1.46±0.02	100
B2	1.4	0	1.48±0.02	105	1.4	0	1.76±0.02	111
B6	18	0	10.10±0.02	106	18	0	18.00±0.03	100
B9	2	0	2.16±0.01	108	2	0	2.00±0.01	100
A-acetate	0.8	2	2.95±0.06	105	0.8	1.2	1.82±0.04	91
D3	0.005	1.2	1.30±0.03	108	0.005	1.0	1.02±0.01	101
K1	0.03	1	1.04±0.01	101	0.03	0.7	0.74±0.01	101

Table 2. Real sample analysis of two different commercially available tablets.

<sup>4</sup>R. Dabre, N. Azaiz, A. Schwämmle, M. Lämmerhofer, W. Lindner, J. Sep. Sci., 2011, in press.

### ChromSword® Auto: RP-WAX optimization

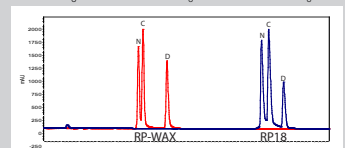
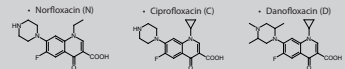
- The first step of optimization consists in performing a few isocratic runs at different organic modifier concentrations and pH in order to define a range. In which all compounds can be separated.

↳ Determination of a mobile phase composition at which the first eluting compounds are well separated (solvent A) and of a second one at which the last eluted compounds are well separated within a short time (solvent B).

- In a second step, the separation gradient is optimized using ChromSword® Auto software in order to obtain the best separation within the shortest time possible.

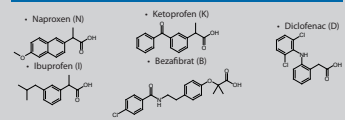
<sup>1</sup> E. Agathos, W. Bicker, M. Lämmerhofer, M. Suljak, R. Kiska, W. Lindner and J. Schumacher, J. Chromatogr. A, 1191 (2008) 171-181.

### Amphoteric compounds: fluoroquinolone antibiotics

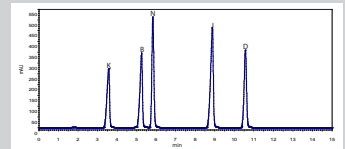


Separation of **amphoteric compounds** can be achieved on RP-WAX material using a **constant salt concentration and constant pH** combined with **increasing amount of organic modifier**. In this case, the RP-WAX stationary phase is used in **standard RP mode**. The shorter retention time in comparison with the standard C18 material is due to the smaller hydrophobicity of the surface modification which is comparable to that of an octyl phase.

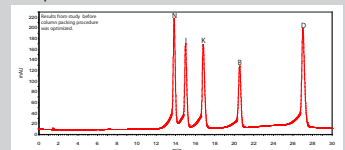
### Acidic compounds: anti-inflammatory drugs



### Separation on RP-18 column



### Separation on RP-WAX column



Even if peak shape and speed of analysis are better on the RP-18 column the five acidic analytes can be **efficiently separated with a completely different order of elution on the RP-WAX column using a combination of salt and organic modifier gradient**.

### Conclusion

**RP-WAX chromatography** is a reasonable **alternative to standard RP or HILIC** methods to separate analytes with different chemical properties by **complementary selectivity principles** using a **combination of several chromatographic modes**.



# Zusammenfassung

Silica-Harze wurden seit der Erfindung der Flüssigchromatographie für die sterische Auftrennung von Analyten durch die Porosität des Silicagels verwendet. Danach wurde Silica verwendet, um polare Verbindungen im normalen Modus zu trennen. In diesem Modus dienen die Silanol-Gruppe auf der Oberfläche der Silica als Interaktionspunkt zwischen Silica-Oberfläche und Analyten. Allerdings wurde die Stabilität und den Einsatzbereich solcher Materialien durch die feste Zusammensetzung der Oberfläche beschränkt.

Später wurden Reversed-Phase-Materialien entwickelt. Hydrophobe Liganden wurden dafür durch Sylanisierung an den Silanol-Gruppen gekoppelt. Diese neueren Materialien sind weniger empfindlich gegenüber aggressiven Chemikalien, und dadurch konnte man Moleküle mit sehr unterschiedlichen Hydrophobizitäten analysieren. Die Elution erfolgt in diesem Fall durch Veränderung der Gehalt an organischem Lösungsmittel in der mobilen Phase. Weiter Chromatographierharze wurden dann entwickelt, um andere Trennungsprobleme anzugehen. Hydrophobe Wechselwirkung Phase (HIC) wurden entwickelt, um die Trennung von hydrophoben Verbindungen mit einem Puffer-gesteuerten Elution für Moleküle, die instabil gegenüber organischen Lösungsmitteln (typischerweise Proteine), zu ermöglichen. Anionen- und Kationenaustausch-Chromatographie (AEC und CEC) wurden für die Trennung von geladenen Molekülen entwickelt. Hydrophile Interaktion Phase (HILIC) wurden für die Trennung von polaren Verbindungen entwickelt (Vorteil gegenüber reines Silica ist die andere Selektivität sowie die bessere Stabilität). Chirale stationäre Phase (CSP) werden für die Trennung chiraler Moleküle verwendet.

Doch in den letzten zehn Jahren ist Mixed-Mode-Chromatographie entstanden, um verschiedene Moleküle mit vielen verschiedenen chemischen Eigenschaften in einem einzigen Lauf auf einer einzigen Phase aufzutrennen. In dieser Studie entwickelten wir ein Ligand mit einer hydrophoben Kette sowie einem schwachen Anionenaustauscher-Gruppe. Durch die Pfropfung der Ligand auf die Oberfläche der Silica-Partikel wurde ein Mixed-Mode-Material entwickelt, der beide Reversed Phase (RP) und schwacher Anionenaustauscher (WAX) Eigenschaften kombiniert.

Der erste Teil der Studie bestand in der Verbesserung der Synthese des patentierten Liganden. Verschiedene chemische und technische Ansätze wurden getestet, um die Synthese zu vereinfachen und die Robustheit des Verfahrens zu verbessern. Die Bindung des Spacer an der Oberfläche, das Endcapping der nicht-umgesetzten Silanolgruppen, die Reaktion des Liganden an den Spacer wurden ebenfalls untersucht. Nachdem jeden Schritt des Herstellungsprozesses optimiert wurde, wurde das Prozess bis zu einer Menge von 500 g durchgeführt, was einer Pre-Production-Skala entspricht.

In einem zweiten Teil wurden viele verschiedene Anwendungen entwickelt, um die Einsatzbereich des Materials festzustellen. Der RP-WAX Material, der in unseren Labors entwickelt worden ist, bietet ein breites Spektrum an Anwendbarkeit für die Trennung von neutrale, saure, basische oder amphotere Verbindungen. Chromatographische Läufe können in vielen unterschiedlichen Modi wie hydrophile und hydrophobe Wechselwirkungen, Ionenausschluss, Ionenaustausch, oder eine Kombination aus mehreren dieser Modi durchgeführt werden. Um die Vielseitigkeit unseres Materials zu zeigen, untersuchten

wir das chromatographische Verhalten von hydrophoben und hydrophilen Verbindungen, sowie von Moleküle mit sauren oder basischen Reste. Es wurden deshalb fett- und wasserlösliche Vitamine, Fluorchinolon-Antibiotika, Betablocker, nicht-steroidale entzündungshemmende Moleküle, anti-Hypercholesterinämie Drogen, unter anderem, getestet. Wir verglichen die Trennung auf Standard RP oder HILIC Material mit der Trennung auf RP-WAX Material. Die Trennung von den meisten komplexen Mischungen kann mit dem Mixed-Mode-Material verbessert werden.

Der RP-WAX Material, der während dieser Studie entwickelt worden ist, soll in 2011 bei Merck KGaA kommerziell erhältlich werden.



# Curriculum Vitae

Romain Dabre  
Frankfurterstrasse 48  
D-64293 Darmstadt  
(06151) 396 33 24  
romain.dabre@gmail.com  
geb. 26. August 1983  
Französisch



## Praxiserfahrung

- Mai 10 – Heute     **Process business development manager** bei **Tosoh Bioscience GmbH**, Stuttgart (Deutschland)
- Apr. 07 – Apr. 10     **Doktorand** in Zusammenarbeit mit der **Universität Wien**, Wien (Österreich) und **Merck KGaA**, Darmstadt (Deutschland) unter der Leitung vom Prof. Wolfgang Lindner:  
*Development and evaluation of silica-based mixed-mode weak ion exchangers including their applications in bioanalytics*
- Okt. 05 – Feb 07     **Forschungsingenieur** bei **Merck KGaA**, Darmstadt (Deutschland), unter der Leitung vom Dr. Achim Schwämmle:  
*Entwicklung eines Verfahrens zur kontinuierlichen Modifizierung von Kieselgelen in einem Säulenreaktor zur Herstellung von neuen RP18-Materialien sowie Anwendung in der präparativen Chromatographie*
- Mär. 05 – Sep. 05     **Diplomand** bei **Merck KGaA**, Darmstadt (Deutschland), unter der Leitung vom Dr. Achim Schwämmle:  
*Magnetische Nanopartikel und Verfahren zu deren Herstellung*
- Apr. 04 – Jul. 04     **Praktikant** bei **Rhodia Acetow GmbH**, Freiburg (Deutschland) unter der Leitung vom Dr. Armin Stein:  
*Optimierung der Reaktion zur Herstellung von Celluloseacetate-basiertes Filter-Tow<sup>TM</sup>*

## Studium

- Apr. 07 – Mär. 11 **Doktoratsstudium analytische Chemie, Universität Wien, Wien**  
(Österreich)
- Sep. 05 **Diplom Ingenieur, Hauptfach Chemie**, Auszeichnung “International Study”  
**Master’s Degree**
- Sep. 02 – Sep. 05 **Ingenieurstudium** bei der **ENSICAen**, Hauptfach Chemie (École Nationale Supérieure d’Ingénieurs de Caen, Frankreich)
- Sep. 00 – Sep. 02 **Vordiplomstudium** in den „Classes Préparatoires aux Grandes Écoles“, Hauptfächer Chemie, Physik und Mathematik, Lycée Victor Hugo (Caen, Frankreich)
- Jul. 00 **Wissenschaftliches Abitur**, Hauptfächer Chemie und Physik

## Sprachkenntnisse

Französisch	Muttersprache
Deutsch	Verhandlungssicher
Englisch	Verhandlungssicher

## EDV-Kenntnisse

Chromatographie	Verschiedene HPLC-UV und HPLC-MS Steuerung- und Auswertung-Software (EZ ChromElite, Bruker MS, Chromeleon, ChromSword Auto...)
Programmierung	Visual Basic, L <sup>A</sup> T <sub>E</sub> X
Sonstiges	Beilstein, MODDE 7.0, Origin, Office Suit, Web und Mail Apps

## Wissenschaftliche Veröffentlichungen

- Patent WO 2009 / 115176 A2  
*Magnetische Nanopartikel und Verfahren zu deren Herstellung*
- Papers **Journal of Chromatography A**, R. Dabre, A. Schwämmle, M. Lämmerhofer, W. Lindner, 1216 (2009) 3473 - 3479  
*Statistical optimization of the silylation reaction of a mercaptosilane with silanol groups on the surface of silica gel*
- Journal of Separation Science**, R. Dabre, N. Azad, A. Schwämmle, M. Lämmerhofer, W. Lindner, 34 (2011) 761 - 772  
*Simultaneous separation and analysis of water- and fat-soluble vitamins on multi-modal reversed phase – weak anion exchange material by HPLC-UV*

Lectures	<b>ISPPP 2008</b> , Baden-Baden (Deutschland) <i>Preparative separation of peptide mixture on a column containing a mixed-mode reversed phase - weak anion exchange material</i>
	<b>ISPPP 2009</b> , Delray-Beach (Florida, USA) <i>An alternative method for peptide mapping using mixed-mode stationary phases</i>
Posters	<b>HPLC 2008</b> , Baltimore (Maryland, USA) <i>Statistical optimization of the silylation reaction of a mercaptosilane with silanol groups on the surface of silica gel</i>
	<b>Recovery 2008</b> , Quebec City (Canada) <i>Purification of peptides and small proteins by means of reversed phase / weak anion exchange mixed mode chromatography</i>
	<b>HPLC 2009</b> , Dresden (Deutschland) <i>Rapid HPLC analysis of pharmaceuticals using 2 <math>\mu</math>m Purospher STAR RP-18e stationary phases</i>
	<b>HPLC 2009</b> , Dresden (Deutschland) <i>A rapid method for the optimization of separation conditions on mixed-mode stationary phases using automated method development software</i>
	<b>Euroanalysis 2009</b> , Innsbruck (Österreich) <i>Separation of several bioactives molecules on mixed-mode stationary phase</i>
	<b>HPLC 2010</b> , Boston (Massachusetts, USA) <i>Validation of a HPLC method for the simultaneous separation of fat- and water-soluble vitamins on mixed-mode stationary phases</i>
	<b>HIC/RPC 2011</b> , Estoril (Portugal) <i>A procedure for optimizing the separation of mixtures of pharmaceutical compounds on RP-WAX stationary phases</i>